NEW PLAYERS AND NEW INTERACTIONS WITHIN THE NATRIURETIC PEPTIDE SYSTEM: MECHANISMS AND PATHOPHYSIOLOGICAL CONSEQUENCES

Xudong Zhu

Submitted in accordance with the requirements for the degree of
Doctor of Philosophy

The University of Hull and The

University of York

Hull York Medical School

September, 2012

Abstract

The natriuretic peptide system plays a pivotal role in the regulation of cardiorenal homeostasis as well as in the pathogenesis of cardiovascular diseases. In this thesis, the biological effects of the newly designed natriuretic peptide (NP) ACNP and mechanisms of the interaction between natriuretic peptide receptor A (NPRA) and B (NPRB) are elucidated. The receptor profiles of different BNPs and degradation profile of hBNP1-42 are also investigated. ACNP stimulates both NPRA and NPRB and thus is more potent and effective compared to human ANP or CNP in stimulating cGMP in primary cells *in vitro*. In sham-operated mice, 4-week treatment with ACNP exerted similar potency in lowering blood pressure compared to that of ANP or CNP. However, ANP, but not ACNP, ameliorated the myocardial infarction-induced left ventricular dysfunction. The lack of benefit of ACNP might relate to its fast degradation by a still unknown enzyme in mouse serum. The interaction between NPRA and NPRB has been suggested since an impaired cGMP generation upon NP stimulation was observed in NPRA/NPRB co-transfected cells. The inhibitory effect of heterogeneous receptor complexes on natural NP/NPR/cGMP signalling were receptor dose-dependent. The attenuation of the CNP/NPRB/cGMP axis is caused by a blocked formation of NPRB mRNA by NPRA and thus decreasing NPRB quantity on the membrane. The attenuated ANP and BNP signalling may involve conformational changes within the NPRA/NPRB heterodimer, leading to less ligand accessibility or ligand-mediated activation of guanylyl cyclise (GC). Furthermore, different forms of BNP have been studied. The N-terminal truncated BNP (mBNP7-32) and the elongated BNP (mBNP1-45) are able to stimulate NPRA, whereas the C-terminal elongated hBNP1-42 is a poor activator of NPRA. Meanwhile, metabolism of hBNP1-42 on kidney membrane was different to that of lung membrane, suggesting specific peptidase(s) in the kidney being important for renal action of hBNP1-42. Taken together, this thesis gives novel insight into the new players and new interactions in the natriuretic peptide system. It provides potential mechanisms in receptor interplay leading to an impaired cGMP generation. It also opens new directions for the better understanding of cardiovascular diseases and may identify completely new treatment options.

Contents

Acknowledgements

This dissertation has been an exciting but often daunting project, although it is merely the tip of the iceberg for my research career, which would have been impossible without the support and encouragement of many people whose confidence in my abilities to explore the challenging hypotheses.

Firstly I am profoundly beholden to Professor Thomas Walther for all his tireless supervision and guidance, for all the rigorous proofreading, and for his hardworking. I am also grateful to my secondary supervisor Dr. Joerg Hardege, and Dr. Francisco Rivero, Dr. Sam Xu, Dr. Yong Wang, Dr. Florian Gembardt, Dr. Yupei Xiao, Anja, Nils, Christian, Pooja, and other lab colleagues for all their accompany and advice, friendship and support. I would also like to express my special thanks to Dr. Burkhard Wiesner and Dr. Jenny Eichhorst from the FMP Berlin, Germany, my colleague Dr. Yong Wang, and Anja for their great input for my thesis and reciprocal collaboration. Furthermore I want to give endless thanks to my family: grandparents, parents, aunts and uncles, cousins, and all the in-laws and out-laws. I would especially like to thank Grandpa Guozhu Zhu and my Grandma Ruixiang Li for their spiritual support, alive or dead, which essentially directed me to achieve this PhD.

I have been blessed with many friends here in Hull, who have all helped to make this city a home for me. Thanks to Kun Shang, Rui Zhao, Elaine Brookes, Mathew Sanderson and all unnamed for your friendship and kindness. Additionally, I am indebted to all residents in 76 Auckland Avenue, for reserving siu yeh for me after overtime working. I have been also blessed with many friends in Giessen, Germany, where I always memorise the pleasant stays as a guest researcher. Thanks to Helene, Sarah, Carolin, Pia, Thana, Azadeh, Bala, Adnan, Erika, Nadia, whose camaraderie and welcome have made my German experience so fruitful and enjoyable. I am grateful to the China Scholarship Council and the University of Hull for providing full scholarship over my 3-year-study; and bursary from the Univerity of Hull and Hull York Medical School for my attendances in various of conferences.

The way ahead is long and no ending, yet high and low I will search with my will unbending.

Xudong Zhu

September, 2012 on Hull campus

Declaration

I confirm that this work is original and that if any passage(s) or diagram(s) have been copied from academic papers, books, the internet or any other sources these areclearly identified by the use of quotation marks and the reference(s) is fully cited.

I certify that, other than where indicated, this is my own work and does not breach the regulations of HYMS, the University of Hull or the University of York regarding plagiarism or academic conduct in examinations.

I have read the HYMS Code of Practice on Academic Misconduct, and state that this piece of work is my own and does not contain any unacknowledged work from any other sources'. If applicable, the declaration should also include; 'I confirm that any patient information obtained to produce this piece of work has been appropriately anonymised'.

Chapter I
Introduction

Chapter 1
Introduction

Some 10,000 articles associated with the natriuretic peptide system (NPS) have been published up to date after the iconic discovery of atrial natriuretic factor (ANF)/atrial natriuretic peptide (ANP) by de Bold and his colleagues in 1981 (de Bold *et al.*, 1981), a cardiac hormone secreted in response to volume expansion inducing plentiful natriuresis. This then led to the cloning of the ANP gene and the isolation of ANP, the first member of natriuretic peptides (NPs) with natriuretic, diuretic, and vasorelaxant activity (Flynn *et al.*, 1983, Misono *et al.*, 1984b). Subsequent investigations by many contributors highlighted the recognition of additional members of this peptide family in many tissues, and the discovery of receptors for these peptides throughout the mammalian species. Such exciting findings led to the speculation that NPs and their cognate receptors would be the basis and targets for the treatment of cardiorenal diseases, including hypertension, acute renal failure, and congestive heart failure. Hence, substantive basic and clinical studies on physiological and pathophysiological functions of the NPS were carried out with the aim to elaborate mechanisms involved in the regulation of cardiovascular, renal, and endocrine homeostasis. Desirably, a foregone conclusion has been addressed that the NPs and their receptors should yield potential therapeutic targets in treating patients with cardiovascular disorders.

1.1. The natriuretic peptide system

The NPS is composed of three structurally similar but genetically distinct peptides, atrial natriuretic peptide (ANP), B-type natriuretic peptide (BNP), and C-type natriuretic peptide (CNP) (Rosenzweig and Seidman, 1991). Urodilatin (URO) is a homologue NP being synthesized in human kidneys, sharing the full amino acid (AA) sequences of human ANP with a 4-AA N-terminal extension through a different post-translational process. These peptides share a highly conserved 17 amino acid (AA) disulfide-linked loop structure (Figure 1).
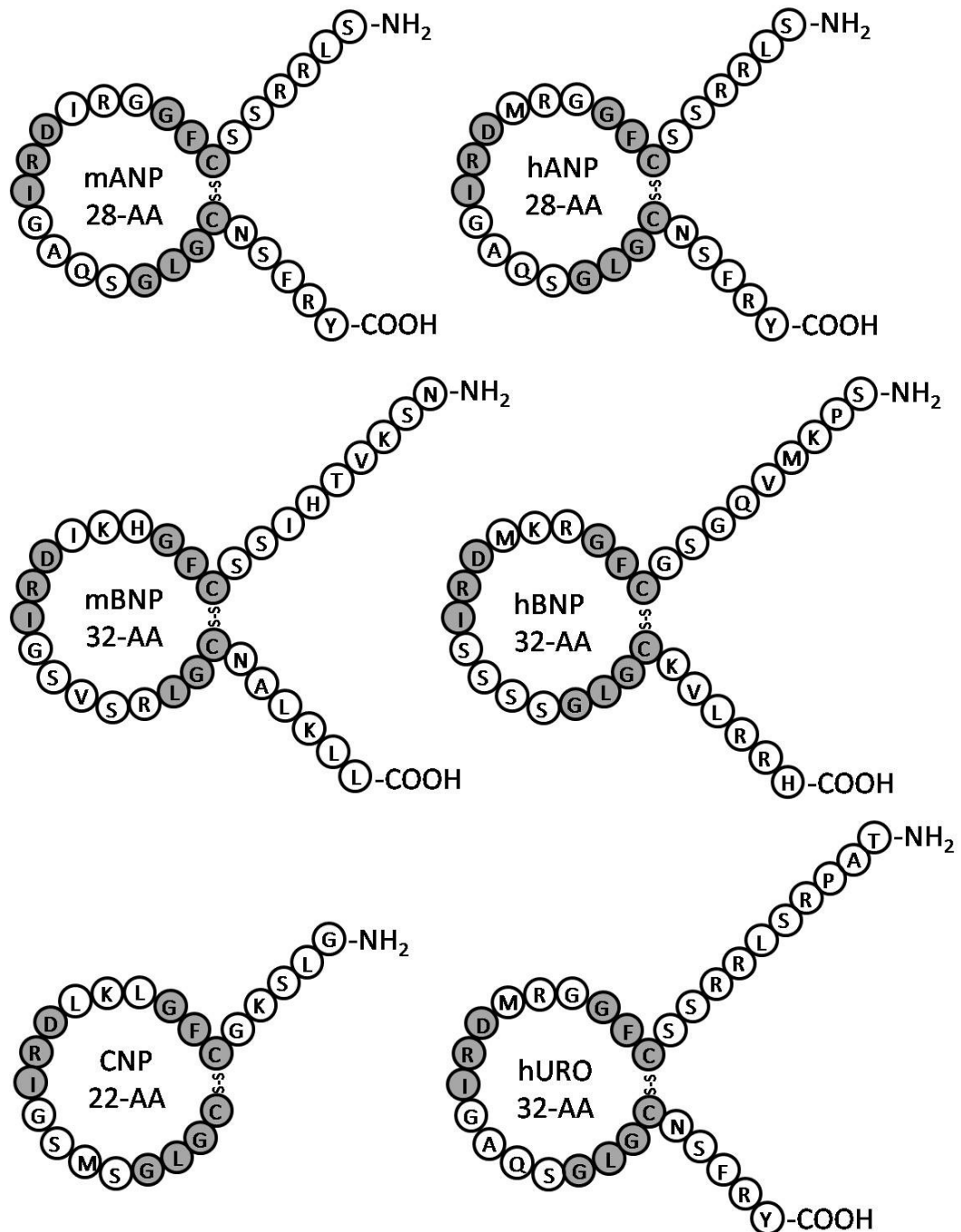
Figure 1. Amino acid sequences of natriuretic peptides. Residues in grey circles denote those conserved between the peptides. mANP, mouse ANP; hANP, human ANP; mBNP, mouse BNP; hBNP, human BNP; CNP sequence is universal in human, porcine, and rodent. hURO, human urodilatin.

This ring structure has been deemed essential for the pharmacological activity of the peptides (Misono *et al.*, 1984a). The biofunctions of NPs are mainly modulated by three different membrane-bound receptor subtypes, natriuretic peptide receptor A, B, and C (NPRA, NPRB and NPRC; also known as NPR1, NPR2, and

3

NPR3) (Koller and Goeddel, 1992, Suga *et al.*, 1992). Many of the responses to NPs have been attributed to the action of cyclic 3',5'-guanosine monophosphate (cGMP) as a second messenger (Potter *et al.*, 2006). Guanylyl cyclases (GC) are the intracellular catalytic domains of the NPRA and NPRB, responsible for the generation of cGMP in response to ligand stimulation. ANP and BNP are ligands of NPRA and play a key role in blood pressure control, while CNP is the most potent ligand known for stimulation of NPRB, exerting vasodilating effects in blood vessels as well as acting as an endothelium-derived hyperpolarising factor (EDHF) (Hobbs *et al.*, 2004). The third member of the NPR family is NPRC. This receptor is homologous in its extracellular domain to NPRA and NPRB, but has only a short 37-AA cytoplasmic domain and is involved in internalisation and clearance of NPs (Maack *et al.*, 1987) (Figure 2). Studies with cloned receptors have shown that all three, ANP, BNP, and CNP bind to NPRC with similar affinity (Anand-Srivastava, 2005). The distribution and function of the NPR are listed in Table 1.

Receptor	Distribution	Ligand	Function
NPRA (GC-A)	vascular smooth muscle cells, endothelial cells, nerve system, adrenal gland, kidney, spleen, heart	ANP, BNP	Lowering arterial pressure and blood volume, inhibiting growth of cardiac myocytes and cardiac fibroblasts
NPRB (GC-B)	Fibroblast, renal tubular cells, mesangial cells, vascular endothelial cells, chondrocytes, brain, uterus	CNP	Cartilaginus ossification, revascularisation
NPRC (clearance receptor)	Endothelium, intestinal epithelial cell, regenerating liver	ANP, BNP, CNP, Osteocrin(Thomas, 2004), cANP4-23 (Maack *et al.*, 1987)	Enhancing water and ions transportation via small intestine and kidney, facilitating growth and differentiation of epithelial cells

Table 1. Members of the NPR family, their distribution, ligands and physiological function.
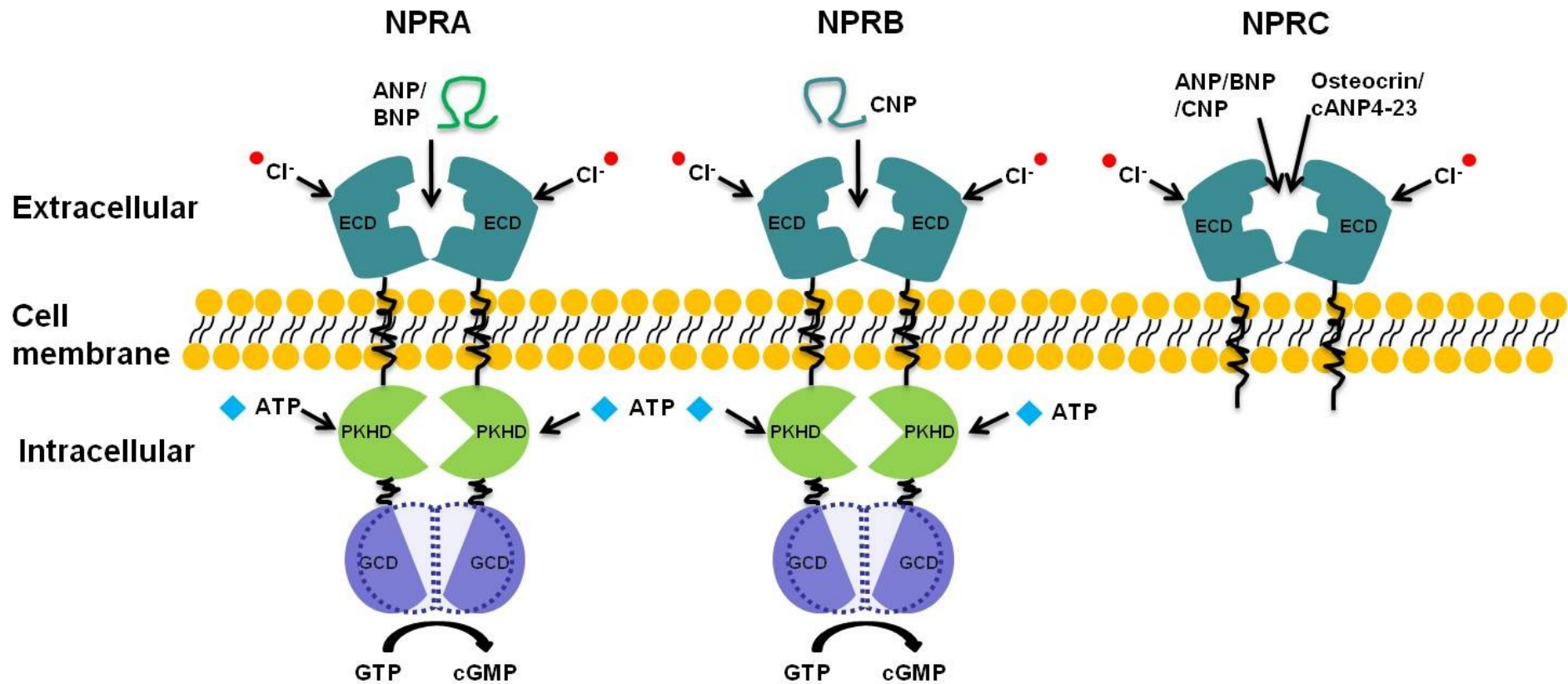
Figure 2. Schematic representation of the natriuretic peptide receptors. NPRA and NPRB share a similar topology including an extracellular ligand binding domain (ECD), a single transmembrane domain, a protein kinase homology domain (PKHD) and a guanylyl cyclase catalytic domain (GCD) in the intracellular portion of the protein. ANP and BNP bind to NPRA with high affinity. CNP binds preferentially to NPRB. NPRC has a similar ECD and transmembrane domain to NPRA and NPRB but lacks PKHD and GCD. NPRC is defined as a clearance receptor with an indiscriminate affinity to all three natriuretic peptides. The chloride-binding site in ECD and ATP-binding site in PKHD are thought to be essential for the ligand binding and transmembrane signal transduction (Potter and Hunter, 2001; Ogawa *et al*, 2010).

1.2. Structural and pathophysiological profiles of natriuretic peptides

1.2.1. The role of ANP under physiological and pathophysiological conditions

The first identified cardiac natriuretic hormone, ANP, originally named atrial natriuretic factor, is mainly produced, stored, and released by cardiac myocytes of the atria in the heart. It is released in response to atrial stretch and a variety of other signals induced by hypervolemia, exercise, or caloric restriction (Potter et al., 2009). The precursor proANP (1-126) is stored in membrane-bound granules in cardiac myocytes. Upon the stimulation, the circulating form of ANP is proteolytically cleaved from proANP to this 28-AA bioactive peptide, which is then constitutively expressed in the ventricle in response to stress induced by increased afterload (e.g. increased ventricular pressure from aortic stenosis) or injury (e.g. myocardial infarction). By binding to its specific receptor, the NPRA, a reduction in blood volume and therefore a reduction in cardiac output and systemic blood pressure is achieved. Lipolysis is increased and renal sodium reabsorption is decreased (de Bold, 1985, Potter et al., 2009). The overall physiological effect of ANP on the body is to suppress the increases in blood pressure and volume caused e.g. by the renin angiotensin system (RAS). Specifically in the kidney, ANP increases the pressure in the glomerular carpillaries via dilating the afferent glomerular arteriole and constricting the efferent glomerular arteriole, thus increasing the glomerular filtration rate (GFR), resulting in greater excretion of sodium and water (Kiberd et al., 1987). Renin and aldosterone secretion are reduced by the adrenal cortex, thereby inhibiting the RAS. Related to the cardiovascular effects, ANP relaxes vascular smooth muscle in arterioles and venules by mediating cGMP release and inhibits cardiac hypertrophy. NPRA-deficient mice develop increased cardiac mass and severe fibrosis and die suddenly (Kuhn et al., 2002). Besides, ANP increases intracellular cGMP levels that induce the phosphorylation of a hormone-sensitive lipase and perilipin A via the activation of a cGMP-dependent protein kinase-I (cGK-I), which controls the lipolysis in human adipocytes (Sengenes et al., 2003). So far, two distinct pathways have been suggested to regulate the effects of ANP, one is mediated by the clearance receptor NPRC possibly via an internalization

mechanism, and the other pathway involves the gradual degradation mainly by neutral endopeptidase (NEP, EC 3.4.24.11). The ring-structure of ANP is destroyed by NEP with a cleavage at Cys-7-Phe-8 bond ensuing biological deactivation of ANP (Vanneste *et al.*, 1988).

The clinical implications of ANP can be inferred from research on the use of ANP or BNP as either diagnostic and prognostic markers or as therapeutic agents in the treatment of heart disease (Gardner, 2003, Munagala *et al.*, 2004). It is suggested that ANP synthesis was significantly augmented in the streptozotocin-induced diabetic rat compared with that in the normal rat. Such enhanced cardiac ANP mRNA level was even greater in spontaneously hypertensive rat (SHR) suffered with streptozotocin-induced diabetes (Matsubara *et al.*, 1990). Importantly, the cardiac ANP mRNA level in the diabetic rats was fully reverted to control levels after insulin therapy, indicating that insulin-deficient diabetes mellitus rather than the cardiac toxicity of streptozotocin could be the principal cause for the altered cardiac ANP synthesis (Matsubara *et al.*, 1990).

1.2.2. The role of BNP under physiological and pathophysiological conditions

B-type natriuretic peptide (BNP), was originally named brain natriuretic peptide, because it was initially identified in the extracts of porcine brain (Sudoh *et al.*, 1988). This 32-AA polypeptide is mainly secreted by the ventricles of the heart in response to excessive stretching of cardiomyocytes. Human BNP is synthesized as a preprohormone of 134 residues containing a signal sequence that is cleaved to yield a 108-AA prohormone (proBNP). proBNP is further cleaved by furin, into two polypeptides: the bioactive 32-AA BNP, along with a 76-AA N-terminal fragment (NT-proBNP: NT-BNP1-76) which is biologically inactive (Sawada *et al.*, 1997, Porcel, 2005). Of note, Kojima *et al.* reported that the mature rat and mouse BNP is of 45-AA (Kojima *et al.*, 1989). The physiological actions of BNP are similar to ANP and include decrease in systemic vascular resistance and central venous pressure as well as an increase in natriuresis. Unlike ANP, BNP was found to be resistant to NEP degradation (Pankow *et al.*, 2009).

The biological half-life of BNP is twice as long as that of ANP, and that of NT-proBNP is even longer. Thus, BNP and NT-proBNP levels in the blood are

more often referred for screening, diagnosis of acute congestive heart failure (CHF) and may be useful to establish prognosis in heart failure than ANP, as both markers are typically higher and they are better predictors in patients with worse outcome (Bhalla *et al.*, 2004). For hospitalised patients with acute decompensated heart failure, BNP has a better prognostic value than any other serum marker or imaging modality in predicting short-term death and rehospitalisation (Logeart *et al.*, 2004). In recent years, clinical investigators have made similar observations in the general population. Elevated BNP or NT-proBNP levels are closely associated with incremental increases in risk for cardiovascular events such as myocardial infarction (MI), stroke, and heart failure (HF) (Kistorp *et al.*, 2005, Costello-Boerrigter *et al.*, 2006). Recently, it has been suggested that elevated serum BNP levels are strongly associated with cardioembolic stroke and increased poststroke mortality, but significantly decreased the odds of good functional outcome at 6 months after ischemic stroke (Rost *et al.*, 2012).

1.2.3. The role of CNP under physiological and pathophysiological conditions

Mature CNP is synthesized from the cleavage of pro-CNP by furin into a 53-AA residue, a form of 22-AA peptide is also identified, yet the enzyme responsible for this 22-AA CNP cleavage has not been clarified. CNP is produced by the vascular endothelium and the central nervous system and has vasodilative properties. It is stored in endothelial cells and is able to induce vasorelaxation by hyperpolarisation (Barton *et al.*, 1998) suggesting that CNP may represent an endothelium derived hyperpolarizing factor (EDHF), participating to the paracrine action of other endothelial vasorelaxant mediators, such as nitric oxide (NO) and prostacyclin. Recent studies have demonstrated that CNP may act as an EDHF in the mesenteric and coronary vascular bed confirming its pivotal role in the regulation of vascular tone and blood flow (Chauhan *et al.*, 2003, Griffith, 2004). Hobbs *et al.* (2004) demonstrated that endothelium-derived CNP is involved in the regulation of the coronary circulation, and NPRC activation underlies the vasorelaxant activity of this peptide. Wang and his colleagues concluded that the over-expression of CNP in cardiomyocytes does not affect ischemia/reperfusion-induced infarct size but prevents cardiac hypertrophy induced by MI (Wang *et al.*, 2007). Woods *et al.* (2007) identified CNP as a key anabolic regulator of endochondral bone growth;

they found that CNP increased expression of enzymes involved in chondroitin sulfate synthesis, which subsequently regulates cellular condensation and glycosaminoglycan synthesis during chondrogenesis. Moreover, compared to other natriuretic peptides, NEP exhibits a higher rate of hydrolysis of CNP suggesting that this enzyme may be more important in regulation of CNP bioavailability (Woods *et al.*, 2007).

1.2.4. The role of urodilatin under physiological and pathophysiological conditions

Urodilatin (URO) was initially isolated by Schulz-Knappe *et al.* in 1988 (Schulz-Knappe *et al.*, 1988). This 32-AA peptide (Figure 1), first extracted in the human urine, is localised in the kidney. URO is primarily distributed in distal tubule of the nephron and secreted luminally to exert a paracrine effect in the nephron mainly at the inner medullar collecting duct where the peptide regulates water and sodium excretion/reabsorption (Goetz *et al.*, 1990, Hildebrandt *et al.*, 1992, Meyer *et al.*, 1996). Since URO derives from the same precursor preproANP and results in highly identical structure of circulating form of ANP, as a consequence it was postulated that NPRA is the physiological receptor for URO and it favours similar potency in many biological response (e.g. natriuresis, diuresis) with that of ANP, and it has been wildly proved (Schulz-Knappe *et al.*, 1990, Goetz, 1991, Saxenhofer *et al.*, 1993, Valentin *et al.*, 1993, Kuse *et al.*, 1996, Carstens *et al.*, 1997, Santos-Neto *et al.*, 2006). In addition, it has been known for some time that the kidney elutes with urodilatin but not ANP, demonstrating URO is little affected by renal enzymes that inactivate ANP (Goetz *et al.*, 1990). More recent studies showed that hyperleptinemia-induced upregulation of Na^+, K^+-ATPase and excessive renal sodium retention contributed to leptin-induced hypertension in hypertensive obese individuals (Beltowski *et al.*, 2004). URO exerted an antagonistic effect via increasing renal dopamine uptake and stimulating the NPRA/cGMP/protein kinase G (PKG) cascade, causing reversible deactivation of renal tubular Na^+, K^+-ATPase, and consequently enhancing natriuretic and diuretic effects with lowering of mean blood pressure (Carstens *et al.*, 1998, Citarella *et al.*, 2009, Vives *et al.*, 2010). Moreover, i.v. bolus injection of URO as compared with ANP resulted in dose-dependent increases in urinary cGMP and Na^+ excretion accompanied by an

elevated GFP and heart rate (HR), with URO being more potent than ANP (Saxenhofer *et al.*, 1990).

1.2.5. Natriuretic peptides by alternative splicing

Technique availability of analysing the vast genome direct a brilliant avenue to the identification of alternatively spliced genes by splicing exons from pre-messenger RNA (mRNA) at variable sites. This process allows individual genes to generate multiple protein isoforms of varying functions. Among them, the mutant
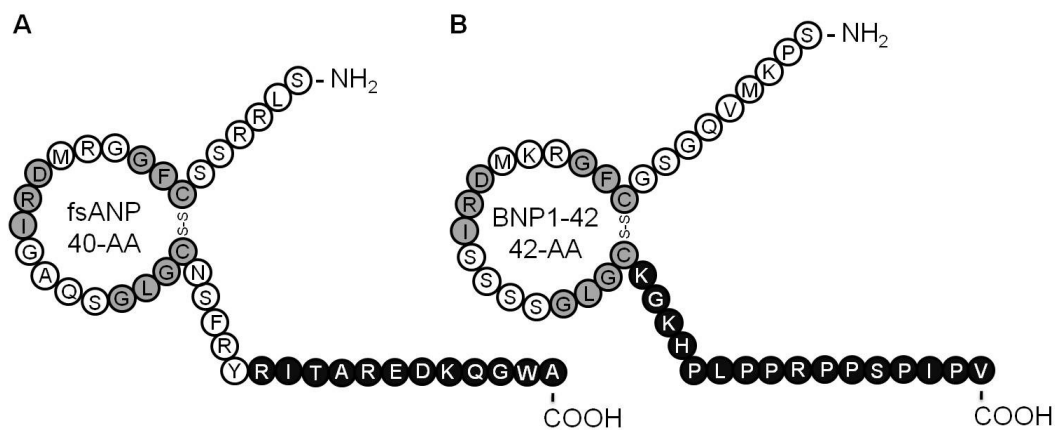
Figure 3. Amino acid sequences of alternatively spliced natriuretic peptides. Residues of fsANP **(A)** and BNP1-42 **(B)** resulting from alternative splicing are in black circles. Residues in grey circles denote those are conserved between the peptides.

ANP (fsANP) was identified as being resistant to proteolytic degradation (Dickey *et al.*, 2009). This 40-AA frameshift product, 12-AA extension to the C terminus of ANP (Figure 3A), was genetically linked to patients with familial atrial fibrillation (Hodgson-Zingman *et al.*, 2008). fsANP induced synthesis of a similar amount of cGMP compared to ANP in primary cardiac fibroblasts (CF) and exerted more potent natriuretic, diuretic, GFR, and renal blood flow enhancing actions than native ANP *in vivo* (McKie *et al.*, 2009). Later, McKie and his colleagues compared the therapeutic potential of fsANP in a canine model of acute angiotensin II (Ang II)-induced hypertension with equimolar human BNP (McKie *et al.*, 2010a). fsANP significantly lowered mean arterial pressure (MAP) and systemic vascular resistance that was even better than BNP. Notably, despite a reduction in blood pressure, renal function was enhanced with significant increases in renal blood flow, GFR, diuresis, and natriuresis after fsANP infusion. fsANP remarkably attenuated Ang II-induced pulmonary capillary wedge pressure elevation, and suppressed Ang II-induced activation of aldosterone. These cardiovascular and renal enhancing actions of

fsANP were accompanied by significant increases in plasma and urinary cGMP (McKie *et al.*, 2010a).

Pan *et al.* (2009) identified an alternative spliced transcript for BNP resulting from intronic retention during BNP transcription in HF patients. This transcript generates ASBNP, a 60-AA peptide with a unique 34-AA carboxyl terminus while retaining the amino terminus and the ring-structure of the native BNP (Pan *et al.*, 2009). Unlike BNP, ASBNP lacks the properties of vasodilating preconstricted arterial rings or stimulating cGMP in vascular cells. Given structural considerations, a carboxyl-terminal truncated form of ASBNP was generated by deleting the last 18-AA in the carboxyl terminus of ASBNP, designated as BNP1-42 (Figure 3B). Pan and colleagues found that BNP1-42 failed to activate NPRA and NPRB in vascular cells, but it could stimulate cGMP in a dose-dependent manner exclusively in isolated canine glomeruli and human mesangial cells. The cGMP effects in mesangial cells were inhibited in a dose-dependent manner by HS-142-1, an inhibitor of particulate guanylyl cyclase receptors (Sano *et al.*, 1992, Pan *et al.*, 2009). In a canine-pacing model of heart failure, BNP1-42 increased GFR, suppressed plasma renin and angiotensin, while inducing natriuresis and diuresis, thus implicating that BNP1-42-stimulated cGMP generation could be mediated via an unknown GC-coupled receptor in the kidney (Pan *et al.*, 2009).

1.3. Structure and function of natriuretic peptide receptors

Natriuretic peptides (ANP, BNP, and CNP) bind and activate specific cognate receptors present on the plasma membranes of a wide variety of target cells. Such ligand/receptor complex leads to a conformational change of structural domain(s) and stimulates intracellular signalling cascades, exerting diverse physiological functions. Molecular cloning and expression of cDNAs have identified three different membrane-bound forms of natriuretic peptide receptors in terms of their ligand specificity: NPRA, NPRB, and NPRC (Figure 2). They are also known as GC-A, GC-B, and the clearance receptor, or as NPR1, NPR2, and NPR3, respectively (Potter *et al.*, 2006).

1.3.1. Structure and function of NPRA

The hormonal activities of ANP and BNP are selectively mediated by NPRA. NPRA is a 118-135 kDa single transmembrane receptor linked to its intrinsic

guanylyl cyclase (GC) (EC 4.6.1.2) activity in the intracellular domain (Figure 2). The basic topology of NPRA is consistent with that identified in the common GC-coupled receptors, containing at least four distinct regions: an ~450-AA extracellular domain (ECD) with a ligand-binding site, a 21-residue single transmembrane domain (TD), an intracellular domain (ICD) comprised of a ~280-AA protein kinase homology domain (PKHD) and a ~250-AA guanylyl cyclase domain (GCD) (Potter and Hunter, 2001). Under basal condition, in absence of ligand, NPRA exists as a homodimer or homotetramer where some key residues in the PKHD are in a highly phosphorylated state, and the catalytic GC activity is inactive (Potter and Hunter, 2001). The binding of the ligand to the pocket structure (one molecule of ligand binds per two molecules of NPRA) in the ECD induces the transmembrane signal transduction, leading to the binding of adenosine triphosphate (ATP) to some high affinity site in PKHD. This ultimately brings the catalytic GCD into an active form (Potter and Hunter, 2001). The crystal structure of the dimerized extracellular hormone-binding domain of NPRA revealed that the transmembrane signalling by the NPRA might be initiated via a hormone-induced rotation mechanism (Ogawa *et al.*, 2004). Recently, it has been suggested that ANP binding to the ECD of NPRA requires chloride, and it is chloride concentration dependent (Ogawa *et al.*, 2010). Nevertheless, the potential significance of this chloride-dependent control mechanism for the BNP-bound NPRA has not been mentioned, and its clarification awaits further physiologic studies.

NPRA has been associated with a number of physiological and pathophysiological functions. NPRA-deficient animals exhibit elevated adrenal Ang II and aldosterone levels, increased blood pressure, cardiac hypertrophy, and ventricular fibrosis (Oliver *et al.*, 1997, Zhao *et al.*, 2007). By contrast, it has been reported that increased expression of NPRA in gene-duplicated mutant mice or increasing number of NPRA gene (Npr1) copies would significantly reduce blood pressure and increase the levels of cGMP (Oliver *et al.*, 1998, Pandey *et al.*, 1999). These findings appear to be in accordance with that ANP and BNP acting via NPRA to antagonise cardiac hypertrophic and fibrotic growth, thus exerting cardioprotective effects in disease states. In human, deletion of Npr1 allele in the 5'-flanking region massively reduced the receptor activity. Interestingly, normotensive individuals in Japan with the Npr1 deletion had left ventricular hypertrophy but

without hypertension (Nakayama *et al.*, 2000). In the presence of pressure overload, reduced myocardial cGMP levels but increased ventricular hypertrophy, fibrosis, filling pressures, and mortality were detected in point mutant (D893A) form of NPRA mice compared with wild type (WT) mice (Patel *et al.*, 2005). Moreover, Npr1 knockout (KO) mice exhibited an impaired ability to initiate a natriuretic response to acute blood volume expansion (Shi *et al.*, 2003), while an augmented natriuresis was achieved by low dose ANP infusion in Npr1-duplicated mice, and such enhancement of natriuresis is Npr1-dose dependent, implicating that NPRA signalling also plays an important role in mediating renal sodium reabsorption (Zhao *et al.*, 2010).

1.3.2. Structure and function of NPRB

The second GC coupled NPR, NPRB, has a structural topology similar to that of NPRA, especially conserved in the GCD with an overall homology of 62% to NPRA in human. Instead, the homology between the ECD of NPRA and NPRB is relatively low at 44%, likely reflective of the unique ligand pharmacology. An explanation for that is that ~130 kDa protein favours specific binding of CNP, but not of ANP or BNP. To date, studies on purified NPRB or its crystal structure has not been reported yet.

NPRB is distributed in many organs/tissues as listed in Table 1. However, in part due to the poor availability of specific inhibitors of the receptor-signalling pathways, the functions of NPRB are still unclear. Nevertheless, this receptor has been strongly implicated in playing a significant counterregulatory role to a variety of growth factors that promote cell proliferation, migration, and hypertrophy, in both cell culture and in a limited number of animal models. Mutations in the human NPRB gene were reported to cause acromesomelic dysplasia, type Maroteaux, a type of skeletal dysplasia (Bartels *et al.*, 2004). Of note, impaired growth of the longitudinal bone seen in the CNP-deficient mice may cause early death, which could also be mediated in part of CNP/NPRB/cGMP signalling pathway (Chusho *et al.*, 2001). Bartels *et al.* detected a higher Npr2 gene expression in the murine uterus than in the ovaries, indicating signalling through NPRB may play a role in uterine development (Bartels *et al.*, 2004). Moreover, Npr2-KO mice have been generated by targeted deletion of exons 3 through 7, which encode the C-termini of the

13

extracellular domain and transmembrane segment of NPRB and the phenotype characterized. The gene deletion resulted in dwarfism and female sterility, further suggesting important functions for this receptor in skeletal growth and the maturation of female reproductive organs (Tamura *et al.*, 2004).

1.3.3. Structure and function of NPRC

NPRC, also known as the natriuretic peptide clearance receptor, is a disulfide-linked homodimer that contains a single intracellular domain of only 37 intracellular amino acids and no guanylyl cyclase activity (Fuller *et al.*, 1988). NPRC is the most promiscuous of the receptors, the ECD of NPRC is approximately 30% identical to that of NPRA and NPRB, binding indiscriminately to all three NPs with the rank order of ligand affinity: ANP $\geq$ CNP > BNP (Suga *et al.*, 1992). The crystal structure studies of NPRC in both quiescent and hormone-bound forms revealed the hormone binding to NPRC with a stoichiometry of one molecule of hormone to two molecules of NPRC, inducing a notable conformational change in the juxtamembrane regions (He *et al.*, 2005). This mechanism of hormone recognition is also evidenced in the response of the NPRA and NPRB ectodomain to ligand binding (Ogawa *et al.*, 2004), implicating such allostery as a general activation signal of NPRs, despite their differing downstream signalling cascades.

Recent studies have implicated NPRC may be involved in signal transduction (Murthy *et al.*, 2000, Pagano and Anand-Srivastava, 2001, Anand-Srivastava, 2005), but the majority of physiological data acknowledge that the principal role of NPRC is to clear natriuretic peptides from the extracellular environment via a receptor-mediated internalisation and enzymatic degradation process. The distinguishing affinity of NPRC for the NP family members may contribute to the longer serum half-life of BNP than that of ANP. Furthermore, NPRC-KO mice displayed slightly decreased blood pressure and mild diuresis that are believed to be due to the longer half-life of circulating NPs arising from their reduced clearance. Additionally, increased body and bone dimensions were observed in Npr3-KO mice. A hypothesis is that NPRC in growing bone modulates the autocrine/paracrine effects of locally produced NPs (mainly CNP) (Matsukawa *et al.*, 1999).

1.4. Natriuretic peptide receptor signalling

1.4.1. Intracellular signalling of NPRA and NPRB

Of considerable potential importance for a better understanding of biological and pathophysiological consequences of NPR signalling is the earlier discovery by Ashman and co-workers of classic intracellular second messenger cGMP in rat urine (Ashman *et al.*, 1963). Later, three cGMP binding proteins, cGMP-dependent protein kinases (PKG), cyclic nucleotide-gated (CNG) channels, and cyclic nucleotide binding phosphodiesterases (PDEs) were discovered and widely investigated regarding their effects on varying targets associated with the natriuretic peptide system (Figure 4).

1.4.1.1. NPRA/NPRB-stimulated GC/cGMP/PKG axis

The cGMP-dependent protein kinases (PKG), also known as cGK, has been vastly studied as a sophisticated cGMP signalling effector. Serine and threonine kinases that are activated by cGMP binding (Lohmann *et al.*, 1997). Two PKG genes, PKG I and PKG II, were identified conducting signals from widespread signalling systems, though mainly via a NO/soluble GC (sGC)/cGMP signalling pathway (Pfeifer *et al.*, 1998, Fiscus, 2002, Rangaswami *et al.*, 2009, Fellner and Arendshorst, 2010). In mammals, PKG I gene consists of α and β isoforms (76kDa) that differ in their N-terminal dimerisation domain, whereas PKG II is a membrane-associated protein of 86 kDa. Vives *et al.* (2010) reported that ANP and URO specifically inhibited Na^+-ATPase activity by activation of the NPRA/cGMP/PKG pathway in luminal membrane and basolateral membranes, suggesting the regulation of NPs on renal sodium excretion, with proximal tubule Na^+-ATPase one possible target (Vives *et al.*, 2010). A recent study in mouse mesangial cells found that ANP/NPRA signalling inhibited the vascular endothelial growth factor-stimulated phosphorylation of mitogen-activated protein kinases (MAPK) and antagonized downstream effector molecules, activating protein-1 (AP-1) and cAMP-response element binding protein (CREB), indicating an inhibitory effect on cell growth and proliferation via the NP/NPRA/PKG axis (Tripathi and Pandey, 2012). Moreover, dwarfism caused by disturbed chondrocyte proliferation was delineated in PKG II-deficient mice (Pfeifer *et al.*, 1996). Later, a similar dwarfism has been reported in the mice model of genetic deletion of CNP or its cognate receptor NPRB (Tamura *et*

al., 2004), suggesting the CNP/NPRB/PKG axis is crucial for bone growth. In contrast, activating mutations in PKG II as well as overexpression of CNP result in general skeletal overgrowth in mice, further demonstrating the positive role of CNP/NPRB/PKG signalling in the regulation of mammalian chondrocyte ossification and cartilage matrix production (Yasoda *et al.*, 2004).
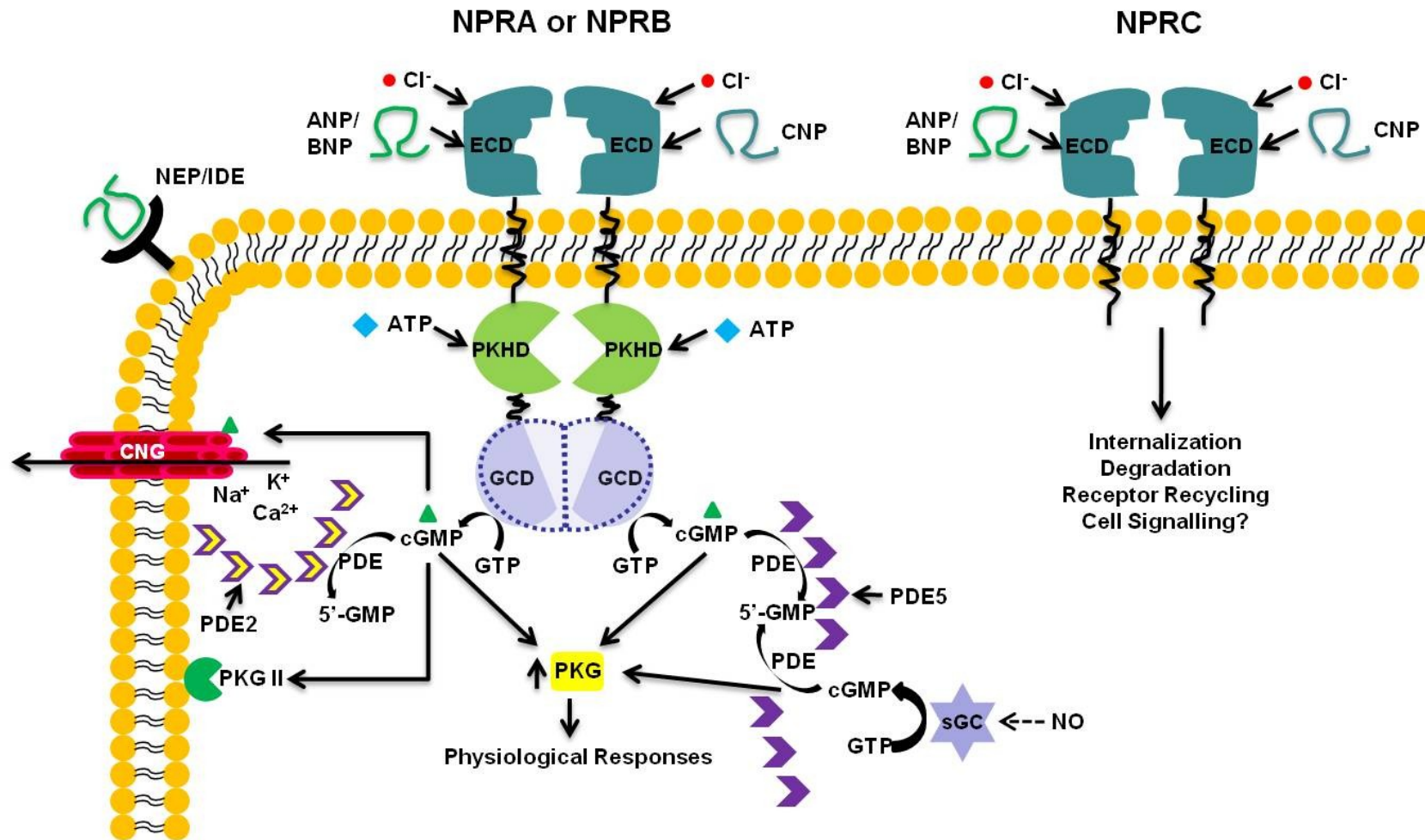
Figure 4. Diagram depicting the NPRs and possible association to the cGMP signalling. NPs bind to either NPRA or NPRB, in a chloride-/ATP-dependent fashion, stimulating the intrinsic GC activity of the receptor. cGMP exerts its biologic effects indirectly through PKG, or CNG channels, or different PDEs. NPs also bind to NPRC, which mediates internalisation, degradation, receptor recycling and other undetermined cell signallings. NPs may also be degraded or metabolized by NEP or IDE.

1.4.1.2. NPRA/NPRB-mediated cGMP/CNG channels activation/inhibition

Cyclic nucleotide-gated (CNG) ion channels modulate ion flux and influx in response to the binding of intracellular cyclic nucleotides, like cAMP and cGMP. Recent studies have demonstrated that cGMP generated by NP/particulate GC (pGC) preferentially regulates plasma membrane–localized targets such as ion channels and pumps, likely in a PKG-dependent manner (Zolle *et al.*, 2000, Zhang *et al.*, 2005). Nanomolar ANP-induced increases in cGMP levels activated CNG channels in a dose-dependent manner, whereas the nitric oxide donor S-nitroso-n-acetylpenicillamine (SNAP) failed to activate CNG channels, indicating that cGMP signals are compartmentalized in the cells (Piggott *et al.*, 2006). Castro *et al.* also reported that pGC and sGC synthesized cGMP in different compartments in adult rat ventricular myocytes, where PKG activation increased the cGMP-gated current response to ANP and amplified the stimulatory effect of ANP on pGC activity. However, such PKG activation in adult cardiomyocytes limited the accumulation of cGMP induced by NO donors via PDE5 stimulation (Castro *et al.*, 2010).

1.4.1.3. NPRA/NPRB-mediated cGMP/PDEs activation/inhibition

PDEs, degrading the phosphodiester bond in the intracellular cyclic nucleotides, are pivotal regulators of signal transduction mediating the localisation, duration, and concentration of these second messengers. To date, 11 PDE isoforms have been characterized based on substrate specificities. PDE4, 7, and 8 are cAMP-specific while PDE5, 6, and 9 are cGMP-selective. The PDE1, 2, 3, 10, and 11 can hydrolyze both cAMP and cGMP (Maurice *et al.*, 2003). Many biological significances of PDEs have been explored associated with their pharmacological inhibition due to the advances in studies of PDE inhibitors (Table 2).

Type		Targets	Function
Nonselective PDE inhibitors	Caffeine	Central nervous system	Stimulant effect, antifatigue
	Theophylline and Aminophylline	Bronchus	Bronchodilator
	1-(5-oxohexyl)-3, 7-dimethylxanthine (Pentoxifylline)	Limb arteries, brain	Treatment for intermittent claudication and vascular dementia
	3-isobutyl-1-methylxanthine (IBMX)	PDEs-riched cells	Attenuate cAMP/cGMP degradation
Selective PDE inhibitors	PDE1 inhibitor (Vinpocetine)	Cerebral vasculature	Cerebral blood-flow enhancing and neuroprotective effects
	PDE2 inhibitor, erythro-9-(2-hydroxy-3-nonyl)adenine (EHNA)	Cardiac myocytes, cortical neurons	Adenosine deaminase inhibitor, increase cGMP
	PDE3 inhibitor (amrinone, cilostazol, milrinone and enoximone.)	Heart	Inotropics for acute HF, treatment for cardiogenic shock
	PDE4 inhibitor (rolipram, mesembrine, ibudilast, roflumilast)	Immune cells, central nervous system	Treatment for chronic obstructive pulmonary disease, bronchodilator
	PDE5 inhibitor (Sildenafil, avanafil, lodenafil, mirodenafil, tadalafil, vardenafil, udenafil)	Smooth muscle cells, lung	Treatment for erectile dysfunction, pulmonary hypertension
	PDE10 inhibitor (papaverine)	Brain, heart, gastrointestinal tract, ureter	Antipsychotics, cerebral and coronary vasodilator

Table 2. Members of the PDE inhibitor family, their targets, and physiological function.

Study of renin and Ang II levels in Npr1-disrupted mice revealed a direct evidence that NPRA activation can inhibit the effects of RAS (Shi *et al.*, 2001). Previous investigation suggested the possible mechanism for the ANP-dependent reductions in cAMP and aldosterone may involve PDE2, where the accentuated ANP/NPRA/cGMP signalling activated PDE2 activity, thereby degrading cAMP, which is the major intracellular determinant for aldosterone synthesis (MacFarland *et al.*, 1991). Castro *et al.* (2006) found that PDE5 controls the soluble but not the particulate pool, whereas the latter is under the exclusive control of PDE2 in cardiac

myocytes, demonstrating that compartmental regulation of cGMP concentration through NPs/pGC or NO/sGC signalling pathways may attribute to the specific PDE distribution (Castro *et al.*, 2006) (Figure 4). He and co-workers further elucidated a juxtamembrane barrier comprised by PDE2 mediated NPs/pGC/cGMP/CNG channels signal cascade via PKG activation, while cGMP generated by sGC activated PKG, leading to an enhanced PDE5 activity and regulating the diffusion of cGMP (Castro *et al.*, 2010).

1.4.2. Intracelluar signalling of NPRC

The intracellular domain-truncated form of NPR, NPRC, interacts with NPs or the specific NPRC agonist, cANP4-23 to inhibit adenylyl cyclase activity through Gi protein (Anand-Srivastava *et al.*, 1990), or to activate the phospholipase C signalling pathway (Resink *et al.*, 1988). Prins *et al.* (1996) demonstrated that both ANP and the ring-truncated peptide of ANP, cANP4-23, could inhibit MAPK uniquely through NPRC in astrocytes, indicating NPRC may also play a role in cell proliferation through inhibition of MAPK (Prins *et al.*, 1996). In addition, cANP4-23 stimulated NPRC in VSMC to decrease cAMP levels and thus activated phosphatidyl inositol turnover signalling, which has been recognized as a major signal transduction pathway for hormones mobilizing intracellular calcium, suggesting NPRC as a key mediator in the feedback control of cAMP levels and phospholipase C signalling (Mouawad *et al.*, 2004). Moreover, Di Fusco and Anand-Srivastava reported that NG-nitro-L-arginine methyl ester (L-NAME)-treated rats exhibited enhanced expression of Gi alpha protein and NPRC-mediated inhibition of adenylyl cyclase activity was abolished, which might be associated to the downregulation of NPRC (Di Fusco and Anand-Srivastava, 2000). This hypothesis was partially confirmed by Lee *et al.* using L-NAME-induced hypertensive rats, which exhibited attenuated expression of NPRA and NPRC mRNA, whereas angiotensin II type 1 (AT1) receptor and angiotensin-converting enzyme (ACE) mRNA expression was upregulated (Lee *et al.*, 2002), indicating there might be the interaction between NPRC and AT1 receptor. Besides, the attenuated inhibition of adenylyl cyclase activity in L-NAME-induced hypertensive rats was restored via oral administration of the AT1 receptor antagonist, losartan (Hashim and Anand-Srivastava, 2004).

1.4.3. Desensitisation of natriuretic peptide receptors

Biochemical studies showed that NPRA and NPRB were desensitized by homologous ligand-induced dephosphorylation of residues at their PKHD (Potter and Garbers, 1992, Potter, 1998), in turn, proper phosphorylation of NPR is the prerequisite for hormone-stimulated guanylyl cyclase activity. Further investigation suggested that homologous (e.g. NPs) desensitisation of NPRs was not due to receptor internalisation or degradation, but mediated by dephosphorylation of specific residues through protein kinase C (PKC)-dependent pathways (Potter and Garbers, 1994, Potter and Hunter, 2000). Of note, heterologous desensitisation also plays a crucial role in unresponsive receptor to hormonal stimulation. It has been shown that increased local concentration of Ang II, endothelin, and other growth factors antagonized the activation of NPRs, which could also be mediated by a protein kinase C-induced dephosphorylation of NPRs (Jaiswal, 1992, Potter and Garbers, 1994, Chrisman and Garbers, 1999). Taken together, these aforementioned mechanisms of homologous or heterologous desensitisation of NPRs may partially explain why patients with cardiovascular diseases (e.g. CHF, cardiac hypertrophy) exhibited elevated plasma NPs levels correlated to severity, but impaired NPR/cGMP response to either endogenous NPs secretion or exogenous NPs administration (Tikkanen *et al.*, 1985, Hirooka *et al.*, 1990).

1.4.4. The interactions between NPRs and other hormone & signalling systems

Accumulating evidence have revealed interactions within the natriuretic peptide system or crosstalk with other peptide systems. Li *et al.* reported an attenuated cardiac hypertrophy and fibrosis in NPRA-deficient mice via inhibiting the endogenous angiotensin II type 1A receptor (AT1A), suggesting NPRA inhibited cardiac remodelling partially via antagonizing AT1A signalling (Li *et al.*, 2002). Besides, responses to both ANP-stimulated NPRA activation and sodium nitroprusside (SNP)-stimulated sGC stimulation were significantly enhanced in endothelial nitric oxide synthase (eNOS) KO mice, demonstrating that deprivation of endothelium-derived NO results in upregulation of the sensitivity of both sGC and pGC *in vivo*. Reciprocally, in NPRA KO mice, ANP failed to lower the MAP as expected, whereas SNP elicited a greater MAP lowering effect in comparison to that

of WT mice. Meanwhile, a cAMP-dependent vasodilator, epoprostenol caused similar haemodynamic changes in both WT and eNOS KO animals, suggesting that the reciprocal regulation of vascular tone is specific to cGMP-generating systems (Madhani *et al.*, 2006). Costa and his colleagues demonstrated that ANP infusion augmented NOS activity in SHR rats, where eNOS stimulation was induced via ANP/NPRC/Gi protein and Ca^{2+}-calmodulin signalling pathway (Costa *et al.*, 2009). In addition, Kinoshita *et al.* reported that the overexpression of transient receptor potential canonical 3/6 (TRPC3/6) in mice lacking guanylyl cyclase domain of NPRA exacerbated cardiac hypertrophy, while ANP acted via the cGMP/PKG pathway to directly inhibit TRPC3/6 activity, which in turn suppressed pro-hypertrophic signalling (Kinoshita *et al.*, 2010). Furthermore, under normal physiological state, calcium homeostasis is achieved via the counterbalance between the ANP/NPRA/cGMP/PKG axis and the Ang II/inositol triphosphate (IP3)/Ca^{2+}_i axis. Klaiber *et al.* found a cGMP-independent pathway when NPRA was desensitized by high ANP levels, causing elevating Ca^{2+}_i levels initiated by the activation of TRPC3/6 channels within a NPRA/TRPC complex (Klaiber *et al.*, 2011). Langenickel *et al.* used COS-7 cells, which were co-transfected with NPRB and the dominant negative NPRB mutant, NPRBΔKC. They found that intracellular cGMP accumulation upon CNP stimulation was blunted with increasing amounts of NPRBΔKC, while non-mutated NPRB homodimers were able to generate cGMP, hence demonstrating NPRBΔKC acts as a dominant-negative molecule for the cardioprotective CNP/NPRB pathway (Langenickel *et al.*, 2006). Our research group studied the cross-talk between the NP system and Ang II/AT1 signalling pathways, and found that co-transfection of NPRC could inhibit the activation of serum response factor and nuclear factor of activated T-cells (NFAT) induced by Ang II/AT1, and this inhibitory effect was dose-dependent.

Recently, the preliminary data showed that NPs/NPRs/cGMP signalling pathway was down-regulated in NPRA and NPRB co-transfected HEK cells in a dose-dependent manner. This finding led the speculation that such unanticipated down-regulated cGMP production may involve the cross-talk between NPRA and NPRB in the context of cardiovascular diseases, e.g. desensitisation/internalisation or heterodimerisation of NPRs under pathophysiological conditions.

1.5. Novel designed natriuretic peptides

The NPs/NPRs/cGMP signalling pathway has long been viewed as a compensatory axis in the setting of CVD, affording beneficial cardiorenal and hemodynamic effects. However, a lack of efficacy for the clinical end point was observed by intravenous injection of recombinant NPs due to reduction in renal perfusion pressure and the potential for reflex sympathetic responses (Voors and van Veldhuisen, 2010, Kilic *et al.*, 2010). Recently, a study involving 7141 patients revealed that the recombinant BNP (Nesiritide®) could lead to significant hypotension accompanied with occasionally severe renal impairment (O'Connor *et al.*, 2011). Hence, as per current primary clinical trial, a thorough validation of efficiency of such recombinant NPs should be addressed, and drugs reducing vascular effects and therefore maintaining renal perfusion pressure and volume unloading functions are sought to be synthesized. Enlightened by Wei *et al.*'s pioneering synthetic peptide (Wei *et al.*, 1993), designated as vasonatrin peptide (VNP), an emerging innovative therapeutic strategy is to engineer designed proteins by manipulating natively occurring peptides by elongating/deleting AA, or combining two or more peptides to create chimeras, which possess favourable therapeutic properties (Foran *et al.*, 2000). Such an approach with natriuretic peptides is advanced in the current study and involves the selection and incorporation of isolated structural determinants from two native peptides that result in a unique peptide with a specific activity profile that could go beyond native peptides as therapeutic agents in cardiovascular diseases.

The VNP of 27-AA was synthesized representing the fusion of 22-AA CNP, complemented with the C-terminus of ANP. VNP combined the venodilating and natriuretic actions of CNP and ANP, respectively, and uniquely favored the arterial vasodilating actions independent to either ANP or CNP (Wei *et al.*, 1993). In 2008, Lisy *et al.* reported the novel design of a chimeric natriuretic peptide, CD-NP (Lisy *et al.*, 2008). This 37-AA peptide possesses the entire 22-AA of CNP together with the 15-AA C-terminus of Dendroaspis natriuretic peptide (DNP). Chen *et al.* discovered that the long C-terminus of DNP may render DNP highly resistant to degradation by NEP contributing to potent natriuretic and diuretic actions (Chen *et al.*, 2002). Thus, the chimera kept the cardiac unloading actions of CNP with minimal hypotensive properties together with the additional renal effects of

natriuresis and dieresis. More recently, a non-vasodilatating NP synthesized from the ring structure of CNP and both C- and N-terminus of URO, termed CU-NP, exerted direct anti-hypertrophic effect through sodium-hydrogen exchanger-1 (NHE-1) inhibition, thereby preventing calcineurin activation and NFAT nuclear import (Kilic *et al.*, 2010). Together, chimeric NPs may afford the promising therapeutic properties targeting the cardiorenal pathophysiology and the specific structural requirements for certain pharmacological actions.

In the current study, we (Zhu *et al.*, 2011) and others (Chen *et al.*, 2011) synthesized ACNP, a designed natriuretic peptide consisting of the N-terminus and C-terminus arms from human ANP and the disulfide bond ring structure of CNP. In normal rats, ACNP has been proved to be more potentially diuretic, natriuretic and hypotensive compared with other NPs, and it is equally efficient to relax rat abdominal aorta compared to either ANP, CNP or VNP (Chen *et al.*, 2011). However, it was not yet investigated the receptor and degradation profile for ACNP and its potency/efficacy in stimulating cGMP generation in different cells. More importantly, under pathophysiological conditions, the pathophysiological effects of ACNP compared with native NPs need to be studied. The intensive *in vitro* and *in vivo s*tudies have been elucidated in Chapter 2.

1.6. Degradation of natriuretic peptides

Generally, there are two proposed mechanisms eliminating NPs, the degradation by peptidases and the receptor-mediated clearance associated with internalisation and subsequent lysosomal hydrolysis (Hirata *et al.*, 1985, Nussenzveig *et al.*, 1990). In regard to the latter one, some dissentions have been raised in terms of receptor internalisation and recycling. Early studies conducted on PC12 cells suggested a rapid internalisation and intracellular recycling mechanism for NPRB, whereas NPRC underwent a lower rate and a lesser extent of internalisation and recycling (Rathinavelu and Isom, 1991). Pandey and colleagues also reported in many different cell types that the majority of the NPRA were internalised after ANP binding, with a smaller portion being recycled to the plasma membrane (Pandey *et al.*, 1986, Pandey, 1992, Pandey, 1993, Pandey *et al.*, 2000). By contrast, Koh *et al.* reported that ANP/NPRA complex in cultured rat mesangial cells and renomedullary interstitial cells did not undergo internalisation or lysosomal

hydrolysis (Koh *et al.*, 1992). Consistent finding was generated by Jewett *et al.*; they found that transiently NPRA-transfected HEK293 cells bound less ANP. Such reduced binding was not related to quantity loss of NPRA mediated by endocytosis, but due to a negative modulation of hormone affinity to NPRA (Jewett *et al.*, 1993). Nevertheless, ligand-mediated internalisation is still a vital mechanism for terminating transmembranal receptor-mediated signalling. More complicated regulations in the cellular signal transduction remain to be definitively defined.

The other pathway involves specific enzymatic degradation, e.g. neprilysin (NEP), the most well-described zinc-dependent enzyme responsible for NPs degradation. However, biochemical studies suggested that murine or human BNP, in contrast to the structurally related ANP and CNP, was resistant to be hydrolyzed by NEP suggesting that its catabolism may involve other NP-degrading peptidases (Smith *et al.*, 2000, Walther *et al.*, 2004a). Using high-performance liquid chromatography (HPLC), our group demonstrated that the native mouse BNP1-32 was metabolized by meprin A (EC 3.4.24.18) to the N-terminal truncated but bioactive metabolite mouse BNP7-32 on the kidney membrane. Further investigation suggested that BNP7-32 was successively catabolized by NEP, leading to renal BNP clearance (Pankow *et al.*, 2007). Moreover, phosphoramidon, a protease inhibitor targeting NEP, prevented the degradation of ANP in HEK293 cells expressing NPRA but not NPRC, indicating the differing degradation mechanisms between NEP and NPRC (Fan *et al.*, 2005).

1.7. Aims of the study

With the attempt to better understand and to generate a more global view on the structure and function of the natriuretic peptide system, especially the effects of native peptides, peptide metabolites, and a novel synthetic peptide under various conditions (e.g. specific receptor binding, receptor heterodimeric complexes) on neurohormonal and haemodynamic profiles, and other pathophysiological consequences, the aims/hypotheses of the PhD thesis are:

● To identify the receptor(s) that mediates the function of ACNP using transfected cells and to investigate its efficacy in generating intracellular cGMP in cultured primary renal cells, endothelial cells, smooth muscle cells, and cardiac fibroblasts in comparison to the native natriuretic peptides ANP and CNP.

- To access the haemodynamic, neurohumoral, pharmacological and other biological properties of ACNP compared with ANP and CNP *in vivo,* with the murine model subjected to left coronary occlusion.

- To test the hypothesis that physical interaction between NPRA and NPRB causes alterations on the transcriptional or translational levels of the receptors, leading to altered NP-mediated cGMP generation; or transcription or translation of NPRs are not influenced, but less NPR is on the membrane due to faster internalisation or delayed reconstitution.

- To examine if a NPRA/NPRB heterodimer leads to conformational change(s) and thus prevents NPs binding to their specific domain or inhibits the activation of guanylyl cyclase domain responsible for cGMP generation.

- To characterise receptor profiles of different B-type natriuretic peptides, and also to investigate the degradation profile of hBNP1-42. It is aimed to identify the difference in hBNP1-42 metabolism/degradation on murine and human kidney membranes by HPLC.

Chapter II

***In vitro* and *in vivo* properties of the newly designed natriuretic peptide ACNP**

Chapter 2
In vitro and *in vivo* properties of the newly designed natriuretic peptide ACNP

2.1. Introduction

Cardiovascular diseases (CVD) are the number one cause of death globally presumably killing more than 20 million people per year by 2030 (cited from http://www.who.int/cardiovascular_diseases/en/). The severity of myocardial infarction (MI) and heart failure (HF), the two main lethal contributors, can be monitored and predicted correlatively by plasma levels of natriuretic peptides (NPs) (von Haehling *et al.*, 2007). In fact, N-terminal pro-atrial natriuretic peptide (NT-proANP) shows significant predictive value for mortality, while NT-proBNP is regarded as an effective biomarker for the diagnosis, risk stratification, and prediction of mortality in patients with HF and MI (Balion *et al.*, 2006, McKie *et al.*, 2011).

Beneficial effects of the natriuretic peptide system which consists of two axes (ANP/BNP-NPRA and CNP-NPRB) have been discussed for decades (Walther *et al.*, 2002). Although cGMP is their common second messenger, these two axes may play different roles under certain circumstances because of different receptor pattern and regulation of peptides and receptors. Human synthetic ANP (carperitide[®]) and BNP (nesiritide[®]) have been confirmed to improve symptoms of patients with acute decompensated heart failure due to their potent natriuresis, diuresis, and arterial dilation (Voors and van Veldhuisen, 2010). However, in some clinical trials, infusion of ANP and BNP increased morbidity and/or mortality, presumably due to NP-induced hypotension and thus renal perfusion (Dontas *et al.*, 2009, O'Connor *et al.*, 2011, Yancy *et al.*, 2008). Also, there are final data missing investigating the influence of differences in heart failure severity, the treatment/dosage given, maximum tolerated dose on the beneficial/side effects of NP administration. Furthermore, under heart failure condition, human NPRA is significantly down-regulated in the heart (Dickey *et al.*, 2007). In contrast, CNP has less potent diuretic and natriuretic actions compared to ANP and BNP, but it is more potent to induce venodilation (Dickey *et al.*, 2008). Importantly, unlike ANP and BNP, the CNP-NPRB axis is still active under chronic heart failure conditions (Dickey *et al.*, 2007).

28

Therefore, it is desirable to design agonists targeting both axes, which can combine the autocrine and paracrine effects of CNP in the heart with the diuretic and natriuretic actions of ANP and BNP in the kidneys, but have less impact on systemic and renal blood pressure. Although intensively searched for, such optimal non-peptidic agonist is not available up to now, mainly due to the fact that natriuretic peptides have a relatively complex 3-D structure. Therefore, inspired by the work on substrate specificity of BNP metabolites for neprilysin (Pankow *et al.*, 2009), different combinations of ring and arms from ANP, BNP, and CNP were tested and finally, we (Zhu *et al.*, 2011) and others (Chen *et al.*, 2011) synthesized ACNP, a synthetic natriuretic peptide consisting of the 6-AA N-terminus and 5-AA C-terminus of human ANP and the disulfide bond ring structure of CNP (Figure 5).
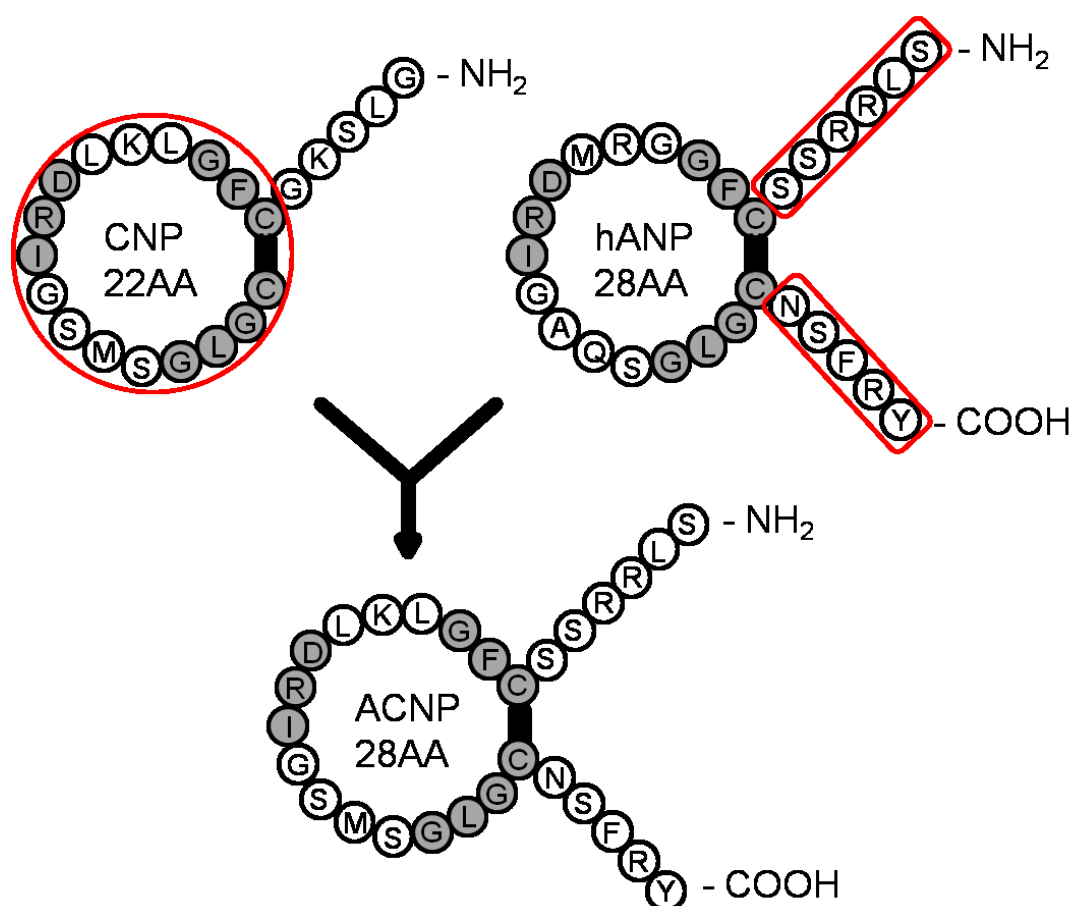
Figure 5. Amino acid sequence of the designed ACNP. The 28-AA ACNP is synthesized from the disulfide bond ring structure of CNP (in red circle) along with N- and C-terminal arms of human ANP (in red rectangle). Residues in grey circles denote those are conserved within the peptides.

In normal rats, Chen *et al.* implicated that natriuretic and diuretic potency of ACNP was higher than that of ANP and CNP, while it had a similar vasorelaxing effect in isolated rat abdominal aorta (Chen *et al.*, 2011). However, there was still a

significant lack in information regarding the receptor(s) that mediates the effects of ACNP and the cell types responsive towards its stimulation. In addition, the cardiorenal and humoral actions of ACNP under pathophysiological conditions remained unclear.

The goals of the following study were: 1) to characterize the receptor(s) profile of ACNP using transfected cells; 2) to investigate its efficacy in generating intracellular cGMP in cultured primary cardiac fibroblasts, renal cells, endothelial cells, and smooth muscle cells in comparison to the native natriuretic peptides ANP and CNP; 3) to assess *in vivo* the hemodynamic and neurohumoral properties of ACNP compared with ANP and CNP in healthy mice and mice with experimental MI; and 4) to investigate the metabolic/degradative profile of ACNP.

2.2. Materials and methods

2.2.1. Animal and housing

Wild-type C57/Bl6 male mice (6- to 8-week old) used as source for primary cell culture were purchased from Harlan Laboratories (Shardlow, UK) and further bred in the animal facility of the University of Hull, Hull, UK. *In vivo* studies were conducted in anesthetized male C57/Bl6 mice (weight 24 - 26g, 11- to 13-week old, Charles River, Sulzfeld, Germany). Mice were either kept with their siblings in Plexiglas cages, or individually housed post surgery in a climate-controlled room (21 ± 1 °C) under a 12 h : 12 h light-dark cycle. Animals were provided with rodent chow and water *ad librium*. All experiments were conducted according to both the Animals (Scientific Procedures) Act 1986, UK, and the guidelines of the Federal Law on the Use of Experimental Animals in Germany, which were further approved by the local authorities.

2.2.2. Reagents

Lyophilized powders of human ANP and CNP, and the designed ACNP peptide had a purity of approximately 95% and were synthesized by Biosyntan GmbH (Berlin-Buch, Germany). Double distilled water (ddH$_2$O) was used as solvent for the powders at varying dilution. The peptide solution was further analyzed by HPLC and mass spectrometry before use. Recombinant neprilysin (NEP) was bought from R&D Systems (Wiesbaden, Germany). The expression vector harbouring recombinant human NPRA cDNA (Genbank accession No. NM_000906.3) was purchased from OriGene Technologies Inc. (Rockville, MD, USA). The human NPRB cDNA fragment (Genbank accession No. NM_003995.3) was amplified via a forward primer 5'-GGAAGGAGTTTAAACCATGGCG-3' and a reverse primer 5'-CCGCACTCGAGTTACAGGAGTCC-3', and was subcloned into pcDNA3.1(-) vector (Invitrogen, Paisley, UK). Cell culture products were purchased from Invitrogen (Karlsruhe, Germany). The QuantiTect$^{®}$ Reverse Transcription Kit and the QuantiTect® SYBR® Green PCR Kit were used from Qiagen GmbH. Alzet® Mini-osmotic pumps (model 2004) were purchased from Charles River (Sulzfeld, Germany). All other chemicals used were obtained from Sigma (Taufkirchen, Germany).

2.2.3. Culture of permanent cells, transfection, and stimulation

Human embryonic kidney cells (HEK293) and the monkey kidney fibroblast cell line COS7 were cultured in Dulbecco modified Eagle medium (DMEM) supplemented with 10% fetal bovine serum (FBS) and penicillin-streptomycin (100 IU/ml to 100 μg/ml). The cultures were maintained at 37 °C in a 5% CO_2 humidified incubator. One day before transfection, cells were plated in 24-well cell culture dishes, and were transiently transfected with 500 ng total DNA per well using 2.5 μl per well PolyFect reagent (Qiagen GmbH, Hilden, Germany)(Pankow *et al.*, 2007). After 24 h, cells were stimulated by the solvent alone, or 10^{-7} M ANP, CNP, or ACNP for 5 min. Dose response curves were done in the same culture and transfection pattern with a 5 min stimulation at various concentrations of NPs. After sucking away the supernatant, 150 μl/well hydrochloric acid (0.1 N) was used to lyse the cells, and the supernatant was then stored at -80 ºC until cGMP measurement.

2.2.4. Isolation and culture of primary cells and their stimulation

Primary aortic smooth muscle cells (VSMC) were derived from the thoracic aortas of 6- to 8-week-old male C57/Bl6 mice and were grown in complete DMEM, as described previously (Pankow *et al.*, 2007). Kidney mesangial cells (MC) were isolated from the same animals according to the protocol by Mene *et al.* with minor modification (Mene and Stoppacciaro, 2009). In brief, kidneys were decapsulated and minced thoroughly in ice-cold RPMI medium. The homogenate was dispersed with 5 ml chilled RPMI medium to a 100-μm nylon filter, sequential sieved with another 10 ml, and then the filtrate transferred to a 70-μm nylon filter. After decapsulated, the glomerular 'cores' were digested with collagenase type II for approximately 30 min, then centrifuged at 1000 rpm for 10 min. The pellet was resuspended in RPMI 1640 medium supplemented with 17% FBS, penicillin/ streptomycin (100 IU/ml to 100 ug/ml), and 0.1 U/mL insulin, and cultured in an incubator with 37 °C and 5% CO_2. Both VSMC and MC were used between passage 2 and 3. Primary cardiac fibroblast (CF) were isolated from wild type C57/Bl6 male mice (6- to 8-week old). Briefly, excised hearts were washed in ice-cold 1× Dulbecco's phosphate buffer saline (1× DPBS) solution. Then ventricular tissues were minced into small pieces by use of 22-gauge blade in a mixture of 0.2% collagenase type 2 and 0.25% trypsin. Minced tissue was then placed into a sterile

50-ml tube and incubated with agitation at 37 °C for 50 min. The supernatant was collected, and the remaining tissue was immersed in digestion solution. The supernatants were pooled and filtered through a 100-μm nylon cell strainer, then centrifuged at 1,000 g for 5 min at 4 °C. The supernatant was removed, and cells were maintained in the fibroblast culture media (DMEM, 10% fetal bovine serum and 1% penicillin/streptomycin/fungizone) and incubated for 2 h at 37 °C with 5% CO_2 and 95% air. Cells were examined for positivity for vimentin. Fibroblasts between passages 2 to 3 were used for experiments.

Primary human dermal microvascular endothelial cells (HDMEC) and bovine aortic endothelial cells (BAEC) were purchased from European Collection of Cell Cultures (Salisbury, UK). All primary cells were plated on 24-well plates until they reached at least 80% confluence, then medium was changed by serum-free medium before stimulation with (VSMC and MC) or without (BAEC and HDMEC) 10 min pretreatment with 3-isobutyl-1-methylxanthine. After stimulation for 5 min with the solvent or one of the three peptides at 10^{-6} M, cells were lyzed by 150 μl/well 0.1 N hydrochloric acid with 0.5% Triton X-100, then stored at -80 °C until cGMP measurement. The same procedures were done for the dose response curve studies, except for the various NP stimulation concentrations. VSMC, MC, and both EC have been charactesized and validated by previous colleagues, and cell morphology is further confirmed under microscopic examination.

2.2.5. Measurement of cGMP

Total cGMP in cell lysate was measured using a commercially available ELISA kit (Enzo Life Sciences, Exeter, UK) according to the manufactures instructions. Final cGMP concentration was expressed as pmol/ml for plasma, or normalized by total protein concentration and expressed as pmol/mg for cell lysate.

2.2.6. Measurement of plasma TNF-α

Plasma TNF-α was measured using a commercially available ELISA kit (RayBiotech, Inc., Heidelberg, Germany) according to the manufactures instructions. Final TNF-α concentration was expressed as pg/ml.

2.2.7. Cell proliferation study

MC, VSMC, and CF were inoculated at 5,000 cells/well in 96-well plate and cultured with 100 μl colourless DMEM supplemented with 0.5% FBS in presence of

either 10 µl 1x DPBS, or 10 µl NPs (final concentration of 10^{-6} M) for 12 h, 24 h, 36 h, and 48 h respectively, 1 h before the end of incubation, 10 µl/well premixed WST-1 reagent was added in 100 µl volume at various time point. The cells were reincubated for another 3 h at 37 °C until the color change (to yellow) was visible to the naked eye. Thereafter, the formazan formed was quantitated as O.D. value at 450 nm subtracted by a 630 nm reference using an absorbance plate reader.

2.2.8. Animal experimental protocols

2.2.8.1. Cardiac surgery

Before starting the surgery, mice was sedated with 4% isoflurane for approximately 3.5 min prior to the intubation. The mice were fixed in the supine position on a heating pad to maintain body temperature. Surgical techniques were employed according to Tarnavski *et al.* with some minor revisions (Tarnavski *et al.*, 2004). Briefly, the intubated mice were anaesthetized and artificially ventilated with a mixture of 70% room air and 30% oxygen including 2 - 2.5% isoflurane for anesthesia. The ventilation rate was set at 90 strokes/min, a peak inspiration pressure of 18 cm H_2O and a positive end expiration pressure of 4 cm H_2O. After the left chest was shaved and disinfected with 70% ethanol, the skin was delicately dissected by a lateral 1.5-cm cut along the left side of the sternum. A 6-0 polypropylene suture was passed along the edge of the incision before the skin was dissected. The subcutaneous tissues were detached along the inferior fringe of the left pectoralis major muscles, and the left pectoralis major muscles were then refracted. The 4th intercostal space was exposed and delicately dissected 1 cm with the aid of microforceps. Self-retaining microretractors were then used to separate the 3rd and 4th ribs enough to get adequate exposure of the operating region, but the ribs were kept intact. MI was produced by permanent ligation using a 7-0 silk suture tied around the left anterior descending coronary artery approximately 1-2 mm from its origin. The ischemic area was identified visually as a result of blanching of the tissue upon ligation. Due to the large animal number, the infarcted size was evaluated by two experienced researchers by the eye. Only mice with infarcted size of > 25% were counted as MI mice. Sham operations were performed identically but loosely ligated the coronary.

2.2.8.2. Minipump implantation

Osmotic minipumps (Alzet, model # 2004) containing either 200 µl saline, or 200 µl (release rate at 0.1 ng/g body weight/min) human ANP, or 200 µl equimolar CNP, or 200 µl equimolar ACNP, were implanted subcutaneously one week post MI (full detailed implantation procedures can be obtained at the following online link: http://www.alzet.com/products/guide_to_use/implantation_and_explantation.html#S Cimplant).

2.2.8.3. Metabolic cage study

Metabolic cage study was performed at Day 28 and 29 post cardiac surgery. Mice were weighed before placed into the metabolic cage system (TSE Systems, Phenomaster, Bad Homburg, Germany). Water and food were available *ad librium* throughout the study. Food/water intake, body weight (BW) changes, urine volume (UV) were measured at the 24 h and 48 h respectively following the placement in metabolic cages. After 48 h, mice were released from metabolic cages and housed in their previous Plexiglas cages. Blood was collected from conscious mice by puncturing the submandibular vessels as previously described (Golde *et al.*, 2005) and collecting about 60-100 µl of the emerging blood into a heparin-containing Eppendorf tube. Blood cells and plasma were separated by centrifugation for 3 min at 12,000 rpm; the plasma was ejected into an Eppendorf tube and frozen at -80 ℃ until used for renal function study.

2.2.8.4. Haemodynamic measurements and pressure-volume loop analyses*

Haemodynamic parameters of the mice were examined 4 weeks post cardiac surgery by cardiac catheterization. A zero-pressure baseline was obtained by placing the pressure sensor in 37 °C saline before the catheter was advanced into the aorta and the left ventricular (LV). The right carotid artery was cannulated by a 1.4-Fr pressure-conductance catheter (Model No. SPR-839, Millar Instruments, Houston, TX, USA). Blood pressure and heart rate were recorded when the catheter was inserted into the right coronay artery. The baseline was recorded for 10 min. The haemodynamic parameters were measured for 5 min after advancing the catheter into LV recording blood pressure signals using the MacLab 3.6/s data acquisition system (AD Instruments). LV systolic pressure (LVSP), LV end-diastolic pressure (LVEDP), and positive and negative first derivatives for maximal rates of LV

pressure development (+dP/dt and -dP/dt) and other parameters were recorded, followed by transient occlusion of the left jugular vein. Subsequently, parallel conductance (Vp) was determined by a 10 µl injection of hypertonic saline (30%) into the left jugular vein to establish the offset due to the conductivity of structures external to the blood pool. The derived Vp was used to exclude the heart muscle influence on volume and thus to correct the pressure-volume (P-V) loop data. All data were analyzed with the LabChart v7.0 Pro software package from AD Instruments. At the end point, 0.5 M EDTA blood was taken under isoflurane anesthesia by puncturing of the left ventricle. Half of the blood samples were used for haematological examination, and the other half underwent centrifugation at 10,000 rpm for 10 min, and the plasma was snap frozen in liquid nitrogen and stored at -80 °C until further processing. After mice were sacrificed, LV, right ventricular (RV), wet lung, spleen, and bilateral kidney weights were obtained. One half of each organ was snap frozen in liquid nitrogen, and the other half was fixed in 4% paraformaldehyde for histological analysis.

2.2.8.5. Measurements of haematological parameters

The fresh EDTA blood samples were collected into sterile 1.5 ml Eppendorf tubes and immediately sent for haematological parameter measurements. Haematological indices were measured with the ADVIA 2120 hematology analyzer (Siemens Healthcare Diagnostics GmbH, Eschborn, Germany) equipped with veterinary software version 5.3.1.-MS. ADVIA 2120 analyses included red blood cells (RBC), white blood cells (WBC), hematocrit (HCT), hemoglobin (HGB), mean corpuscular haemoglobin (MCH) concentration, platelet count (PLT), and WBC differential (including neutrophils (Neut), lymphocytes (Lymph), monocytes (Mono), eosinophils (Eos) and basophils (Baso)).

2.2.9. One-step quantitative real-time PCR

Total RNA from LV and kidney tissue were extracted by Trizol® with subsequent chloroform-isopropanol extraction according to the manufacture's protocol (Invitrogen, Paisley, UK). The RNA concentration and purity were determined via NanoDrop 1000 Spectrophotometer (Thermo Fisher Scientific Inc., East Sussex, UK). Ten ng of RNA was used as template to determine mouse BNP mRNA, mouse collagen type I, and the reference gene mouse glyceraldehyde 3-

phosphate dehydrogenase (GAPDH) mRNA expression in an ABI StepOnePlus™ Real-Time PCR System (Applied Biosystems). Quantitative real-time PCR was carried out using one-step QuantiTect SYBR Green RT-PCR Kit and specific primers for mouse BNP (NM_008726), mouse Collagen type I (NM_007742), and mouse GAPDH (NM_008084) according to the manufacturer's instructions (Qiagen GmbH, Crawley, UK). Melting curve analyses were performed to monitor PCR product purity.

2.2.10. Natriuretic peptides degradation studies*

Human ANP, BNP, CNP, and ACNP in the concentration of 10^{-5} M were incubated with 100 µl recombinant human NEP (1 µl stock solution first diluted with 9 µl Assay Buffer (Assay Buffer: 50 mM Tris, 0.05% Brij35, pH 9.0), and then further diluted in 50 mM Tris buffer to a final volume of 100 µl) at 37 °C for 10 or 60 min. Additionally, 10^{-5} M of each NP was incubated with serum solution (1 : 12.5 diluted) from either human, or mouse and rat at 37 °C for 30 min. The reaction was stopped by adding perchloric acid (0.35 M). After centrifugation, the supernatant has been analyzed with High-Performance-Liquid-Chromatography using an UV-Detector. A linear gradient (Buffer A: acetonitrile with 0.05 % trifluoracetic acid; and Buffer B: double distilled water with 0.05% trifluoracetic acid) for both analyses was used to separate peptides on a RP Nucleosil 100 C12 column (Phenomenex, Torrance, CA, USA). Peak areas have been calculated with the LabSolutions® software from Shimadzu.

2.2.11. Statistical analysis

Results are expressed throughout as the mean ± SEM unless otherwise indicated. For the cell culture studies, each experiment was performed in triplicate in 2 or 3 separate experiments. Differences between groups were calculated using unpaired Student's t-tests. Physiological parameters in study groups were compared with one-way ANOVA, and Turkey post analysis. Two-way ANOVA was used to compare the main group effects of ANP, CNP, and ACNP in dose-response curves. EC_{50} values were calculated by using sigmoidal dose response curve fit in GraphPad Prism 5.0 (GraphPad Software, San Diego, CA, USA). Delta values were calculated by subtracting the MAP, or LVSP, or LVEDP, or dP/dt in sham-operated mice from each sample in MI group. Survival curves of the sham and MI mice were calculated

by Kaplan and Meier analysis method. A P value of < 0.05 was considered as significant.

*Haemodynamic and degradation studies were conducted in cooperation with Dr. Yong Wang and Anja Schwiebs, respectively, from Excellence Cluster Cardio-Pulmonary System, Justus-Liebig-Universität Giessen, Germany.

2.3. Results

2.3.1. ACNP is an activator of both NPRA and NPRB

2.3.1.1. Characterisation of ACNP/cGMP signalling in transfected cells

While we and others identified ACNP to be bioactive (Chen *et al.*, 2011, Zhu *et al.*, 2011), it was not clear which receptor mediates the described beneficial effects of this designed peptide. To define the associated receptors, HEK293 cells were transfected with plasmids harboring human NPRA or NPRB cDNA and stimulated with the solvent only, or 10^{-7} M of human ANP, CNP, or ACNP. As expected, ANP, but not CNP, dramatically increased cGMP concentration compared to vehicle control in NPRA-transfected cells. ACNP was able to stimulate cGMP generation almost equally potent as ANP (Figure 6A). By contrast, CNP stimulation significantly enhanced cGMP generation in NPRB-transfected HEK293 cells, while ANP could not stimulate cGMP generation. Impressively, ACNP also stimulated cGMP in NPRB-transfected cells with similar efficacy as CNP (Figure 6B).
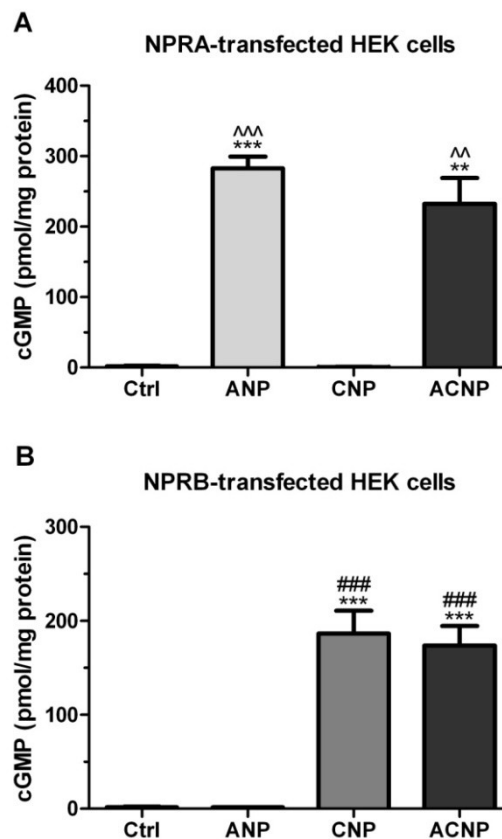
Figure 6. Generation of cGMP in NPRA- or NPRB-transfected HEK293 cells. **(A)** Absolute values of cGMP generation with NPRA-transfected HEK293 cells; **(B)** Absolute values of cGMP generation with NPRB-transfected HEK293 cells. Experiments were conducted in 3 independent settings as triplicates. **$P < 0.01$, ***$P < 0.001$ *vs.* control (Ctrl); ###$P < 0.001$ *vs.* ANP; ^^$P < 0.01$, ^^^$P < 0.001$ *vs.* CNP.

To check whether these findings were limited to HEK293 cells or are a general phenomenon, another reference cell line, COS7, was stimulated with equimolar natriuretic peptides. Comparable to HEK293 cells, ACNP could also stimulate both receptors in COS7 cells with slightly, but not significant less efficacy than ANP to NPRA (Figure 7A), but with similar one to CNP in NPRB-transfected cells (Figure 7B).
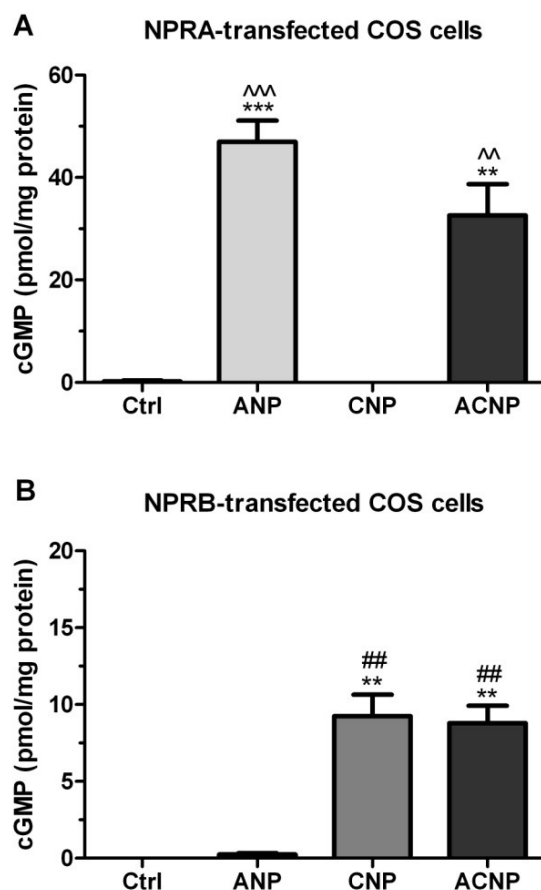
Figure 7. Generation of cGMP in NPRA- or NPRB-transfected COS7 cells. **(A)** Absolute values of cGMP generation with NPRA-transfected COS7 cells; **(B)** Absolute values of cGMP generation with NPRB-transfected COS7 cells. Experiments were conducted in 3 independent settings as triplicates. $**P < 0.01$, $***P < 0.001$ *vs.* control (Ctrl); $\#\#P < 0.01$ *vs.* ANP; $^{\wedge\wedge}P < 0.01$, $^{\wedge\wedge\wedge}P < 0.001$ *vs.* CNP.

This receptor profile has been further confirmed by dose-response curves in transfected HEK293 cells identifying ACNP to have a very low EC_{50} being almost as low as the one for ANP (Figure 8A), whereby the two curves were not significantly different. Dose-response curves in NPRB transfected cells identified an even better potency of ACNP in stimulating cGMP generation via the NPRB receptor compared to the endogenous ligand CNP in HEK293 cells, although ACNP was significantly less efficient than CNP ($P < 0.001$) (Figure 8B).

40
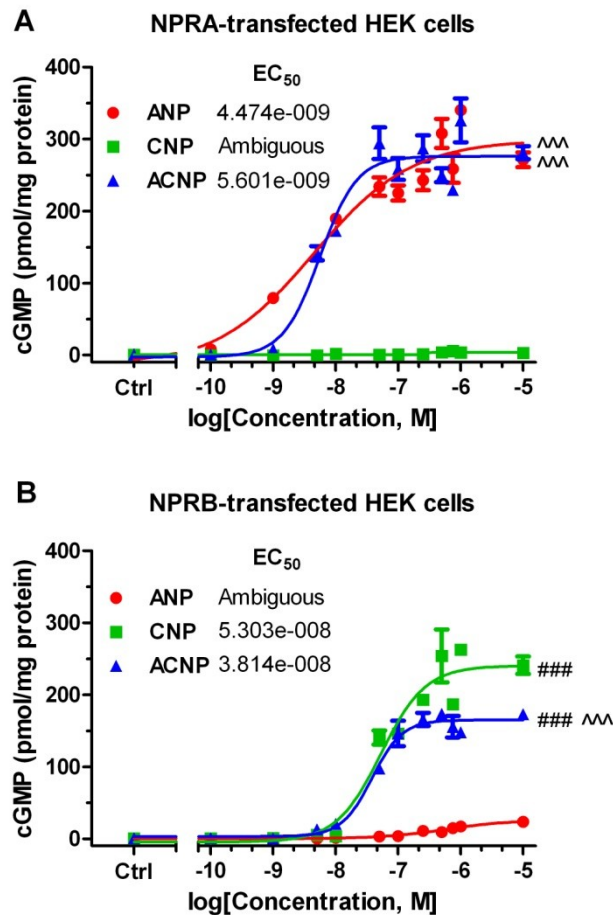
Figure 8. Dose-response curves in NPRA- or NPRB-transfected HEK293 cells. **(A)** Dose-response curves and EC_{50} calculation in NPRA-transfected HEK293 cells; **(B)** Dose-response curves and EC_{50} calculation in NPRB-transfected HEK293 cells. Human ANP, CNP, and ACNP ranging from a concentration of 10^{-10} to 10^{-5} M were used. Experiments were conducted in 3 independent settings as triplicates. ###$P < 0.001$ *vs*. ANP; ^^^$P < 0.001$ *vs*. CNP.

2.3.1.2. Characterisation of ACNP/cGMP signalling in primary cells

Above results suggested that the recombinant human ACNP can stimulate cGMP generation via both natriuretic receptors, NPRA and NPRB, with slightly lower or equal efficacy than the endogenous ligands. To test whether similar results can be generated in primary cell lines which play a crucial role in cardiovascular regulation and with endogenous expression of different proportions of the NPRA and NPRB, search was performed for additive effects of ACNP in those cells. Firstly, HDMEC were stimulated with 10^{-6} M of the peptides. Such endothelial cells have no significant NPRB expression as shown by very minor cGMP response on CNP stimulation but had robust NPRA expression as illustrated by the strong cGMP

signal induced by ANP (Liang *et al.*, 2007)(Figure 9). In such cells, ACNP was equally efficient as ANP.
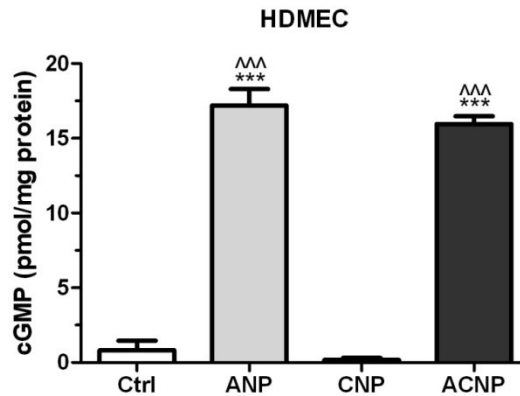
Figure 9. Generation of cGMP in human dermal microvascular endothelial cells (HDMEC). cGMP generation after stimulation with either solvent (control), 10^{-6} M of human ANP, CNP or ACNP was presented from 3 independent experimental settings as triplicates. ***$P < 0.001$ *vs.* control (Ctrl); ^^^$P < 0.001$ *vs.* CNP.
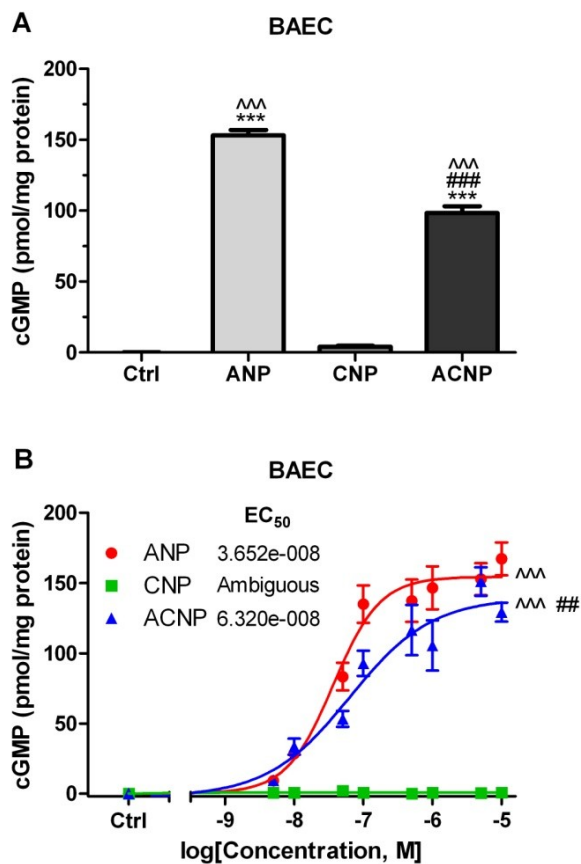
Figure 10. Generation of cGMP in bovine aortic endothelial cells (BAEC). **(A)** cGMP generation after stimulation with either solvent (control), 10^{-6} M of human ANP, CNP, or ACNP is presented from at least 3 independent experiments. **(B)** cGMP generation after stimulation with either solvent (control), human ANP, CNP, or ACNP ranging from a concentration of 10^{-9} to 10^{-5} M were used and EC_{50} values of each NP curve determined. ***$P < 0.001$ *vs.* control (Ctrl); ##$P < 0.01$, ###$P < 0.001$ *vs.* ANP; ^^^$P < 0.001$ *vs.* CNP.

42

A similar cGMP stimulation pattern, although with significantly less cGMP generation by ACNP compared to ANP, could be observed in BAEC, used to exclude species-specific expression of such receptors or receptor signalling profile in EC of different species (Figure 10A). Consistently, dose-response curves in BAEC exhibited lower potency of ACNP compared to ANP (EC$_{50}$: ANP: 3.7×10^{-8} M; ACNP: 6.3×10^{-8} M), with significant differences between the two curves ($P < 0.01$) (Figure 10B).

In contrast, in kidney MC, which express mostly NPRB (Suga *et al.*, 1992), CNP stimulated cGMP generation to a much higher extent than ANP (Figure 11A). Due to the minor, but still significant expression of NPRA, which the designed peptide could also stimulate, ACNP was even more efficient than CNP and therefore the most efficient NP tested. Dose-response curves in such cells revealed higher potency of ACNP compared to CNP, with significant differences between the two curves ($P < 0.05$) (Figure 11B).
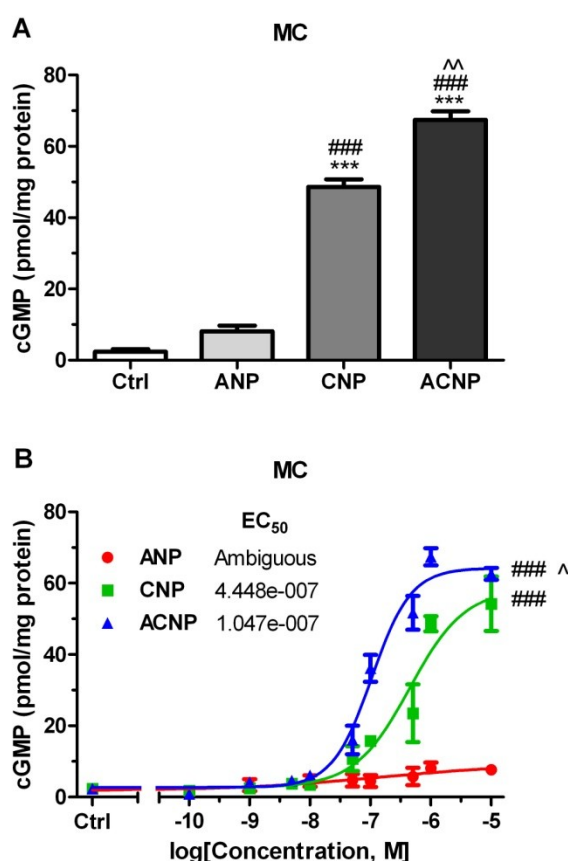
Figure 11. Generation of cGMP in primary mesangial cells (MC). **(A)** cGMP generation after stimulation with either solvent (control), 10^{-6} M of human ANP, CNP, or ACNP is presented from at least 3 independent experiments. **(B)** cGMP generation after stimulation with either solvent (control), human ANP, CNP, or ACNP ranging from a concentration of 10^{-10} to 10^{-5} M were used and EC$_{50}$ values of each NP curve determined. ***$P < 0.001$ *vs.* control (Ctrl); ###$P < 0.001$ *vs.* ANP; ^$P < 0.05$, ^^$P < 0.01$ *vs.* CNP.

This additive effect from endogenous NPRA expression was even more obvious in primary vascular smooth muscle cells (Figure 12A), which has been described as cells expressing predominantly NPRB but also robust amounts of NPRA (Suga *et al.*, 1992, Pankow *et al.*, 2007). ACNP generated significantly higher cGMP concentration than CNP whereby such level was comparable to the sum of cGMP generated by ANP and CNP (Figure 12A). Consequently, dose-response curves in VSMC revealed higher potency of ACNP compared to CNP (EC$_{50}$: CNP: 2.3×10^{-7} M; ACNP: 6.3×10^{-8} M), with significant differences between the two curves ($P < 0.01$) (Figure 12B).
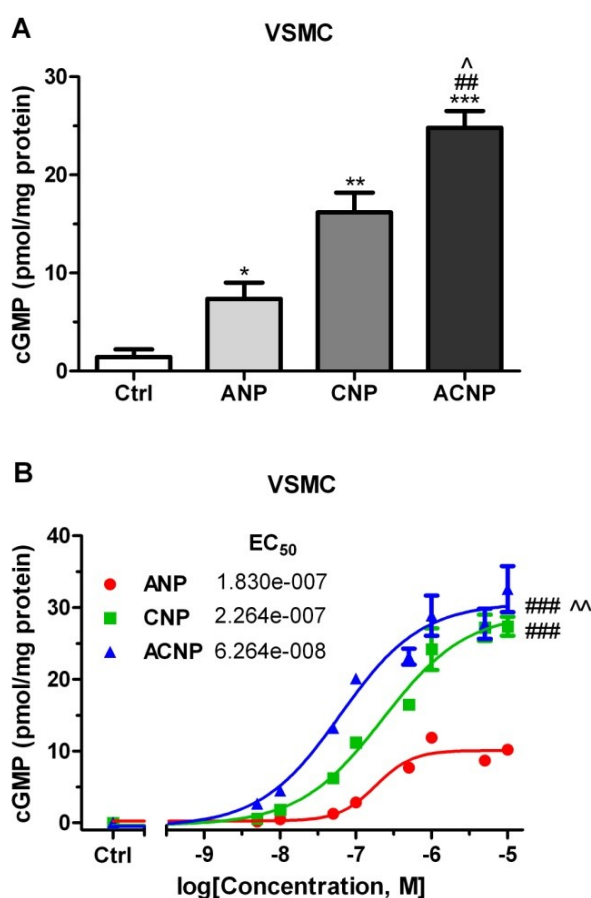
Figure 12. Generation of cGMP in primary vascular smooth muscle cells (VSMC). **(A)** cGMP generation after stimulation with either solvent (control), 10^{-6} M of human ANP, CNP, or ACNP is presented from at least 3 independent experiments. **(B)** cGMP generation after stimulation with either solvent (control), human ANP, CNP, or ACNP ranging from a concentration of 10^{-9} to 10^{-5} M were used and EC$_{50}$ values of each NP curve determined. *$P < 0.05$, **$P < 0.01$, ***$P < 0.001$ *vs.* control (Ctrl); ##$P < 0.01$, ###$P < 0.001$ *vs.* ANP; ^$P < 0.05$, ^^$P < 0.01$ *vs.* CNP.

Moreover, another NPRB-rich cell type, CF, depicted a very similar cGMP stimulation pattern in comparison to either MC or VSMC (Figure 13A). 10^{-6} M of CNP stimulated cGMP generation to a much higher extent than ANP ($P < 0.01$).

Equimolar ACNP could stimulate such cells more efficiently than CNP due to additive cGMP production by the minor expressed of NPRA, though not significant. Therefore, dose-response curves in CF showed higher efficacy of ACNP compared to CNP ($P < 0.05$), though no difference in their potency (Figure 13B).
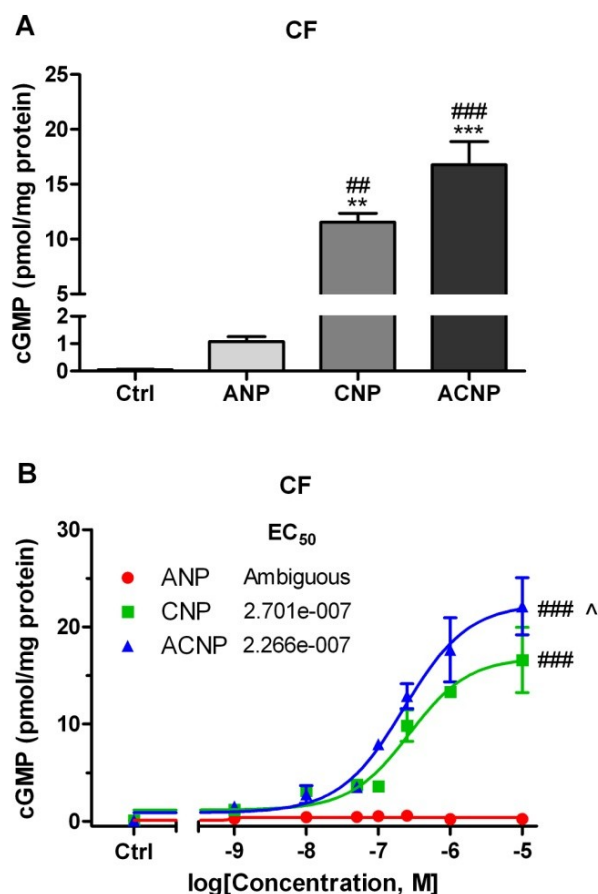
Figure 13. Generation of cGMP in primary cardiac fibroblasts (CF). **(A)** cGMP generation after stimulation with either solvent (control), 10^{-6} M of human ANP, CNP, or ACNP is presented from at least 3 independent experiments. **(B)** cGMP generation after stimulation with either solvent (control), human ANP, CNP, or ACNP ranging from a concentration of 10^{-9} to 10^{-5} M were used and EC$_{50}$ values of each NP curve determined. **$P < 0.01$, ***$P < 0.001$ *vs.* control (Ctrl); ##$P < 0.01$, ###$P < 0.001$ *vs.* ANP; ^$P < 0.05$ *vs.* CNP.

2.3.2. Cell proliferation study in different primary cells

To quantify the proliferative effect of natriuretic peptides on three different primary cells, either solvent (Ctrl), 10^{-6} M of ANP, CNP, or ACNP were incubated with MC, VSMC, and CF for 12 h, 24 h, 36 h, and 48 h, respectively. One hour before the end of each incubation period, the premixed WST-1 reagent was added to each well and incubated for another 3h to assay the cell proliferation. As shown in

Figure 14A, ANP did not influence the MC proliferation along with the time elapse and exhibited similar ΔOD changes compared to control cells.
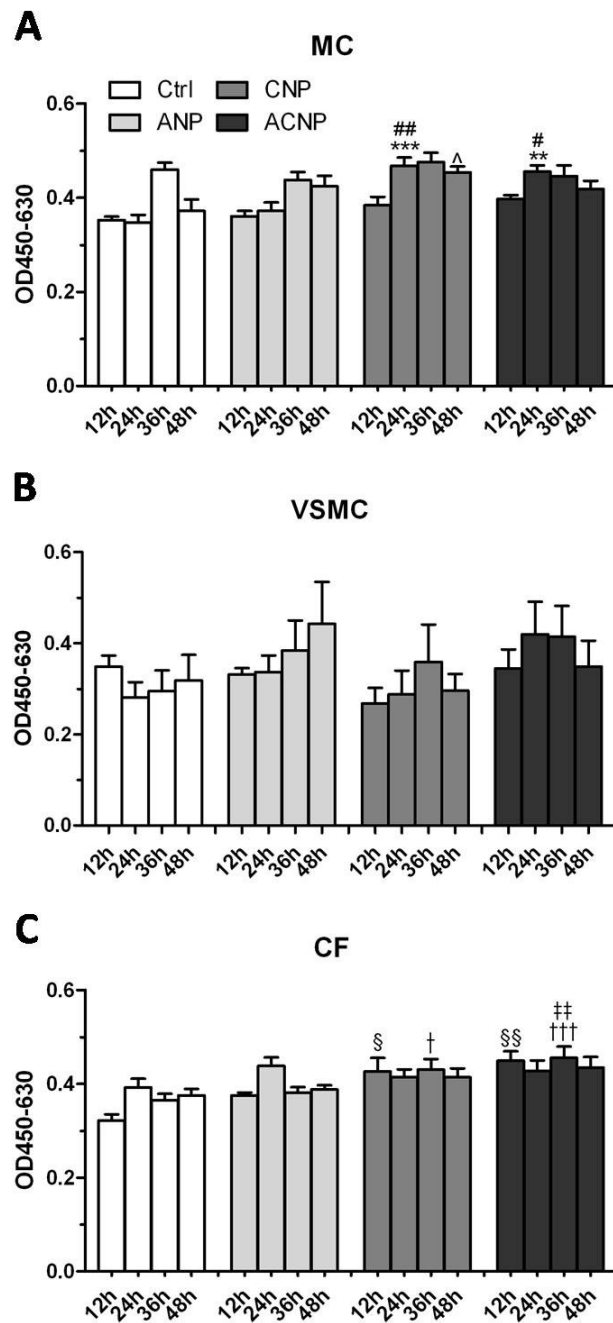
Figure 14. Comparison of proliferation of different primary cells in response to natriuretic peptides. **(A)** MC; **(B)** VSMC; and **(C)** CF were incubated in presence of 10^{-6} M of NPs, or equivolume 1x DPBS (Ctrl). (n = 6 wells per group). §$P<0.05$, §§$P<0.01$ *vs.* 12h-Ctrl; **$P<0.01$, ***$P<0.001$ *vs.* 24h-Ctrl; †$P<0.05$, †††$P<0.001$ *vs.* 36h-Ctrl; #$P<0.05$, ^$P<0.05$ *vs.* 48h-Ctrl; ##$P<0.01$ *vs.* 24h-ANP; ‡‡$P<0.01$ *vs.* 36h-ANP.

At 24h, MC grew significantly faster in CNP and ACNP preincubated wells than those of control and ANP, but maintained in a non-proliferative stage afterwards. A similar pattern of cell proliferation after pre-incubation with CNP and

ACNP was found in VSMC (Figure 14B), with no significant changes of ΔOD in comparison with control cells. ANP treated VSMC displayed a slightly but not statistically significant increase of OD value by the time elapse (Figure 14B). In CF, natriuretic peptide-treated cells showed an overall increase in ΔOD over control cells at different time points, whereby CNP and ACNP demonstrated an identical cell proliferation pattern (Figure 14C).

2.3.3. ACNP in a mouse model of myocardial infarction

2.3.3.1 Survival after MI

To test the cardiorenal and humoral actions of ACNP under pathophysiological condition, a MI mouse model was established via permanent ligation of the left coronary artery. Sham operation was done with a loose ligature around the left coronary artery. MI areas were visualized in the anterior wall, lateral wall, or posterior wall of the left ventricle respectively as early as 24 h following the ligation. As shown in Figure 15, the left ventricular wall in MI groups was significantly thinner in comparison to that of sham groups 5 weeks post MI, associated with visable left ventricular hypertrophy. However, no significant difference in cardiac morphology was observed within either four sham subgroups, or MI subgroups.
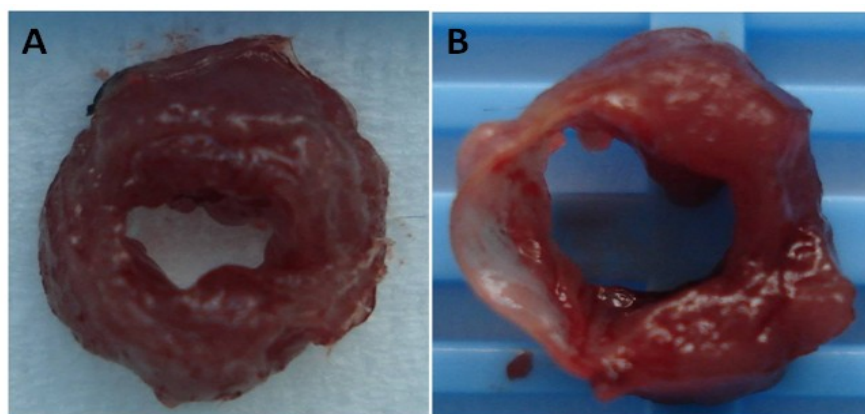
Figure 15. Representative photos of the heart cross-sections 5 weeks post operation. **(A)** Sham operation; **(B)** MI operation.

As MI is associated with high mortality, survival data of pooled sham groups and MI groups were analysed (Figure 16). Overall, sham group showed a 8.2% (4/49) mortality and all death occurred within 7 days post surgery. MI group exhibited 40.4% (23/57) mortality overall and majority of death occurred within 7 days post surgery. Of note, no differences in mortality rate were found among the different MI groups. All deaths in sham group and 3 deaths in MI group were due to trachea damage-

induced dehydration, while most of the deaths in the MI group were caused by cardiac rupture, except one was euthanized due to blindness.
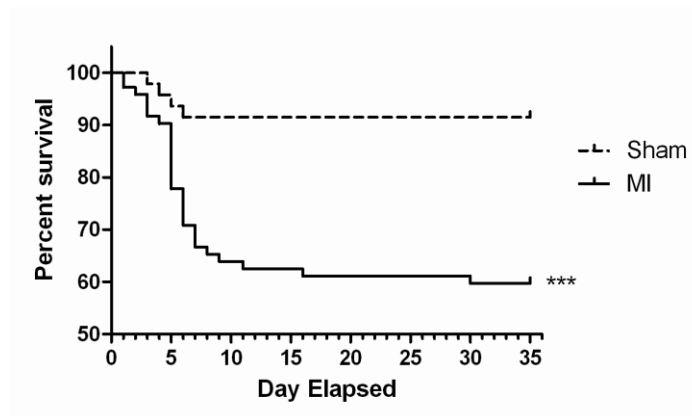
Figure 16. Mortality rate in sham and MI mice. Survival curves used Kaplan-Meier estimates. ***$P < 0.001$ *vs.* sham.

2.3.3.2 Metabolic cage study

To access the natriuretic and diuretic effects of the tested NPs and their impact on drinking and feeding behavior, mice were housed individually in a metabolic cage for 48h at the end of week 4 post MI. As shown in Figure 17, except a decrease
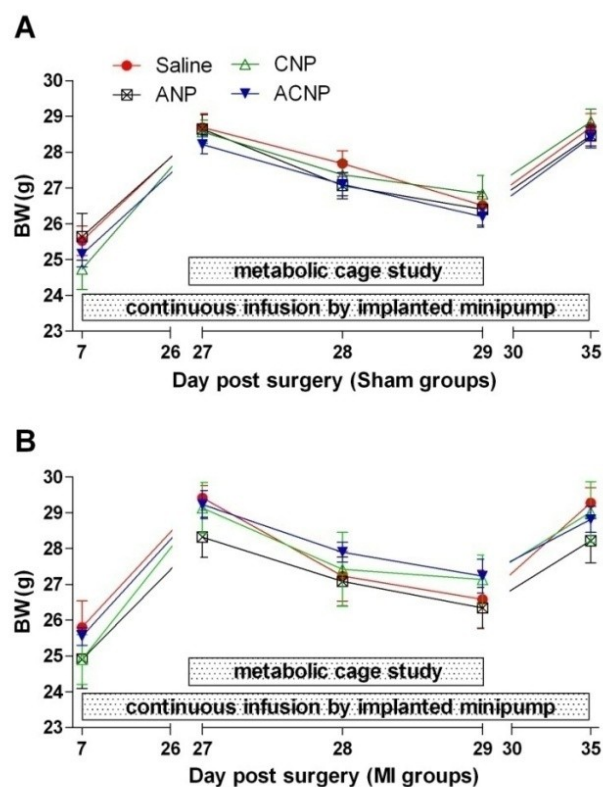
Figure 17. Body weight(BW) changes in sham and MI groups. **(A)** BW changes in sham groups; **(B)** BW changes in MI groups. BW were weighed at Day7, 27, 28, 29, and Day35, respectively.

48

during the period in metabolic cage, BW of mice were increased over time and there were no significant differences within the sham and MI groups at Day 7, 27, 28, 29, and Day 35, indicating that these three NPs had no effect on BW (Figure 17).

After 24 h adaptive time, metabolic cages were cleaned and mice re-entered cages immediately for a second 24 h-monitoring. The 24 h and 48 h urines were collected by the container of the metabolic cage, and UV was calculated (Figure 18). All sham subgroups had a similar UV during 24-48 h except Sham-ACNP group, showing 30% less urine excretion, although not statistically significant. MI-saline group showed a similar urine excretion compared that of sham-saline group, whereas MI-ANP group displayed the minimum UV during the second 24 h period, with nearly one third reduction compared to sham-ANP, although not statistically significant. An identical significantly enhanced urine excretion was observed in both MI-CNP and MI-ACNP groups in comparison to MI-ANP group ($P < 0.05$). Only the MI-ACNP group exhibited more diuresis in comparison to its sham group, with a 40% UV increase compared with that of sham-ACNP group ($P < 0.05$).
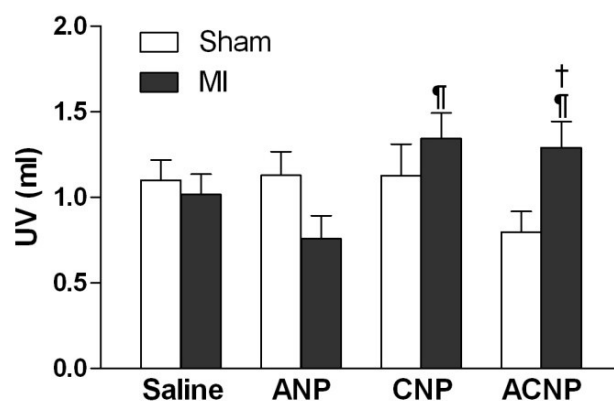
Figure 18. Urine volume (UV) changes in sham and MI groups. UV were calculated at the 24-48 h of metabolic cage study. Data represent the mean ± SEM (n = 6 - 8 per group). [†]$P < 0.05$ *vs.* sham-ACNP; [¶]$P < 0.05$ *vs.* MI-ANP.

2.3.3.3 Organ weights comparison in sham and MI animals

To compare changes in organ mass and to evaluate visceral lesions (e.g. cardiac hypertrophy and pulmonary edema) within the sham and MI groups 5 weeks post surgery, heart (LV and RV, no atrium), wet lung, average of bilateral kidney, and whole spleen weight normalised by tibia length (organ weight/tibia length) were immediately calculated after mice were sacrificed. No differences in tibia growth were seen between the 8 subgroups after 4-week saline or NP infusion (Figure 19A).

49
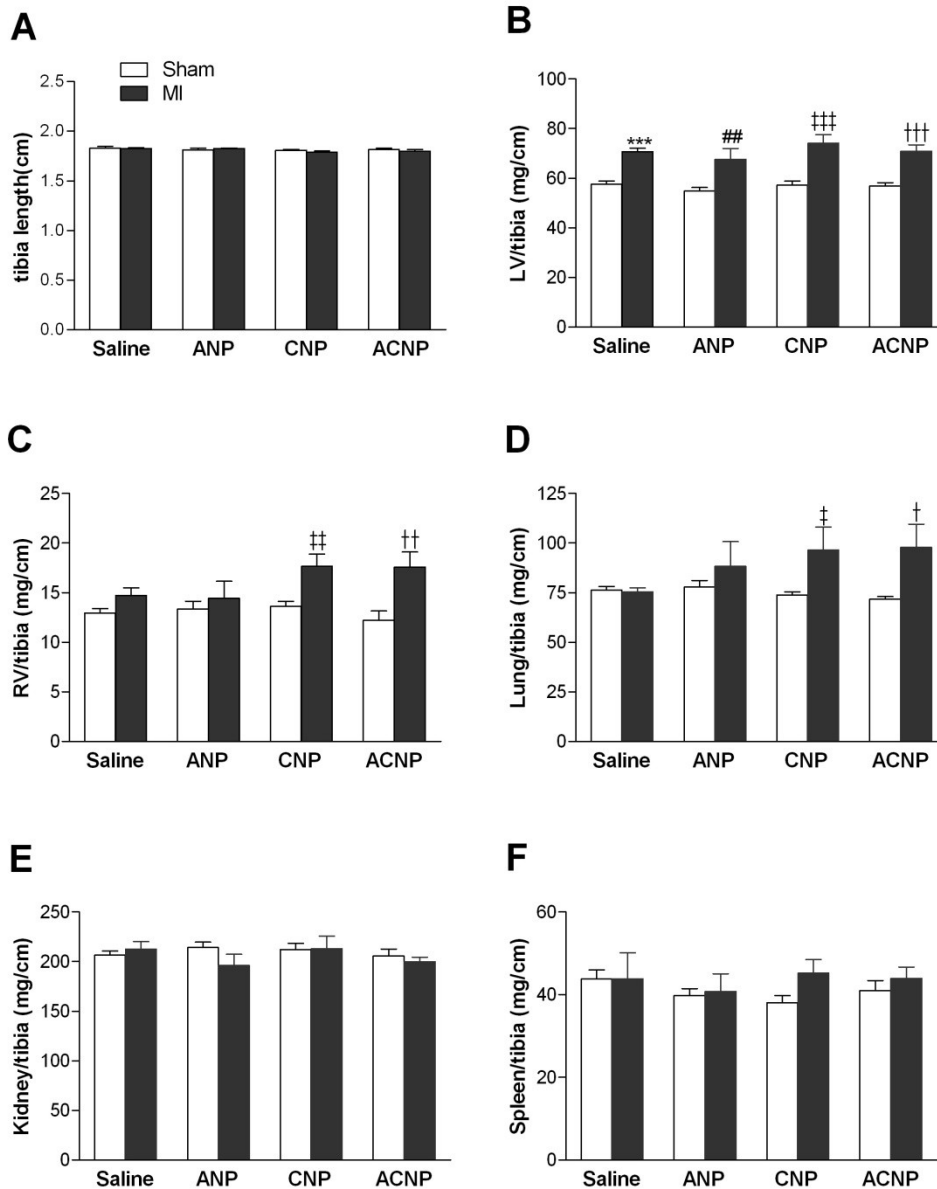
Figure 19. Comparisons of organ mass-to-tibia length in sham and MI groups. **(A)** Tibia length; **(B)** LV mass/tibia length; **(C)** RV mass/tibia length; **(D)** Lung mass/tibia length; **(E)** kidney mass/tibia length; and **(F)** Spleen mass/tibia length. Data represent the mean ± SEM (n = 6 - 8 per group). ***$P < 0.001$ *vs.* sham-saline; ##$P < 0.01$ *vs.* sham-ANP, ‡$P < 0.05$, ‡‡$P < 0.01$, ‡‡‡$P < 0.001$ *vs.* sham-CNP; †$P < 0.05$, ††$P < 0.01$, †††$P < 0.001$ *vs.* sham-ACNP.

However, a clear LV hypertrophy was displayed in all MI groups. The LV weight-to-tibia length ratios in all MI groups were illustrating with no significant differences within MI groups (Figure 19B). RV weight-to-tibia length ratios in MI-saline group slightly increased comparable to the ANP-infused MI mice. By contrast, RV weight in both MI-CNP and MI-ACNP groups were significantly increased compared to their sham-operated peptide groups (Figure 19C). This was congruent with the development of the lung weight, where both MI-CNP and MI-ACNP

50

groups showed a remarkable increase in pulmonary weight (Figure 19D), whereas no significant difference was observed in either saline or ANP groups post MI. However, saline or NP infusion did not change the kidney or spleen weight in either sham or MI groups (Figure 19E&F). These data demonstrate that CNP and ACNP might play negative roles in the development of cardiac hypertrophy and pulmonary edema under MI condition.

2.3.3.4 Cardiac remodelling and function in sham and MI animals

All animals were implanted with osmotic minipumps containing either saline or different NPs at a stable flow rate for 4 weeks, and haemodynamic measurements were performed to evaluate cardiac remodelling and function at the end point (5 weeks post MI). There was no difference in most of cardiac function parameters between peptides in sham groups. Compared to the sham groups, a slight decrease in MAP after MI was found in saline-infused mice, while it was significantly decreased in ANP-infused group. However, it did not differ in CNP- or ACNP-infused mice post MI (Figure 20A). All four MI groups experienced an impaired systolic function, since indices such as LVSP and ejection fraction (EF%) were decreased compared to sham groups, with no significant differences within the MI groups (Figure 20B and Table 3). Elevated LVEDP were seen in all groups subjected to MI except ANP-treated mice, which had a very minor decrease (Figure 20C). This finding was supported by the indices of LV systolic and diastolic function, as peak rate of pressure rise (dP/dt_{max}) (Figure 20E), peak rate of pressure decline (dP/dt_{min}) (Figure 20F), and ventricular isovolumic relaxation time constant (Tau), where ANP attenuated LV dyfunction after MI (Table 3). The P-V loops (Figure 21) obtained from individual sham-operated or infarcted mice further illustrated the improvement in dP/dt_{max} and dP/dt_{min} in ANP-treated animal, five weeks post MI. LV end-systolic and -diastolic pressures/volumes were reduced compared to that of sham animals. Due to dilation of the chamber and a decrease in contractility with time post-MI, a characteristic right-shift in the P-V loops and a decline in amplitude of the pressure signal indicated a greater LV operating volume in saline, CNP, and ACNP infused animals (Figure 21A, C&D), while the MI-ANP group exhibited a minimal right-shift compared with other MI groups (Figure 21B). Moreover, stroke work/stroke volume, cardiac ouput, and Tau indicated better performance in ANP-infused mice post MI (Table 3). Collectively, ANP, but not CNP and ACNP, preserved LV

function post MI. Further, a decreased HR was found in MI-saline group compared to sham-saline (ΔHR-saline: −72.2 ± 10.3 bpm), while no statistical differences was observed in the remaining NP groups (Figure 20D). Of note, LV hypertrophy in MI groups also affected the cardiac dilatation, where clear increases of volume at maximal and minimal pressure were seen in MI mice in comparison to that of sham-operated mice (Table 3).
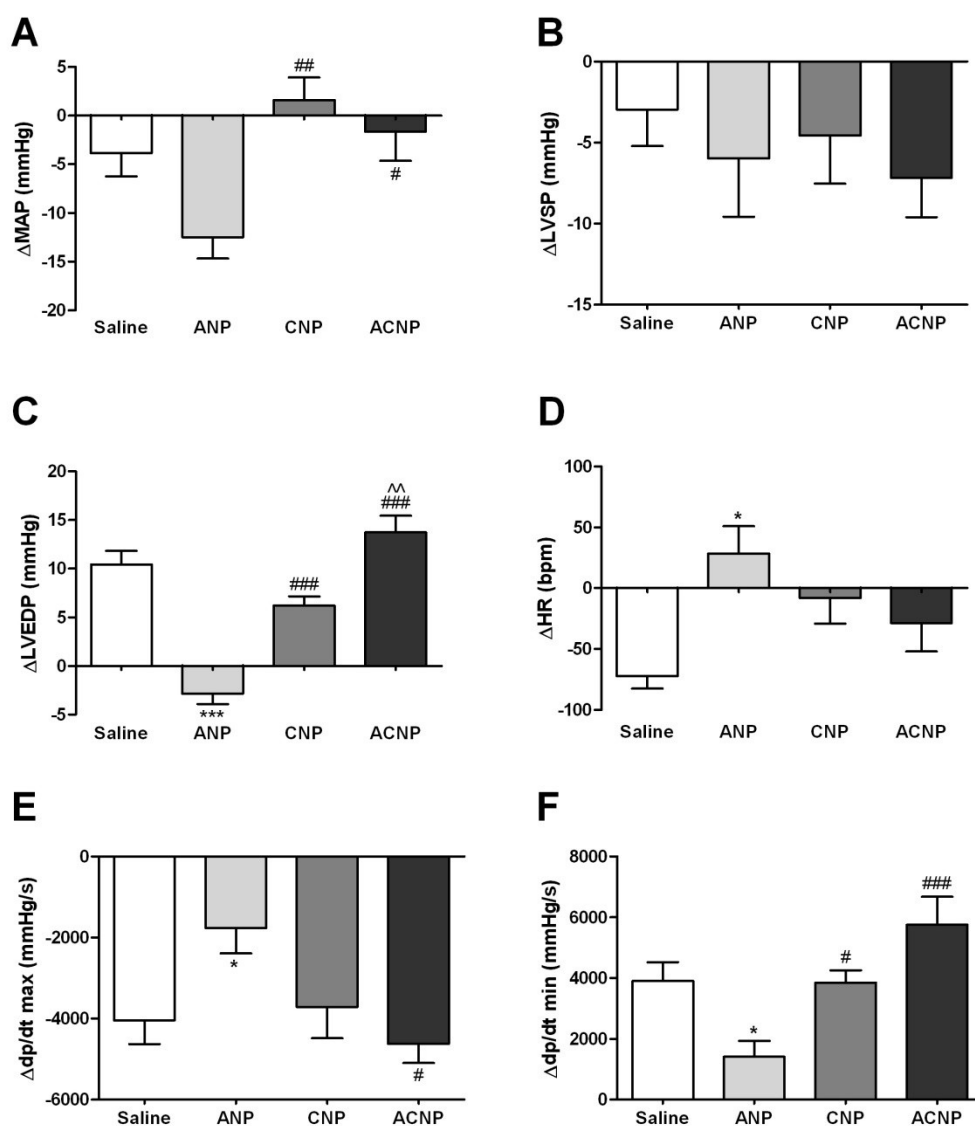
Figure 20. Cardiac function comparisons in sham/MI mice. Effects of NPs or saline on **(A)** Mean arterial pressure; **(B)** Left ventricular systolic pressure; **(C)** Left ventricular end diastolic pressure; **(D)** LV systolic function parameter dP/dt_{max}; **(E)** LV diastolic function parameter dP/dt_{min}; and **(F)** Heart rate. Data represent the mean ± SEM (n = 6 - 8 per group). *$P < 0.05$ *vs.* Saline; #$P < 0.05$, ##$P < 0.01$, ###$P < 0.001$ *vs.* ANP; ^^$P < 0.01$ *vs.* CNP.

Parameters	Sham				MI			
	Saline	ANP	CNP	ACNP	Saline	ANP	CNP	ACNP
SW (mmHg*RVU)	819.1±51.00	732.7±79.51	681.2±48.38	714.6±61.52	413.9±108.5**	537.7±146.5	399.1±86.15‡	411.7±86.71†
CO (RVU/min)	6067±265.0	4901±493.0	4756±393.2*	4972±172.5**	3901±809.6*	4698±973.8	4218±343.6	3855±502.2
SV (RVU)	10.21±0.55	8.82±0.71	8.36±0.59*	8.49±0.42*	6.95±1.25*	8.17±1.57	7.22±0.53	7.02±1.01
Vmax (RVU)	17.65±1.23	17.71±1.47	15.75±1.21	14.38±1.71	22.7±1.89*	23.85±2.23#	24.37±3.59‡	24.06±2.12††
Vmin (RVU)	7.45±1.21	8.89±1.12	7.39±1.07	5.89±1.66	15.75±2.65**	15.68±1.69##	17.15±3.94‡‡	17.03±1.65†††
Ves (RVU)	7.95±1.21	9.56±1.21	7.90±1.16	6.42±1.66	16.72±2.55**	16.62±1.65##	17.86±3.85‡‡	17.92±1.63†††
Ved (RVU)	17.29±1.26	17.20±1.50	15.26±1.18	13.75±1.81	22.47±1.81*	23.51±2.07#	23.84±3.75‡	23.59±2.06††
SBP (mmHg)	91.55±2.53	95.21±2.43	92.04±3.10	91.25±3.07	87.76±4.23	81.73±3.08##	90.58±2.84	86.29±1.81
DBP (mmHg)	65.5±2.47	67.26±2.18	64.33±2.11	61.52±3.05	61.59±4.43	55.30±4.00#^	67.48±2.00	61.53±1.69^
MAP (mmHg)	74.18±2.37	76.57±2.22	73.56±2.31	71.43±2.99	70.31±4.17	64.11±3.60#	75.18±2.19	69.79±1.64
Pmax (mmHg)	98.36±2.02	100.45±3.95	101.89±3.96	97.43±2.26	90.98±5.11	91.02±2.14	88.36±2.24‡	87.66±2.48†
Pmin (mmHg)	0.47±0.73	2.68±0.70*†	3.89±1.30*†	-0.77±0.97	8.25±2.44**	2.46±0.86	7.33±3.40	10.87±2.65†††¶
Pmean (mmHg)	40.41±1.78	45.70±2.72	45.93±2.29†	36.85±3.15	44.91±2.53¶	36.85±1.14	44.19±2.57¶	46.00±2.22†¶
Pdev (mmHg)	95.11±3.27	91.31±3.64	98.00±4.28	98.20±2.16	73.07±11.12*	88.56±2.82	81.02±4.64‡	76.79±3.42†††¶
Pes (mmHg)	90.47±2.48	94.44±3.31	96.12±4.53	89.65±3.28	89.19±5.05	88.22±1.41	86.33±2.19	85.63±2.57
Ped (mmHg)	4.91±1.33	7.99±1.44†	8.17±1.49†	2.78±1.50	13.78±2.91**¶	4.99±0.93	13.45±3.83	17.52±2.25†††¶
HR (bpm)	597.8±8.92	553.4±27.60	565.6±13.49	589.3±21.80	552.84±16.26*	568.52±16.01	582.89±8.32	554.66±14.65
EF (%)	61.88±4.50	51.79±3.31	55.85±4.54	63.82±5.88	34.13±7.34**	35.19±5.37#	33.6±5.91‡	30.13±2.86††
Ea (mmHg/RVU)	9.48±0.71	11.4±0.59	11.94±1.00	10.68±0.40	15.76±2.00*	13.04±3.77	12.24±0.76	13.38±1.58
PowMax (mmHg/s)	14136±2892	10309±2362	10307±1589	10845±1902	14417±3594	10101±1330	7331±1745	11999±1934
dP/dt max (mmHg/s)	10582±557.0	9079±495.5	9339±756.4	10490±527.6	6683±1134**	7318±392.0#	5999±658.0‡	5243±340.2†††¶¶
dP/dt min (mmHg/s)	-9339±547.2	-8195±487.2	-8382±504.6	-9842±826.8	-5383±1156**	-6834±614.0	-4709±614.2‡‡	-4236±311.3†††¶¶
dV/dt max (RVU/s)	517.6±53.04	455.2±38.45	421.5±58.40	421.8±50.17	431.9±89.92	386.8±54.39	486.6±44.71	409.1±36.34
dV/dt min (RVU/s)	-575.2±59.72	-385.9±38.50*	-348.4±29.85**	-433.1±39.39	-420.3±93.24	-553.4±160.0	-433.1±28.66	-310.2±41.58
P@dV/dt min (mmHg)	7.93±3.33	10.43±3.52	9.42±3.87	2.20±2.04	18.48±4.90	7.36±3.91	19.63±13.63	15.35±3.36††
P@dP/dt max (mmHg)	61.17±3.22	63.25±5.87	60.13±2.76	56.17±3.12	64.49±11.83	52.61±2.01	53.56±1.71	51.42±2.57
V@dP/dt max (RVU)	17.04±1.18	17.47±1.44	15.46±1.21	14.05±1.71	21.69±1.95	22.73±1.80	23.28±3.60‡	23.34±2.14††
V@dP/dt min (RVU)	7.76±1.18	9.12±1.11	7.84±1.24	6.06±1.64	16.28±2.60**	16.01±1.62##	17.82±4.45‡	17.32±1.61†††
PVA (mmHg*RVU)	852.8±668.9	213.4±818.3	2121±671.2	2279±638.0	-2043±3085	1326±3041	-390.31±362.2	4163±3151
PE (mmHg*RVU)	33.86±661.3	-519.3±825.7	1457±697.8	1564±627.6	-2457±3048	788.4±2956	-789.5±424.0	3750±3168
CE	0.87±0.26	0.84±0.79	-0.18±0.66	-0.16±0.38*	-0.28±0.31	0.02±0.23	0.27±0.49	-0.42±0.62
Tau (ms)	6.25±0.58	7.99±0.80†	8.01±0.88†	5.02±0.67	13.25±3.93*	7.22±0.79	10.14±1.30	11.44±1.12†††¶

Table 3. Haemodynamic parameters in mice 5 weeks after induction of myocardial infarction or sham operation. SW, stroke work; CO, cardiac output; SV, stroke volume; V_{max}, maximum volume; V_{min}, minimum volume; V_{es}, end-systolic volume; V_{ed}, end-diastolic volume; SBP, systolic blood pressure; DBP, diastolic blood pressure; MAP, mean arterial pressure; P_{max}, maximum pressure; P_{min}, minimum pressure; P_{mean}, mean pressure; P_{dev}, developed pressure; P_{es}, end-systolic pressure; P_{ed}, end-diastolic pressure; HR, heart rate; EF, eject fraction; Ea, arterial elastance (measure of ventricular afterload); PowMax, maximum power; dP/dt_{max}, peak rate of pressure rise; dP/dt_{min}, peak rate of pressure decline; dV/dt_{max}, peak rate of volume rise; dV/dt_{min}, peak rate of volume decline; $P@dV/dt_{max}$, pressure at peak rate of volume rise; $P@dV/dt_{min}$, pressure at peak rate of volume decline; $V@dP/dt_{max}$, volume at peak rate of pressure rise; $V@dP/dt_{min}$, volume at peak rate of pressure decline; PVA, pressure volume area; PE, potential energy; CE, cardiac efficiency; Tau, relaxation time constant (calculated by Glantz method). Data represent the mean ± SEM (n = 6 - 8 per group). $*P < 0.05$, $**P < 0.01$, $***P < 0.001$ $vs.$ sham-saline; $†P < 0.05$, $††P < 0.01$, $†††P < 0.001$ $vs.$ sham-ACNP; $‡P < 0.05$, $‡‡P < 0.01$ $vs.$ sham-CNP; $#P < 0.05$ $vs.$ sham-ANP; $¶P < 0.05$, $¶¶P < 0.01$ $vs.$ MI-ANP; $^P < 0.05$ $vs.$ MI-CNP.
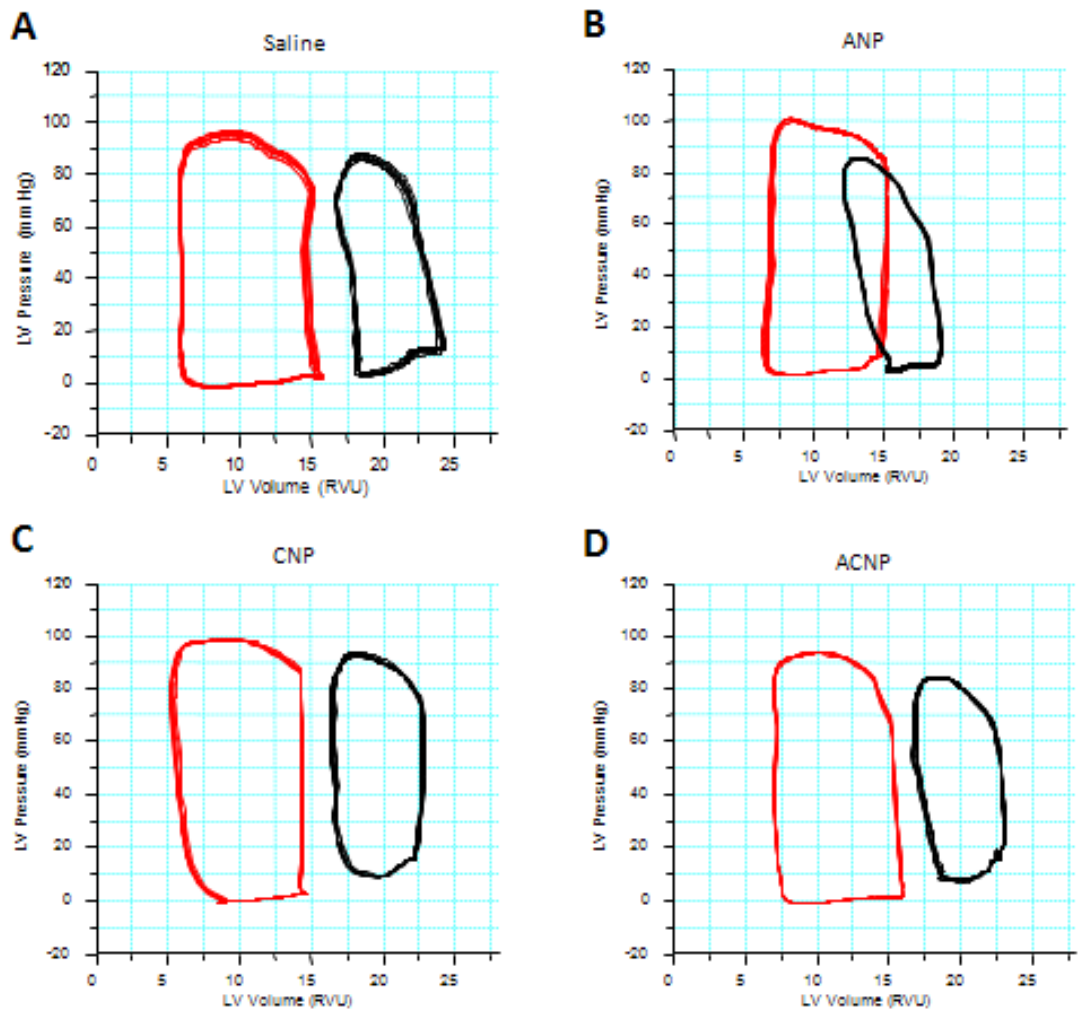
Figure 21. Representative pressure-volume loops from sham and MI mice 5 weeks post cardiac surgery. The red loops denote sham-operated mice, whereas the black loops denote MI mice. **(A)** Saline; **(B)** ANP; **(C)** CNP; **(D)** ACNP. Data represent the mean ± SEM (n = 6 - 8 per group).

2.3.4. Haematological comparison and TNF-α levels in sham/MI animals

To compare haematological parameters within sham and MI groups, EDTA-blood samples taken from individual mice at the end of experiment were immediately analyzed and subjected to haematological analysis. Red blood cell (RBC) counts and platelet (PLT) counts did not differ between sham- and MI-operated mice (Figure 22A and B). Meanwhile, there were also no changes in haemoglobin (HGB) concentrations, hematocrit (HCT) values, and mean corpuscular haemoglobin (MCH) concentrations within sham and MI groups (Appendix 1).
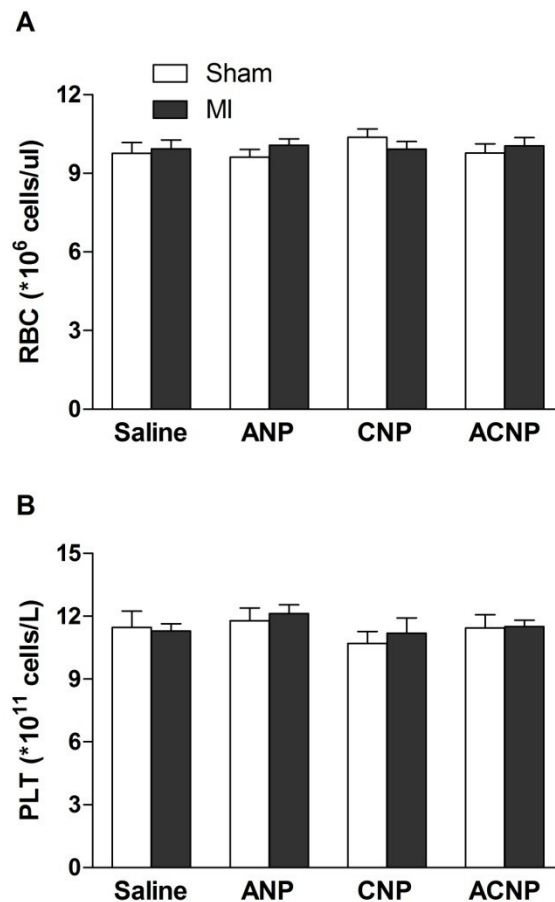
Figure 22. Haematological parameters within sham and MI groups. **(A)** Red blood cells (RBC) counts; **(B)** Platelet (PLT) counts. Data represent the mean ± SEM (n = 6 - 8 per group).

The number of white blood cells (WBC) was not different between all groups under sham conditions, however, it was significantly increased in natriuretic peptide-infused MI animals, except for MI-CNP group (Figure 23A). To find the contributor(s) to the elevated WBC counts, three main sub populations of WBC were further investigated. No significant difference in neutrophils concentration was seen after 4-week NP administration in both sham and MI groups (Figure 23B). In contrast, the major component in mouse WBC, lymphocytes, and the cytophagic factor monocytes exhibited identical quantitative changes compared to that of total WBC (Figure 23C and D).
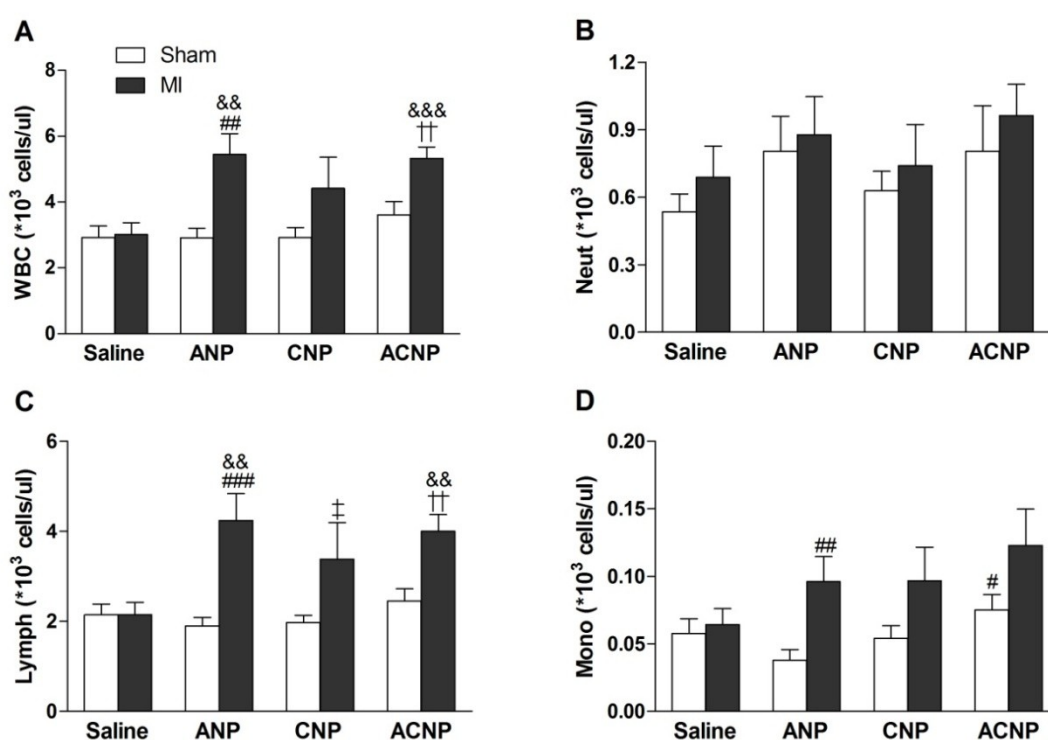
Figure 23. Hematological parameters within sham/MI groups. **(A)** White blood cells (WBC); **(B)** Neutrophils (Neut); **(C)** Lymphocytes (Lymph); **(D)** Monocytes (Mono). Data represent the mean ± SEM (n = 6 - 8 per group). $^{\&\&}P < 0.01$, $^{\&\&\&}P < 0.001$ $vs.$ MI-saline; $^{\#}P < 0.05$, $^{\#\#}P < 0.01$, $^{\#\#\#}P < 0.001$ $vs.$ sham-ANP; $^{\ddagger}P < 0.05$ $vs.$ sham-CNP; $^{\dagger\dagger}P < 0.01$, $^{\dagger\dagger\dagger}P < 0.001$ $vs.$ sham-ACNP.

To further explore whether such NP-induced leukocytosis could stimulate certain cytokine secrection in terms of immune response to e.g. inflammation, the concentration of tumor necrosis factor-alpha (TNF-α) in plasma was measured. No statistically significant differences were seen depending on either NP treatment or MI (Figure 24). Taken together, these results suggest that 4-week exogenous NP

administration may cause changes in WBC counts and differential but this does not lead to secretion of proinflammatory cytokines in sham or MI mice.
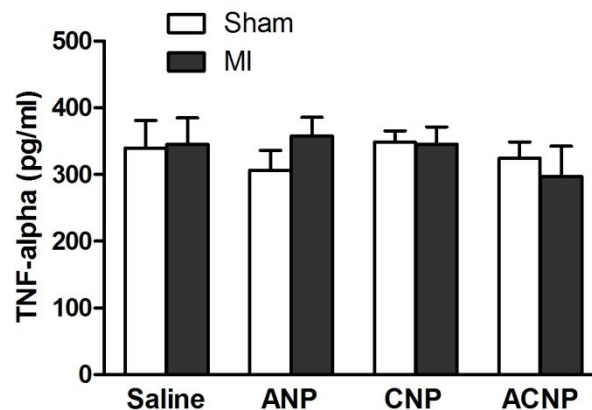
Figure 24. Tumor necrosis factor-α production in sham and MI mouse plasma. Data represent the mean ± SEM (n = 6 - 8 per group).

2.3.5. Plasma cGMP levels and quantification of markers of cardiac failure

Previous data depicted significant increases of heart and LV mass in left coronary artery ligated mice *vs.* sham-operated mice (Figure 19), indicating that MI led to cardiac hypertrophy, regardless of saline infusion or NP infusion. To investigate whether the changes of organ weight in different NP groups would affect the expression levels of cardiorenal biochemical markers, and to check whether the alterations of levels of such markers are dependent on MI and/or NPs, plasma levels of cGMP and mRNA expression levels of mouse BNP and collagen type I were examined, which are associated with cardiac failure and fibrosis, respectively. In sham-operated groups, ACNP slightly increased cGMP, yet not statistically significant. Under MI condition, plasma cGMP level was significantly upregulated in saline group compared to that in sham-saline group, while elevated plasma cGMP levels in comparison to their sham pattern were observed in all MI-NP groups, although not statistically significant (Figure 25A). mRNA levels of cardiac BNP were significantly elevated after MI in all groups without a significant inter-group difference (Figure 25B), while no differences were seen in renal BNP mRNA levels among the groups (Figure 25C). mRNA levels of cardiac collagen type I did not differ between all sham groups, while it exhibited a significant increase post MI,

except for MI-ANP (Figure 25D). Moreover, elevated renal collagen type I mRNA levels were found in all MI groups except for saline group (Figure 25E).
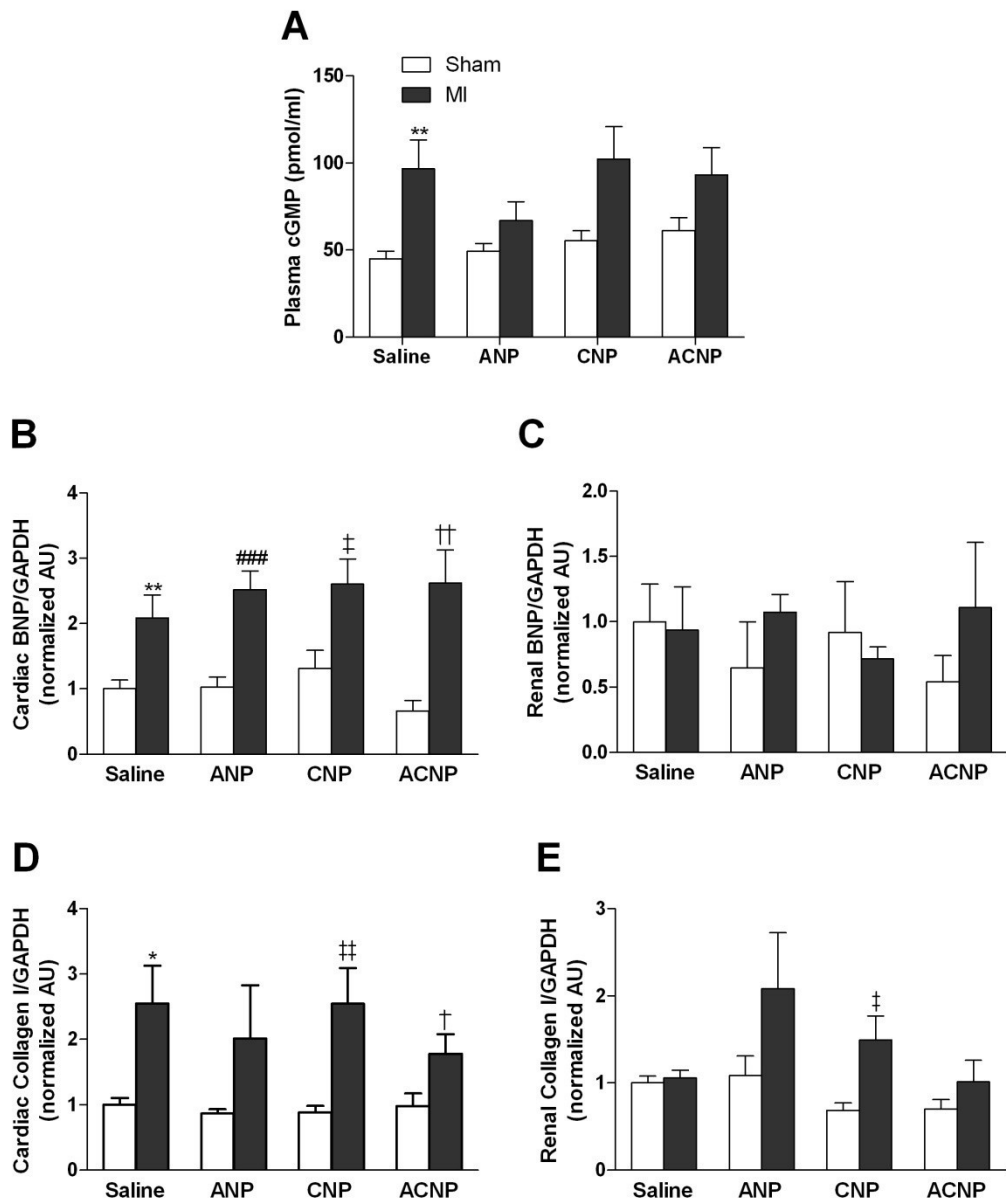
Figure 25. Changes in plasma cGMP levels and real-time PCR quantification of cardiac and renal BNP and collagen type I mRNA in sham and MI mice. **(A)** Comparisons of plasma cGMP levels between sham and MI groups; **(B)** Comparisons of cardiac BNP mRNA level between sham and MI groups; **(C)** Comparisons of renal BNP mRNA level between sham and MI groups; **(D)** Comparisons of cardiac collagen type I mRNA level between sham and MI groups; **(E)** Comparisons of renal collagen type I mRNA level between sham and MI groups. Sham-saline group is normalised as 1.0. Data represent the mean ± SEM (n = 6 - 8 per group). *$P < 0.05$, **$P < 0.01$ $vs.$ sham-saline; ###$P < 0.05$ $vs.$ sham-ANP. ‡$P < 0.05$, ⧣$P < 0.01$ $vs.$ sham-CNP; †$P < 0.05$, ††$P < 0.01$ $vs.$ sham-ACNP.

2.3.6. Degradation profiles of different NPs

ACNP has been identified to be equally potent in stimulating the two independent natriuretic peptide receptors, NPRA and NPRB, and to be thus more efficient in primary cells to stimulate the generation of the protective cGMP under *in vitro* condition. However, *in vivo* study suggested that ANP, but not ACNP, ameliorated the MI-induced LV dysfunction. Hence, to identify the mechanisms which lead to the discrepancy between *in vitro* and *in vivo* data in mice, human ANP, CNP, and ACNP as well as the NEP-resistant human BNP as an internal control were incubated together with recombinant human NEP, a well-known enzyme mediating natriuretic peptide degradation (Pankow and Schwiebs *et al.*, 2009). After 10 min incubation period, nearly no degradation for BNP was detected, whereas 22% of ACNP, 31% of ANP, and 30% of CNP was degraded by NEP (Figure 26A). After 60 min incubation, there was still more than 80% of hBNP remaining, while most of ACNP was degraded by NEP, comparable to the degradation rate of ANP and CNP (Figure 26B).
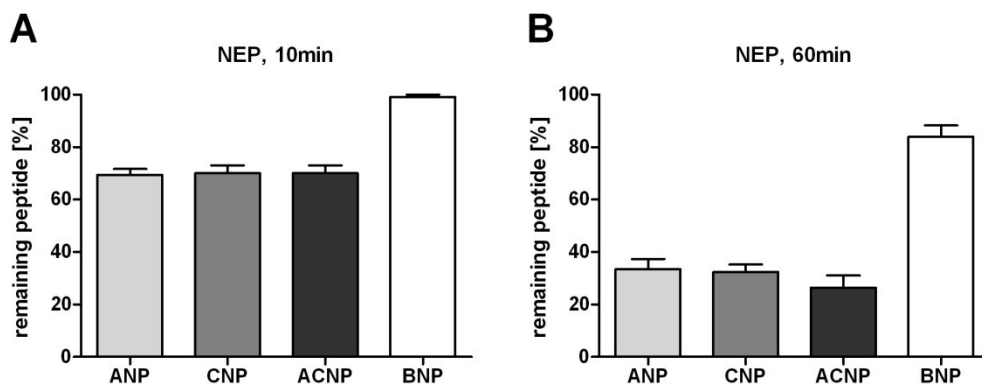
Figure 26. Degradation percentage of natriuretic peptides. **(A)** Remaining NPs after 10 min incubation with NEP; **(B)** Remaining human NPs after 60 min incubation with NEP. Data represent the mean ± SEM (n = 3 per group).

While different degradation rate of NEP are not responsible for the discrepancy between the *in vitro* and *in vivo* data, further analyses were conducted on the degradation of NPs in serum of three different species. In mouse serum, ACNP was degraded faster (43% degraded) compared to ANP (33% degraded) and CNP (8% degraded) after 30 min incubation (Figure 27A). A similar degradation profile for all three natriuretic peptides could be found if incubated with rat serum (Figure 27B). Similar to other sera, in human serum, a 30% degradation of CNP

could be observed, but a significant degradation of both ANP (43% degraded) and ACNP (61% degraded) after 30 min incubation (Figure 27C).
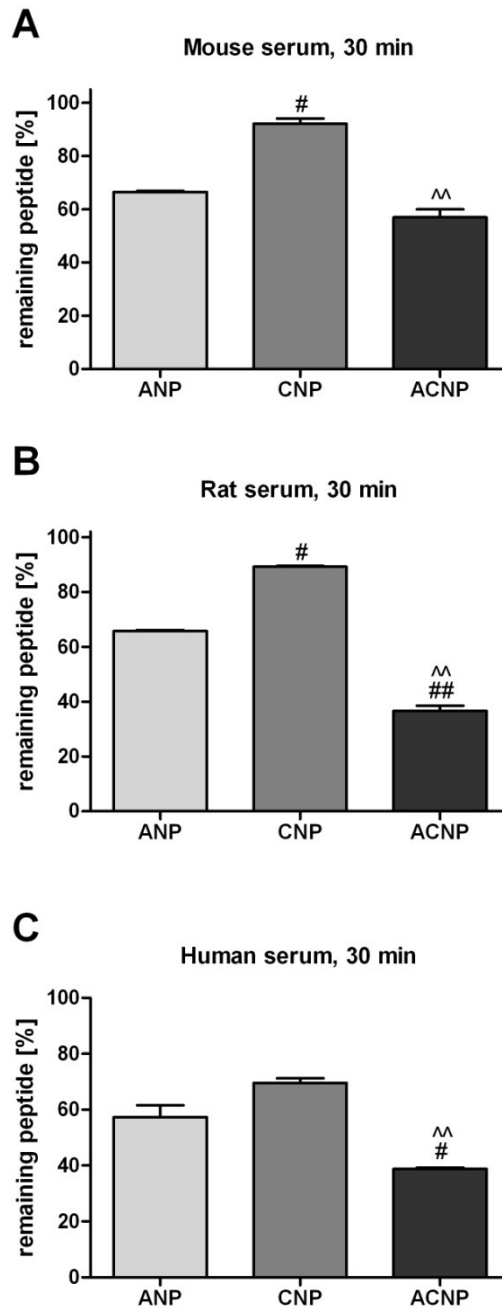
Figure 27. Percentage of degradation of natriuretic peptides. **(A)** Remaining NPs after 30 min incubation with mouse serum; **(B)** Remaining NPs after 30 min incubation with rat serum; and **(C)** Remaining NPs after 30 min incubation with human serum. Data represent the mean ± SEM (n = 3 per group). #$P < 0.05$, ##$P < 0.01$ *vs.* ANP; ^^$P < 0.01$ *vs.* CNP.

To further investigate the stability of ACNP in comparison to ANP and CNP, mouse and rat kidney membrane preparations where many peptidases (e.g. NEP, meprin A, dipeptidyl peptidases, etc.) are highly expressed were used to characterize

their degradation profile. No differences were seen among these three NPs on the degradation rate with mouse kidney membranes (Figure 28), whereby the degradation rate is much faster with rat kidney membranes (Figure 28B) than with mouse preparations (Figure 28A). Interestingly, ANP was fastest degraded on rat kidney membrane
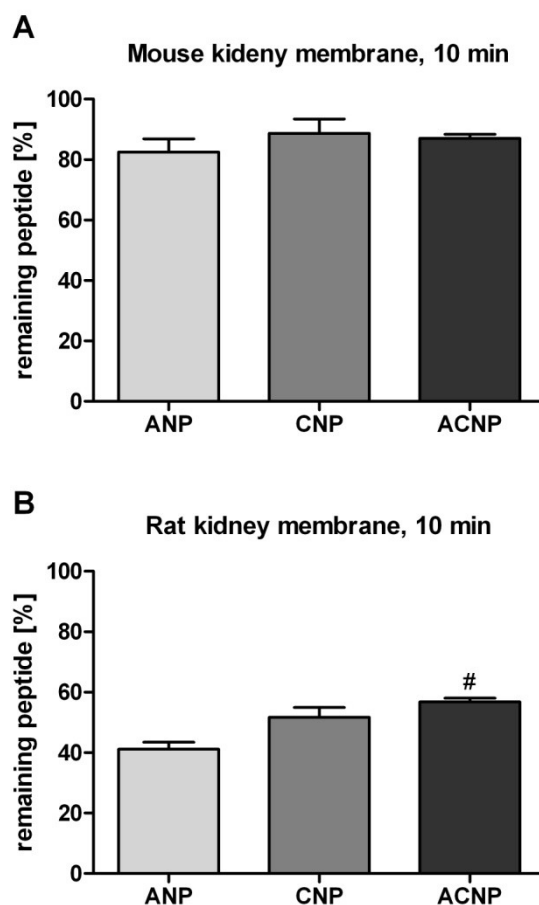
Figure 28. Percentage of degradation of natriuretic peptides. **(A)** Remaining human NPs after 10 min incubation with mouse kidney membrane preparations; **(B)** Remaining human NPs after 10 min incubation with rat kidney membrane preparations. Data represent the mean ± SEM (n = 3 per group). [#]$P < 0.05$ *vs.* ANP.

2.4. Discussion

This study is the first to define the receptor(s) profile of the newly designed ACNP and to compare the potential therapeutic actions of ACNP in a MI model in mice with naturally occuring natriuretic peptides. The cell proliferative, degradative and humoral profiles for ACNP and natural NPs were also characterised. Importantly, ACNP is a ligand for both natriuretic peptide receptors (NPR), the NPRA and NPRB, and consequently more potent in stimulating cGMP in primary cells expressing both receptors in different ratios. In sham-operated mice, 4-week treatment with ACNP exerted similar potency in lowering blood pressure compared to that of ANP or CNP. However, under MI condition, ANP, but not ACNP, ameliorated the myocardial infarction-induced left ventricular dysfunction. The lacking benefit of ACNP might relate to its fast degradation by an unknown enzyme(s) existing in mouse serum as well as in rat or human serum, whereas impairment of cardiac function was less pronounced in MI-ANP group in comparison to other MI groups where a less infarcted size was observed in MI-ANP mice.

Chimeric peptides have been developed to possess favorable therapeutic properties of naturally occurring natriuretic peptides (e.g. to circumvent the hypotensive nature of BNP, to preserve or augment renal function in HF patients). The novel designed CD-NP (Lisy et al., 2008), is a partial agonist of human NPRA and NPRB with a lower potency in mediating cGMP generation than their natural peptides in either NPRA or NPRB overexpressing HEK293 cells. By contrast, the newly designed ACNP, composed of sequences of the ANP arms and the CNP ring (Walther and Schwiebs, 2012), acts as a dual activator of NPRA and NPRB with similar potencies to their endogenous peptides in receptor transfected HEK293 cells. Of note, ACNP has been found more potent to generate intracellular cGMP in various primary cultured cells, as aortic VSMC, kidney MC, and CF, than the native natriuretic peptides ANP and CNP. The enhanced potency of ACNP for NPRA and NPRB compared to CD-NP could be an explanation of ligand binding to NPRA or NPRB hindered by long C-terminus of CD-NP, where the C-terminal fragment was unable to induce a cGMP response in either NPRA or NPRB expressing cells but increased resistance to NEP proteolysis (Dickey and Potter, 2011, Dickey et al., 2008). In addition, it is noticed that ACNP stimulation was less strong in NPRA-

transfected cells and ECs exclusively express NPRA compared to ANP, while it is equipotent as CNP in NPRB-transfected cells. Consequently, a stronger signal of ACNP than of CNP could be seen in MC predominantly expressing NPRB (Suga *et al.*, 1992). Due to parallel expression of NPRA, although minor, ACNP can stimulate both receptors to generate cGMP and thus ACNP-stimulated cGMP is additive to the one of ANP and CNP. This significant increase in efficacy is also confirmed in primary VSMC which express mainly NPRB but NPRA to a higher extent than the MC. The cGMP generation of both receptors mediated by ACNP is additive and makes ACNP the most effective peptide in such cells. It is worth noting that the significant less cGMP generation by ACNP compared to ANP in bovine endothelial cells suggests a species-related difference in bovine-derived NPR/cGMP signalling stimulated by human NPs or chimera, with ANP being less influenced due to a better ligand/receptor filling. Indeed, evidence by Schoenfeld *et al.* suggested that human NPRA is less sensitive than rat or mouse NPRA to cGMP response after agonist stimulation (Schoenfeld *et al.*, 1995). Thus, testing different models/species when evaluating compounds for therapeutic potential is of great importance.

Discrepant observations regarding proliferative/anti-proliferative effect of NPs have been reported and is still of controversy. A dominant view is that NPs exert inhibitory effect towards cell proliferation induced by Ang II, endothelin-1 (ET-1), norepinephrine (NE) and other cell growth factors in many cell types, including CF, VSMC, EC, and MC (Kohno *et al.*, 1993, Morishita *et al.*, 1994, Fujisaki *et al.*, 1995, Calderone *et al.*, 1998). CNP has been shown antiproliferative effect in the absence of CVD (Horio *et al.*, 2003) and in models of acute myocardial ischemia (Hobbs *et al.*, 2004, Soeki *et al.*, 2005), the chimeric CD-NP also suppressed cell proliferation in cultured human fibroblasts (Lisy *et al.*, 2008). In contrast, some have suggested proliferative properties of NPs but mainly focusing on CNP. Khambata *et al.* concluded that CNP facilitates proliferation of human umbilical vein endothelial cells (HUVEC) and inhibits rat aortic SMC growth concentration-dependently in NPRC knockout mice (Khambata *et al.*, 2011). Lenz *et al.* suggested CNP may enhance the proliferation of human osteoblasts (Lenz *et al.*, 2010).

Proliferative studies here have revealed minor differences between ANP, CNP, and ACNP in comparison to non-NP treated controls in VSMC. ANP shows little proliferative/anti-proliferative effect on all three types of cells investigated, whereas

CNP and ACNP present an increased ΔOD compared to control MC and CF at certain incubation time points. The addition of cell growth factors, independent experimental protocols, and NP treatment period may account for the discrepancy from the dominant view. Firstly, different cell growth factors were used in previous studies, whereas no additives were preincubated to the investigated cells except 1x DPBS (control), or 10^{-6} M of NPs. Such discrepancy in cell pretreatment might lead to the different findings regarding the effects of NPs on cell proliferation. Secondly, investigated cells were maintained in DMEM supplemented with 10^{-6} M of NPs and 0.5% FBS, and were subjected to either 12 h-, 24 h-, 36 h-, or 48 h-incubation period prior to 3h-incubation with the cell proliferation reagent WST-1, but in previous studies cells were maintained in serum-free or 1% FBS DMEM for 24-48 h, and the effects of NPs on DNA synthesis of different cells were evaluated by the incorporation of 0.5 μCi/well ^{3}H-thymidin for a further 24 h. Hence, there is no strong evidence supporting that NPs could remarkably potentiate/inhibit cell proliferation in absence of cell growth factors. Further experiments testing the inhibition/promotion of cell proliferation by NPs should be performed in presence and absence of certain cell growth factors.

Novel designed peptides have been shown many favourable effects *in vitro* and *in vivo*. A less but still clear hypotensive effect was observed upon the infusion of CD-NP in dogs (Lisy *et al.*, 2008), while the non-vasodilatating CU-NP was able to reduce cardiomyocyte hypertrophy induced by hypertrophic stimuli, e.g. phenylephrine, angiotensin II, and endothelin-1 (Kilic *et al.*, 2010). Chen *et al.* have implicated that natriuretic and diuretic potencies of ACNP are higher than that of ANP and CNP in normal rat models, while it has a similar vasorelaxing effect in isolated rat abdominal aorta (Chen *et al.*, 2011). Thus, such findings together with our promising *in vitro* data led to the suggestion that administration of ACNP may exert a better cardioprotective effect in the settings of CVD, such as MI and chronic HF. This chapter is the first to assess how ACNP affects cardiorenal function, in both sham- and MI-mice.

Cardiac remodelling after the onset of MI is accompanied by structural changes in the LV, such as chamber dilatation, wall thinning in the infarcted region, and hypertrophy in the viable region. These findings agree with previous reports in mouse and rat models of MI (Pfeffer *et al.*, 1991, Patten *et al.*, 1998, Lutgens *et al.*,

1999). It has been suggested that infarct size was highly correlated with cardiac systolic dysfunction (Takagawa *et al.*, 2007). Indeed, mice with an infarcted size of < 25% (such mice did not count as MI/sham mice) have shown little difference in haemodynamic parameters compared to sham-operated mice in present study, while all MI mice experienced impaired cardiac function with remarkable reductions of pressure-volume parameters (e.g. SW, SV, CO, EF%, and peak dP/dt) and increases of other load-dependent/independent parameters (e.g. V_{es}, V_{ed}, peak V@dP/dt, and Tau), which agree with previous studies of varying models (Wang *et al.*, 2007, Shioura *et al.*, 2007, Pokreisz *et al.*, 2009). Of note, infusion of ANP, but not CNP or ACNP, has exhibited a less biased PV loop and thus less pronounced impairment in the haemodynamic parameters tested in comparison to that of MI-saline group. The mechanism of such cardiac-protective properties observed in MI-ANP group could be multifactorial. First, infusion of ANP has been shown to elicit protective effects against ischaemia/reperfusion (I/R) in isolated rat hearts (Okawa *et al.*, 2003), while such beneficial effect on I/R injury was absent using cardiomyocyte-restricted over-expression of CNP (Wang *et al.*, 2007). *In vitro* data suggest that ANP is more efficient to stimulate cGMP compared to equimolar CNP or ACNP in NPRA-transfected cells, hence, it can be speculated that infusion of ANP could induce a better ventricular performance and reduce the load on heart possibly via NPRA/cGMP related vasodilatation. Secondly, ANP in the circulation is derived primarily from myocardium, whereas CNP is mainly derived from endothelial cells and the central nervous system. When cardiac remodelling occurs induced by e.g. MI and HF, endogenous ANP would be dramatically secreted in an autocrine manner in response to the increased afterload, which makes an additive benefit besides subcutaneous absorption of the NPs by local capillaries. Third, a less average of infarcted size was obtained in MI-ANP (33.4%) and MI-saline (32.7%) groups in comparison to that of MI-CNP (38.9%) and MI-ACNP (39.0%) groups. This discrepancy in infarcted size could be attribute to the different effect of saline and three NPs on myofibroblast and endothelial cell proliferation during murine myocardial infarct repair (Virag and Murry, 2003), where CNP and ACNP may have a stronger anti-proliferative effect on such cells. As a result, MI-ANP group favours a less pronounced impairment in LV function, but not for MI-saline group, presumably due to no beneficial cGMP generated by saline.

NPRB is suggested being involved in preventing cardiac hypertrophy in heart failure (Langenickel *et al.*, 2006). *In vivo* administration of CNP via osmotic minipumps ameliorated cardiac hypertrophy and significantly improved cardiac function in rats 2 weeks post MI (Soeki *et al.*, 2005). Such anti-hypertropic effect was also comfirmed by Wang *et al.* in MI mice with cardiomyocyte-restricted over-expressing of CNP. In present chapter, however, neither saline nor NP administration via osmotic minipumps attenuate MI-induced LV hypertrophy. Species-specific differences, independent approaches of NP delivery, and unequal MI duration may account for this discrepancy. As in the study by Wang *et al.*, CNP originated from the cardiomyocytes in transgenic mice were used and thus acted in an autocrine way; Soeki *et al.* (2005) applied CNP by minipump intravenously to MI rat model for 2 weeks, however, in current chapter, NPs were given via 4-week minipump infusion that resulted in a slow systemic administration, thereby exposing the myocardium to a much lower concentration and consequently a less anti-hypertrophic effect. Interestingly, RV hypertrophy accompanied by elevated lung mass was prevented in MI-ANP and MI-saline groups but still presented in MI-CNP and MI-ACNP groups. A possible explanation could be that MI-induced LV dysfunction causes elevated LVEDP, in some severe cases (i.e. larger infarcted size observed in MI-CNP and MI-ACNP groups) lung edema could be seen which might lead to anomalous pulmonary venous return and thus elevated pulmonary arterial pressure, and eventually, causing RV hypertrophy. In addition, it has been evidenced that CNP acts as a local endogenous inhibitor of vascular ACE activity in the human forearm resistance vessels (Davidson *et al.*, 1996), recently our unpublished data suggest that increased CNP level in circulation may stimulate Ang II effect, both implicating that CNP may exhibit detrimental effect post MI via activating ACE/AngII axis.

Although the cardiac function was not preserved in ACNP-infused mice 5 weeks post MI, diuretic effect was enhanced in ACNP-MI group, whereas a significant less urine flow was seen in MI-ANP group compared to that of MI-CNP and MI-ACNP groups. This agrees with the finding by Chen *et al.* that ACNP was more potently natriuretic and diuretic after intravenous injection (Chen *et al.*, 2011). However, CNP retained an unexcepted diuresis, as CNP is thought to lack renal action in healthy human (Clavell *et al.*, 1993, La Villa *et al.*, 1998). This

66

contradiction may be related to pathological circumstance (e.g. MI) in present study, it is possible that a less degraded level of CNP osmosed through renal capillary decreases local blood pressure, thus enhances renal blood flow and diuresis. However, this is speculative and would require additional studies to confirm.

Furthermore, MI induced a clear increase in plasma cGMP levels, but the increase was to a less extent in MI-ANP mice compared to other MI groups, implicating that plasma cGMP elevation is more depending on MI than on NP infusion. The less increase in plasma cGMP in MI-ANP group could be an explanation of less infarcted size observed in MI-ANP mice led to less severity of LV dysfunction as mentioned above. Although current experiments do not allow the identification of the mechanisms responsible for this increased cGMP level induced by MI, which may be related to the induction of cardiac NO synthesis after MI. Another possibility is that increased cGMP levels may inhibit cAMP hydrolysis, augmenting LV cAMP levels and contractile function after MI and thereby limiting the stimulus to adverse LV remodelling. Moreover, HF markers such as cardiac BNP and collagen type I mRNA levels were all evelated post MI, regardless of NP or saline infusion, while renal BNP and collagen type I mRNA levels did not differ between the sham and MI groups, except for increased collagen type I mRNA level in MI-CNP group. These findings confirm that augmented level of cardiac functional markers (BNP gene expression, collagen type I gene expression) are associated with MI (Goetze et al., 2003), while suggesting that increased level of cardiac fibrosis indicator (collagen type I mRNA) is more related to MI than NP infusion. It is worth noting that, haematological studies demonstrated elevated WBC counts in NP groups but not saline group post MI. A further check in three main cell types in WBC (Neut, Lymph, and Mono counts) suggested an increased activity of immune system against MI and/or NP infusion, which also could predict coronary artery disease (e.g. MI) risk (Horne et al., 2005). Of note, such leukocytosis might also partly attribute to anesthesia described before (Kress and Eberlein, 1992). Indiscriminate plasma TNF-α concentration among all the groups suggested that such NP-induced leukocytosis did not stimulate certain cytokine secrection in terms of immune response to e.g. inflammation, although extensive cardiomyocyte necrosis was found after coronary artery occlusion (Frangogiannis et al., 2002). Taken together, these results suggest that 4-week exogenous NP administration may

cause changes in WBC counts and differential but this does not lead to secretion of proinflammatory cytokines in sham or MI mice.

Previous studies demonstrated at least *in vitro,* that NEP could efficiently degrade ANP and CNP (Brandt *et al.*, 1997, Kenny *et al.*, 1993), whilst BNP was resistant to be degraded by NEP, implicating the existence of NEP-independent peptidase(s) in the degradation process of BNP (Walther *et al.*, 2004a, Walther *et al.*, 2004b). Later, our group discovered the necessity of BNP truncation to make it accessible for NEP degradation, whereby the first peptidase we identified to initiate such truncation was the metallopeptidase meprin A (Pankow *et al.*, 2007). Due to ACNP is a hybrid of ANP and CNP, it might not be surprising that it is also an excellent substrate for NEP, and thus can be easily inactivated by NEP due to the opening of the ring structure. However, since more peptidases than NEP are able to degrade NPs, the stability of ACNP in serum was also investigated in comparison to its two parent NPs, ANP and CNP. In all three investigated species, CNP was most stable, while ACNP was fastest degraded. This finding could be a perfect explainanation for the failure of ACNP to ameliorate the MI-induced LV dysfunction *in vivo*, although the ability of ACNP to activate both NPRA and NPRB may prove doubly beneficial in regards to inhibiting cardiac remodelling. One speculation is that the cleavage site targeted by the responsible peptidase(s) in the serum may locate differently in ANP and CNP (e.g. cleavage site on the arms for ANP while in the ring loop for CNP), where the responsible peptidase(s) has lower accessibility to CNP than to ANP due to their spatial structure differences. Given the above speculation, ACNP therefore would have two recognition sites (both on the arm and in the ring loop) in one molecule and thus it could be easier to be captured by the peptidase(s). Moreover, the length of the N- and C-terminus of a NP was suggested as a potential determinant for the degradation rate of the NP by NEP, since longer N- and C-terminal extensions may cause spatial clashes and impede the correct orientation of the NP within the cave of NEP, leading to the inability of NEP to hydrolyse the target site in the ring structure (Pankow *et al.*, 2009). Indeed, it has been shown that DNP with the long 15-AA C-terminus is also highly resistant to NEP proteolysis (Dickey and Potter, 2011). Consequently, such finding is of great importance when evaluating ACNP as a potential new treatment option for CVD. Since ACNP is less stable than the endogenous NPs, it might fail to be more

effective than ANP and/or CNP, although it is more potent in generating cGMP and has a very promising receptor profile. Hence, studies should be performed to identify amino acid substitutions in ACNP ensuring higher stability of ACNP in blood, but preserving its properties. Although approaches like elongating C-terminus of the NPs/chimeric NPs may extend their half-life, the tailing may also lead to poorer cGMP generation. Further investigation regarding the responsible peptidase(s) for ACNP degradation in the serum is urgently required.

In conclusion, the present chapter demonstrates that the novel chimeric natriuretic peptide ACNP could be a promising therapeutic agent as it stimulates both NPRA and NPRB. Further investigations on peptide stability and on specific proteases being responsible for the proteolysis of the ACNP, and the development of inhibitors of such protease(s) or structural modification of ACNP may help to increase the half-life time of ACNP-based drugs, selectively and efficiently stimulating the protective cardiorenal effects of ACNP. Though many limitations ahead, such worthwhile attempt will open the avenue for the design of novel peptidic agonists acting on both beneficial axes of the natriuretic peptide system.

Chapter III

The mechanism and biological consequences of the interaction between NPRA and NPRB

Chapter 3

The mechanism and biological consequences of the interaction between NPRA and NPRB

3.1. Introduction

CVD are one of the leading causes of death in developed countries (cited from: http://apps.who.int/ghodata/?vid=10012). Unfortunately, rare explanation could thoroughly elaborate the underlying pathogenesis. The NPS plays a pivotal role in the regulation of cardiorenal homeostasis as well as in the pathogenesis of CVD (Levin *et al.*, 1998). Two homologous membrane-bound receptor subtypes, natriuretic peptide receptor A and B (NPRA and NPRB) generate the second messenger cGMP upon binding of the NPs (Potter *et al.*, 2006). The third member of NPR family, NPRC, has been regarded as a clearance receptor involving the receptor internalisation and degradation (Matsukawa *et al.*, 1999). Under certain pathological circumstances, NPRs undergo either homologous desensitisation (via NP binding) or heterologous desensitisation (inhibiting NPRs/cGMP generation via activator of PKC, e.g. phorbol 12-myristate 13-acetate) leading to unresponsive receptor to hormonal stimulation (Jaiswal, 1992, Potter and Garbers, 1992, Potter and Garbers, 1994, Potter, 1998). The inhibited signal transduction in NPs/NPRs/cGMP axis leads to the failure in counteracting its antagonising axes, as ACE/Ang II/AT1 receptor axis of the renin angiotensin system.

Crystal structural studies suggest that natriuretic peptide receptors exist as homodimers. ANP and BNP preferentially bind to NPRA while CNP selectively binds to NPRB in a 1:2 ligand:receptor stoichiometry (Potter *et al.*, 2009). As shown in Chapter 2, the designed natriuretic peptide ACNP acts as a potent dual activator of both NPRA and NPRB with an equal potency as the endogenous ligands in mediating cGMP generation. Of note, it is widely regarded that most of functions and effects of ANP & BNP/NPRA and CNP/NPRB complexes are exerted through activating the intracellular guanylyl cyclase domains and consequently the bioactive second messenger, cGMP (Kuhn, 2003, Potter, 2005). However, many CVD patients have shown elevated plasma NP levels but blunted cGMP formation and endocrine effects of endogenous/exogenous NP. A large randomized trial with recombinant BNP (nesiritide) also suggested that BNP fails to reduce mortality or

71

rehospitalisation in heart failure patients (O'Connor *et al.*, 2011). More recently, our unpublished data revealed an inhibited cGMP generation upon NP stimulation in human NPRA and rat/mouse NPRB double-transfected cells (Appendix 4), implicating such unanticipated consequence may involve the cross-talk between NPRA and NPRB in the context of CVD, e.g. desensitisation/internalisation, heterodimerisation, or altered proportion of NPRs, under pathophysiological conditions.

However, there was still a significant lack in information regarding the mechanisms of interaction between NPRA and NPRB. Such understanding could be also beneficial as the basis for pathogenetic explanations in CVD patients. The hypotheses of the studies in this chapter were: 1) Down-regulated natriuretic peptide receptor expression on transcriptional or translational levels leads to lower NP-mediated cGMP generation; or transcription or translation of NPRs are not influenced, but less NPRs are in the membrane; 2) Physical interaction between NPRA and NPRB by forming a NPRA/NPRB heterodimer leads to comformational changes of the receptors, and thus prevents NPs binding to their specific domain or inhibits the activation of guanylyl cyclase domain leading to less/no cGMP generation.

3.2. Materials and methods

3.2.1. Materials and reagents

Juvenile FVBN and C57/Bl6 mice (6- to 8-week old) were supplied by Charles River (Margate, Kent, UK), and further bred in the animal facility of the University of Hull according to the Animals (Scientific Procedures) Act 1986, UK. Primers were purchased from either Invitrogen (Paisley, UK) or Qiagen (Crawley, UK). small interfering RNA against NPRA and NPRB (siRNA-NPRA and siRNA-NPRB), QIAprep Spin Miniprep Kit, Plasmid Maxi Kit, Polyfect transfection reagent, Hiperfect transfection reagent, QuantiTect SYBR Green RT-PCR Kit were all bought from Qiagen (Crawley, UK). The rapid DNA ligation kit and competent *E.coli* were supplied by Promega (Southampton, UK). All natriuretic peptides were synthesized by Biosyntan GmbH (Berlin-Buch, Germany) and had a purity of approximately 95%. Double distilled water (ddH2O) was used as solvent for the powders at varying dilution. The peptide solution was further analyzed by HPLC and mass spectrometry before used for experiments. The expression vectors harbouring recombinant human NPRA cDNA (Genbank accession No. NM_000906.1) and mouse NPRB cDNA (Genbank accession No. BC042470.1) were purchased from OriGene Technologies Inc. (Rockville, MD, USA). Human NPRA-eYFP (Genbank accession No. NM_000906.1) and NPRB-eCFP (Genbank accession No. NM_003995.3) constructs were bought from GeneCopoeia (Rockville, MD). Biometra Standard Power Pack P25 was purchased as the low voltage power supply for electrophoresis and blotting (Biometra GmbH, Goettingen, Germany). The LivingColor® GFP polyclonal antibodies were obtained from ClonTech (Saint-Germain-en-Laye, France). The anti-calreticulin antibody (Cat. No. ab2907) was obtained from Abcam (Cambridge, UK). Goat anti-rabbit IgG-HRP were bought from Santa Cruz (Heidelberg, Germany). The cGMP kit was purchased from Enzo life sciences (Exeter, UK). Random primers, Lipofectamine 2000 transfection reagent, the mammalian expression vector pcDNA3.1(-), penicillin/streptomycin, FBS, sodium pyruvate were all bought from Life Technologies (Paisley, UK). All restriction enzymes and their respective buffers were obtained from either Roche (Welwyn Garden City, UK) or New England Biolabs (Hitchin, UK). DMEM, RPMI1640 were from PAA laboratories (Somerset, UK). All other chemicals and reagents were mentioned where appropriate.

3.2.2. Plasmid construction

3.2.2.1 Mouse lung isolation

Juvenile, male C57/Bl6 mice were killed by dislocation of the neck in accordance with The Animals (scientific procedures) act 1986. An incision was made longitudinally down the front of the animal, then opened the thoracic cavity by scissoring diaphragm and part of ribs, carefully cut out lung tissue, and immediately went to '3.2.2.2 mRNA extraction', or stored the tissue in liquid nitrogen (LN).

3.2.2.2 mRNA extraction

Freshly isolated or LN-reserved lung tissue were immediately placed into a 15 ml Falcon tube containing 1.5 ml Trizol, homogenized at highest speed for 1 min under ice-incubated condition to maintain RNA stability. After that, the homogenate was taken to room temperature (RT) for 10 min, then transferred to a 1.5 ml Eppendorf tube containing 0.3 ml chloroform and subsequently vortexed vigorously, and incubated at RT for 2 to 3 min. The tube was then centrifuged at 4 °C, 10,000 rpm for 30 min, the supernatant was transferred to a new tube mixed with 0.5 ml isopropanol, incubated at RT for 10 min. A second centrifuge step was carried out at 4 °C, 12,000 rpm for 10 min, then discarded the supernatant, washed the pellet with 1.5 ml 70% ethanol. A final centrifugation was performed at 4 °C, 7500 rpm for 8 min, then discarded ethanol and inverted the tube on fluff out tissue for 15 to 20 min to dry the pellet. The eluted RNA was dissolved in 100 µl diethylpyrocarbonate (DEPC)-treated water, mixed at 55 °C for 10 to 15 min in the thermomixer (500 rpm). Recovered mRNA was then quantified using a spectrophotometer and stored at -80 °C until use.

3.2.2.3 Reverse transcription

Messenger RNA was reverse transcribed into stable cDNA by M-MLV reverse transcriptase (M-MLV RT). The reverse transcription reaction comprised of 4 µg of mRNA, 0.5 mM dNTP mix, 1.8 nM of random primer oligonucleotides, 0.01 M DTT, 10 U of Moloney Murine Reverse Transcriptase and 5x First-Strand Buffer from the Invitrogen M-MLV RT kit to a total volume of 20 µl. To remove RNA complementary to the cDNA, 1 µl (2 U) of *E. coli* RNase H was added into the cDNA solution and incubated at 37 °C for 20 min. The reaction was performed as

74

described in Table 4, and cDNA was subsequently stored at -20 °C. The thermal cycler (Eppendorf Mastercycler® gradient) was programmed to run the following cycles:

Process	Temperature (°C)	Time (Minutes)
Enzyme Activation	37°C (before adding reverse transcriptase)	2
	25°C (after 1µl reverse transcriptase)	10
Annealing and Extension	37°C	50
Enzyme Inactivation	70°C	15

Table 4. Reverse transcription PCR cycles.

3.2.2.4 Amplification of mouse NPRA cDNA and TA ligation

Mouse NPRA (mNPRA) cDNA possesses an open reading frame (ORF) of 3,174 nucleotides (accession number NM_008727.5). Primers were designed to amplify the product in two separate but overlapping fragments (Table 5 and Figure 29). Primer mNPRA51 was designed prior to the start codon of the mNPRA sequence, while primer mNPRA31 included the stop codon (TGA) to allow positional cloning. Another pair of primers (mNPRA52 and mNPRA32) was used containing a *Nde I* restriction site (CATATG) in between to allow two fragments' position specific ligation.

Fragment	Primers' name	Sequence	Annealing Temperature (°C)
mNPRA 1st half	mNPRA 51	CCGTCGCTGCGCTCGCTGAGGCC	58
	mNPRA 32	GCAGAATGAGCACTTGACCAG	
mNPRA 2nd half	mNPRA 52	CAAGACAGCATACTATAAGGGC	57
	mNPRA 31	GCAGCACTCGAGGCTTGACCTAC	

Table 5. Primer details and conditions of mNPRA PCR. The stop codon was underlined.

Expand Long Template (ELT) PCR (Roche) was used with the aim to efficiently amplify the fragments. Each PCR was performed in an Eppendorf Mastercycler® gradient with 5 µl 10x PCR buffer with $MgCl_2$, 2 µl cDNA, 0.3 µmol of each primer, 0.35 mM dNTP, and 0.75 µl ELT enzyme mix in a 50 µl reaction volume. Specific PCR conditions for each product are given in Table 6. The PCR thermal cycler was programmed to run the following cycles:

	Temperature	Time	Cycles
Initial denaturation	94°C	2min	1
Denaturation	94°C	10s	10
Annealing	55°C	30s	
Elongation	68°C	1min12s	
Denaturation	94°C	15s	20
Annealing	55°C	30s	
Elongation	68°C	1min12s+20s cycle elongation for each successive cycle	
Final elongation	68°C	7min	1
Cooling	4°C	Unlimited time	

Table 6. Extended long template PCR cycles.

Once the two fragments (1st half and 2nd half of mNPRA cDNA) had been generated and gel purified, rapid ligation was performed respectively to ligate the 1st of mNPRA cDNA fragment and 2nd half into pGEM® T-Easy vector, before conducting a final ligation procedure to link 1st half with 2nd half (the whole open reading frame of mNPRA). The recombinant T-easy constructs were enzyme digested (*Acc I*, *EcoR I* and *Nde I*) and sequenced to identify mutants and inserts orientation. The ligation products, were subsequently gel purified before undergoing restriction digest and then ligation into vector pcDNA3.1(-).

Figure 29. Diagramatic representation of the ORF of mNPRA, showing the primer and restriction enzyme positions within the sequence.

3.2.2.5 Restriction digest of vectors and dephosphorylation of pcDNA3.1(-)

The vector pcDNA3.1(-) was digested with *Not I* and dephosphorylated in order to linearise the vector and reveal the *Not I* cohesive ends for 1st half and 2nd half mNPRA. Meanwhile, the pGEM® T-easy vectors with correct inserts were digested by the restriction enzymes *Not I* and *Nde I* respectively, to be ligated later with the dephosphorylated pcDNA3.1(-). *Not I* and *Nde I* exhibit optimum activity at same temperature. Therefore in a total volume of 20 µl, 5 µl of each T-easy vector was separately incubated with 5 U of *Not I* and *Nde I* for 1 h at 37 °C in a reaction mixture containing 10x Roche Buffer H, and DNase/RNase free water. Same procedure was performed for pcDNA3.1(-) except using *Not I* restriction enzyme only. Following the incubation, digested pcDNA3.1(-) was gel purified once and dephosphorylated by 2 U Alkaline Phosphatase (Calf Intestinal Phosphatase, CIP) in NEB buffer 4. The total reaction was incubated at 37 °C for another 1 h. The digested fragments from T-easy vectors and dephosphorylated product were then gel purified to remove the unwanted, cleaved portion of DNA, dissolved in DNase/RNase free water and stored at -20 °C.

3.2.2.6 Ligation of 1st and 2nd fragments into pcDNA3.1(-)

Both two fragments were mixed together into one ligation. The ligation reaction contained 2 µl of 10x ligation buffer, 6 µl of each linearised fragment from T-easy vector, 5 µl of dephosphorylated pcDNA3.1(-), and 1 µl of T4 ligase to have a final volume of 20 µl. The reaction was incubated at RT for 1 h. As negative control, an identical reaction was set up with 12 µl of DNase/RNase free water in place of the inserts, 1st and 2nd mNPRA. A second gel purification was applied, the product was dissolved in DNase/RNase free water and enzyme digested to identify insert orientation, finally stored at -20 °C.

3.2.2.7 Amplification of human NPRB cDNA

Human NPRB (hNPRB) cDNA (Genbank accession No. NM_003995.3) was extracted from the commercially purchased hNPRB-CFP (Genecopoeia, Rockville, MD) by designing two primers containing two restriction sites (*Pme I*: GTTTAAAC, blunted overhang; *Xho I*: CTCGAG, cohesive overhang), and with the stop codon where appropriate (Table 7).

Fragment	Primers' name	Sequence	Annealing Temperature (°C)
hNPRB	5'-hNPRB	GGA A GGA **GTTTAAAC**CA T GGC G	68
	3'-hNPRB	CCGCA **CTCGAG**<u>TTA</u>CA GGA GT CC	

Table 7. Primer details and conditions of hNPRB PCR. The restriction sites were in bold and the stop codon was underlined.

Phusion® High-Fidelity DNA Polymerase (New England Biolabs Ltd., Hitchin, UK) was used with the aim to efficiently amplify the fragments (3171bp). PCR was performed in an Eppendorf Mastercycler® gradient with 5 µl 5x PCR buffer with $MgCl_2$, 1 µl cDNA template, 0.3 µmol of each primer, 0.35 mM dNTP, and 0.5 µl Phusion DNA polymerase in a 25 µl reaction volume. Specific PCR conditions for each product are given in Table 8. The PCR thermal cycler was programmed to run the following cycles:

	Temperature	Time	Cycles
Initial denaturation	98°C	30s	1
Denaturation	98°C	10s	35
Annealing	68°C	30s	
Elongation	72°C	1min	
Final elongation	72°C	7min	1
Cooling	4°C	Unlimited time	

Table 8. PCR Amplification of human NPRB cDNA using Phusion® High-Fidelity DNA polymerase.

3.2.2.8 A-tailing for human NPRB cDNA and TA ligation

The 3171bp cDNA fragment was gel purified first, the A-tailing procedure was performed in an Eppendorf Mastercycler® gradient with 2 µl 10x PCR buffer with $MgCl_2$, 16 µl purified cDNA template, 0.5 µl dATP (0.1 mM), and 1.5 µl Taq DNA polymerase in a 20 µl reaction volume. The mixture was then incubated at 72 °C for 20 to 30 min.

Rapid ligation was performed to ligate hNPRB cDNA fragment into pGEM® T-Easy vector according to manufacture's protocol (Promega, Southampton, UK). The recombinant T-easy constructs were enzyme digested (*Sal I* and *Xba I*) and sequenced to identify mutants and inserts orientation. The ligation products, were

subsequently gel purified before undergoing restriction digest and then ligation into vector pcDNA3.1(-).

3.2.2.9 Restriction digest of recombinant T-easy constructs and ligation with dephosphorylated pcDNA3.1(-)

The T-easy hNPRB construct was digested by *Not I* and incubated for 1 h at 37 °C in a total 20 µl reaction volume, which contained 3 µl recombinant construct, 1 µl 10x Roche Buffer H, 1 µl *Not I* (5 U), and 5 µl DNase/RNase free water. The linearised fragment was then extracted via gel electrophoresis and purified by a PureLink^{TM} PCR Purification Kit (Invitrogen, Paisley, UK). The purified fragment with *Not I* cohesive end was finally ligated to the dephosphorylated pcDNA3.1(-) vector also containing *Not I* overhang. The final ligation reaction contained 2 µl of 10x ligation buffer, 6 µl of linearised hNPRB fragment from T-easy vector, 3 µl of dephosphorylated pcDNA3.1(-),1 µl of T4 ligase, and 8 µl DNase/RNase free water to have a final volume of 20 µl. The reaction was incubated at RT for 1 h. As negative control, an identical reaction was set up with 12 µl of DNase/RNase free water in place of the insert. A second gel purification was applied, the product was dissolved in DNase/RNase free water and enzyme digested to identify insert orientation, finally stored at -20 °C.

3.2.2.10 Transformation

Competent *E.coli* cells (Promega, Southampton, UK) were allowed to thaw on ice. 10 µl of each ligation product, mNPRA and hNPRB (refer to 3.2.2.6 and 3.2.2.9) were added into 50 µl *E.coli* respectively, and incubated for 30 min on ice. The cells were then heat shocked by placing the reaction into a thermomixer at 42 °C for 50 sec before placing back onto ice for 2 min. LB broth (800 µl for each at 37 °C, without any antibiotics) was then applied to the *E.coli* tubes before being placed in a shaking incubator (500 rpm) for 1 h at 37 ºC. After that, 150 µl of each *E.coli* were plated on LB Agar plates containing 100 µg/ml ampicillin, 50 µg/ml X-Gal, and placed the LB-agar plates in an incubator at 37 °C overnight, the remaining were stored at 4 °C.

3.2.2.11 Screening colonies

The blue-white screen was used for the detection of successful ligations. Theoretically, plasmid contains bacterial lacZ gene can produce β-galactosidase if its ORF is not interrupted by insert DNA. Together with α peptide expressed by hosting *E.coli* strain, functional β-galactosidase can be produced by transforming wild type lacZ containing plamid into *E.coli* and the β-galactosidase can turn the X-gal into a blue colour products. When a foreign DNA is inserted into the multiple cloning site (MCS) within the lacZ gene, the open reading frame of lacZ is changed and will not produce β-galactosidase therefore the recombinant colony will be in white colour. Here, single white bacterial colonies from the transformed *E.coli* were individually selected with a 20 µl pipette tip and placed straight into separate 15 ml Falcon tube containing 3 ml of LB broth and 7 µl of 100 µg/ml Ampicillin. The Falcon tubes were then placed in a shaking incubator at 37 °C overnight to allow the colonies to grow.

Plasmid DNA was extracted from the expanded colonies and purified according to the Miniprep isolation protocol (Qiagen, Crawley, UK). Restriction digest analyses (For mNPRA using *Xho I*, cut 3 times; for hNPRB using *Eco47-III* & *Xba I*) were performed to ascertain whether the plasmid contained the right orientation insert. For each digest 5 µl of the plasmid miniprep was used. Following digestion each reaction was run on a 1.0% agarose gel and visualised by UV illumination. All cloned constructs were confirmed by DNA sequencing (York-Bioscience, Heslington, UK). After the products were sequencing proved, maxiprep would be performed to generate high yields of plasmid DNA for later cell transfection.

3.2.3. Culture of cells, transfection, and stimulation

Culture of permanent cells and primary cells refers to 2.2.3 and 2.2.4. One day before transfection, HEK293 cells and COS7 cells of 90% confluency were plated in 24-well cell culture dishes, and were transiently transfected according to the following Table 9. After 24 h, cells were stimulated by the solvent alone, or ANP, BNP, CNP, or ACNP for 5 min. After sucking away the supernatant, 150 µl/well hydrochloric acid (0.1 N) was used to lyse the cells, and the lysed cells were

subjected to centrifugation at 1,200 rpm for 10 min. The supernatant was then stored at -80 ºC until cGMP measurement.

Cell lines	Cells per well	Volume of medium (µl)	DNA per well (diluted into 20 µl suspension)			siRNA per well (diluted into 20 µl suspension)			Transfection reagent per well (diluted into 20 µl suspension)
			0.25 µg NPRA	0.25 µg NPRB	0.25 µg pcDNA	22 nM siCtrl	22 nM siNPRA	22 nM siNPRB	
HEK293	2×10^5	400	√	-	√	-	-	-	2.5
HEK293	2×10^5	400	-	√	√	-	-	-	2.5
HEK293	2×10^5	400	√	√	-	-	-	-	2.5
HEK293	2×10^5	400	√	√	-	√	-	-	2.5
HEK293	2×10^5	400	√	√	-	-	√	-	2.5
HEK293	2×10^5	400	√	√	-	-	-	√	2.5
COS7	1.8×10^5	400	√	-	√	-	-	-	2.5
COS7	1.8×10^5	400	-	√	√	-	-	-	2.5
COS7	1.8×10^5	400	√	√	-	-	-	-	2.5

Table 9. Different transient transfection combinations of permanent cell lines. Lipofectamine ™ 2000 was used for plasmid-DNA transfection and co-transfection of siRNA and plasmid DNA.

3.2.4. Measurement of cGMP

Measurement of cGMP refers to 2.2.5.

3.2.5. Preparations of cytoplasmic and membrane fractions

HEK293 cells (2×10^6 cells per 6-cm Petri dish at 90% confluency) were used for membrane preparations and transfected according to Table 10&11.

Groups \ Elements	pcDNA3.1(-)	NPRA	NPRA-YFP	NPRB-CFP
Control	6 µg	-	-	-
100% NPRA	4 µg	2 µg	-	-
100% NPRB-CFP	4 µg	-	-	2 µg
25% NPRA+100% NPRB-CFP	3.5 µg	0.5 µg	-	2 µg
50% NPRA+100% NPRB-CFP	3 µg	1 µg	-	2 µg
100% NPRA+100% NPRB-CFP	2 µg	2 µg	-	2 µg
200% NPRA+100% NPRB-CFP	-	4 µg	-	2 µg

Table 10. Different transient transfection combinations of permanent cell lines. A total of 6 µg plasmid-DNA per group was transfected for 24 h with 30 µl/dish Polyfect transfection reagent. Two microgram of either human NPRA or human NPRB-CFP regards as 100%.

Elements / Groups	pcDNA3.1(-)	NPRB	NPRA-YFP	NPRB-CFP
Control	6 µg	-	-	-
100%NPRB	4 µg	2 µg	-	-
100%NPRA-YFP	4 µg	-	2 µg	-
25%NPRB+100% NPRA-YFP	3.5 µg	0.5 µg	-	2 µg
50%NPRB+100% NPRA-YFP	3 µg	1 µg	-	2 µg
100%NPRB+100% NPRA-YFP	2 µg	2 µg	-	2 µg
200%NPRB+100% NPRA-YFP	-	4 µg	-	2 µg

Table 11. Different transient transfection combinations of permanent cell lines. A total of 6 µg plasmid-DNA per group was transfected for 24 h with 30 µl/dish Polyfect transfection reagent. Two microgram of either human NPRB or human NPRA-YFP regards as 100%.

After 24 h incubation, transfected cells were harvested and centrifuged at 3,000 g, RT for 5 min. The supernatants were discarded, and the pellets were resuspended in 800 µl 50 mM Tris (pH 7.5). The following steps were all manipulated on ice in case of overheated and subsequently cells might be damaged. The resuspension was homogenised for 1 min at 24,000 rpm and the homogenates were then ultrasound treated for 10 sec using a Dawe Soniprobe type 7533A (Branson Sonic Power Co., Danbury, CT). After that, the ultrasound treated cells solution was centrifuged at 40,000 g, 4 °C for 22 min. The supernatants were collected as cytosol part. The pellets were resuspended in radio-immunoprecipitation assay (RIPA) buffer (150 mM NaCl, 10 mM Tris pH 7.2, 0.1% SDS, 1% Triton X-100, 1% deoxycholate and 5 mM EDTA) as membrane part. The protein was quantified by a bicinchoninic acid (BCA) protein assay kit (Thermo Fisher Scientific, Cramlington, UK). Both membrane and cytosol preparations were stored at -80°C ready for use.

3.2.6. Western blot analysis

Each of memebrane and cytosol preparations was supplied with 5 µl of 6x loading buffer and filled up with ddH$_2$O to an end volume of 30 µl and incubated at 95°C for 10 min. A 10 µg protein was loaded into stacking gel at 80 Volts and separated in a 10 % separation gel at 120 Volts, and subjected to SDS-PAGE for 3h using a Mini-PROTEAN Tetra System (Bio-Rad Laboratories, Hertfordshire, UK). After that, the gel was blotted by 0.8 mA/cm^2 for 1 h (Semi-Dry-Blotter PEGASUS,

PHASE GmbH, Luebeck, Germany). Proteins were electrically transferred onto the polyvinylidene fluoride (PVDF) membrane (Millipore, Consett, UK, Immobilon-P Transfer Membrane Pore Size 0.45 μm) and the membrane was blocked with 5 % milk powder (Carl Roth GmbH + Co. KG, Karlsruhe, Germany) in 1x Tris buffered saline-with Tween-20 (TBS-T) (3 g TrisBase, 8.8 g NaCl, 0.2 g KCl plus 500 μl Tween-20, pH 7.4, autoclaved) at RT for 1 h. After the blocking, the PVDF membrane was carefully cut into two pieces (Upper piece of ≥ 90 kDa incubated with Living Colors Full-length A.v. polyclonal antibody; lower piece of ≤ 90kDa incubated with anti-calreticulin antibody). The Living Colors Full-length A.v. polyclonal antibody and the house-keeping protein anti-calreticulin antibody (both diluted to 1:1000 in 1xTBST with 5% milk) were incubated onto the upper and lower pieces of membrane overnight at 4°C, respectively. Before the secondary antibody was added, the membrane was washed for 30 min with 1x TBS-T changing every 5 min. The membrane was incubated for 1 h with the secondary antibody (goat anti-rabbit IgG-HRP, diluted to 1:2000 1x TBS-T with 3% milk) at RT and washed two times for 15 min with 1x TBS-T. The specific bands were visualised by ECL Plus Western Blotting Detection Reagents (GE Healthcare Life Sciences, Amersham Place, Buckinghamshire, UK) as instructed in the user manual (Amersham ECL Plus Western Blotting Detection Reagents, Product Booklet, Codes RPN2132/2133). The targeted bands were then developed, fixed in a dark room via Hyperfilm ECL (GE Healthcare Life Sciences, Amersham Place, Buckinghamshire, UK). Finally, the developed film was scanned and analyzed via the ImageJ program, which is a Java-based open source image enumeration software package freely downloadable from the US National Institute of Health website (http://rsbweb.nih.gov/ij/). The signal intensity of the proteins of interest was calculated against the signal intensity of house-keeping proteins (anti-calreticulin).

3.2.6. RNA preparation and one-step quantitative real-time polymerase chain reaction

Culture of the HEK293 cells refers to 2.2.3. One day before transfection, HEK293 cells of 90% confluency were plated in 6-well cell culture dishes, and were transiently transfected according to the following Table 12.

Sets / Elements	Control	100% NPRA	NPRB	25%	50%	100%	200%
pcDNA3.1(-)	6 µg	4 µg	4 µg	3.5 µg	3 µg	2 µg	-
X%NPRA	-	2 µg	-	0.5 µg	1 µg	2 µg	4 µg
100% NPRB	-	-	2 µg	2 µg	2 µg	2 µg	2 µg

Table 12. Detailed parameters for transient transfection of HEK293 cells with different formats. A total of 6 µg plasmid-DNA per group was transfected for 24 h with 30 µl/dish Polyfect transfection reagent. 2 µg of either human NPRA or human NPRB regards as 100%.

After 24 h, total RNA from transfected HEK293 cells was extracted by Trizol® with subsequent chloroform-isopropanol extraction according to the manufacture's protocol (Invitrogen, Paisley, UK). The RNA concentration and purity were determined via NanoDrop 1000 Spectrophotometer (Thermo Fisher Scientific Inc., East Sussex, UK). Ten ng of RNA was used as template to determine human NPRA gene, human NPRB gene and the reference gene human glyceraldehyde 3-phosphate dehydrogenase (GAPDH) mRNA expression in an ABI StepOnePlus™ Real-Time PCR System (Applied Biosystems). Quantitative real-time PCR was carried out using one-step QuantiTect SYBR Green RT-PCR Kit and specific primers for human NPRA (NM_000906), human NPRB (NM_000907) or human GAPDH (NM_002046) according to the manufacturer's instructions (Qiagen GmbH, Crawley, UK). Melting curve analyses were performed to monitor PCR product purity. Relative quantification of the gene expression output was performed using Sequence Detection System software (SDS v2.2.1, ABI). The SDS utilizes relative quantification of gene expression by way of the comparative CT method where the relative quantity (RQ) = $2^{-\Delta\Delta C_T}$, C_T is defined as the threshold cycle where the target gene surpasses a defined amplification.

3.2.7. Fluorescence resonance energy transfer*

Fluorescence resonance energy transfer (FRET) experiments were performed 24 h after transfection of HEK293 cells. Cells were maintained at room temperature in a Ringer modified saline (NaCl 125 mmol/L, KCl 5 mmol/L, Na_3PO_4 1 mmol/L, $MgSO_4$ 1 mmol/L, Hepes 20 mmol/L, Glucose 5.5 mmol/L, $CaCl_2$ 1 mmol/L, pH 7.4), and an LSM510 NLO multiphoton laser scanning microscope (ZEISS, Jena, Germany) equipped with a tunable Titan-Sapphir-Laser (2-photon-absorption) and a 40x or 100x oil objective lens was used for the detection of FRET. CFP and YFP were used as the donor and acceptor fluorophore, respectively, since the emission

spectrum of CFP overlaps with the excitation spectrum of YFP (CFP was excited at ~436 nm and emitted at ~480nm, whereas the acceptor YFP was excited at ~480nm and emitted at ~532nm). The donor (CFP) was excited at 810 nm (two photon technique) and due to the META detector, a λ-stack (spectrum) from 436 to 650 nm with a resolution of 10 nm was detected. Such settings were used throughout the whole experiment, excluding the direct excitation of the acceptor (YFP) at the excitation wavelength of the donor at 810 nm. Cells with equal expression levels of CFP and YFP were selected and imaging was performed at RT. The detected spectra were normalized to 1.0 at 468 nm. The signal value at 532 nm was calculated as the point of maximal YFP intensity. Acceptor photobleaching experiments were not performed, but the increase in CFP intensity due to acceptor bleaching was calculated out of the unbleached CFP spectrum as described before (Teichmann et al., 2012b, Teichmann et al., 2012a). The FRET efficiency (E_T) was calculated according to the following equation:

$$E_T(\%) = 1 - \frac{I_{DA}}{I_D} \times 100 = \frac{1}{1 + (R/R_0)^6} \times 100$$

where the intensities I_{DA} and I_D describe the fluorescence of the donors in presence and absence of the acceptor, respectively. The Förster radius R_0 is the distance when E_T is 50%. It is depended on the type of fluorescence molecule. For CFP (donor) and YFP (acceptor) a value of $R_0 = 4.9$ nm is used (Sourjik and Berg, 2002). By detection of fluorescence intensities, E_T can be calculated and with known R_0, the distance R between donor and acceptor can be determined. This equation can be expressed as:

$$E_T(\%) = (1 - \frac{\sum\limits_{436}^{489} I_{DA}(\lambda)}{\sum\limits_{436}^{489} I_D(\lambda)}) \times 100$$

where the donor intensitiy after acceptor bleaching is calculated as follows:

$$\sum\limits_{436}^{489} I_D(\lambda) = \sum\limits_{436}^{489} \hat{I}_{DA}(\lambda) + \sum\limits_{436}^{489} \hat{I}_{DA}(\lambda) \times \frac{\left[(\sum\limits_{436}^{650} \hat{I}_{DA}(\lambda) - \sum\limits_{436}^{650} \hat{I}_D(\lambda)) \times \frac{\phi_D}{\phi_A}\right]}{\sum\limits_{436}^{650} \hat{I}_{DA}(\lambda)}$$

where $\hat{I}_{DA}$ is the normalized fluorescence intensity of CFP in absence of YFP, and $\hat{I}_D$ is the normalized fluorescence intensity of CFP after the bleaching of YFP. The parameter Φ_D and Φ_A are the fluorescence quantum yields of CFP (0.4) and YFP (0.61), respectively (Tsien, 1998). The variable $\hat{I}$ describes the normalized fluorescence spectra with a maximum of 1.0 at 468 nm.

3.2.8. Statistical analysis

Results are expressed throughout as the mean ± SEM unless otherwise indicated. For cell culture studies, each experiment was performed in triplicate in 2 or 3 separate experiments. Differences between groups were compared with one-way ANOVA followed by the Bonferroni posttest when the global test was significant. Two-way ANOVA was used to compare the main group effects of ANP, BNP, CNP, and ACNP in dose-response curves, and to test the differences of FRET signal between NPRB-CFP single- and NPRA-YFP/NPRB-CFP co-transfected cells. EC_{50} values were calculated by using sigmoidal dose response curve fit in GraphPad Prism 5.0 (GraphPad Software, San Diego, CA, USA). A P value of < 0.05 was considered as significant.

* The FRET assay was conducted in cooperation with Dr. Burkhard Wiesner, from Leibniz-Institut für Molekulare Pharmakologie (FMP), Berlin, Germany.

3.3. Results

3.3.1. Generation of mNPRA and hNPRB constructs

mNPRA cDNA was successfully amplified from mouse lung cDNA consisting of two overlapping fragments (1801bp 1st mNPRA and 1531bp 2nd mNPRA, see Figure 29). Each fragment was ligated into T-easy vector, and the reconstructed T-easy vectors containing either 1st mNPRA or 2nd mNPRA fragment were confirmed by restriction enzyme digestion, where two bands at 3330bp and 1486bp occur to prove correct 1st mNPRA construct, while three bands at 2998bp, 1548bp, and 275bp occur to prove correct 2nd mNPRA construct. Then, the 1st mNPRA and 2nd mNPRA fragments were extracted from their T-easy vectors by *Not I* and *Nde I* and successfully subcloned into the *Not I* digested and dephosphorylated vector pcDNA3.1(-). The reconstructed pcDNA3.1(-) vectors containing full-length mNPRA were screened by restriction enzyme digestion (Figure 30C).
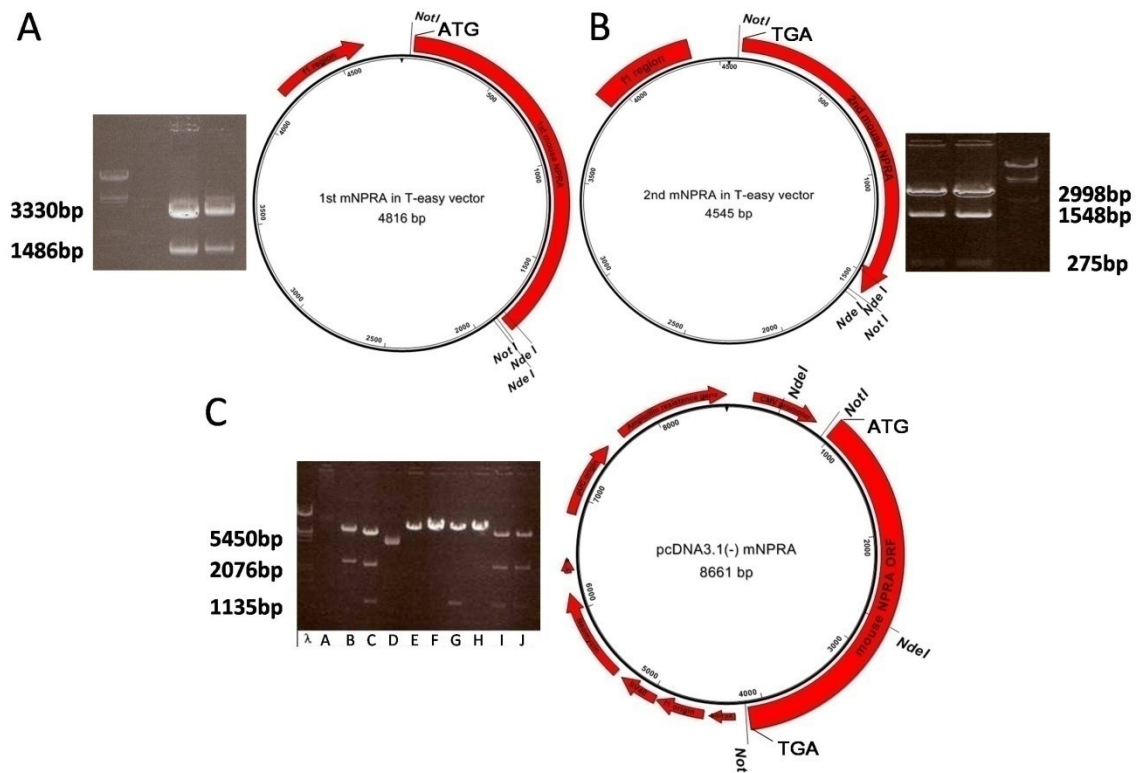
Figure 30. Plasmid generation of 1st mNPRA, 2nd mNPRA fragments in T-easy vectors, and full-length mNPRA in pcDNA3.1(-) confirmation by gel electrophoresis using enzyme digestion. mNPRA was amplified by amplifying two overlapping fragments (1st mNPRA and 2nd mNPRA) from mouse lung cDNA. **(A)** Restriction enzyme digestion and plasmid chart of pGEM T-easy 1st half mNPRA. λ marker indicated fragments size. Both lanes were digested by *Acc I* to prove for correct inserts. **(B)** Restriction enzyme digestion and plasmid chart of pGEM T-easy 2nd half mNPRA. λ marker indicated fragments size. Both lanes were digested by *EcoR I* to prove for correct inserts. **(C)** Restriction enzyme digestion and plasmid chart of pcDNA3.1(-) mNPRA. λ marker indicated fragments size. Lane A, B were digested by *Nde I*, while Lane C to J were digedted by *Xho I*. Lane B, C, I, and J were proven as the correct inserts, while others were either wrong oriented inserts, or unexpected fragments.

88

hNPRB cDNA was successfully extracted from the commericially purchased hNPRB-CFP vector (GeneCopoeia, Rockville, MD) using a primer pair (5'-hNPRB and 3'-hNPRB) covering the start and stop codon of the full-length hNPRB cDNA (Figure 31A). After A-tailing procedure, the 3171bp fragment was ligated into T-easy vector and confirmed by restriction enzyme digestion (Figure 31B&C). The hNPRB fragment (3207bp) was extracted from the fused T-easy hNPRB construct digested by *Not I* (Figure 31D). the 3207bp fragment was successfully subcloned into the *Not I* ended dephosphorylated pcDNA3.1(-) vector (Figure 31E&F). None nucleotide DNA polymerase error was identified in either mNPRA or hNPRB cDNA compared to their published sequences (Appendix 3&4).
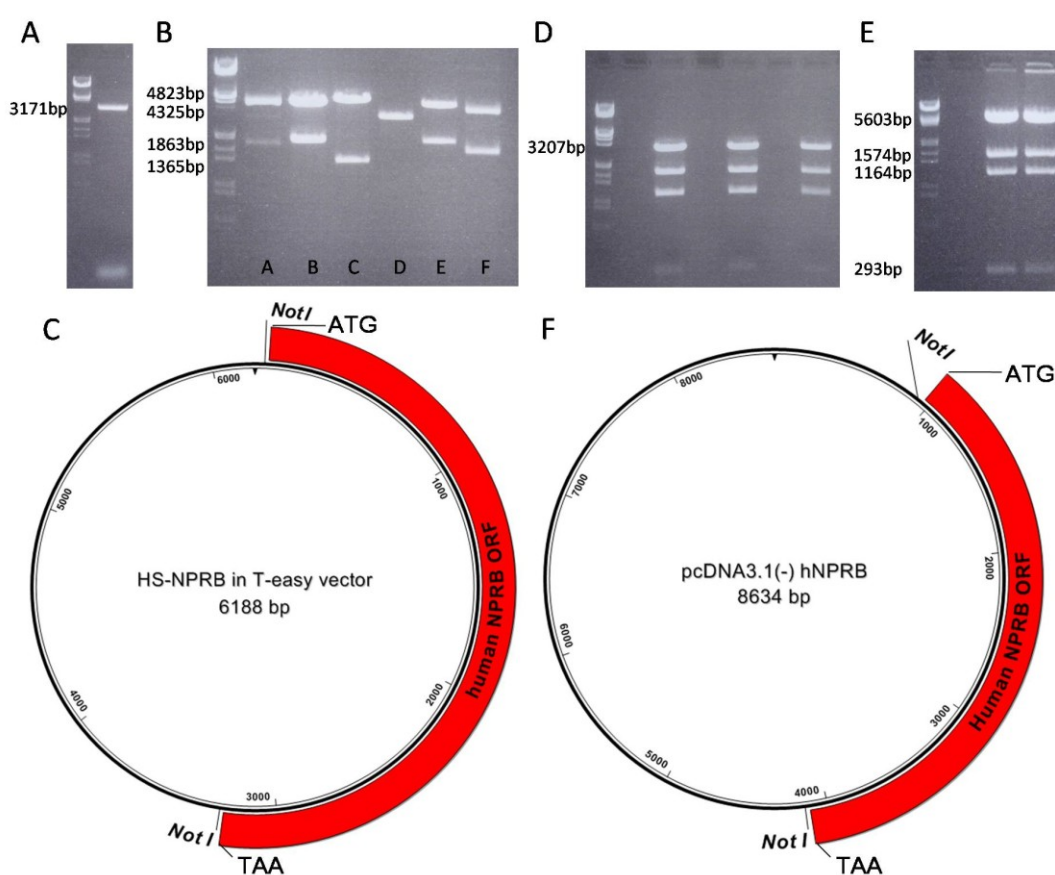
Figure 31. Plasmid generation of hNPRB in T-easy vector, and hNPRB in pcDNA3.1(-) confirmation by gel electrophoresis using enzyme digestion. **(A)** Extraction of hNPRB fragment (3171bp) via high fidelity PCR. λ marker indicated fragments size. **(B)** Restriction enzyme digestion of pGEM T-easy hNPRB. λ marker indicated fragments size. Bands in Lane 2, 5 (U-orientation) and Lane 3 (N-orientation) were proven as correct inserts, which were digested by *Sal I* & *Xba I*. **(C)** Plasmid chart of human NPRB in T-easy vector. **(D)** Extraction of human NPRB fragment (3207bp) by *Not I*. λ marker indicated fragments size. **(E)** Restriction enzyme digestion of pcDNA3.1(-) hNPRB. λ marker indicated fragments size. Both lanes were digested by *Eco47-III* & *Xba I*, and proven as correct inserts. **(F)** Plasmid chart of the newly generated plasmid merging hNPRB and pcDNA3.1 (-) vector.

3.3.2. NP/cGMP signalling is attenuated in human NPRA and human NPRB double-transfected cells

Data presented previously suggested that a dramatically down-regulated NP/cGMP generation occurred in the co-transfection of human NPRA and rat/mouse NPRB (Appendix 4). To exclude the species-related influence causing such blunted cGMP generation, mouse NPRA and human NPRB were cloned respectively, allowing the investigation the interaction of receptors of the same species. As shown in Figure 32, human NPR-transfected HEK293 cells were stimulated with 10^{-7} M of different NPs and the receptor triggered increase in intracellular cGMP measured.
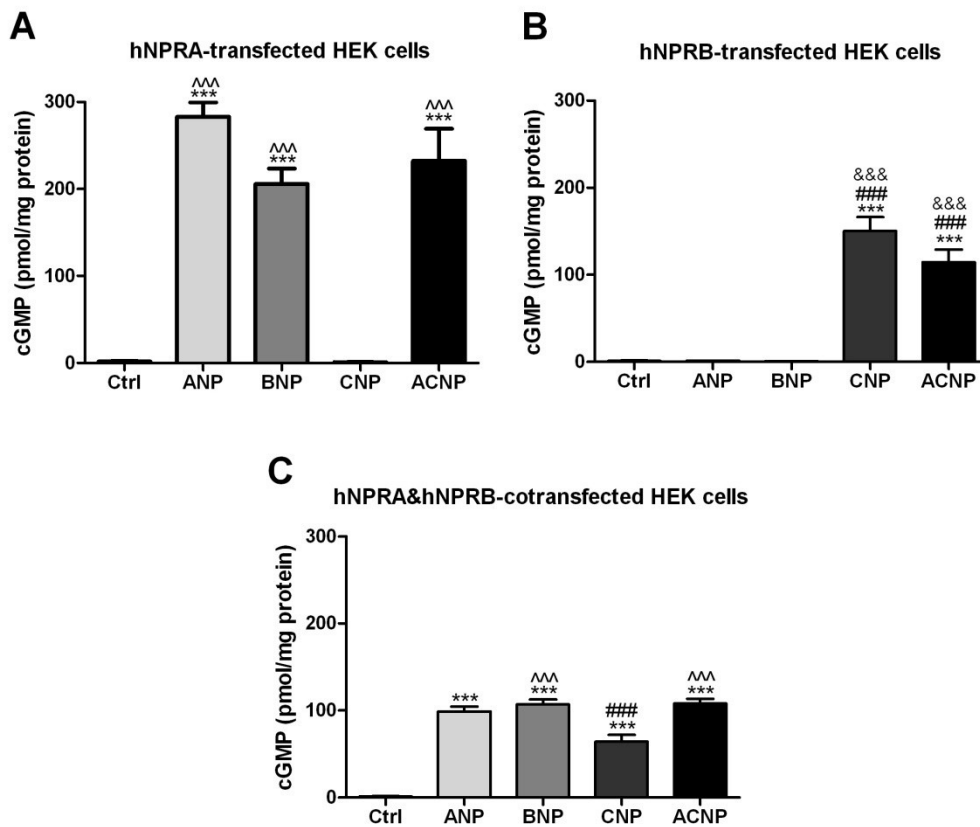
Figure 32. cGMP generation stimulated by 10^{-7} M of human NPs in human receptor single- or double-transfected HEK293 cells. **(A)** Absolute values of cGMP generation in hNPRA single-transfected HEK293 cells; **(B)** Absolute values of cGMP generation in hNPRB single-transfected HEK293 cells; **(C)** Absolute values of cGMP generation in hNPRA and hNPRB double-transfected HEK293 cells. Experiments were conducted in 3 independent settings as triplicates. ***P < 0.001 *vs.* control (Ctrl); ###*P* < 0.001 *vs.* ANP; &&&*P* < 0.001 *vs.* BNP; ^^^*P* < 0.001 *vs.* CNP.

CNP stimulated hNPRB, but not hNPRA (Figure 32A&B). ACNP stimulated NPRA mediated cGMP generation, though less efficient than ANP, similar to BNP (Figure 32A). Additionally, ACNP stimulated NPRB mediated cGMP release in comparable to CNP, where neither ANP nor BNP were able to mediate cGMP generation (Figure 32B). In double-transfected cells, the ANP-mediated cGMP generation was dramatically down-regulated by 65% compared to NPRA single-transfected cells, while BNP-mediated cGMP production was decreased by 48%. In comparison to NPRB single-transfected cells, 57% less cGMP production was seen stimulated by CNP. By contrast, ACNP stimulated a similar cGMP generation compared with that in NPRB-transfected HEK293 cells, but only 50% from that of NPRA-transfected HEK293 cells (Figure 32C).

3.3.3. Comparison of effects of siRNA-NPR on NP/cGMP signalling in human NPRA and human NPRB double-transfected cells

To test whether reduction in co-transfetced NPR quantity could restore NP-mediated cGMP production in double-transfected cells, siRNA against either human NPRA (siRNA-NPRA) or NPRB (siRNA-NPRB), or scrambled siRNA (siCtrl) as internal control were co-transfected with the NPRA/NPRB double-transfected HEK 293 cells. Identically, a very similar cGMP generation pattern was seen in NPRA/NPRB/siCtrl triple-transfected HEK293 cells compared to that in NPRA/NPRB double-transfected HEK cells (Figure 33A). By applying siRNA-NPRA, ANP and BNP mediated NPRA/cGMP signalling were totally abolished, whereas CNP/cGMP signalling was fully restored to that of NPRB-transfected HEK293 cells (Figure 33B). Such findings suggest that the inhibition of the expression of NPRA can restore NPRB/cGMP signalling. Notably, ACNP/cGMP signalling was even enhanced compared to the NPRB-transfected cells, with a similar cGMP production to that of NPRA-transfected cells (Figure 33B). However, no down-regulation of CNP/cGMP signalling or restoration of NPRA/cGMP signalling was observed after co-transfecting with siRNA against NPRB to the NPRA/NPRB double-transfected HEK293 cells (Figure 33C).
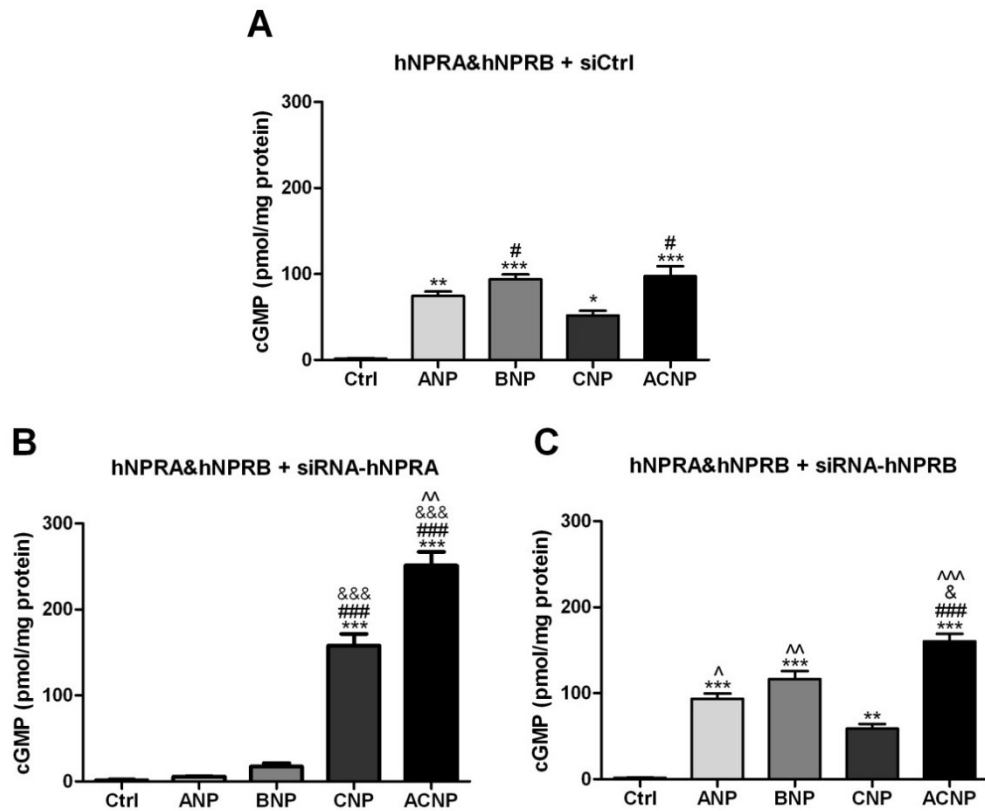
Figure 33. cGMP generation stimulated by 10^{-7} M of human NPs in double-transfected HEK293 cells in presence of either 22nM siCtrl, or equimolar siRNA-hNPRA, or siRNA-hNPRB. **(A)** Absolute values of cGMP generation in siCtrl/hNPRA/hNPRB co-transfected HEK293 cells. **(B)** Absolute values of cGMP generation in siRNA-hNPRA/hNPRA/hNPRB co-transfected HEK293 cells. **(C)** Absolute values of cGMP generation in siRNA-hNPRB/hNPRA/hNPRB co-transfected HEK293 cells. Experiments were conducted in 3 independent settings as triplicates. *$P < 0.05$, **$P < 0.01$, ***$P < 0.001$ *vs.* control (Ctrl); #$P < 0.05$, ###$P < 0.001$ *vs.* ANP; &$P < 0.05$, &&&$P < 0.001$ *vs.* BNP; ^$P < 0.05$, ^^$P < 0.01$, ^^^$P < 0.001$ *vs.* CNP.

3.3.4. The attenuated cGMP signalling in NPRA and NPRB co-transfection is not species restricted

To test whether the attenuated cGMP signalling in hNPRA/hNPRB co-transfection can be reproduced, HEK293 cells were single- or double-transfected with plasmids harboring mNPRA or mNPRB cDNA in presence or absence of siRNA against either mNPRA or mNPRB. After 24 h, such cells were stimulated with the solvent only, or 10^{-7} M of mouse ANP, BNP, CNP, or ACNP. A very similar cGMP stimulation pattern was found in mNPRA-transfected HEK293 cells in comparison of that in hNPRA-transfected cells (Figure 32A), although mouse BNP mediated a similar cGMP generation than mouse ANP. Both stimulated cGMP slightly more than ACNP although not being significant (Figure 34A). CNP activated mNPRB to increase cGMP levels, while neither ANP nor BNP was able to

mediate significant cGMP response (Figure 34B). Interestingly, equimolar ACNP was even more potent in stimulation of cGMP generation in mNPRB-transfected HEK293 cells compared to CNP ($P < 0.001$; Figure 34B), where CNP/cGMP was slightly stronger than ACNP in hNPRB-transfected HEK293 cells ($P > 0.05$; Figure 32B). The ANP/NPRA/cGMP signalling pathway in mNPRA/mNPRB co-transfected HEK293 cells was down-regulated by 34% and thus to a less extent than that in cells transfected with human receptors (65%; Figure 32C). Similarly, BNP/cGMP signalling in mNPRA/mNPRB co-transfected HEK293 cells was downregulated by 29%, while it was 48% in cells transfected with human receptors. However, CNP/cGMP signalling was blunted by 77% in mouse receptor co-transfected cells in comparison to that of 57% in human receptor co-transfected cells. In contrast, ACNP was much less affected and stimulated a similar cGMP generation compared with that in mNPRA-transfected HEK293 cells (Figure 34C).
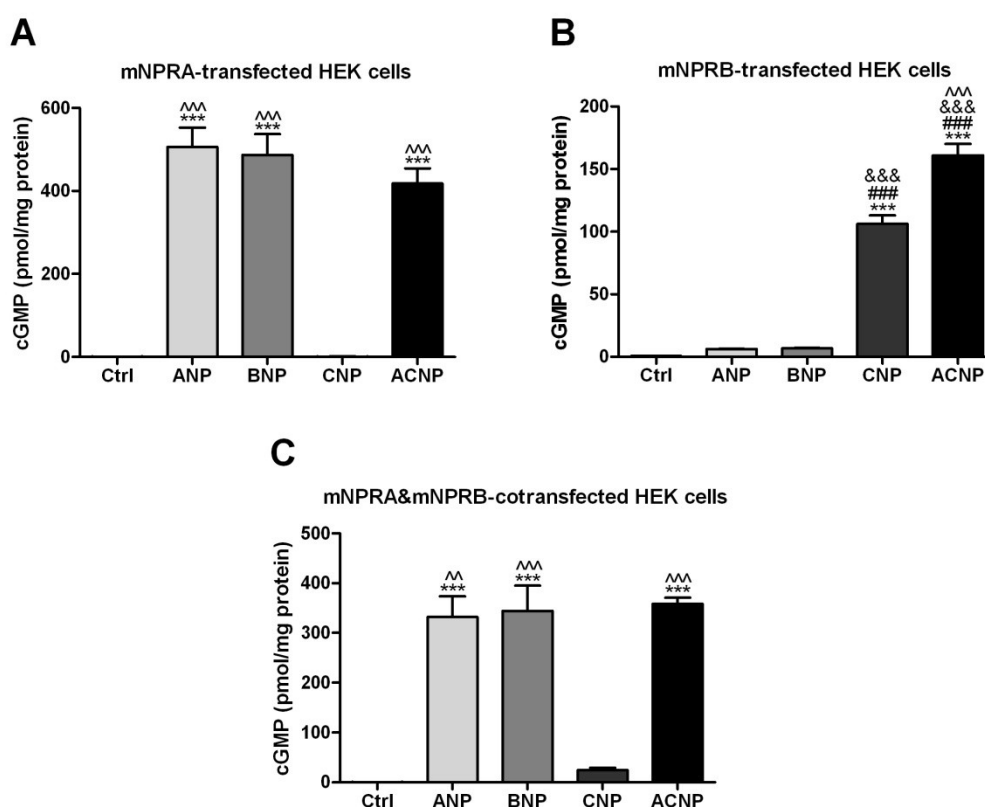
Figure 34. cGMP generation stimulated by 10^{-7} M of mouse ANP, mouse BNP, CNP, and ACNP in double-transfected HEK293 cells. **(A)** Absolute values of cGMP generation in mNPRA single-transfected HEK293 cells; **(B)** Absolute values of cGMP generation in mNPRB single-transfected HEK293 cells; **(C)** Absolute values of cGMP generation in mNPRA/mNPRB double-transfected HEK293 cells. Experiments were conducted in 3 independent settings as triplicates. ***$P < 0.001$ *vs.* control (Ctrl); ###$P < 0.001$ *vs.* ANP; &&&$P < 0.001$ *vs.* BNP; ^^$P < 0.01$, ^^^$P < 0.001$ *vs.* CNP.

Identically, a very similar cGMP generation pattern was seen in NPRA/NPRB/siCtrl triple-transfected HEK293 cells (Figure 35A) compared to the NPRA/NPRB double-transfected HEK cells. By applying siRNA against mNPRA, nearly half of mouse ANP, mouse BNP and ACNP mediated NPRA/cGMP signalling were inhibited compared to the double-transfected pattern (Figure 35B). However, CNP/cGMP signalling was not restored (Figure 35B). Further, CNP-mediated cGMP formation was totally abolished whilst no significant restoration of NPRA/cGMP signalling were observed after co-transfecting siRNA against mNPRB to the mNPRA/mNPRB double-transfected HEK293 cells (Figure 35C), indicating the mechanism of interaction within mNPRA and mNPRB may differ from that of human species. Nevertheless, the attenuated NP/cGMP signalling was confirmed in double-trasfected cells regardless of receptor origin.
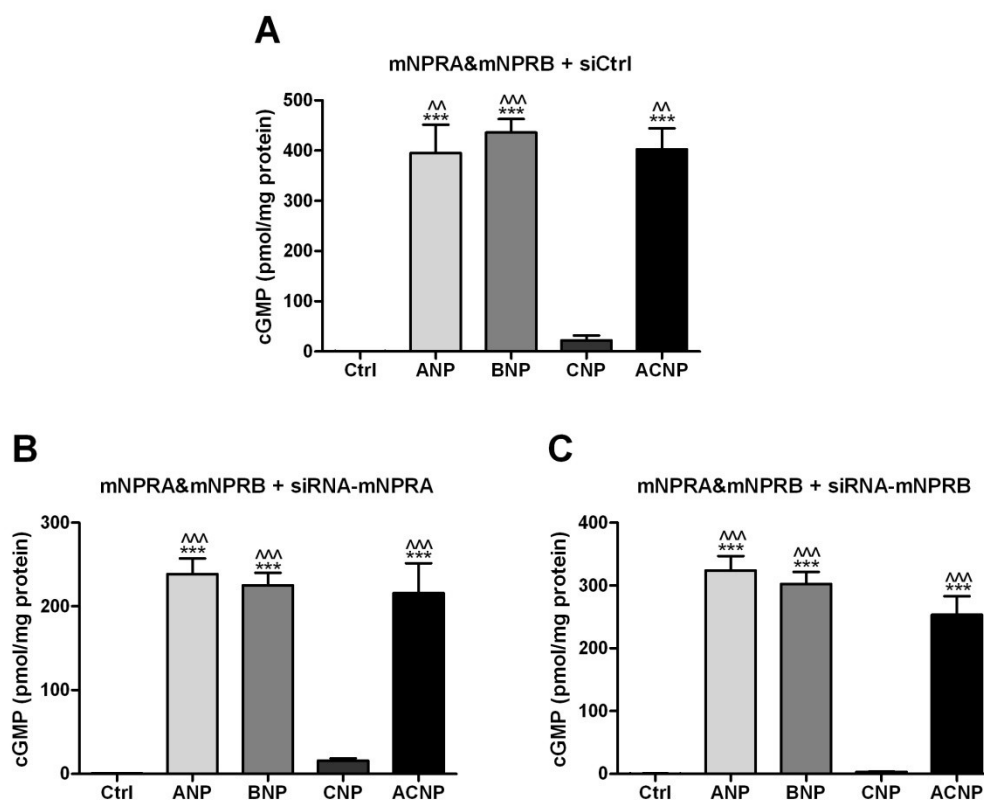
Figure 35. cGMP generation stimulated by 10^{-7} M of mouse ANP, mouse BNP, CNP, and ACNP in double-transfected HEK293 cells in presence of either 22nM siCtrl, or equimolar siRNA-mNPRA, or siRNA-mNPRB. **(A)** Absolute values of cGMP generation in siCtrl, mouse NPRA and NPRB co-transfected HEK293 cells. **(B)** Absolute values of cGMP generation in siRNA against mouse NPRA, mouse NPRA and NPRB triple-transfected HEK293 cells. **(C)** Absolute values of cGMP generation in siRNA against mouse NPRB, mouse NPRA and NPRB triple-transfected HEK293 cells. Experiments were conducted in 2 independent settings as triplicates. $***P < 0.001$ *vs.* control (Ctrl); $^{\wedge\wedge}P < 0.01$, $^{\wedge\wedge\wedge}P < 0.001$ *vs.* CNP.

3.3.5. The inhibitory effect of receptor co-transfection is dose-dependent

To investigate whether the co-transfection of NPRA and NPRB leading to less cGMP production is dose-dependent, and to test if such attenuated NP/NPR/cGMP signalling in double-transfected cells could be abolished by using siRNA against hNPRA or hNPRB, different proportions of hNPRA and hNPRB in presence or absence of siCtrl/siRNA were co-transfected in HEK293 cells and such cells stimulated with either 10^{-7} M of human ANP, BNP, or CNP. All three NPs activated their natural receptors by leading to a rapid cGMP generation. ANP and BNP stimulated cGMP generation decreased upon the co-transfection of hNPRA with increasing ratio of hNPRB (Figure 36A&B), and these dose-dependent inhibitory effects could not be restored by siRNA against hNPRB as found before (Figure 33C).
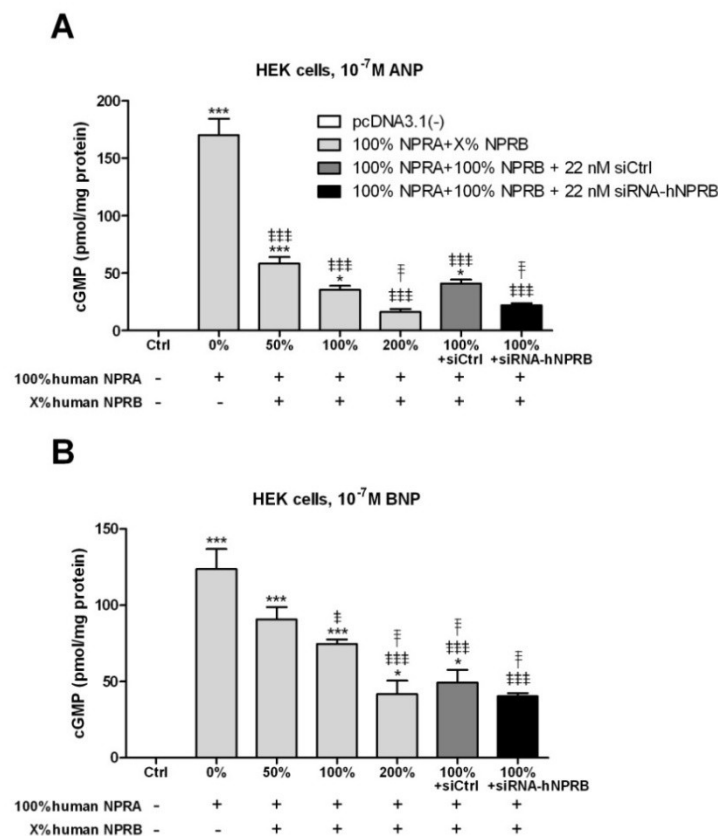
Figure 36. Comparisons of cGMP generation stimulated by 10^{-7} M of human ANP and human BNP in HEK293 cells transfected with different proportions of hNPRA/hNPRB/siCtrl/siRNA-hNPRB. **(A)** Absolute values of cGMP generation stimulated by human ANP upon the co-transfection with hNPRA and increasing ratio of hNPRB in presence or absence of siCtrl/siRNA-hNPRB; **(B)** Absolute values of cGMP generation stimulated by human BNP upon the co-transfection with hNPRA and increasing ratio of hNPRB in presence or absence of siCtrl/siRNA-hNPRB. * $P < 0.05$, *** $P < 0.001$ *vs.* Ctrl; ‡ $P < 0.05$, ‡‡‡ $P < 0.001$ *vs.* 100% hNPRB + 0% hNPRA; $\bar{\mp}$ $P < 0.05$ *vs.* 100% hNPRB + 50% hNPRA.

Interestingly, the effect of hNPRA cotransfection on CNP-mediated cGMP generation was less pronounced than that of hNPRB influencing hNPRA mediated cGMP signalling. There is no downregulation of cGMP generation after cotransfecting 0.25 µg (50%) NPRA co-transfected with 0.5 µg (100%) NPRB, but the cGMP signalling was attenuated by further increasing concentrations of hNPRA co-transfected with 100% hNPRB in a dose-dependent manner. In contrast, a detectable but not significacnt restoration of cGMP generation was seen by applying siRNA against hNPRA (restored by 49% *vs.* 200%NPRA + 100%NPRB) (Figure 37).
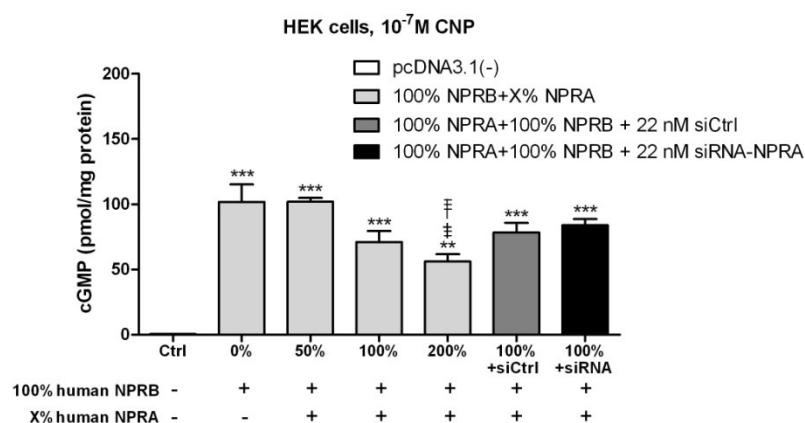
Figure 37. Comparisons of cGMP generation stimulated by 10^{-7} M of CNP in HEK293 cells. Absolute values of cGMP generation stimulated by CNP upon the co-transfection with human NPRB and increasing concentration of human NPRA in presence or absence of siCtrl/siRNA-hNPRA. **$P < 0.01$, ***$P < 0.001$ *vs.* Ctrl; ‡$P < 0.05$ *vs.* 100% hNPRB + 0% hNPRA; ‡$P < 0.05$ *vs.* 100% hNPRB + 50% hNPRA.

3.3.6. Characterisation of NPs/NPRs/cGMP signalling in transfected primary cells

Above results suggested that there is a dose-dependent inhibitory effect on cGMP generation upon NP stimulation in NPRA/NPRB double-transfected HEK293 cells. To test whether such attenuated NP/cGMP mediated by receptors interaction can be reproduced in primary cell lines transfected with exogenous NPRA or NPRB, two cultured primary cell types with inversely proportion of endogenously expressed NPRA and NPRB were used. Mesangial cells (MC) predominately expressing NPRB and human dermal microvascular endothelial cells (HDMEC) endogenously expressing NPRA were transfected with mNPRA and hNPRB, respectively, in presence or absence of siRNA against either mNPRA or hNPRB. In untransfected

MC, 10^{-6} M of mouse ANP or BNP generated only one tenth cGMP in comparison to CNP (Figure 38A). ANP/cGMP and BNP/cGMP signalling were rapidly activated after transfecting with mNPRA, whilst CNP/cGMP signalling was ~30% attenuated compared to the untransfected cells (Figure 38B). A similar result was seen in mNPRA and siCtrl co-transfected MC (Figure 38C). By applying siRNA again mNPRA to mNPRA-transfected MC, ANP- and BNP-mediated cGMP generation was significantly inhibited, while CNP/cGMP signalling was partially restored by 23% in comparison of that in mNPRA-transfected MC (Figure 38D), but not significantly higher than that in untransfected MC.
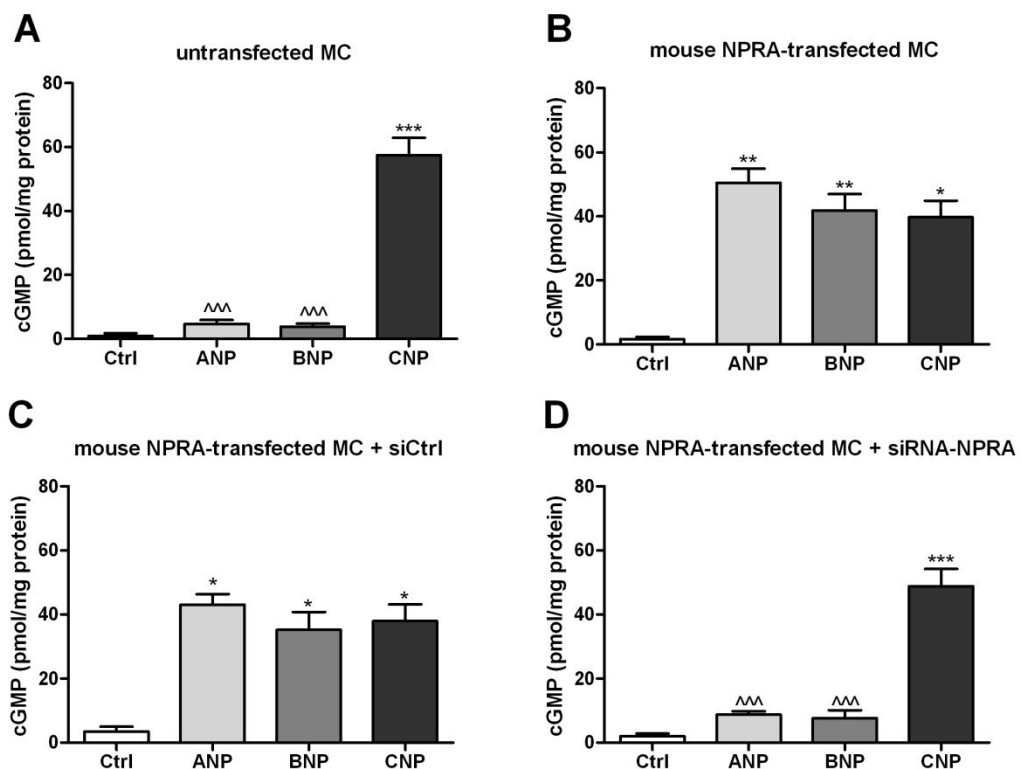
Figure 38. Comparison of cGMP generation stimulated by 10^{-6} M of mouse ANP, mouse BNP, and CNP in untransfected and transfected MC. **(A)** Absolute values of cGMP generation in untransfected MC; **(B)** Absolute values of cGMP generation in mNPRA single-transfected MC; **(C)** Absolute values of cGMP generation in mNPRA and siCtrl double-transfected MC; **(D)** Absolute values of cGMP generation in mNPRA and siRNA-mNPRA double-transfected MC. Experiments were conducted in 3 independent settings as triplicates. $*P < 0.05$, $**P < 0.01$, $***P < 0.001$ *vs.* control (Ctrl); $^{\wedge\wedge\wedge}P < 0.001$ *vs.* CNP.

Further, the endogenous NPRA-rich HDMEC were stimulated with either solvent, or 10^{-6} M of human ANP, BNP, or CNP. In untransfected HDMEC, which has only little endogenous NPRB, CNP failed to mediate cGMP release as expected, while ANP induced a strong cGMP signal being significantly higher than that of

BNP (Figure 39A). CNP/cGMP signalling was rapidly activated after transfecting with human NPRB, accompanied with a slight but not significant decrease in ANP- and BNP-mediated cGMP formation (Figure 39B). Similarly, siCtrl did not affect the cGMP formation (Figure 39C). Moreover, the down-regulated ANP/cGMP and BNP/cGMP signalling were not restored via siRNA against NPRB, where CNP/cGMP signalling was interfered and had a more than 70% decrease versus that of NPRB-transfected HDMEC (Figure 39D). Thus, these data validated the substantial NPRA and NPRB interaction through both axes of exogenous/exogenous and exogenous/endogenous receptor interplays, which might involve complicated and distinct mechanisms.
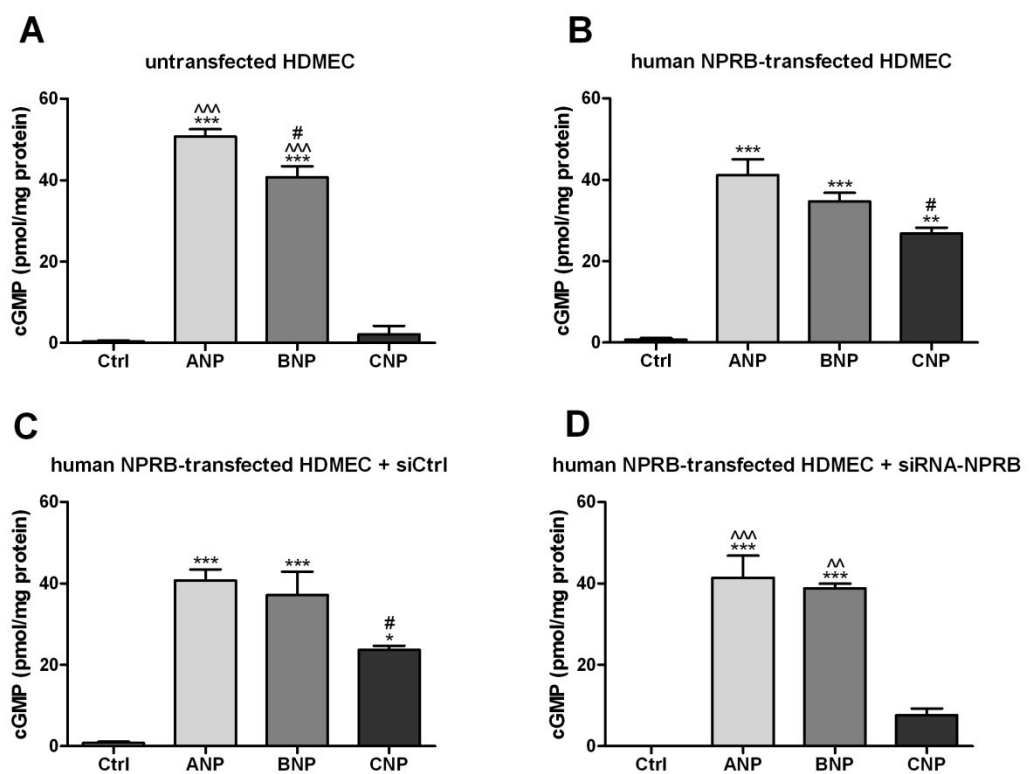
Figure 39. Comparison of cGMP generation in untransfected and transfected HDMEC. **(A)** Absolute values of cGMP generation in untransfected HDMEC; **(B)** Absolute values of cGMP generation in hNPRB single-transfected HDMEC; **(C)** Absolute values of cGMP generation in hNPRB and siCtrl double-transfected HDMEC; **(D)** Absolute values of cGMP generation in hNPRB and siRNA-hNPRB double-transfected HDMEC. Experiments were conducted in 3 independent settings as triplicates. $*P < 0.05$, $**P < 0.01$, $***P < 0.001$ $vs.$ control (Ctrl); $\#P < 0.05$ $vs.$ ANP; $^{\wedge\wedge}P < 0.01$, $^{\wedge\wedge\wedge}P < 0.001$ $vs.$ CNP.

3.3.7. Evaluation of NPRA and NPRB interaction by Western blotting

To test if NPRA down-regulates NPRB expression on translational levels leading to lower CNP-mediated cGMP generation; or translation of NPRB is not influenced by NPRA, but less NPRB is on the membrane due to altered internalisation, immunoblots were performed to assess the interaction of human NPRB-CFP with different ratio of untagged human NPRA in membrane and cytoplasma preparation. Living Colors antibody was used as the primary antibody and Calreticulin was used as a housekeeping protein (spanning 64-70kDa). As shown in Figure 40, NPRB-CFP appeared as a strong band whose apparent molecular mass (spanning 130-135kDa) agrees with previous estimation (Tian and Yang, 2006, Abdelalim and Tooyama, 2009). No NPRB-CFP-associated immunoactivity was seen in pcDNA3.1(-) or NPRA transfected membrane samples, while the strongest band occured in membrane of NPRB-CFP single transfected cells. A decreasing immunoreactivity of NPRB-CFP was seen in the membrane preparations by increasing the concentration of co-transfected NPRA. In contrast, in the cytosol, no detectable signal was found in any transfection pattern, suggesting the absence of internlisation occurred during the interaction between NPRA and NPRB (Appendix 5). Taken together, these data implicate that the transcription or translation of NPRB might be inhibited by NPRA in a dose dependent manner.
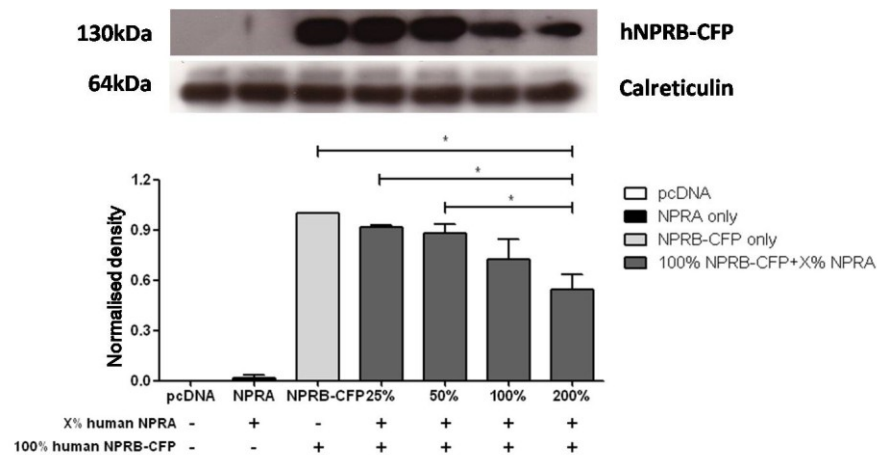
Figure 40. Comparison of human NPRB-CFP protein levels in HEK293 cell membrane preparations co-transfected with human NPRB-CFP and different concentration of human NPRA. HEK293 cells were single-transfected with either 0.5 µg pcDNA3.1(-) vector, or 0.5 µg human NPRA (as 100%), or 0.5µg human NPRB-CFP (as 100%); or double-transfected with 100% NPRB-CFP plus various concentration of NPRA. Cell membrane samples were prepared and analysed by western blot with a Living Colors antibody raised against CFP tag, or calreticulin. Experiments were conducted in 3 independent settings as triplicates. The immunoreactivity of sample of 100% single NPRB-CFP transfection was normalized as 1.0. Each lane of a 10% PAGE was loaded with 10 µg of membrane protein.

Inversely, to test the hypothesis that NPRB down-regulates NPRA expression on translational level leading to lower ANP- and BNP-mediated cGMP generation, or translation of NPRA is not influenced by NPRB, but less NPRA is on the membrane due to altered internalization, an identical procedure was conducted with untagged human NPRB and human NPRA-YFP, instead of aforementioned human NPRA and human NPRB-CFP. As shown in Figure 41, NPRA-YFP appeared as a broad band of immunoreactivity whose apparent molecular mass (spanning 130-135kDa) agrees with previous estimation (Liu *et al.*, 2010, You and Laychock, 2011). No human NPRA-YFP-associated immunoreactivity was observed in pcDNA3.1(-) or human NPRB transfected membrane samples, while the normalized densities of targeted bands were all similar among the 100% NPRA-YFP lane and the lanes co-transfected with varying concentration of human NPRB (Figure 41). This indicates that the down-regulation of ANP- and BNP-medaited cGMP generation in double-transfected cells is not due to a translational alteration of NPRA. Moreover, in the cytosol, no detectable signal was found in any transfection pattern, suggesting again the absence of internlization occurring during the interaction between NPRA and NPRB in ligand-unstimulated cells (Appendix 6).
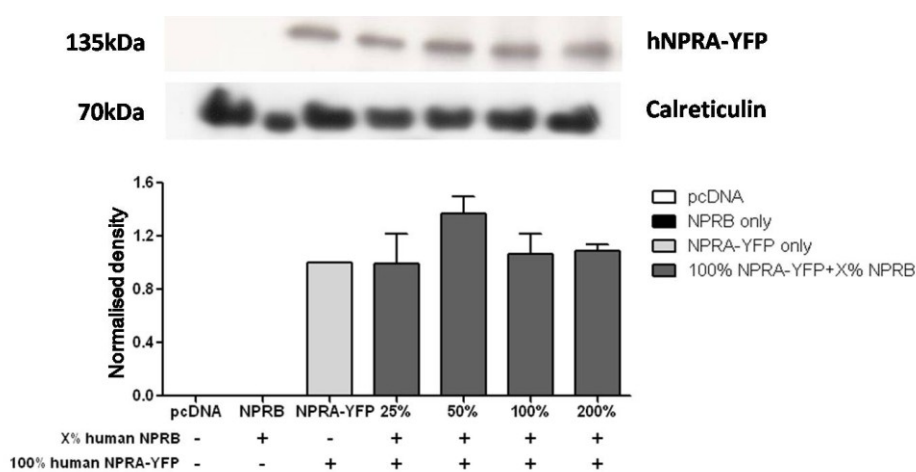
Figure 41. Comparison of human NPRA-YFP protein levels in HEK293 cell membrane preparations co-transfected with human NPRA-YFP and different concentration of human NPRB. HEK293 cells were single-transfected with either 0.5 µg pcDNA3.1(-) vector, or 0.5 µg human NPRB (as 100%), or 0.5 µg human NPRA-YFP (as 100%); or double-transfected with 100% NPRA-YFP plus various ratio of NPRB. Cell membrane samples were prepared and analysed by western blot with a Living Colors antibody raised against YFP tag, or calreticulin. Experiments were conducted in 3 independent settings as triplicates. The immunoreactivity of sample of 100% single NPRA-YFP transfection was normalized as 1.0. Each lane of a 10% PAGE was loaded with 10 µg of membrane protein.

3.3.8. Quantification of NPRA and NPRB mRNA expression in transfected HEK293 cells

To further assess whether the interaction between NPRA and NPRB leading to impaired cGMP generation was due to transcriptional alteration or direct intervention on translational level, 24 h after transfection, cells were harvested and RNA was isolated. Quantitative RT-PCR was performed to determine the changes in human NPRA and NPRB mRNA in transfected HEK293 cells, respectively.
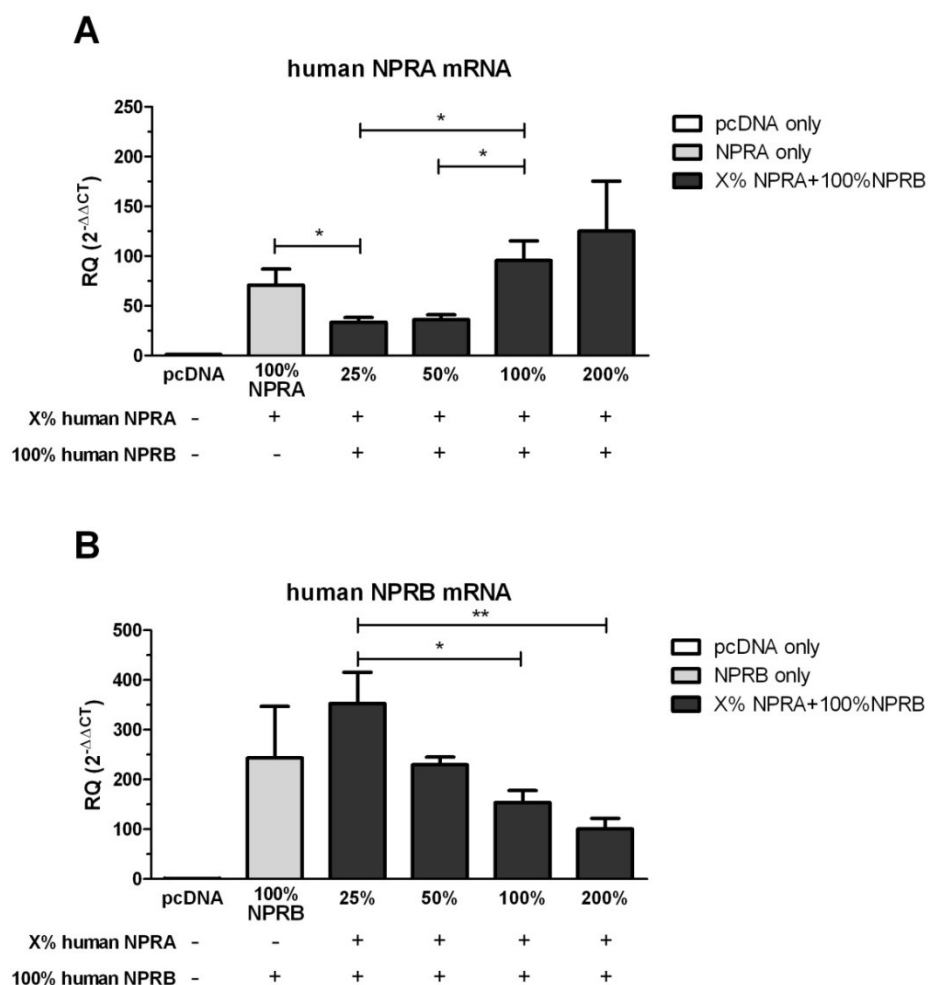
Figure 42. Real-time PCR quantification of human NPRs in receptor transfected HEK293 cells. **(A)** Relative quantity (RQ) of human NPRA Mrna expression; **(B)** Relative quantity (RQ) of human NPRB mRNA expression. HEK293 cells were single-transfected with either 0.5 μg pcDNA3.1(-) vector, or 0.5 μg human NPRA (as 100%), or 0.5μg human NPRB (as 100%); or double-transfected with 100% NPRB plus various ratio of NPRA. Relative quantity (RQ) is normalized to human GAPDH level. Data represent the mean ± SEM (n = 6 per group).

As shown in Figure 42A, relative quantity (RQ) of human NPRA mRNA was gradually increased by raising the concentration of human NPRA (from 25% to 200%) in human NPRB-transfected HEK293 cells. In contrast, RQ of human NPRB

mRNA displayed a gradient reduction when co-transfected with an increasing portion of human NPRA (Figure 42B), suggesting NPRA inhibits CNP/NPRB/cGMP signalling on transcriptional level.

3.3.9. Physical interaction between NPRA and NPRB

To further investigate if a direct physical interaction of NPRA and NPRB occurs, human NPRB-CFP and NPRA-YFP were co-expressed in HEK293 cells and FRET signals were analyzed as a measurement for direct interaction between both receptors when two fluorophores are in close proximity to each other. Both CFP signal (Figure 43A) and YFP signal (Figure 43B) were detected in hNPRA-YFP/hNPRB-CFP co-transfected HEK293 cells using the CFP and YFP channel, respectively. Merged signal (Figure 43C) demonstrated the coexpression of hNPRA-YFP and hNPRB-CFP in the double-transfected cells.
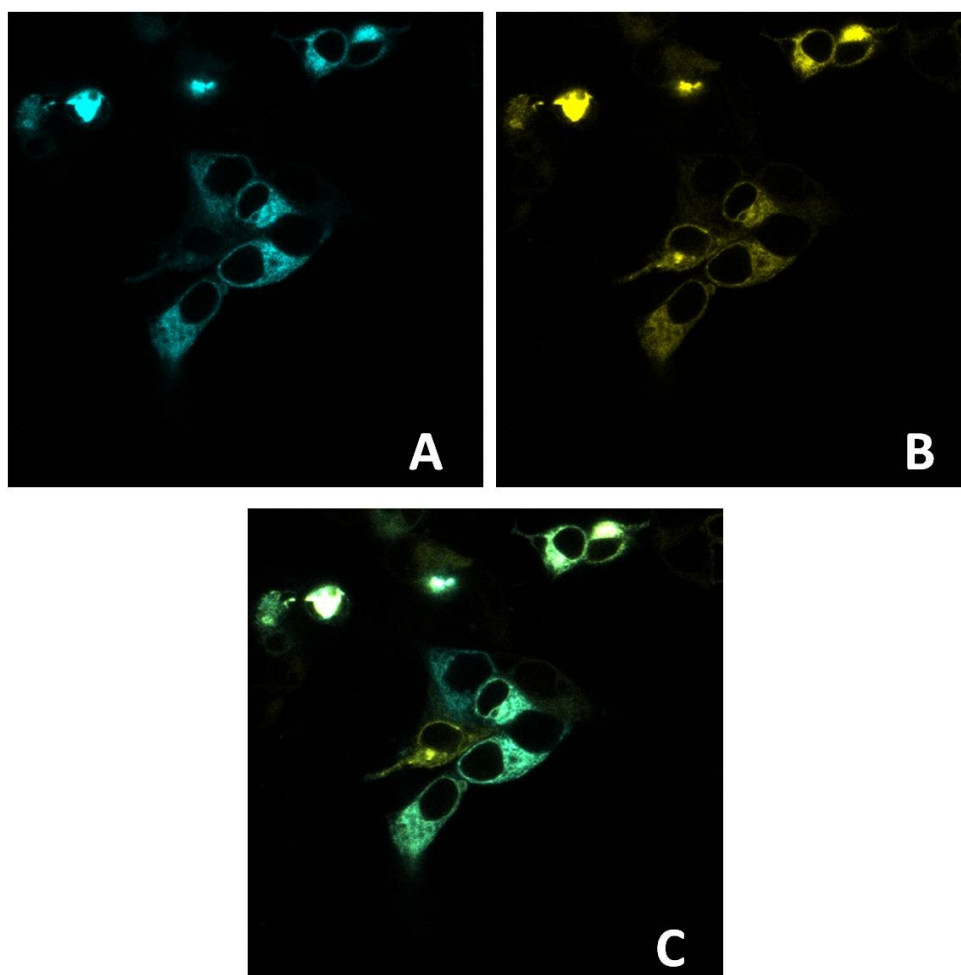
Figure 43. Representative images illustrating the coexpression of human NPRA-YFP and human NPRB-CFP. **(A)** HEK293 cells expressing the targeted human NPRB-CFP using the CFP channel; **(B)** HEK293 cells expressing the targeted human NPRA-YFP using the YFP channel; **(C)** The overlay of HEK293 cells co-expressing hNPRA-YFP and hNPRB-CFP. Images were captured with Zeiss LSM510 using 40× oil objective.

Compared to the fluorescence intensity of NPRB-CFP alone, decrease in donor (CFP) emission (at ~480 nm) and increase in acceptor (YFP) emission (at ~532 nm) intensities was observed in co-transfection of NPRB-CFP and NPRA-YFP (Figure 44), and these signal values are significantly different between the single NPRB-CFP spectrum and that of co-transfection of NPRB-CFP and NPRA-YFP ($P < 0.001$). Furthermore, the distance between the two fluorophores was determined ($R = 7.42 \pm 0.89$ nm) by knowing the FRET efficiency ($E_T = 8.99 \pm 4.05$), demonstrating the energy transfer occurred when two fluorophores were close to each other enough (distance of the donor and acceptor molecules < 10 nm) and interacting with each other.
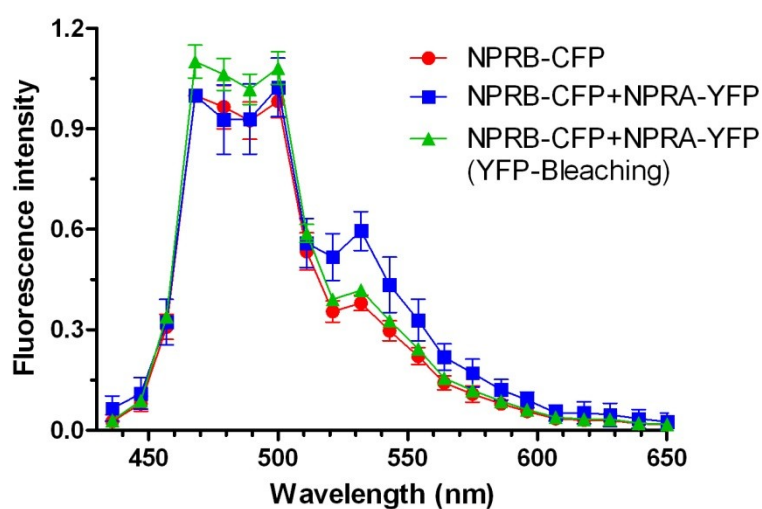
Figure 44. Fluorescence spectra of human NPRB-CFP alone, human NPRB-CFP plus human NPRA-YFP, and human NPRB-CFP plus human NPRA-YFP (YFP-bleaching). Data represent the mean ± SD (n = 46-49 per group).

3.4. Discussion

Characterisation of the crosstalk among different signalling pathways that involve cardiovascular pathogenesis should lead to a better understanding of molecular and cellular processes and ultimately, leading to the discovery of novel and fundamental therapeutic options for CVD. In this chapter, a NPRA/NPRB interplay was uncovered involving the down-regulated NP-mediated cGMP signalling via their cognate receptors in the cells double-transfected with NPRA and NPRB. Such inhibitory effect on signalling of heterogeneous receptor complexes by receptor co-transfection was dose-dependent. Interestingly, the data revealed that increasing concentration of NPRA co-transfected with NPRB leads to a reduced generation of NPRB mRNA and thus to decrease the amount of NPRB protein in the membrane, which consequently results in the observed lower cGMP release stimulated by CNP in NPRA/NPRB double-transfected cells in comparison to NPRB single-transfected cells. In contrast, by increasing concentration of NPRB in NPRA, it is revealed that the decreased cGMP formation stimulated by ANP and BNP in co-transfected cells is not attributed to lowered receptor quantity in the membrane, but very likely due to the newly identified physical interaction of the two receptors, causing conformational change of the NPRA receptor in NPRA/NPRB heterodimer, thereby reducing the GC activity after ligand stimulation.

The protein interaction between NPRA and NPRB is not species related, because the down-regulation of cGMP formation was observed in cells double-transfected with NPRA and NPRB of different species. Using analysis with basic local alignment search tool (BLAST) revealed that such concordant attenuated cGMP signalling in receptor combinations of different species possibly results from a relatively high homology of 87% between human NPRA (accession number NM_000906.3) and mouse/rat NPRA (accession number NM_012613.1 for rat, and NM_008727.5 for mouse), and of 91% between human NPRB (accession number NM_003995.3) and mouse/rat NPRB (accession number NM_053838.1 for rat, and NM_173788.3 for mouse). Yet, NP mediated cGMP formation in cells double-transfected with NPRA and NPRB is incompletely understood, the ratio of NPRA and NPRB in living cells/tissues has not been quantified in pathophysiological states (Dickey *et al.*, 2007). Previous studies demonstrated cGMP generation in primary cells expressing different concentrations of NPRA and NPRB (Suga *et al.*, 1992,

Pankow *et al.*, 2007, Potter *et al.*, 2006), and different receptor distribution was shown in isolated tissue/organs (Ritter *et al.*, 1995, Del Ry *et al.*, 2010). Thus, the here generated data demonstrate for the first time an attenuated cGMP generation in equal amount of NPRA/NPRB double-transfected cells after equimolar NP stimulation in comparison to single-transfected cells using the same receptor cDNA concentrations as in double-transfected cells. Many reports have suggested that NPRA exists as a homodimer (Rondeau *et al.*, 1995, Ogawa *et al.*, 2004, Misono *et al.*, 2011). It was shown for the NPRA homodimer that a rotation at the transmembrane domain after ligand binding is associated with the signal transduction, thereby leading to the activation of the GC domain (Parat *et al.*, 2010). Crystallographic studies also showed a minor extent of conformational difference between the unliganded and liganded forms of the NPRA ECD, supporting the concept of conformational change as the basis for intracellular signalling (Ogawa *et al.*, 2004). The present study demonstrate that using the same amounts of receptor plasmid DNA for transfection, CNP mediated cGMP formation in NPRB-transfected cells is less pronounced than NPRA/cGMP formation stimulated by ANP or BNP. This is in well congruence with former findings (Pankow *et al.*, 2007). One possible explanation could be that the receptor rotation in the CNP/NPRB complex leads to a less extent of intracellularly GC activation in comparison to that in ANP/NPRA or BNP/NPRA complex by e.g. less significant rotation, and thus resulting in less cGMP generation. Although such rotational mechanism in NPRB activation requires further investigation, it could then be speculated that the combination of a better and less good transmembrane domain in the investigated heterodimers leads to a significant inhibition of the intracellular signalling by the more efficient ANP/BNP.

In addition, it could be shown here that ACNP is an activator for NPRA and NPRB and can stimulate an augmented cGMP release in primary cells expressing both receptors (Zhu *et al.*, 2011). Thus, it was postulated that ACNP could exert additive cGMP production in NPRA/NPRB double-transfected cells. However, in current study, ACNP only showed a similar cGMP generation compared to that of ANP and BNP (Figure 32C and 38C). The model of altered rotation/activation in such heterodimers could explain this. While NPRB is down-regulated in NPRA/NPRB double-transfected cells, the signals of NPRA in complexes with the remaining NPRB could be not as good as the NPRA alone. Langenickel *et al.*

demonstrate that intracellular cGMP accumulation upon CNP stimulation was blunted in COS-7 cells co-transfected with NPRB and a dominant negative NPRB mutant, NPRBΔKC, while native NPRB homodimers were able to generate cGMP (Langenickel *et al.*, 2006), implicating that such alteration in signalling efficacy can be due to disturbed interaction resulting from domains of the receptors in the heterodimers compared to the optimal interaction of such domains in homodimers. Hence, altered rotation and thus alteration in signalling efficacy in the NPRA/NPRB heterodimer blunts the expected additive effect of ACNP in stimulating both receptors.

It has been shown in Chapter 2 that ACNP stimulated an augmented cGMP release in primary cells, e.g. MC, VSMC, and CF, what should not be expected taking the data in double-transfected cells. However, presumably the unbalanced ratio between NPRA and NPRB in these primary cells (predominant NPRB but also minor NPRA expression) leads to a very limited receptor heterodimerisation. Indeed, co-expression of 50% NPRA with 100% NPRB in HEK293 cells had almost no inhibitory effect on CNP-mediated cGMP generation (Figure 37C). Furthermore, in NPRA single-transfected cells, ANP was more potent than BNP in stimulating cGMP as shown here (Figure 32A and 39A) and by others (Kambayashi et al., 1990, Nakao et al., 1991). It is also suggested that BNP was approximately 10-fold less potent than ANP (Koller and Goeddel, 1992). When the cells were co-transfected with both NPRA and NPRB, however, ANP was less potent than BNP in generating cGMP in double-transfected HEK293 cells (Figure 32A&C and Figure 34A&B). This is likely due to the structural differences between ANP and BNP, allowing BNP under co-transfection condition, to better interact with the NPRA/NPRB heterodimer and leading to a better transmembrane rotation in comparison to the one initiated by ANP, and subsequently to more stirring GC activity. Of note, the importance of other determinants for a normal transmembrane signalling such as association, spatial position, and binding angle of the ligand/receptor complex cannot be excluded, since natriuretic peptides are small polypeptides with a relative disordered conformation in solution (Carpenter *et al.*, 1997).

siRNA-NPRA and siRNA-NPRB have been successfully used in many applications to knock down NPRA and NPRB expression, respectively (Wang et al., 2008, Kong et al., 2008, Wang et al., 2011, Simon et al., 2009). Here, it was shown

that siRNA-NPRA could efficiently abolish human NPRA/cGMP formation and restore CNP-mediated NPRB/cGMP signalling in the double-transfected HEK293 cells and NPRA-transfected MC. One explanation could be that the siRNA-NPRA balances the NPRA/NPRB ratio similar to primary cells where the NPRA effect on NPRB expression and NPRB on heterodimer-associated reduction in efficacy of ANP/BNP are minor. Surprisingly, the siRNA-NPRA intervention ameliorated ACNP/cGMP signalling in the double-transfected HEK293 cells to a better performance than that in NPRB-transfected HEK293 cells, reaching a comparable cGMP generation as that in NPRA-transfected HEK293 cells. It has been documented by Ribeiro *et al.* that reduced transfection efficiency occurred while increasing the size of the plasmid (Ribeiro *et al.*, 2012). Hence, such enhanced ACNP/cGMP signalling could also be attributed to the competitive transfection efficiency between the empty vector (pcDNA3.1(-)) and the NPR constructs. Because the NPRB transfection contained equal amount of pcDNA3.1(-) co-transfected with NPRB, the transfection efficiency of the empty vector (5427 bp) is presumably higher than that of the larger NPRB construct (8634 bp). Deducibly, the commercial human NPRA construct (~8200 bp) should also have a similar or slightly better transfection efficiency than NPRB. Consequently, compared to the ACNP/cGMP signalling in NPRB-transfected cells which were also transfected with the empty vector (Figure 32B), a higher transfection efficiency of NRPB could be achieved after silencing the NPRA via siRNA and ensuing an augmented ACNP/cGMP signalling without the transfection competition from either NPRA or the empty vector.

However, apart from the slightly increased ACNP-mediated cGMP generation in NPRA/NPRB double-transfected HEK293 cells and inhibition of CNP-mediated NPRB/cGMP signalling in NPRB-transfected HDMEC are seen in current study, siRNA-NPRB failed to suppress CNP/NPRB signalling as well as to restore ANP- or BNP-mediated NPRA/cGMP signalling in NPRA/NPRB double-transfected HEK293 cells. It is very likely the siRNA-NPRB did not work properly. However, it has been observed a reduced CNP-mediated cGMP formation in NPRB-transfected HDMEC (Figure 39D). Nevertheless, experiments should be repeated using siRNA-NPRB from other companies to confirm whether there is a different

mechanism of NPRB interacts with NPRA, leading to an irreversible down-regulated NPRA/cGMP signalling.

Western blotting assay in transfected cell membrane preparations of various NPR ratios revealed that the NPRB protein expression in double-transfected cells is counterregulated by NPRA in a dose-dependent manner, but NPRA quantity on the membrane is not influenced by NPRB co-transfection. Although emerging specific NPRA or NPRB antibodies have been generated and reportedly functioned in many applications, neither these described antibodies previously (Tian and Yang, 2006, You and Laychock, 2010) nor other primary antibodies purchased elsewhere worked properly in western blotting. Therefore, in the experiments of Chapter 3 (data not shown), the NPRA tagged with enhanced YFP and NPRB tagged with enhanced CFP both at C-terminus were used in combination with untagged NPRs in co-transfection experiments. Here, no fluorescent protein signal was detected in the cytoplasm for both tagged receptors (Appendix 5&6). This makes it unlikely that the less NPRB on the membrane would attribute to faster internalisation under NPRA and NPRB interaction, since this should have had led to a stronger intracellular signal in double-transfected cells. A previous study on interaction between Mas and AT1 receptor (Von Bohlen and Halbach *et al.*, 2000) showed that the membrane-bound AT1 receptor expression was not restricted to the cell membrane but also occurred in the cytoplasm, suggesting the possibility of internalised AT1 receptors via Mas interaction. Meanwhile, the discrepancy in protein level alteration between the preparations of NPRA/NPRB-CFP and NPRB/NPRA-YFP leads to further consideration on the regulation of transcriptional level on NPRB. Thereupon, the mRNA regulation of both NPRA and NPRB were investigated in receptor transfected HEK293 cells. Such experiments confirmed that dose-dependent inhibition of NPRB transcription occurs with increasing NPRA in transfected cells (Figure 42), thereby reducing the quantity of NPRB on the membrane. Such decreased NPRB is then the key factor for the attenuated CNP/NPRB/cGMP signalling in NPRA/NPRB double-transfected cells.

However, it is hard to deduce the same mechanism for the down-regulated NPRA/cGMP signalling. No direct evidence supports that NPRA is affected by NPRB on transcriptional- or translational level leading to reduced ANP/BNP effects in double-transfected cells. Previous studies demonstrated that NPRA is desensitized

in the failing human heart (Tsutamoto et al., 1993, Kuhn, 2003) despite of elevated N-terminal pro-NP and NP levels in patients with hypertensive cardiac hypertrophy and heart failure (McKie et al., 2010b, McKie et al., 2011), causing an impairment in cGMP formation and preventing the diverse cardioprotective NP functions. Additionally, neither NPRA nor NPRB were internalised or degraded in response to NP binding (Fan *et al.*, 2005). Here it is demonstrated that with increasing concentration of NPRB co-transfected with stable concentration of NPRA, the decreased cGMP formation stimulated by ANP and BNP in co-transfected cells is not attributed to a change in receptor quantity either on NPRA mRNA or protein level, but very likely due to the following two potential reasons: 1) Less ANP/BNP interacts with the NPRA caused by the less accessibility to the binding domain built by the NPRA/NPRB heterodimer, which is presumably due to conformational change in the 'binding-pocket' structure. 2) The affinity is unchanged but the ligand-receptor complexes experience an altered NP-induced rotation in the juxtamembrane region that partly hinder the two intracellular domains to change into the active conformation, thereby reducing the GC activity. Here it is shown with FRET assay that energy transfer occurred and a significant difference between the spectrum of NPRB-CFP homodimer and that of NPRB-CFP/NPRA-YFP heterodimer, demonstrating the two different fluorophores were interacting with each other. By using cysteine substitution of the extracellular juxtamembrane domain of NPRA which leads to an unpaired $Cys432$ and results in spontaneous disulfide bridge formation, Labrecque *et al.* indicated that the juxtamembrane regions of the ECD subunits should be juxtaposed (Labrecque *et al.*, 1999). However, mutation $D435C$, producing an unpaired $Cys435$ three residues distal to $Cys432$, leading to a disulfide bridge only upon NPRA activation by ANP (Labrecque *et al.*, 2001). These results are compatible with a conformational change of the juxtamembrane domain that was also documented by Parat *et al.* using FRET autoquenching (Parat *et al.*, 2010). It therefore led to the speculation that the unanticipated down-regulated NPRA/cGMP generation in certain types of CVD, e.g. hypertention, heart failure, etc. may involve physical interaction between NPRA and NPRB, leading to a conformational change at the binding site(s) or inhibited GC activation between the two receptors. Still, it would be of interest to determine the exact conformational changes in the NPRA/NPRB heterodimer in presence of NP, which might finally identify the mechanism for such impaired ANP/BNP signalling in double-transfected cells.
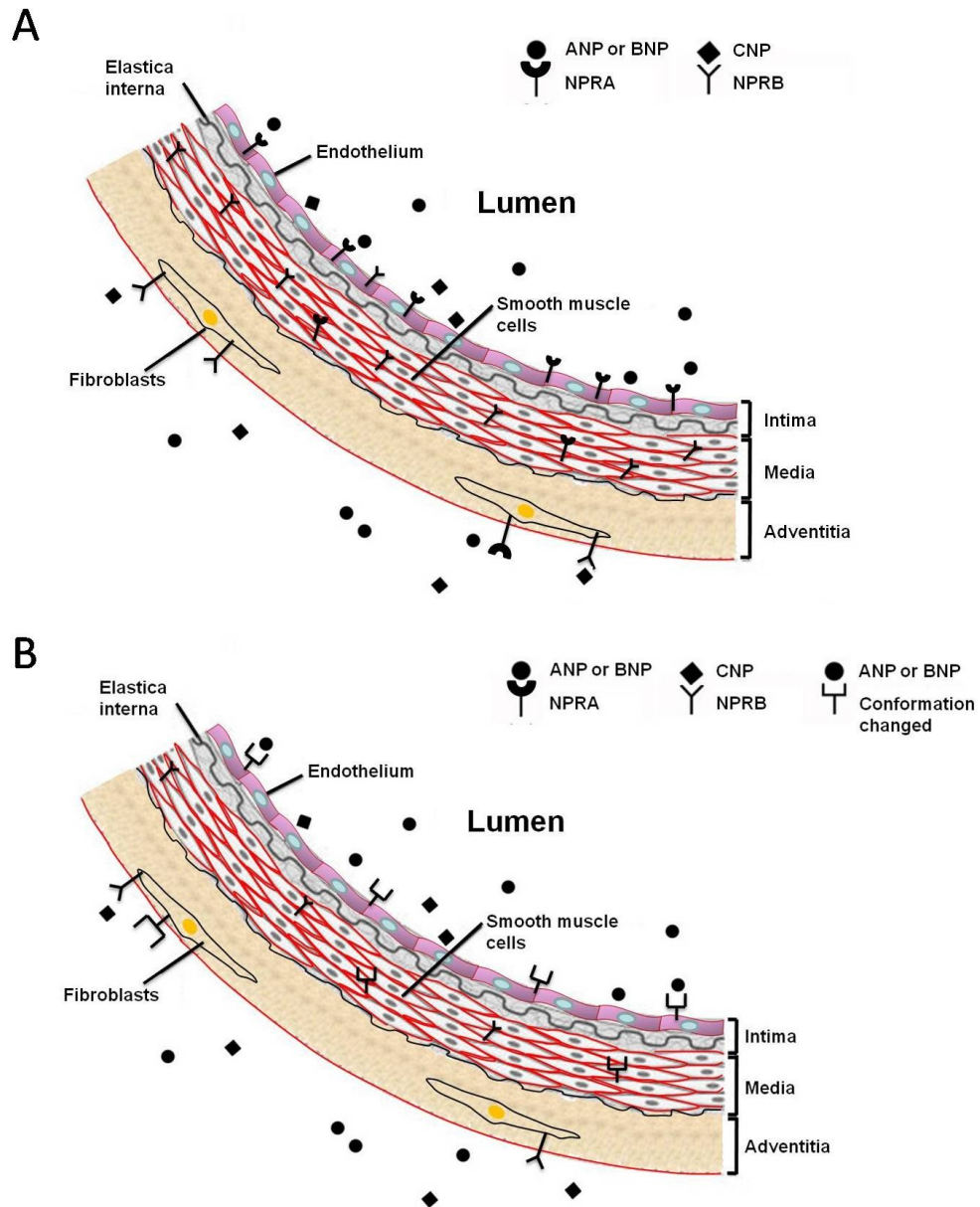
Figure 45. Anatomy of arterial wall and NPR distribution under normal and abnormal states. **(A)** Anatomy of normal arterial wall and NPR distribution. The vessel wall consists of three layers (intima, media, and adventitia). The innermost layer is mainly formed by elastica interna and endothelial cells, which is in direct contact with the blood blow in the lumen. The outermost layer is the tunica externa (also known as adventitia) and is composed of connective tissue and some fibroblasts. Between intima and adventitia is the tunica media, this layer is made up by elastic tissue and smooth muscle cells. The NPRs are distributed differently in these types of cells with unbalanced proportions, NPs bind to their cognate receptors and mediate cGMP release to exert vasodilating effect. **(B)** Anatomy of abnormal arterial wall and impaired NPR distribution. The conformation of NPRA is changed after interacting with NPRB, which may inhibit the GC domain activation and attenuated its cGMP signalling. NPRB/cGMP signalling is also affected by the interaction of NPRA and less NPRB are present on the cell membrane. Consequently, the overall effects of NPRA and NPRB interaction lead to the dysfunction of NPs/NPRs/cGMP axis in regulating vasculature tone.

A proposed model for the impaired vasorelaxation in the artery has been raised in which, under normal condition, NPRA and NPRB have different distributions in the vessel layers, NPRA are preferentially located on the endothelium and also partly in VSMC and fibroblasts, whereas NPRB preferentially anchor on VSMC and fibroblasts (Figure 45A). Under pathological condition, NPRA and NPRB interaction leads to a conformational change in the binding domain of the NPRA while the NPRB is down-regulated on the cell membrane, blocking the NPR/cGMP signalling and thus causing the dysfunction in regulating vasculature tone (Figure 45B). Indeed, the finding that NPRA had a physical interaction with NPRB in the FRET assay may support this notion (Figure 44). In that regard, the precise site(s) of the interaction remains to be determined.

Moreover, it has been reported that the clearance receptor is the most abundant NPR in most tissues (Maack, 1992). It also has been shown in VSMC that knockdown of NPRA enhanced NPRC expression and signalling (Li *et al.*, 2011). In present study, the interaction between NPRA (or NPRB) and NPRC was not investigated, but first orientating experiments indicate that the co-transfection of NPRA with NPRC or NPRB with NPRC showed at least no significant influence on cGMP production stimulated by ANP/BNP or CNP (Appendix 7). This cannot exclude the possibility that a NPRA/NPRC or NPRB/NPRC heteromeric complexes play an unseen role in mediating cAMP signalling, since it has been suggested that NPRC regulates adenylyl cyclase activity (Mouawad *et al.*, 2004). Nevertheless, it will be of interest to further investigate how these three NPRs might influence each other in receptor complexes and whether such interaction might play a role in the patients with CVD, also by comparing the NPRs distribution in tissue of healthy people. Also, it is urged to identify whether any receptor conformation might lead to intracellular signalling alteration in response to different NPs. This might also allow the identification of a pharmacologically-distinct receptor (complex) signalling specifically in response to certain peptide, and finally, to open the avenue for a better understanding of the pathogenesis of CVD.

Chapter IV

The receptor profiles of different B-type natriuretic peptides and the degradation profile of BNP1-42

Chapter 4

The receptor profiles of different B-type natriuretic peptides and the degradation profile of BNP1-42

4.1. Introduction

BNP has been viewed as a potent cardiac hormone in regulating blood vessel tone and kidney function, exerting natriuretic, anti-hypertrophic, anti-fibrotic, and BP-lowering effects, with the longest AA sequence compared to its structurally similar but genetically distinct homologous peptides, ANP and CNP. Meanwhile, BNP and the inactive N-terminal proBNP serve as biomarkers for many CVD, such as decompensated HF, due to their high negative predictive values (Hunt *et al.*, 1997, McCullough *et al.*, 2002, Maisel *et al.*, 2002, Maisel *et al.*, 2004). The synthesis of mature human BNP (hBNP1-32) occurs almost exclusively in the ventricular myocardium. Different molecular weight forms of BNP can be generated through distinct cleavages of the BNP precursor, proBNP which has a length of 108 AA, or from alternative RNA splicing, as the ASBNP (Pan *et al.*, 2009) (Figure 46). Notably, apart from the mature mouse BNP (mBNP1-32), another circulating form of mBNP was isolated and determined as mBNP1-45, with a 22-AA N-terminus (Steinhelper, 1993, Sudoh *et al.*, 1989) (Figure 47).

Many physiological responses of BNP are mediated by cGMP formation via BNP binding to NPRA, and its clearance from the circulation mainly involves the common NP clearance receptor NPRC. Besides, the circulating BNP level could also be controlled via glomerular filtration and degradation by peptidases, to generate different BNP metabolites/catabolites with or without bioactivity. Interestingly, our laboratory reported that mouse BNP7-32 (mBNP7-32) was yielded from mature mBNP1-32 by murine renal metallopeptidase meprin A (EC 3.4.24.18) (Figure 47) (Pankow *et al.*, 2007), and it is BNP8-32 in human (hBNP8-32) (Walther, 2007). Both mBNP7-32 and hBNP8-32, but neither BNP1-32 nor BNP3-32 (a BNP metabolite cleaved by dipeptidyl peptidase IV at N-terminus of BNP1-32) (Brandt *et al.*, 2006), are substrates of NEP (Brandt *et al.*, 2006, Pankow *et al.*, 2007, Boerrigter *et al.*, 2009). Later, Boerrigter *et al.* suggested that hBNP8-32 has a similar haemodynamic but reduced renal effect *in vivo* compared with native hBNP1-32 (Boerrigter *et al.*, 2009), indicating that such different BNPs resulting

from enzymatic processing may have different receptor profiles and thus physiological function. Moreover, it has been described in 1.2.5 that the designed C-terminal truncated form of ASBNP, namely BNP1-42, had little vasodilating effect but a preserved renal action, e.g. stimulating cGMP in MC and glomeruli, increasing GFR and suppressing plasma renin and angiotensin, and inducing natriuresis and diuresis (Pan *et al.*, 2009), implicating there might be an undefined pGC linked receptor in MC with hBNP1-42 as a potential ligand, or there might be a cell-type specific peptidase which rapidly metabolizes hBNP1-42 to a bioactive one in MC.
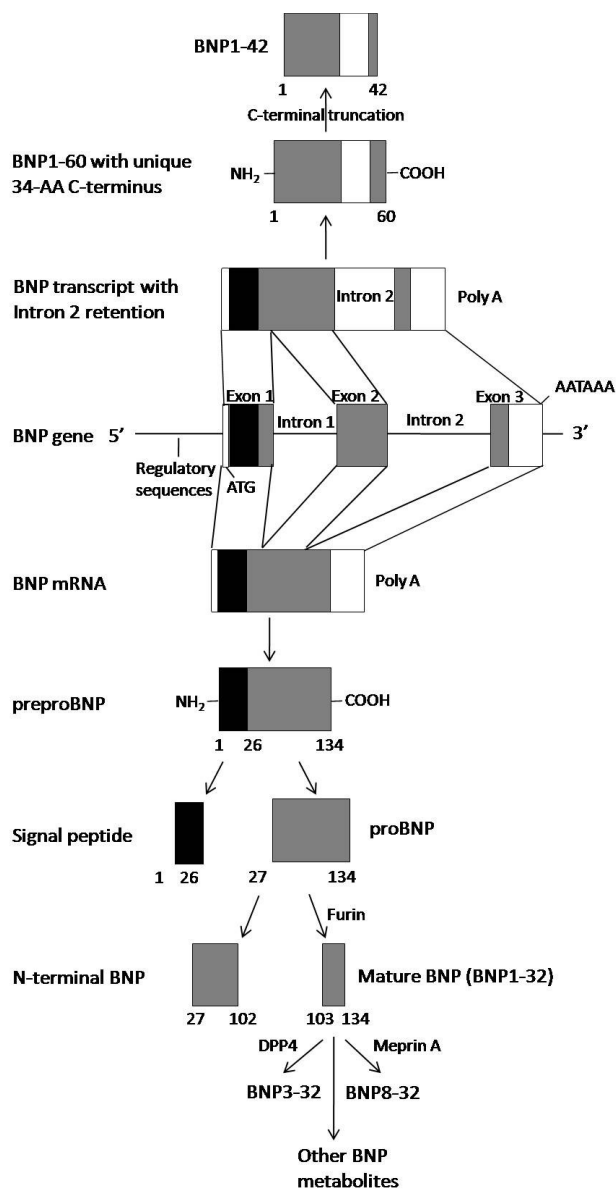
Figure 46. Scheme of the genetic structure of the human BNP gene and the biosynthetic pathways for the human BNP, BNP1-42, and BNP metabolites. BNP1-42 was designed by a 18-AA deletion at C-terminus of ASBNP (BNP1-60), which is an alternative spliced transcript for BNP resulting from intron 2 retention (Pan *et al.*, 2009). BNP3-32 is the product of dipeptidyl-peptidase IV (DPP4)-cleaved BNP1-32, while BNP8-32 is a metabolite of BNP1-32 cleaved by meprin A.
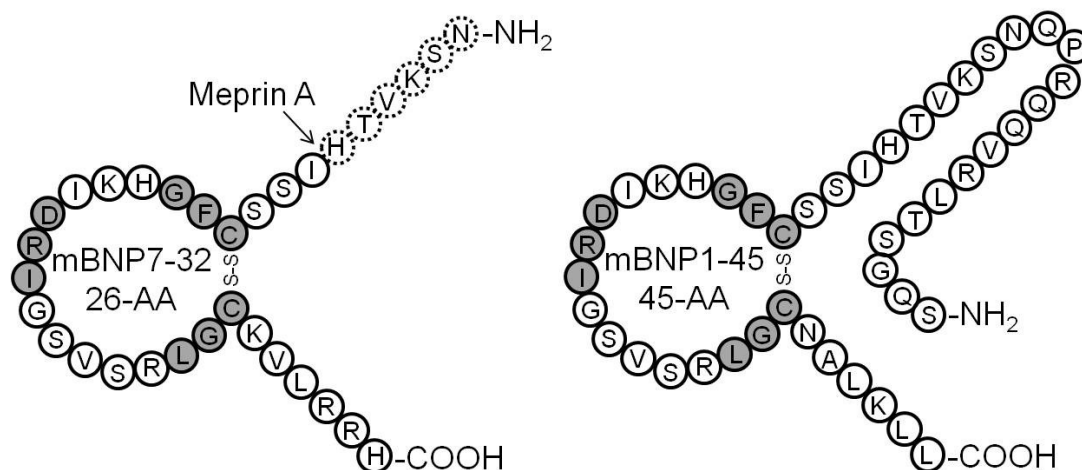
Figure 47. Amino acid sequences of mouse BNP7-32 and mouse BNP1-45. Residues in grey circles denote those are conserved among the mouse natriuretic peptides. Circles in dotted boundaries denote the disappearance of those amino acids from mBNP1-32. The arrow indicates the cleavage site of meprin A.

This chapter aims to identify specific receptor profiles of different BNPs, including two murine BNPs, the N-terminal elongated mBNP1-45 and N-terminal truncated mBNP7-32, and also the human BNP variant, hBNP1-42, resulting from a truncated version of the alternative spliced transcript of hBNP (Pan *et al.*, 2009). The potency and efficacy of these BNPs in stimulating cGMP generation were studied in various cell types (transfected HEK293 cells, cultured primary BAEC, HDMEC, VSMC, and MC) in comparison to their native BNP, mBNP1-32 and hBNP1-32, respectively. Meanwhile, it is also aimed to explore if the metabolism/degradation of hBNP1-42 differs from that of native BNP, whereby peptide degradation by NEP or murine lung and kidney membranes were specifically examined by HPLC.

4.2. Materials and methods

4.2.1. Materials and reagents

mBNP7-32, mBNP1-45, and hBNP1-42 were synthesized by Biosyntan GmbH (Berlin-Buch, Germany) with a purity of 95%. All other materials and reagents refers to 3.2.1.

4.2.2. Culture of cells, transfection, and stimulation

Culture of the permanent cells and primary cells, transfection, and cell stimulation refer to 2.2.3 and 2.2.4. Exclusively Lipofectamine 2000 transfection reagent was used for plasmid DNA transfection.

4.2.3. Measurement of cGMP

Measurement of cGMP has been described in 2.2.5.

4.2.4. Membrane preparations

Mouse lung and kidney membranes were prepared by homogenising whole tissue pieces in a 50 mM Tris buffer (pH 7.4) with an IKA Ultra-Turrax® T25 homogeniser (Staufen, Germany). Samples were centrifuged at 40,000 g to separate membranes from cytosol. After a washing step, the pellet was resuspended in 50 mM Tris buffer and stored at -80 °C. The total protein content of the membrane preparations was determined by BCA assay and adjusted depending on the experiment.

4.2.5. Degradation of BNP1-42 by membrane preparations and recombinant human NEP

hBNP1-42 was incubated with different membrane preparations (mentioned in 4.2.4) in Tris buffer (50 mM, pH 7.5) supplemented with 0.1% BSA (Tris/BSA - buffer) at 37 °C. Additionally, hBNP1-42 in the concentration of 10^{-5} M was incubated with 100 µl recombinant human NEP (1 µl stock solution first diluted with 9 µl Assay Buffer (Assay Buffer: 50 mM Tris, 0.05% Brij35, pH 9.0), and then further diluted in 50 mM Tris buffer to a final volume of 100 µl) at 37 °C for 10 or 30 min. The reaction was stopped by adding perchloric acid (0.35 M). After centrifugation, the supernatant has been analyzed with High-Performance-Liquid-Chromatography using an UV-Detector. A linear gradient (Buffer A: acetonitrile

with 0.05 % trifluoracetic acid; and Buffer B: double distilled water with 0.05% trifluoracetic acid) for both analyses was used to separate peptides on a RP Nucleosil 100 C12 column (Phenomenex, Torrance, CA, USA). Peak areas have been calculated with the LabSolutions® software from Shimadzu.

4.2.6. Statistical analysis

Results are expressed throughout as the mean $\pm$ SEM unless otherwise indicated. For the cell culture studies, each experiment was performed in triplicate in 2 or 3 independent experiments. Differences between groups were compared with one-way ANOVA followed by the Bonferroni posttest when the global test was significant. Two-way ANOVA was used to compare the main group effects of hBNP1-32, hBNP1-42, mBNP1-32, and mBNP1-45 in dose-response curves. EC_{50} values were calculated by using sigmoidal dose response curve fit in GraphPad Prism 5.0 (GraphPad Software, San Diego, CA, USA). A P value of < 0.05 was considered as significant.

4.3. Results

4.3.1. Characterisation of cGMP generation by different BNPs in receptor transfected cells

In human NPRA-transfected HEK293 cells, total cGMP concentration increased only one fifth with 10^{-6} M of hBNP1-42 compared to the cGMP stimulated with equimolar hBNP1-32 (Figure 48A). Neither hBNP1-32 nor hBNP1-42 were able to mediate robust cGMP generation in human NPRB-transfected HEK293 cells, though hBNP1-32 significantly stimulated the human NPRB versus the control (Figure 48B). Dose-response curves confirmed hBNP1-32 to be more efficient than hBNP1-42 in NPRA-transfected HEK293 cells. Such curves also exhibited a significantly lower EC_{50} and thus a higher potency of hBNP1-32 than that of hBNP1-42 ($P < 0.001$; Figure 48C).
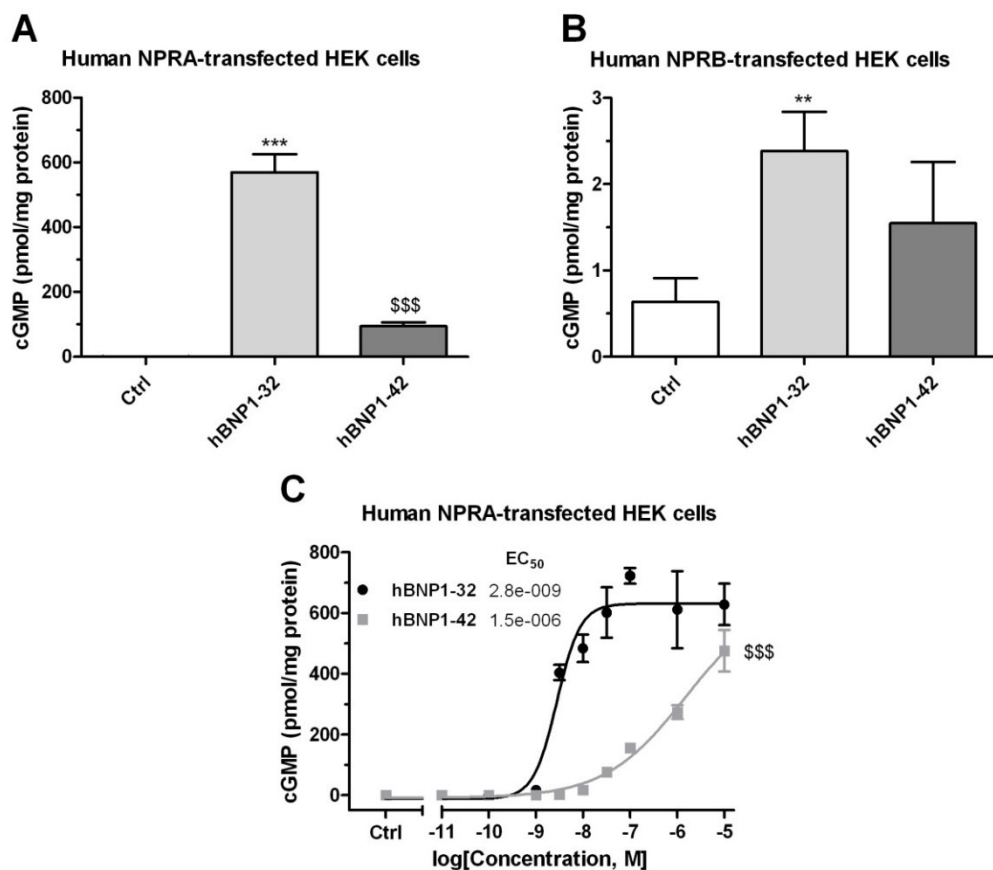
Figure 48. Comparison of cGMP generation by hBNP1-32 or hBNP1-42 in receptor transfected HEK293 cells. **(A)** Absolute values of cGMP generation with human NPRA-transfected HEK293 cells; **(B)** Absolute values of cGMP generation with human NPRB-transfected HEK293 cells; **(C)** Dose-response curves stimulated by 10^{-11} to 10^{-5} M hBNP1-32 and hBNP1-42 in human NPRA-transfected HEK293 cells. Experiments were conducted in 3 independent settings as triplicates. **$P < 0.01$, ***$P < 0.001$ *vs*. control (Ctrl); $^{\$\$\$}P < 0.001$ *vs*. hBNP1-32.

To evaluate the efficacy of murine BNPs to stimulate cGMP generation, 10^{-6} M of mBNP1-32, mBNP1-45, or mBNP7-32 were incubated with HEK293 cells transfected by mouse NPRs. All three murine BNPs were able to mediate potent cGMP generation with no significant differences among them (Figure 49A). Similar to the hBNPs in Figure 48B, none of the mBNPs was able to elicit robust cGMP formation via mouse NPRB (Figure 49B). Dose-response curves identified mBNP1-45 as the most potent BNP with an approximately 4-fold lower EC_{50} in comparison to mBNP1-32 and mBNP7-32 (Figure 49C), although there were no differences in maximal efficacy in cGMP formation among them.
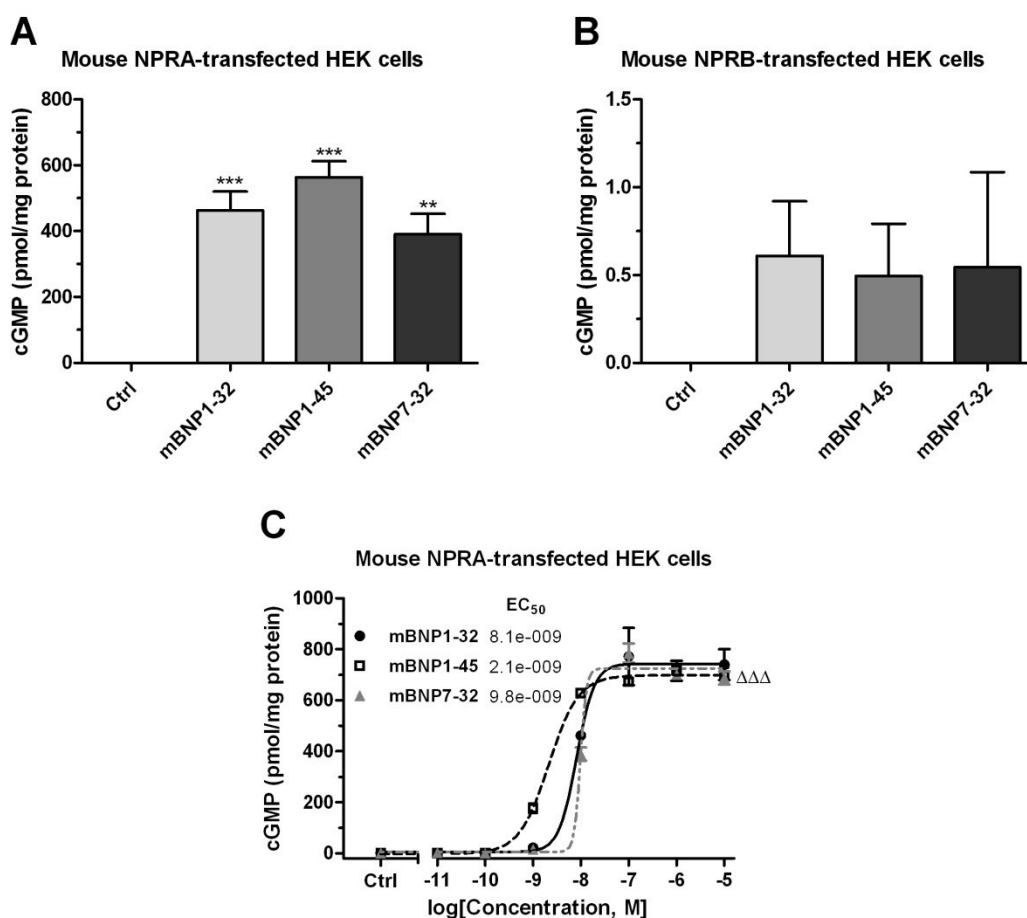
Figure 49. Comparison of cGMP generation by mBNP1-32, mBNP1-45, or mBNP7-32 in mouse receptor transfected HEK293 cells. **(A)** Absolute values of cGMP generation with mouse NPRA-transfected HEK293 cells; **(B)** Absolute values of cGMP generation with mouse NPRB-transfected HEK293 cells; **(C)** Dose-response curves stimulated by 10^{-11} to 10^{-5} M mBNP1-32, mBNP1-45, and mBNP7-32 in mouse NPRA-transfected HEK293 cells. Experiments were conducted in 3 independent settings as triplicates. $**P < 0.01$, $***P < 0.001$ *vs.* control (Ctrl); $^{\Delta\Delta\Delta}P < 0.001$ mBNP7-32 *vs.* mBNP1-45.

4.3.2. Characterisation of cGMP generation by different BNPs in primary cells

To further evaluate the specific receptor profile of the investigated BNPs in cultured primary cells with varying NPRA and NPRB expression, and also to test if activation of GC in the mouse kidney cells by hBNP1-42 may result in similar cGMP accumulation compared to native BNP was seen in human kidney cells before (Pan *et al.*, 2009), firstly HDMEC predominantly expressing NPRA were stimulated with 10^{-6} M of each BNP. The most efficacious NP among the BNPs was hBNP1-32, increasing the cGMP level ~50-fold above basal, whereas hBNP1-42 had least efficacy yielding cGMP levels being only one third of hBNP1-32 (Figure 50). Probably due to the species difference between the murine ligands and endogenous human receptor, the three mouse BNPs had a similar cGMP production but were less efficacious than hBNP1-32 ($P > 0.05$, Figure 50).
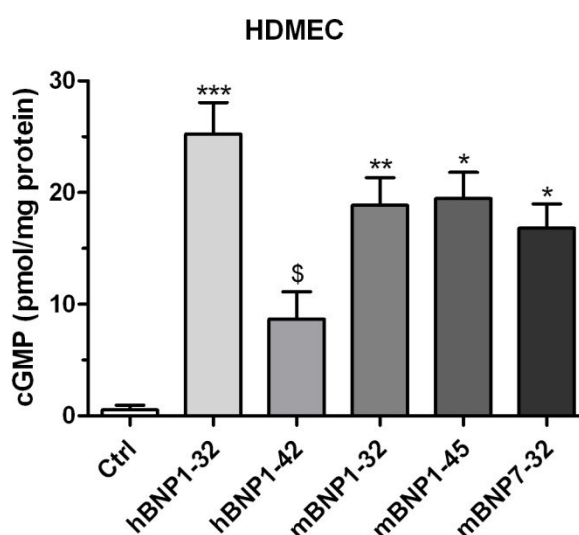
Figure 50. Generation of cGMP in cultured primary human dermal microvascular endothelial cells. Absolute values of cGMP generation are given after stimulation with either solvent (control), or 10^{-6} M of different BNPs. Experiments were conducted in 2 independent settings as triplicates. *$P < 0.05$, **$P < 0.01$, ***$P < 0.001$ *vs.* control (Ctrl); $^{\$}P < 0.001$ *vs.* hBNP1-32.

By contrast, in mouse kidney MC, where NPRB is mainly expressed, hBNP1-32 was 2.1-fold more efficacious than hBNP1-42, but apparently its cGMP generation was much lower compared to that of the mouse BNPs (Figure 51A). A similar cGMP stimulation pattern was found in VSMC, which express both NPRA and NPRB. Interestingly, no difference between hBNP1-32 and hBNP1-42 was detected in such cells (figure 51B).
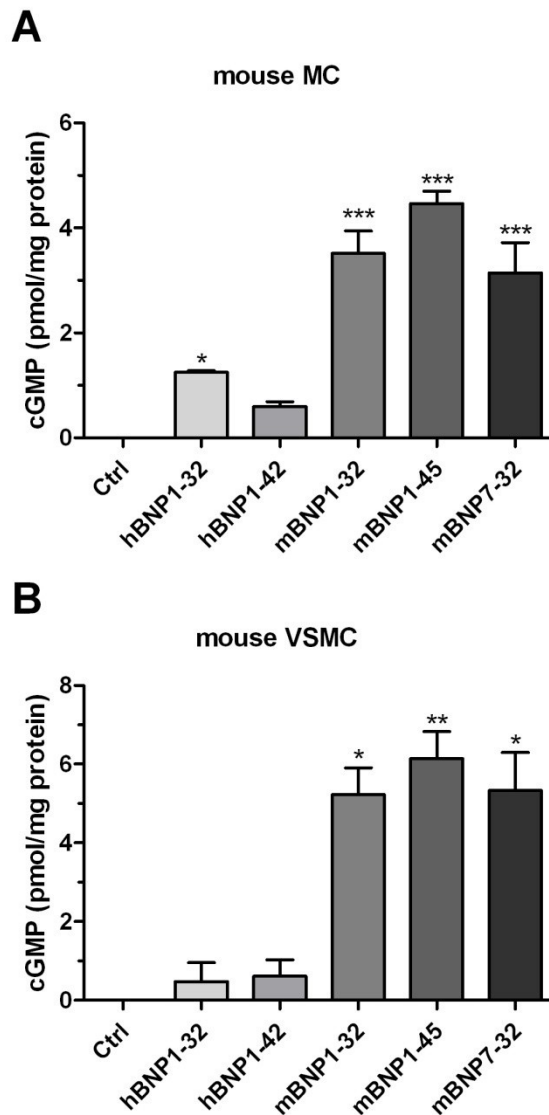
Figure 51. Generation of cGMP in cultured primary cells. **(A)** mouse mesangial cells; **(B)** mouse vascular smooth muscle cells. Absolute values of cGMP generation are given after stimulation with either solvent (control), or 10^{-6} M of different BNPs. Experiments were conducted in 2 independent settings as triplicates. $*P < 0.05$, $**P < 0.01$, $***P < 0.001$ *vs.* control (Ctrl).

4.3.3. Characterisation of the degradation profile of hBNP1-42

To investigate whether the different relation of hBNP1-42 to hBNP1-32 effects in different primary cells is due to its undefined metabolic signature, the degradation profile of hBNP1-42 was characterised by incubating it with human recombinant NEP and membrane preparations of different species and organs. After 10 min incubation with NEP, nearly no degradation occurred for both hBNPs, whereas 28.2% of CNP was degraded by NEP (Figure 52A). After 30 min incubation, there was still 89.6% hBNP1-32 remaining, while one third of BNP1-42 was degraded by NEP. At

the same time 68.1% CNP was degraded (Figure 52A). These results suggest that hBNP1-42 is a better substrate than hBNP1-32 but still not as good as the classical substrate CNP. Further analyses were conducted on the catabolism of hBNP1-42 on both murine lung and kidney membrane preparations. By using HPLC it was identified that hBNP1-42 was degraded much faster by the kidney membrane than lung membrane (Figure 52B).
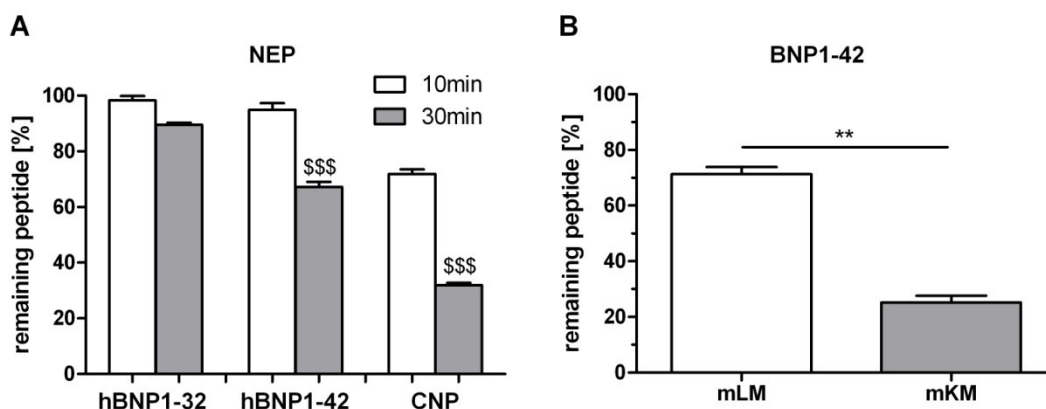
Figure 52. Percentage of degradation of natriuretic peptides by recombinant human neprilysin or by murine lung membrane (mLM) and kidney membrane (mKM). **(A)** hBNP1-32, hBNP1-42, and CNP of 10^{-5} M were incubated with NEP for 10 or 30 min. **(B)** Remaining BNP1-42 percentage after 10min incubation with mLM and mKM. Experiments were conducted in 2 independent settings as duplicates. $^{\$\$\$}P < 0.001$ *vs.* hBNP1-32.

Interestingly, apart from the significant difference in hBNP1-42 degradation rate in murine membrane preparations, the metabolisms/degradation products of hBNP1-42 also differed between lung and kidney membranes. As seen in Figure 54A ignoring the background before 8 min and after 25 min, a unique peak appeared at 21 min when using only hBNP1-42. After co-incubating with either lung or kidney membrane preparations, the hBNP1-42 peak became smaller, while three metabolisms/degradation peaks came up at different time points in mouse lung membrane preparation (Figure 53B). By contrast, three more undefined peaks (at 8.5, 16 and 20 min) occurred in the kidney membrane while did not exist in the lung membrane (Figure 53B&C).
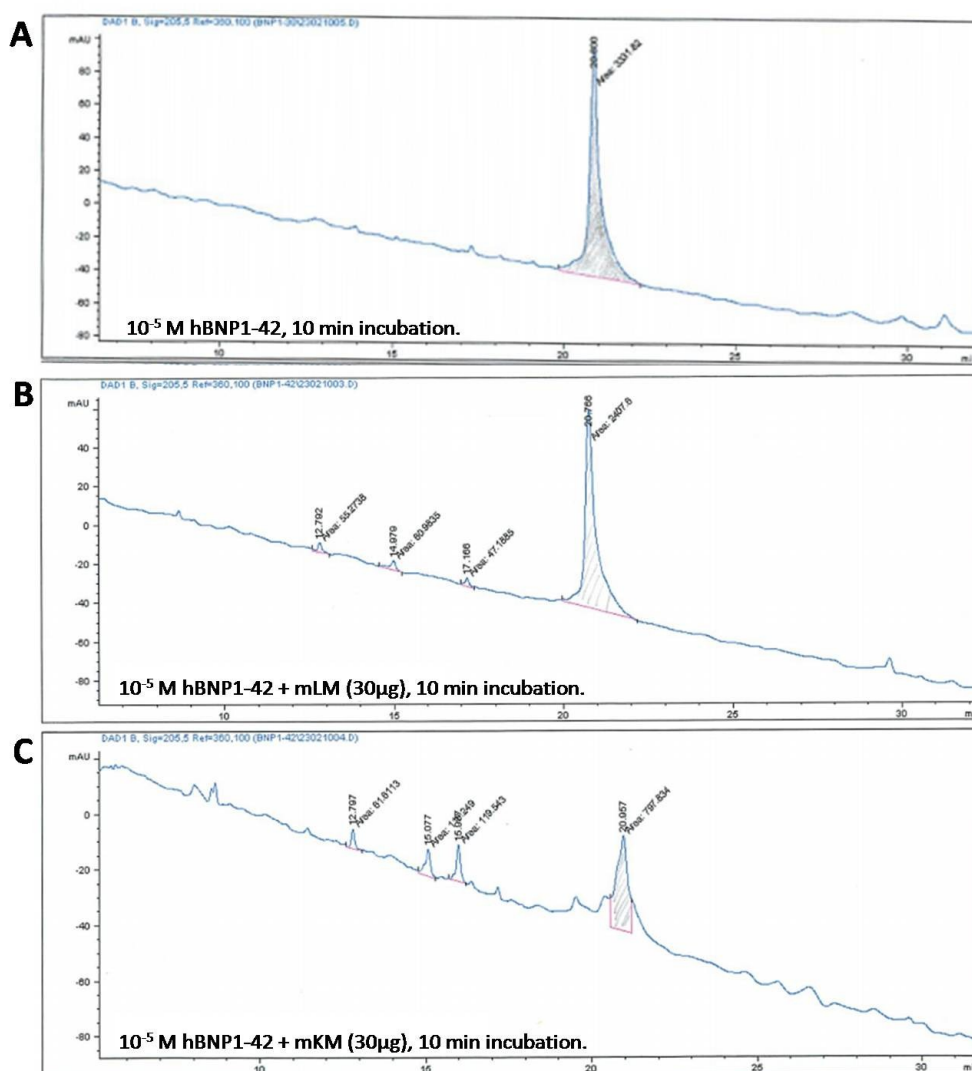
Figure 53. Representative HPLC chromatograms of metabolisms/degradation of hBNP1-42 in murine lung and kidney membranes. **(A)** hBNP1-42 alone; **(B)** hBNP1-42 with murine lung membranes (mLM). hBNP1-42 of 10^{-5} M were incubated with 30 µg mLM preparations for 10 min. **(C)** hBNP1-42 with murine kidney membranes (mKM). hBNP1-42 at 10^{-5} M were incubated with 30 µg mKM preparations for 10 min.

Given the species difference in aforementioned HPLC degradation study (human peptide and murine membrane preparations), it could be that hBNP1-42 is differently truncated by human kidney and lung membranes. Hence, a similar degradation study was carried out in human lung and kidney membrane preparations. As for human, hBNP1-42 was also faster degraded by the kidney membrane than lung membrane (Figure 54), though less dramatic in comparison to that with murine membranes. A different hBNP1-42 metabolism profile could also be seen between lung and kidney membrane preparations. Two different peaks (at 17 and 22 min) either occurred in the lung membrane (at 17 min) or in the kidney membrane (at 22

min) (Figure 55B&C), although three out of four product peaks (at 8.5, 12.5, and 19.5 min) occurred both in the lung membrane or kidney membrane.
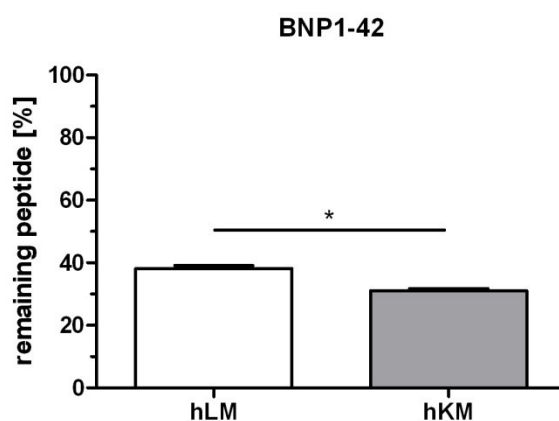
Figure 54. Remaining BNP1-42 percentage after 10min incubation in human lung membrane (hLM) or human kidney membrane (hKM). Experiments were conducted in 2 independent settings as duplicates.
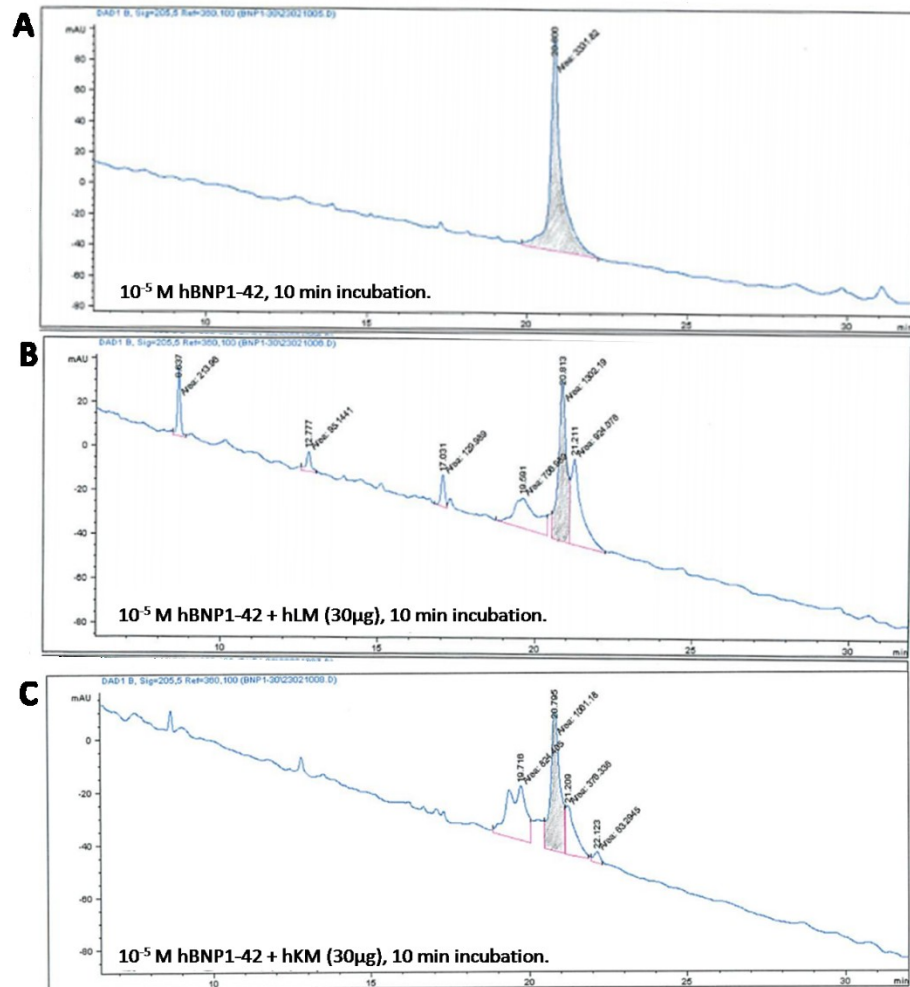
Figure 55. Representative HPLC chromatograms of metabolisms/degradation of hBNP1-42 in human lung and kidney membranes. **(A)** hBNP1-42 alone; **(B)** hBNP1-42 with human lung membranes (hLM). hBNP1-42 of 10^{-5} M were incubated with 30 µg hLM preparations for 10 min. **(C)** hBNP1-42 with human kidney membranes (hKM). hBNP1-42 of 10^{-5} M were incubated with 30 µg hKM preparations for 10 min.

4.4. Discussion

In this chapter, the receptor profiles of different molecular weight forms of BNP in different species, i.e. mBNP7-32, mBNP1-45, and hBNP1-42 were investigated. In addition, the degradation profile of hBNP1-42 *in vitro* was identified. Similar to the finding of cGMP generation by Pankow *et al.* (2007), the mBNP1-32 metabolite mBNP7-32, could activate NPRA and increase cGMP generation with no statistical difference to mBNP1-32 and mBNP1-45 in either mouse NPRA-transfected HEK293 cells, or primary HDMEC, mouse MC and mouse VSMC. In contrast, hBNP1-42 mediated significant lower cGMP formation in human NPRA-transfected HEK293 cells and endogenous NPRA-rich HDMEC when compared to the native hBNP1-32. Meanwhile, very limited cGMP generation by either hBNP1-32 or hBNP1-42 has been observed in mouse MC and VSMC, where have endogenously predominant NPRB but also minor NPRA expression. These findings agree with the previous description that hBNP1-42 lacked vascular effects (Pan *et al.*, 2009), suggesting that hBNP1-42 is neither a potent activator of NPRA nor NPRB. In addition, HPLC identified that hBNP1-42 is degraded much faster by the kidney membrane than lung membrane, and metabolism of hBNP1-42 on both human and murine kidney membrane are different from that of lung membrane, implicating there might be a specific peptidase in the kidney metabolising hBNP1-42.

Some evidences have suggested that proteases in the circulation degrade proBNP1-108 into many bioactive or inactive fragments of BNP isoforms, e.g. furin has been demonstrated to cleave proBNP1-108 into NT-proBNP and BNP1-32 (Sawada *et al.*, 1997); whereas corin-mediated cleavage led to the production of BNP4-32 (Semenov *et al.*, 2010). Other studies revealed that BNP could also be metabolised to BNP3-32, BNP5-32, BNP7-32, BNP8-32, BNP2-31, BNP5-31, BNP1-30, BNP4-27 by various proteolytic enzymes (Shimizu *et al.*, 2002, Walther *et al.*, 2004a, Walther, 2007, Schellenberger *et al.*, 2009, Schwiebs *et al.*, 2011). By using matrix assisted laser desorption ionization-time of flight mass spectrometry (MALDI-T of MS) immunoassay, our group has manifested the existence of mBNP7-32 on mouse lung membrane, which at least *in vitro* is produced from mature mBNP1-32 by meprin A (Pankow *et al.*, 2007). Meanwhile, it is hBNP8-32 for hBNP1-32 after enzymatic processing by the renal meprin A (Walther, 2007).

126

Boerrigter *et al.* (2007) declared that the N-terminal truncated BNP3-32 has reduced vasodilating and natriuretic bioactivity compared with BNP1-32 *in vivo* (Boerrigter *et al.*, 2007), however, the ability of BNP3-32 in stimulating cGMP has not been determined. Another N-terminal truncated BNP (hBNP8-32) has shown a similar haemodynamic but reduced renal effect *in vivo* compared with native hBNP1-32 (Boerrigter *et al.*, 2009). Such findings led to the speculation that the reduced bioactivity may involve a less cGMP formation mediated by these BNP metabolites. In that regard, Pankow *et al.* (2007) found a less pronounced but preserved cGMP formation by mBNP7-32 than mBNP1-32 in human NPRA-transfected cells, although the species differences between the ligand and receptor may lead to a discrepancy in its cGMP signalling.

To increase the knowledge regarding the receptor profile and bioactivity of N-terminal truncated mBNP7-32, a cell-based assay measuring cGMP production was performed with native mBNP1-32 and the N-terminal elongated mBNP1-45. Here it shows that mBNP7-32 selectively activates mouse NPRA and displays slight lower potency and efficacy in cGMP production but no statistically differences compared with mBNP1-32 or mBNP1-45 in either receptor transfected HEK293 cells or primary cells. This could be explained by the slightly lowered receptor affinity of mBNP7-32 compared to native ligands, which agrees with a previous report by Dickey and Potter that the length or size of NPs might be associated with the receptor affinity (Dickey and Potter, 2011). ANP of 28-AA is proven to be more potent than BNP of 32-AA in cGMP production because of the higher affinity to the NPRA (Potter *et al.*, 2006, Pankow *et al.*, 2007). However, a contradiction to the suggestion by Dickey and Potter is that the N-terminal elongated mBNP1-45 could stimulate cGMP generation with a tendency toward increased activity but no significant difference when comparing its potency with that of mBNP1-32, and it is significant when comparing with that of mBNP7-32. Besides, our unpublished data also suggest a C-terminal truncated BNP (mBNP1-30) favours a better efficacy and higher potency in generating cGMP in comparison to native mBNP1-32. Consequently, receptor affinity may not necessarily depend on NP size/length. Further studies are required to clarify the effect of NP size/length in receptor affinity and their relevance. Another explanation for the marginally less cGMP production mediated by mBNP7-32 could be that it is faster degraded to inactive fragments than mBNP1-32 (Pankow *et al.*, 2007) and mBNP1-45. Previous study also implied a

presumptive association between the size of NPs and their degradability by NEP, where they demonstrated that mBNP1-32 cleaved by meprin A to become a substrate for NEP (Pankow *et al.*, 2007). Although study presented here has not investigated the degradability of mBNP1-45 by NEP, very unlikely that mBNP1-45 is accessible to the binding cavity of NEP, as the truncation by meprin A is the prerequisite for fast mBNP clearance (Pankow *et al.*, 2007). The degradation profile of the bioactive BNP metabolites requires further elucidation.

Previous study by Pan *et al.* (2009) identified an alternative spliced transcript for BNP resulting from intronic retention, namely ASBNP. Unlike native BNP, ASBNP of 34-AA reconstituted C-terminus failed to stimulate cGMP in vascular cells or vasorelax pre-constricted arterial rings. Given structural considerations, the designed hBNP1-42 with a shortened C-terminus was generated resulting from the end 18-AA deletion of ASBNP (hBNP1-60), though it is still longer than native BNP1-32. Congruently, data presented here show that hBNP1-42 is a poor activator of NPRA with a EC_{50} of three orders of magnitude higher compared to that of hBNP1-32 in NPRA-transfected HEK293 cells. This is possibly due to the long C-terminus of hBNP1-42 and thus lowering its affinity to NPRA. It is worth noting that, the C-terminus of hBNP1-42 is reconstituted and it is completely different from that of hBNP1-32, such difference in AA composition may also influence the ability of NP to stimulate cGMP. Therefore, further experiments should be performed to test whether the long C-terminus of hBNP1-42 or specific AA in the C-terminus being responsible for the NPRA activation.

Moreover, unlike the finding by Pan *et al.* (2009) that hBNP1-42 could equipotently stimulate cGMP as hBNP1-32 in cultured human MC, hBNP1-42 could only mediate half of cGMP generation of hBNP1-32 in mouse MC. The species-specific difference, independent experimental treatment may account for this discrepancy. Firstly, human kidney/MC were used in previous study (Pan *et al.*, 2009), whereas murine kidney/MC were investigated in this chapter. As compared to mBNP1-32, hBNP1-32 was much less potent in activating endogenous mouse NPRA in mouse MC (Figure 51A), which is in keeping with the data demonstrating the attenuated hBNP1-32-mediated cGMP generation in mouse NPRA-transfected cells (Figure 56). Secondly, the human MC were stimulated with 10^{-5} M of hBNP1-32 or hBNP1-42 for 10 min in the previous study by Pan *et al.*, but a protocol of 5

min of 10^{-6} M NPs stimulation in mouse MC was used in this chapter. Thirdly, there might be another receptor in human MC that is not in mouse MC or does not respond to hBNP1-42. Thus, only further experiments using human MC to be stimulated with hBNP1-32 and hBNP1-42 for a same incubation time can clarify on this discrepancy.
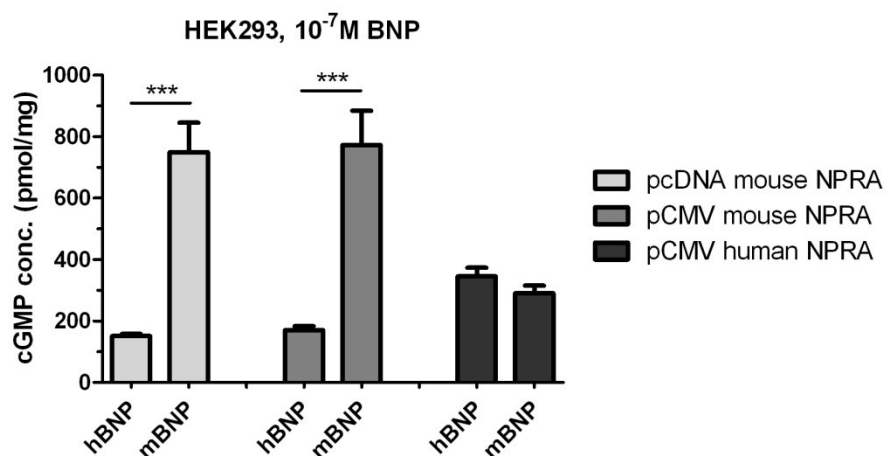
Figure 56. cGMP generation comparisons of transfected HEK293 cells. Three NPRA constructs (two commercial purchased pCMV NPRA of human and mouse species and cloned pcDNA3.1(-) mouse NPRA) were tested.

A slight decreased cGMP production by mouse BNPs in HDMEC which express endogenous human NPRA (Figure 50), and an even obvious decreased cGMP pattern by human BNPs in mouse MC and VSMC (Figure 51) could be seen in data presented in this chapter. One possible explanation is that human BNP has lower affinity to mouse NPRA, which has been aforementioned. In addition, evidence by Schoenfeld and his colleagues suggested that human NPRA is less sensitive than rat or mouse NPRA to the changes in the loop structure of ANP and to the species differences in BNP (Schoenfeld *et al.*, 1995), which is well congruent with the finding that hBNP mediated mNPRA/cGMP generation is significantly less than that of mBNP, whereas no significant difference occurs in human NPRA pattern (Figure 56). Therefore, it could lead to a further speculation that the species differences in activity and NPR specificity of BNP might be correlated to different AA composition in the peptide sequence. It may also related to propensity to form beta-sheet structures, flexibility patterns, dynamics properties and free conformations explored during the BNP simulation (Papaleo *et al.*, 2010).

Surprisingly, Pan *et al.* (2009) presented that hBNP1-42 favored distinct renal effects but lacked the dose-limiting hypotensive effects of BNP. It is of interest to

see if inhibiting NEP activity could further potentiate the renal action of hBNP1-42. Data presented here indicate that hBNP1-42 does not serve as a good NEP substrate since it was degraded by NEP at a relatively low speed compared to CNP. Hence, pharmacological blockage of NEP activity may not influence the renal action of hBNP1-42. However, HPLC data indicated a faster degradation of hBNP1-42 in the mouse kidney membrane than mouse lung membrane, and its metabolites/catabolites on the kidney membrane were different from that of lung membrane (Figure 53). Such discrepancy in the metabolism of hBNP1-42 indicates a tissue/organ-specific metabolic mechanism. Given the different species consideration, hBNP1-42 metabolism on human kidney and lung membrane were also studied. Congruently, hBNP1-42 was faster degraded on human kidney membrane than lung membrane (Figure 54), and a different hBNP1-42 metabolism profile could be observed between human lung and kidney membrane preparations (Figure 55). Of note, the degradation product peaks differed between human and mouse species, regardless of lung or kidney membrane preparations. The exact metabolites should be determined by using LC-MS and MALDI-T of MS to unveil the species-directed metabolism differences in the near future. Meanwhile, incorporating with the data from Pan *et al.* (2009), such findings also suggest that there might be a specific peptidase in the kidney metabolising hBNP1-42 to a bioactive BNP, or there is an unknown GC-linked receptor mediating the biofunction of hBNP1-42 in the kidney. The responsible peptidase(s)/receptor for selective renal actions of hBNP1-42 will require further study.

In conclusion, current study suggests that the species/degradability/sequence of NP may influence the receptor specificity and activity of different BNPs. Thus, sequence modification of BNPs or other NPs and identification of novel NP targets (e.g. specific pepdidase) in specific tissue/organ may lead to an advanced development of NP-based drug with desirable therpeutic effects and half-life.

Chapter V

Summary, general discussion and open questions

Chapter 5
Summary, general discussion and open questions

5.1. Summary

This study elucidates the pathophysiological consequences of the newly designed natriuretic peptide ACNP *in vitro* and *in vivo*, and explores the mechanisms of new interactions between the two functional receptors of the natriuretic peptide system, NPRA and NPRB. Also briefly, it has a glance at various BNP metabolites and the designed BNP variant, hBNP1-42, which is a truncated version of a hBNP (BNP1-60) that is production of an alternative spliced transcript. By using a variety of techniques involving biochemical, molecular biological, cellular biological, pharmacological and pathophysiological studies, the objectives/hypotheses of this thesis were tested and major findings are outline below:

1) The designed ACNP stimulates both NPRA and NPRB with similar potencies and efficacies to their endogenous peptides in receptor transfected HEK293 cells and COS7 cells. An augmented cGMP formation in comparison to ANP and CNP was seen in cultured primary cells (MC, VSMC, CF, BAEC, and HDMEC) having varying NPRA and NPRB distributions.

2) In sham-operated mice, ACNP exerted similar potency in lowering blood pressure compared to that of ANP or CNP. However, after myocardial infarction, only ANP, but not CNP or ACNP, ameliorated the MI-induced LV dysfunction. It is speculated that the lacking benefit of ACNP might relate to its poor resistance against degradation by an unknown enzyme(s) in mouse serum.

3) A down-regulated cGMP generation upon NP stimulation was observed in NPRA and NPRB double-transfected cells, and such inhibitory effect of heterogeneous receptor complexes on natural NP/NPR/cGMP signalling was dose-dependent. The attenuated CNP/NPRB/cGMP axis can be restored via silencing the NPRA expression using siRNA-NPRA; however, the impaired ANP- and BNP-mediated NPRA/cGMP signalling pathway in double-transfected cells was irresponsive to the application of siRNA-NPRB.

4) The increasing concentration of NPRA in cells co-transfected with NPRB leads to a supressed formation of NPRB mRNA and thus decreasing the amount of

NPRB protein on the membrane, which results in a lower cGMP release by CNP in such co-transfected cells. However, impaired ANP and BNP signalling in double-transfected cells may not attribute to the receptor quantity alteration either from mRNA or protein level, but might due to the observed physical interaction between NPRA and NPRB that causes conformational changes within the receptor heterodimer, leading to less ligand accessibility or ligand mediated activation of GC.

5) hBNP1-42 is a poor NPRA activator. HPLC identified that hBNP1-42 is degraded much faster by the kidney membrane than lung membrane, and metabolisms of hBNP1-42 on the kidney membrane is different from that of lung membrane, suggesting a specific peptidase in the kidney metabolising hBNP1-42.

6) The N-terminal truncated BNP (mBNP7-32) and the elongated BNP (mBNP1-45) are able to stimulate NPRA comparable to the native BNP1-32, whereas the C-terminal reconstituted BNP (hBNP1-42) only can mediate a much less pronounced NPRA/cGMP formation. Such findings suggest the BNP-mediated NPRA/cGMP signalling may involve a specific recognition site(s) in the C-terminus of BNP.

Taken together, the data of this thesis give a novel insight into the new players and new interactions within the NP system. By searching the potential mechanisms of receptor-receptor interplay leading to an impaired cGMP generation, it may provide very promising treatment options and open novel directions for a better understanding of the aetiology of CVD.

5.2. General discussion

5.2.1 The sequence/structure of natriuretic peptides define the receptor specificity and their degradation pattern

The NPS exerts a unique pleiotropic strategy in regulating cardiovascular and renal homeostasis (Levin *et al.*, 1998, Rubattu *et al.*, 2008). However, exogenous administration of native ANP and BNP has been met with success but also limitations. Any treatment with only a single NP seems insufficient to address the complex interaction between structural, functional, neurohumoral, and renal mechanisms involved in the diseases. Thus, innovative therapeutic strategies emerged to engineer designed proteins via manipulating natively occurring peptides (e.g. elongating/deleting AA, or combining parts of two or more peptides to create

new chimeras), which may possess favorable therapeutic properties. Among the emerging chimeric peptides, we (Zhu *et al.*, 2011) and others (Chen *et al.*, 2011) synthesised ACNP, composed of the ring structure from CNP and the N- and C-terminus from human ANP.

In vitro studies with ACNP by measuring cGMP responses in transfected immortalized cells and cultured primary cells show that ACNP stimulates both NPRA and NPRB. Meanwhile, augmented cGMP release by ACNP is found in different primary cells, e.g. MC, VSMC, and CF. *In vivo* studies by Chen *et al.* implicates that natriuretic and diuretic potencies of ACNP are higher than that of ANP and CNP in normal rat, while it has a similar but not enhanced vasorelaxing effect in isolated rat abdominal aorta (Chen *et al.*, 2011). However, ACNP is fast degraded by NEP and in serum, which may partly explain its lacking cardioprotective effects towards mice subjected to MI. Another chimeric NP, designated as CD-NP (cenderitide), has been previously described (Lisy *et al.*, 2008, Dickey and Potter, 2011). CD-NP possesses the entire CNP structure and elongated C-terminus from DNP. In contrast, this designer peptide succeeds the merit of DNP in coping against proteolytic inactivation (Dickey and Potter, 2011), although it shows less potency and efficacy in mediating cGMP formation in comparison to ACNP, presumably due to the long C-terminus of CD-NP decreases its receptor affinity. Such favourable or unfavourable properties of ACNP and CD-NP led to some conjecture regarding the relation between the sequence/structure of natriuretic peptides and their receptor specificity/degradation pattern.

It has been reported that the highly conserved ring structure of a NP with a Cys-Cys disulfide bond determinatively participates in stimulation of cGMP accumulation (Misono *et al.*, 1984a, Schoenfeld *et al.*, 1995, Papaleo *et al.*, 2010). Especially, the sequence Leu9-Lys10-Leu11 in the ring portion of CNP executed essential roles for both elevation of cGMP and selectivity of the ligand for NPRB (Furuya *et al.*, 1992). Since CNP lacks the C-terminus, it could be deduced that the C-terminus may involve in the NPRA activation. By comparing the AA sequence among the NPs, it could be found that the common arginine (Arg) at the fourth position of C-terminus of human ANP (Arg27)/BNP (Arg30)/DNP (Arg27)/ACNP (Arg27) may play a crucial role for selectivity of the ligand for human NPRA,

although no substantial investigation has been reported and required further confirmation.

A 4-fold less cGMP formation mediated by human BNP in comparison to mouse BNP has been observed in mouse NPRA-transfected HEK293 cells, whereas no significant down-regulation of cGMP production is seen in mouse BNP/human NPRA stimulation pattern (Figure 56). This finding agrees with a previous report by Schoenfeld and his colleagues that human NPRA is less sensitive than rat or mouse NPRA to changes in the loop structure of ANP and to the species differences in BNP (Schoenfeld *et al.*, 1995), indicating the species differences in activity and NPR specificity of CNP and ANP/BNP might be correlated to different AA composition of the cyclic loop and C-terminus, also probably, related to propensity to form beta-sheet structures, flexibility patterns, dynamics properties and free conformations explored during the simulation (Papaleo *et al.*, 2010).

Furthermore, enzymatic processing of a NP hormone does not merely involve in degradation, it could also be essential modification of a specific peptide to take different actions in verying targets/organs. Undoubtedly, chimeras are designed for a better biofunction exertion combining dispersive effects from two or more distinct peptides, its degradation profile should be also considered and examined. NEP (EC 3.4.24.11), a ubiquitous peptidase with a very broad substrate spectrum, is always used to check the substrate specificity of a NP. The length of the N- and C-terminus of a NP has been found as a potential determinant for the degradation rate of the NP by NEP (Pankow *et al.*, 2009), although human BNP containing a considerably longer N-terminus compared to ANP, is resistant to be degraded directly by NEP. Longer N- and/or C-terminal extensions may cause spatial clashes and impede the correct orientation of the NP within the cave of NEP, leading to the inability of NEP to hydrolyse the target site in the ring structure (Pankow *et al.*, 2009). Deducibly, DNP with the long C-terminus of 15-AA is highly resistant to NEP proteolysis (Dickey and Potter, 2011). In current thesis, ACNP shared a similar degradation rate in comparison to that of ANP and CNP when incubated with NEP overtime, all these three NPs were significantly faster degraded than BNP. Therefore, approaches like enlongating C-terminal tail of the NPs/chimeric NPs may extend their half-life and thus potentiate the beneficial effects, although the elongated C-terminal tail may lead to poorer cGMP generation. Besides, data presented here suggest that ACNP is

faster degraded in mouse serum, implicating there might be peptidase(s) degrading ACNP in the serum and ACNP is a good substrate. Further investigations on specific proteases being responsible for the proteolysis of the NP and development of protease inhibitors may help to increase the half-life of NP-based drugs and selectively manipulating cardiorenal effects of the NPs by regulating NP proteolysis on target organs. Taken together, omnifarious considerations on the relation between AA sequence/structure of NP and receptor specificity/enzymatic degradation are necessary when designing chimeric peptides.

5.2.2 Mechanisms for the altered cGMP generation and its importance for cardiovascular diseases

The role of cGMP as a second messenger in cardiovascular physiology and pathology has been widely appreciated (Kuhn, 2004, Tsai and Kass, 2009, Kemp-Harper and Schmidt, 2009). Aberrant cGMP production and/or signalling may multifactorially occur due to e.g. abnormal NP degradation/metabolism, mutant(s) in protein structure, imbalance between two antagonisms e.g. NP system and RAS, leading to many cardiovascular disorders such as cardiac hypertrophy, hypertension, atherosclerosis, coronary artery disease and diabetic complications. Indeed, Santos *et al.* found that angiotensin-(1-7) was an endogenous ligand for the G protein-coupled receptor Mas (Santos *et al.*, 2003). Kostenis *et al.* showed that Mas could hetero-oligomerize with the AT1 receptor and by inhibiting the actions of Ang II, demonstrating the interaction between Mas and AT1 within the renin angiotensin system (Kostenis *et al.*, 2005). In this regard, current study in the NPRA and NPRB interaction leading to desensitisation of NPRs might serve as one possible mechanism for these pathophysiological consequences. Under normal physiological condition, either NPRA or NPRB is predominately expressed and they are distributed unequally in certain types of cells or organs (Table 1), exerting pleiotropic biofunctions with relative functional division and cooperation. Reciprocally, impaired NPRs activity or redistribution of NPRs proportion may occur during the pathophysiological exacerbation. Western blot and quantitative RT-PCR analyses for the inhibited CNP/NPRB/cGMP signalling pathway provided further evidence that the lowered NPRB mRNA level in NPRA/NPRB co-transfected HEK293 cells led to the less NPRB in the cell membrane. It is worth noting that, many studies have shown that post-translational modification are

essential for protein folding, stability, cell-surface expression and signalling (Helenius, 1994, Taylor and Drickamer, 2003, Helenius and Aebi, 2004). Failure in N-glycosylation of the AT1 receptor showed the disappearance of receptor on the plasma membrane, but retention in the endoplasmic reticulum (ER) (Deslauriers *et al.*, 1999). Similarly another group also report that the functional expression of D5 dopamine receptors at the cell surface of HEK293 cells required the addition of N-linked glycosylation (Karpa *et al.*, 1999). It was seen in the FRET result that the fluorophores tagged at C-terminus of both receptors were predominantly expressed intracellularly. Hence, current study cannot exclude the possibility that the impaired processes of post-translational modifications (e.g. N-glycosylation) attribute to the decreased NPRB expression on the membrane, presumably related to ER or Golgi apparatus. The effect of protein modification on receptor expression during receptor interaction need to be further studied.

Kim and colleagues used monocrotaline to induce cardiac hypertrophy. In monocrotaline-treated rats with pulmonary hypertension, specific ^{125}I-labelled rat ANP binding to hypertrophied RV endocardium almost disappeared and the cyclase activities of both NPRA and NPRB were significantly decreased in membranes from the monocrotaline-treated rats, despite the plasma levels of ANP and BNP were increased by 5-fold compared with controls (Kim *et al.*, 1999). Singh *et al.* demonstrated a significant downregulation in the density of NPRA in heart and coronary artery of patients with ischemic heart disease, which may explain, in part, the attenuated NP response in such patient group (Singh *et al.*, 2006). Dickey and colleagues reported that in normal hearts, 10^{-6} M of CNP increased about 70% pGC activity in that of ANP response by measuring cGMP formation. In contrast, NPRA activity was reduced in failed heart preparations, whereas NPRB activity remained unchanged (Dickey *et al.*, 2007). Therefore, evidence in this thesis may provide the mechanism for the decrease in NPRA activity in the failed heart. It was shown that attenuated cGMP expression in equal amount of NPRA and NPRB double-transfected cells after equimolar NP stimulation (Figure 32C). Moreover, the inhibitory effect of NPRA on NPRB was accentated in a dose-dependent manner, and vice versa (Figure 36 and 37). Different from the findings of the attenuated NPRB signalling, the impaired NPRA signalling may involve in an independent mechanism, e.g. conformational change(s) on receptor structure, presumably caused

by the physical interaction in the NPRA/NPRB heterodimer. A schematic diagram illustrates the hypothesised receptor desensitisation after NPRA/NPRB interaction (Figure 57).
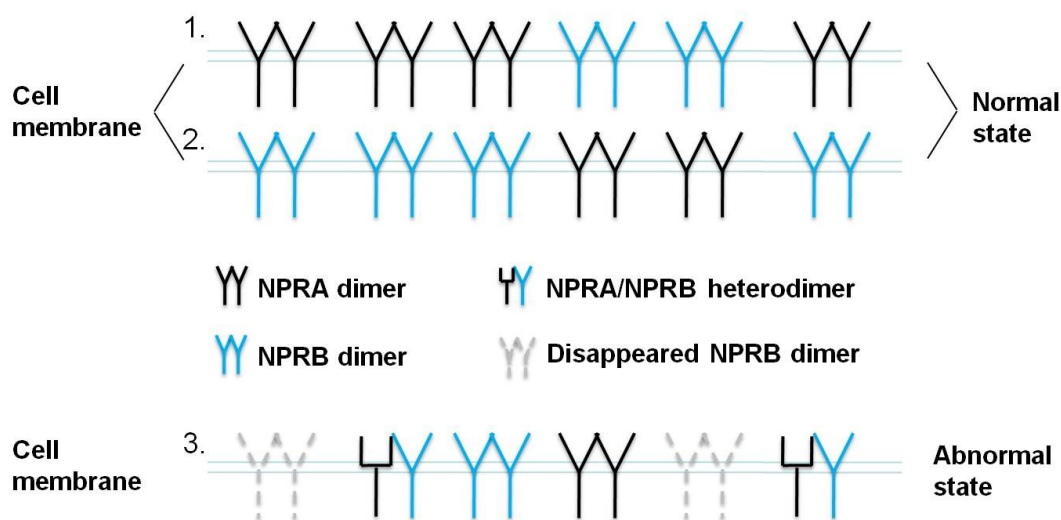
Figure 57. Diagram depicting the normal and abnormal status of NPR on the cell membrane. Upon the interaction between NPRA and NPRB, the NPRB quantity on the membrane is decreased while NPRA experiences a conformational change on the extracellular domain, both having an attenuated cGMP formation. **1.** Normal NPRA and NPRB distributions and structures in NPRA-dominant expressing cells (e.g. ECs); **2.** Normal NPRA and NPRB distributions and structures in NPRB-dominant expressing cells (e.g. MC, CF); **3.** Abnormal NPRA and NPRB distributions and structures in either NPRA- or NPRB-dominant expressing cells. The 'YY' shape structures in black and blue colour indicate NPRA homodimers and NPRB homodimers, respectively. The conformation-altered NPRA in black in combination with 'Y' shape NPRB in blue indicate NPRA/NPRB heterodimers. The dotted 'YY' structures in grey indicate the disappearance of NPRB on the membrane due to its interaction with NPRA.

Nevertheless, the exact conformational change occurring during activation of NPRA in NPRA/NPRB heterodimer is still largely unknown. One speculation is that NPRA homodimer and NPRA/NPRB heterodimer coexist in the double-transfected cells (e.g. 50% for each). It could be that the attenuated cGMP generation in double-transfected cells is not mediated by the 50% heterodimer, but from the 50% homodimer. Presumably the NPRA/NPRB heterodimer cannot mediate cGMP signalling due to its faulty conformational change, ensuing the failure in GC activation. While the homodimer retains its function since a correct alteration at the positioning of the receptor subunits and thus enabling the GC catalysis (Ogawa *et al.*, 2004, Misono *et al.*, 2011). It therefore requires further experiments to reveal if a failed/wrong rotation elicited by NPRA and NPRB interaction in NPRA/NPRB heterodimer occurs, subsequently hindering the intracellular GC catalysis.

Overall, these findings provide potential mechanisms for the interaction between NPRA and NPRB, and give an alternative and promising hypothesis among the numerous contributors for the pathogenesis and aetiology of CVD.

5.3. Study limitations and open questions

There are several limitations in this thesis. First, the *in vivo* property studies of human derived ACNP as well as its parent peptides, ANP and CNP, were carried out in a mouse model. Although human ANP shares very similar AA sequence and structure with mouse ANP (Met12 in human ANP and Ile12 in mouse), and the AA sequence and structure of CNP have been found universal among most species (procine, mouse, rat, human, and dog), it cannot exclude the possibility that receptor binding and peptide metabolism for ANP and ACNP may differ between murine and human. Therefore, the findings in mouse model cannot be certainly extrapolated to human. Second, the degradation studies of ACNP were performed in diluted serum samples (1:12.5 dilution) due to the pure serum samples could not go through the capillary in the HPLC machine, and the NP concentrations were far more than the normal physiological level since the peptide peaks would be undetectable with lower NP concentrations. More importantly, due to the shortage of blood samples from the MI mice in this study, the proposed degradation profiles of different NPs incubating with such MI blood are not investigated. Thus, it is unknown whether the dilution of the blood samples (both normal blood and MI blood) and the excessive NP concentrations would cause a different degradation profile in disease conditions. Third, elevated endogenous NP levels (e.g. BNP) are usually associated with certain pathological states. Could it be possible that local endogenous NPs exert cardiorenal effect in a more direct and efficient manner compared to exogenous NP administration? And could it be that NPRA/NPRB interation involved in the desensitisation of NPRs and forming NPRA/NPRB heterodimer, any direct evidence *in vivo*? Fourth, due to the experimental condition limitation, the binding study of NP, especially ACNP to the different receptors was not included. The conformational change at extracellular binding site(s) of NPRA and NPRB heterodimers after ligand binding remains unknown. Finally, the anesthesia used in the ACNP MI experiment might affect the response to the peptides (Matsukawa *et al.*, 1993).

Consequently, with the aim to better understand the structure and function of the natriuretic peptide system, and to generate a more global view on it, especially the effects of native peptides, peptide metabolites, and synthetic peptides under various conditions (e.g. specific receptor binding, undefined receptor(s), receptor heterodimeric or heterotrimeric complexes) on neurohormonal and haemodynamic profiles, and other physiological consequences, the following open questions will be investigated in future: 1) What is(are) the sequence determinant(s) influencing the agonist selectivity for different species of NPRs? Does the structure and sequence of ACNP help to understand the structure of the binding pockets of NPRA, NPRB, and NPRC? 2) Whether the degradation profile of ACNP in pathological (e.g. MI) condition be different from that in normal condition? If so, it may account for the hindering of beneficial cardiac effects of ACNP in mice post MI. 3) What is the peptidase(s) being responsible for the fast degradation of ACNP in serum? If found, it might be promising to seek the mechanism to prevent degradation via a) modification of the ACNP amino acid sequence or b) by specifically inhibiting this peptidase(s). Such approaches will extend the half-life of ACNP and thus potentiate the beneficial effects of ACNP. 4) Whether the broad receptor profile of ACNP and other chimeric peptides is a benefit or drawback in a therapeutic setting. Could ACNP have more unwanted effects in these targets when used to treat cardiovascular ailments, as compared to e.g. BNP? 5) Apart from examining the functional indicator (e.g. cAMP, cGMP), how NPRA/NPRC, NPRB/NPRC, NPRA/NPRB/NPRC would structurally influence each other in the receptor complexes under pathological conditions. It would be very interesting to see if any receptor conformation might change intracellular signalling alteration in response to mature NPs and their identified metabolites. This might also allow the identification of a pharmacologically-distinct receptor (complex) signalling specifically in response to one of peptide metabolites. 6) Whether any post-translational processes (e.g. glycosylation, phophorylation) regulate cell-surface NPRs concentration/activation, since such modifications have been shown to be important for many biofunctions including protein folding, stability, intracellular trafficking, cell-surface expression and signal transduction (Helenius, 1994, Taylor and Drickamer, 2003, Helenius and Aebi, 2004). If so, whether the lowered NPRB quantity in the cell membrane involves the interaction with elements of the ER-based quality control processes.

References

ABDELALIM, E. M. & TOOYAMA, I. (2009) BNP signaling is crucial for embryonic stem cell proliferation. *PLoS One,* 4**,** e5341.

ANAND-SRIVASTAVA, M. B. (2005) Natriuretic peptide receptor-C signaling and regulation. *Peptides,* 26**,** 1044-59.

ANAND-SRIVASTAVA, M. B., SAIRAM, M. R. & CANTIN, M. (1990) Ring-deleted analogs of atrial natriuretic factor inhibit adenylate cyclase/cAMP system. Possible coupling of clearance atrial natriuretic factor receptors to adenylate cyclase/cAMP signal transduction system. *J Biol Chem,* 265**,** 8566-72.

ASHMAN, D. F., LIPTON, R., MELICOW, M. M. & PRICE, T. D. (1963) Isolation of adenosine 3', 5'-monophosphate and guanosine 3', 5'-monophosphate from rat urine. *Biochem Biophys Res Commun,* 11**,** 330-4.

BALION, C., SANTAGUIDA, P. L., HILL, S., WORSTER, A., MCQUEEN, M., OREMUS, M., MCKELVIE, R., BOOKER, L., FAGBEMI, J., REICHERT, S. & RAINA, P. (2006) Testing for BNP and NT-proBNP in the diagnosis and prognosis of heart failure. *Evid Rep Technol Assess (Full Rep)***,** 1-147.

BARTELS, C. F., BUKULMEZ, H., PADAYATTI, P., RHEE, D. K., VAN RAVENSWAAIJ-ARTS, C., PAULI, R. M., MUNDLOS, S., CHITAYAT, D., SHIH, L. Y., AL-GAZALI, L. I., KANT, S., COLE, T., MORTON, J., CORMIER-DAIRE, V., FAIVRE, L., LEES, M., KIRK, J., MORTIER, G. R., LEROY, J., ZABEL, B., KIM, C. A., CROW, Y., BRAVERMAN, N. E., VAN DEN AKKER, F. & WARMAN, M. L. (2004) Mutations in the transmembrane natriuretic peptide receptor NPR-B impair skeletal growth and cause acromesomelic dysplasia, type Maroteaux. *Am J Hum Genet,* 75**,** 27-34.

BARTON, M., BENY, J. L., D'USCIO, L. V., WYSS, T., NOLL, G. & LUSCHER, T. F. (1998) Endothelium-independent relaxation and hyperpolarization to C-type natriuretic peptide in porcine coronary arteries. *J Cardiovasc Pharmacol,* 31**,** 377-83.

BELTOWSKI, J., JAMROZ-WISNIEWSKA, A., BORKOWSKA, E. & WOJCICKA, G. (2004) Up-regulation of renal Na+, K+-ATPase: the possible novel mechanism of leptin-induced hypertension. *Pol J Pharmacol,* 56**,** 213-22.

BHALLA, V., WILLIS, S. & MAISEL, A. S. (2004) B-type natriuretic peptide: the level and the drug--partners in the diagnosis of congestive heart failure. *Congest Heart Fail,* 10**,** 3-27.

BOERRIGTER, G., COSTELLO-BOERRIGTER, L. C., HARTY, G. J., HUNTLEY, B. K., CATALIOTTI, A., LAPP, H. & BURNETT, J. C., JR. (2009) B-type natriuretic peptide 8-32, which is produced from mature BNP 1-32 by the metalloprotease meprin A, has reduced bioactivity. *Am J Physiol Regul Integr Comp Physiol,* 296**,** R1744-50.

BOERRIGTER, G., COSTELLO-BOERRIGTER, L. C., HARTY, G. J., LAPP, H. & BURNETT, J. C., JR. (2007) Des-serine-proline brain natriuretic peptide 3-32 in cardiorenal regulation. *Am J Physiol Regul Integr Comp Physiol,* 292**,** R897-901.

BRANDT, I., LAMBEIR, A. M., KETELSLEGERS, J. M., VANDERHEYDEN, M., SCHARPE, S. & DE MEESTER, I. (2006) Dipeptidyl-peptidase IV converts intact B-type natriuretic peptide into its des-SerPro form. *Clin Chem,* 52**,** 82-7.

BRANDT, R. R., MATTINGLY, M. T., CLAVELL, A. L., BARCLAY, P. L. & BURNETT, J. C., JR. (1997) Neutral endopeptidase regulates C-type natriuretic peptide metabolism but does not potentiate its bioactivity in vivo. *Hypertension,* 30**,** 184-90.

CALDERONE, A., THAIK, C. M., TAKAHASHI, N., CHANG, D. L. & COLUCCI, W. S. (1998) Nitric oxide, atrial natriuretic peptide, and cyclic GMP inhibit the growth-promoting effects of norepinephrine in cardiac myocytes and fibroblasts. *J Clin Invest,* 101**,** 812-8.

CARPENTER, K. A., WILKES, B. C., DE LEAN, A., FOURNIER, A. & SCHILLER, P. W. (1997) Hydrophobic forces are responsible for the folding of a highly potent natriuretic peptide analogue at a membrane mimetic surface: an NMR study. *Biopolymers,* 42**,** 37-48.

CARSTENS, J., JENSEN, K. T., IVARSEN, P., RASMUSSEN, L. M. & PEDERSEN, E. B. (1997) Development of a urodilatin-specific antibody and radioimmunoassay for urodilatin in human urine. *Clin Chem,* 43**,** 638-43.

CARSTENS, J., JENSEN, K. T. & PEDERSEN, E. B. (1998) Metabolism and action of urodilatin infusion in healthy volunteers. *Clin Pharmacol Ther,* 64**,** 73-86.

CASTRO, L. R., SCHITTL, J. & FISCHMEISTER, R. (2010) Feedback control through cGMP-dependent protein kinase contributes to differential regulation and compartmentation of cGMP in rat cardiac myocytes. *Circ Res,* 107**,** 1232-40.

CASTRO, L. R., VERDE, I., COOPER, D. M. & FISCHMEISTER, R. (2006) Cyclic guanosine monophosphate compartmentation in rat cardiac myocytes. *Circulation,* 113**,** 2221-8.

CHAUHAN, S. D., NILSSON, H., AHLUWALIA, A. & HOBBS, A. J. (2003) Release of C-type natriuretic peptide accounts for the biological activity of endothelium-derived hyperpolarizing factor. *Proc Natl Acad Sci U S A,* 100**,** 1426-31.

CHEN, B. Y., CHEN, J. K., ZHU, M. Z., ZHANG, D. L., SUN, J. S., PEI, J. M., FENG, H. S., ZHU, X. X., JIN, J. & YU, J. (2011) AC-NP: a novel chimeric peptide with natriuretic and vasorelaxing actions. *PLoS One,* 6**,** e20477.

CHEN, H. H., LAINCHBURY, J. G. & BURNETT, J. C., JR. (2002) Natriuretic peptide receptors and neutral endopeptidase in mediating the renal actions of a new therapeutic synthetic natriuretic peptide dendroaspis natriuretic peptide. *J Am Coll Cardiol,* 40**,** 1186-91.

CHRISMAN, T. D. & GARBERS, D. L. (1999) Reciprocal antagonism coordinates C-type natriuretic peptide and mitogen-signaling pathways in fibroblasts. *J Biol Chem,* 274**,** 4293-9.

CHUSHO, H., TAMURA, N., OGAWA, Y., YASODA, A., SUDA, M., MIYAZAWA, T., NAKAMURA, K., NAKAO, K., KURIHARA, T., KOMATSU, Y., ITOH, H., TANAKA, K., SAITO, Y. & KATSUKI, M. (2001) Dwarfism and early death in mice lacking C-type natriuretic peptide. *Proc Natl Acad Sci U S A,* 98**,** 4016-21.

CITARELLA, M. R., CHOI, M. R., GIRONACCI, M. M., MEDICI, C., CORREA, A. H. & FERNANDEZ, B. E. (2009) Urodilatin and dopamine: a new interaction in the kidney. *Regul Pept,* 153**,** 19-24.

CLAVELL, A. L., STINGO, A. J., WEI, C. M., HEUBLEIN, D. M. & BURNETT, J. C., JR. (1993) C-type natriuretic peptide: a selective cardiovascular peptide. *Am J Physiol,* 264**,** R290-5.

COSTA, M. A., ELESGARAY, R., CANIFFI, C., FELLET, A., MAC LAUGHLIN, M. & ARRANZ, C. (2009) Role of nitric oxide as a key mediator on cardiovascular actions of atrial natriuretic peptide in spontaneously hypertensive rats. *Am J Physiol Heart Circ Physiol,* 298**,** H778-86.

COSTELLO-BOERRIGTER, L. C., BOERRIGTER, G., REDFIELD, M. M., RODEHEFFER, R. J., URBAN, L. H., MAHONEY, D. W., JACOBSEN, S. J., HEUBLEIN, D. M. & BURNETT, J. C., JR. (2006) Amino-terminal pro-B-type natriuretic peptide and B-type natriuretic peptide in the general community: determinants and detection of left ventricular dysfunction. *J Am Coll Cardiol,* 47**,** 345-53.

DAVIDSON, N. C., BARR, C. S. & STRUTHERS, A. D. (1996) C-type natriuretic peptide. An endogenous inhibitor of vascular angiotensin-converting enzyme activity. *Circulation,* 93**,** 1155-9.

DE BOLD, A. J. (1985) Atrial natriuretic factor: a hormone produced by the heart. *Science,* 230**,** 767-70.

DE BOLD, A. J., BORENSTEIN, H. B., VERESS, A. T. & SONNENBERG, H. (1981) A rapid and potent natriuretic response to intravenous injection of atrial myocardial extract in rats. *Life Sci,* 28**,** 89-94.

DEL RY, S., CABIATI, M., LIONETTI, V. & GIANNESSI, D. (2010) NPR-B, the C-type natriuretic peptide specific receptor, is the predominant biological receptor in mouse and pig myocardial tissue. *Minerva Endocrinol.*

DESLAURIERS, B., PONCE, C., LOMBARD, C., LARGUIER, R., BONNAFOUS, J. C. & MARIE, J. (1999) N-glycosylation requirements for the AT1a angiotensin II receptor delivery to the plasma membrane. *Biochem J,* 339 (Pt 2)**,** 397-405.

DI FUSCO, F. & ANAND-SRIVASTAVA, M. B. (2000) Enhanced expression of Gi proteins in non-hypertrophic hearts from rats with hypertension-induced by L-NAME treatment. *J Hypertens,* 18**,** 1081-90.

DICKEY, D. M., BURNETT, J. C., JR. & POTTER, L. R. (2008) Novel bifunctional natriuretic peptides as potential therapeutics. *J Biol Chem,* 283**,** 35003-9.

DICKEY, D. M., FLORA, D. R., BRYAN, P. M., XU, X., CHEN, Y. & POTTER, L. R. (2007) Differential regulation of membrane guanylyl cyclases in congestive heart failure: natriuretic peptide receptor (NPR)-B, Not NPR-A, is the predominant natriuretic peptide receptor in the failing heart. *Endocrinology,* 148**,** 3518-22.

DICKEY, D. M. & POTTER, L. R. (2011) Dendroaspis natriuretic peptide and the designer natriuretic peptide, CD-NP, are resistant to proteolytic inactivation. *J Mol Cell Cardiol,* 51**,** 67-71.

DICKEY, D. M., YODER, A. R. & POTTER, L. R. (2009) A familial mutation renders atrial natriuretic Peptide resistant to proteolytic degradation. *J Biol Chem,* 284**,** 19196-202.

DONTAS, I. D., XANTHOS, T., DONTAS, I., LELOVAS, P. & PAPADIMITRIOU, L. (2009) Impact of nesiritide on renal function and

mortality in patients suffering from heart failure. *Cardiovasc Drugs Ther,* 23**,** 221-33.

FAN, D., BRYAN, P. M., ANTOS, L. K., POTTHAST, R. J. & POTTER, L. R. (2005) Down-regulation does not mediate natriuretic peptide-dependent desensitization of natriuretic peptide receptor (NPR)-A or NPR-B: guanylyl cyclase-linked natriuretic peptide receptors do not internalize. *Mol Pharmacol,* 67**,** 174-83.

FELLNER, S. K. & ARENDSHORST, W. J. (2010) Complex interactions of NO/cGMP/PKG systems on Ca2+ signaling in afferent arteriolar vascular smooth muscle. *Am J Physiol Heart Circ Physiol,* 298**,** H144-51.

FISCUS, R. R. (2002) Involvement of cyclic GMP and protein kinase G in the regulation of apoptosis and survival in neural cells. *Neurosignals,* 11**,** 175-90.

FLYNN, T. G., DE BOLD, M. L. & DE BOLD, A. J. (1983) The amino acid sequence of an atrial peptide with potent diuretic and natriuretic properties. *Biochem Biophys Res Commun,* 117**,** 859-65.

FORAN, S. E., CARR, D. B., LIPKOWSKI, A. W., MASZCZYNSKA, I., MARCHAND, J. E., MISICKA, A., BEINBORN, M., KOPIN, A. S. & KREAM, R. M. (2000) A substance P-opioid chimeric peptide as a unique nontolerance-forming analgesic. *Proc Natl Acad Sci U S A,* 97**,** 7621-6.

FRANGOGIANNIS, N. G., SMITH, C. W. & ENTMAN, M. L. (2002) The inflammatory response in myocardial infarction. *Cardiovasc Res,* 53**,** 31-47.

FUJISAKI, H., ITO, H., HIRATA, Y., TANAKA, M., HATA, M., LIN, M., ADACHI, S., AKIMOTO, H., MARUMO, F. & HIROE, M. (1995) Natriuretic peptides inhibit angiotensin II-induced proliferation of rat cardiac fibroblasts by blocking endothelin-1 gene expression. *J Clin Invest,* 96**,** 1059-65.

FULLER, F., PORTER, J. G., ARFSTEN, A. E., MILLER, J., SCHILLING, J. W., SCARBOROUGH, R. M., LEWICKI, J. A. & SCHENK, D. B. (1988) Atrial natriuretic peptide clearance receptor. Complete sequence and functional expression of cDNA clones. *J Biol Chem,* 263**,** 9395-401.

FURUYA, M., TAWARAGI, Y., MINAMITAKE, Y., KITAJIMA, Y., FUCHIMURA, K., TANAKA, S., MINAMINO, N., KANGAWA, K. & MATSUO, H. (1992) Structural requirements of C-type natriuretic peptide for elevation of cyclic GMP in cultured vascular smooth muscle cells. *Biochem Biophys Res Commun,* 183**,** 964-9.

GARDNER, D. G. (2003) Natriuretic peptides: markers or modulators of cardiac hypertrophy? *Trends Endocrinol Metab,* 14**,** 411-6.

GOETZ, K., DRUMMER, C., ZHU, J. L., LEADLEY, R., FIEDLER, F. & GERZER, R. (1990) Evidence that urodilatin, rather than ANP, regulates renal sodium excretion. *J Am Soc Nephrol,* 1**,** 867-74.

GOETZ, K. L. (1991) Renal natriuretic peptide (urodilatin?) and atriopeptin: evolving concepts. *Am J Physiol,* 261**,** F921-32.

GOETZE, J. P., CHRISTOFFERSEN, C., PERKO, M., ARENDRUP, H., REHFELD, J. F., KASTRUP, J. & NIELSEN, L. B. (2003) Increased cardiac BNP expression associated with myocardial ischemia. *FASEB J,* 17**,** 1105-7.

GRIFFITH, T. M. (2004) Endothelium-dependent smooth muscle hyperpolarization: do gap junctions provide a unifying hypothesis? *Br J Pharmacol,* 141**,** 881-903.

HASHIM, S. & ANAND-SRIVASTAVA, M. B. (2004) Losartan-induced attenuation of blood pressure in L-NAME hypertensive rats is associated

144

with reversal of the enhanced expression of Gi alpha proteins. *J Hypertens,* 22, 181-90.

HE, X. L., DUKKIPATI, A., WANG, X. & GARCIA, K. C. (2005) A new paradigm for hormone recognition and allosteric receptor activation revealed from structural studies of NPR-C. *Peptides,* 26, 1035-43.

HELENIUS, A. (1994) How N-linked oligosaccharides affect glycoprotein folding in the endoplasmic reticulum. *Mol Biol Cell,* 5, 253-65.

HELENIUS, A. & AEBI, M. (2004) Roles of N-linked glycans in the endoplasmic reticulum. *Annu Rev Biochem,* 73, 1019-49.

HILDEBRANDT, D. A., MIZELLE, H. L., BRANDS, M. W. & HALL, J. E. (1992) Comparison of renal actions of urodilatin and atrial natriuretic peptide. *Am J Physiol,* 262, R395-9.

HIRATA, Y., TAKATA, S., TOMITA, M. & TAKAICHI, S. (1985) Binding, internalization, and degradation of atrial natriuretic peptide in cultured vascular smooth muscle cells of rat. *Biochem Biophys Res Commun,* 132, 976-84.

HIROOKA, Y., TAKESHITA, A., IMAIZUMI, T., SUZUKI, S., YOSHIDA, M., ANDO, S. & NAKAMURA, M. (1990) Attenuated forearm vasodilative response to intra-arterial atrial natriuretic peptide in patients with heart failure. *Circulation,* 82, 147-53.

HOBBS, A., FOSTER, P., PRESCOTT, C., SCOTLAND, R. & AHLUWALIA, A. (2004) Natriuretic peptide receptor-C regulates coronary blood flow and prevents myocardial ischemia/reperfusion injury: novel cardioprotective role for endothelium-derived C-type natriuretic peptide. *Circulation,* 110, 1231-5.

HODGSON-ZINGMAN, D. M., KARST, M. L., ZINGMAN, L. V., HEUBLEIN, D. M., DARBAR, D., HERRON, K. J., BALLEW, J. D., DE ANDRADE, M., BURNETT, J. C., JR. & OLSON, T. M. (2008) Atrial natriuretic peptide frameshift mutation in familial atrial fibrillation. *N Engl J Med,* 359, 158-65.

HORIO, T., TOKUDOME, T., MAKI, T., YOSHIHARA, F., SUGA, S., NISHIKIMI, T., KOJIMA, M., KAWANO, Y. & KANGAWA, K. (2003) Gene expression, secretion, and autocrine action of C-type natriuretic peptide in cultured adult rat cardiac fibroblasts. *Endocrinology,* 144, 2279-84.

HORNE, B. D., ANDERSON, J. L., JOHN, J. M., WEAVER, A., BAIR, T. L., JENSEN, K. R., RENLUND, D. G. & MUHLESTEIN, J. B. (2005) Which white blood cell subtypes predict increased cardiovascular risk? *J Am Coll Cardiol,* 45, 1638-43.

HUNT, P. J., RICHARDS, A. M., NICHOLLS, M. G., YANDLE, T. G., DOUGHTY, R. N. & ESPINER, E. A. (1997) Immunoreactive amino-terminal pro-brain natriuretic peptide (NT-PROBNP): a new marker of cardiac impairment. *Clin Endocrinol (Oxf),* 47, 287-96.

JAISWAL, R. K. (1992) Endothelin inhibits the atrial natriuretic factor stimulated cGMP production by activating the protein kinase C in rat aortic smooth muscle cells. *Biochem Biophys Res Commun,* 182, 395-402.

JEWETT, J. R., KOLLER, K. J., GOEDDEL, D. V. & LOWE, D. G. (1993) Hormonal induction of low affinity receptor guanylyl cyclase. *EMBO J,* 12, 769-77.

KAMBAYASHI, Y., NAKAO, K., KIMURA, H., KAWABATA, T., NAKAMURA, M., INOUYE, K., YOSHIDA, N. & IMURA, H. (1990) Biological characterization of human brain natriuretic peptide (BNP) and rat BNP:

species-specific actions of BNP. *Biochem Biophys Res Commun,* 173**,** 599-605.

KARPA, K. D., LIDOW, M. S., PICKERING, M. T., LEVENSON, R. & BERGSON, C. (1999) N-linked glycosylation is required for plasma membrane localization of D5, but not D1, dopamine receptors in transfected mammalian cells. *Mol Pharmacol,* 56**,** 1071-8.

KEMP-HARPER, B. & SCHMIDT, H. H. (2009) cGMP in the vasculature. *Handb Exp Pharmacol***,** 447-67.

KENNY, A. J., BOURNE, A. & INGRAM, J. (1993) Hydrolysis of human and pig brain natriuretic peptides, urodilatin, C-type natriuretic peptide and some C-receptor ligands by endopeptidase-24.11. *Biochem J,* 291 (Pt 1)**,** 83-8.

KIBERD, B. A., LARSON, T. S., ROBERTSON, C. R. & JAMISON, R. L. (1987) Effect of atrial natriuretic peptide on vasa recta blood flow in the rat. *Am J Physiol,* 252**,** F1112-7.

KILIC, A., RAJAPUROHITAM, V., SANDBERG, S. M., ZEIDAN, A., HUNTER, J. C., SAID FARUQ, N., LEE, C. Y., BURNETT, J. C., JR. & KARMAZYN, M. (2010) A novel chimeric natriuretic peptide reduces cardiomyocyte hypertrophy through the NHE-1-calcineurin pathway. *Cardiovasc Res,* 88**,** 434-42.

KIM, S. Z., CHO, K. W. & KIM, S. H. (1999) Modulation of endocardial natriuretic peptide receptors in right ventricular hypertrophy. *Am J Physiol,* 277**,** H2280-9.

KINOSHITA, H., KUWAHARA, K., NISHIDA, M., JIAN, Z., RONG, X., KIYONAKA, S., KUWABARA, Y., KUROSE, H., INOUE, R., MORI, Y., LI, Y., NAKAGAWA, Y., USAMI, S., FUJIWARA, M., YAMADA, Y., MINAMI, T., UESHIMA, K. & NAKAO, K. (2010) Inhibition of TRPC6 channel activity contributes to the antihypertrophic effects of natriuretic peptides-guanylyl cyclase-A signaling in the heart. *Circ Res,* 106**,** 1849-60.

KISTORP, C., RAYMOND, I., PEDERSEN, F., GUSTAFSSON, F., FABER, J. & HILDEBRANDT, P. (2005) N-terminal pro-brain natriuretic peptide, C-reactive protein, and urinary albumin levels as predictors of mortality and cardiovascular events in older adults. *JAMA,* 293**,** 1609-16.

KLAIBER, M., DANKWORTH, B., KRUSE, M., HARTMANN, M., NIKOLAEV, V. O., YANG, R. B., VOLKER, K., GASSNER, B., OBERWINKLER, H., FEIL, R., FREICHEL, M., GROSCHNER, K., SKRYABIN, B. V., FRANTZ, S., BIRNBAUMER, L., PONGS, O. & KUHN, M. (2011) A cardiac pathway of cyclic GMP-independent signaling of guanylyl cyclase A, the receptor for atrial natriuretic peptide. *Proc Natl Acad Sci U S A,* 108**,** 18500-5.

KOH, G. Y., NUSSENZVEIG, D. R., OKOLICANY, J., PRICE, D. A. & MAACK, T. (1992) Dynamics of atrial natriuretic factor-guanylate cyclase receptors and receptor-ligand complexes in cultured glomerular mesangial and renomedullary interstitial cells. *J Biol Chem,* 267**,** 11987-94.

KOHNO, M., IKEDA, M., JOHCHI, M., HORIO, T., YASUNARI, K., KURIHARA, N. & TAKEDA, T. (1993) Interaction of PDGF and natriuretic peptides on mesangial cell proliferation and endothelin secretion. *Am J Physiol,* 265**,** E673-9.

KOJIMA, M., MINAMINO, N., KANGAWA, K. & MATSUO, H. (1989) Cloning and sequence analysis of cDNA encoding a precursor for rat brain natriuretic peptide. *Biochem Biophys Res Commun,* 159**,** 1420-6.

KOLLER, K. J. & GOEDDEL, D. V. (1992) Molecular biology of the natriuretic peptides and their receptors. *Circulation,* 86**,** 1081-8.

KONG, X., WANG, X., XU, W., BEHERA, S., HELLERMANN, G., KUMAR, A., LOCKEY, R. F., MOHAPATRA, S. & MOHAPATRA, S. S. (2008) Natriuretic peptide receptor a as a novel anticancer target. *Cancer Res,* 68**,** 249-56.

KOSTENIS, E., MILLIGAN, G., CHRISTOPOULOS, A., SANCHEZ-FERRER, C. F., HERINGER-WALTHER, S., SEXTON, P. M., GEMBARDT, F., KELLETT, E., MARTINI, L., VANDERHEYDEN, P., SCHULTHEISS, H. P. & WALTHER, T. (2005) G-protein-coupled receptor Mas is a physiological antagonist of the angiotensin II type 1 receptor. *Circulation,* 111**,** 1806-13.

KRESS, H. G. & EBERLEIN, T. (1992) [Effect of anesthesia and operation on essential immune functions]. *Anasthesiol Intensivmed Notfallmed Schmerzther,* 27**,** 393-402.

KUHN, M. (2003) Structure, regulation, and function of mammalian membrane guanylyl cyclase receptors, with a focus on guanylyl cyclase-A. *Circ Res,* 93**,** 700-9.

KUHN, M. (2004) Molecular physiology of natriuretic peptide signalling. *Basic Res Cardiol,* 99**,** 76-82.

KUSE, E. R., MEYER, M., CONSTANTIN, R., OLDHAFER, K., SCHLITT, H. J., SCHULZ-KNAPPE, P., UBERBACHER, H. J., PICHLMAYR, R. & FORSSMANN, W. G. (1996) [Urodilatin (INN: ularitide). A new peptide in the treatment of acute kidney failure following liver transplantation]. *Anaesthesist,* 45**,** 351-8.

LA VILLA, G., MANNELLI, M., LAZZERI, C., VECCHIARINO, S., DE FEO, M. L., TOSTI GUERRA, C., BANDINELLI, R., FOSCHI, M. & FRANCHI, F. (1998) Different effects of atrial and C-type natriuretic peptide on the urinary excretion of endothelin-1 in man. *Clin Sci (Lond),* 95**,** 595-602.

LABRECQUE, J., MC NICOLL, N., MARQUIS, M. & DE LEAN, A. (1999) A disulfide-bridged mutant of natriuretic peptide receptor-A displays constitutive activity. Role of receptor dimerization in signal transduction. *J Biol Chem,* 274**,** 9752-9.

LANGENICKEL, T. H., BUTTGEREIT, J., PAGEL-LANGENICKEL, I., LINDNER, M., MONTI, J., BEUERLEIN, K., AL-SAADI, N., PLEHM, R., POPOVA, E., TANK, J., DIETZ, R., WILLENBROCK, R. & BADER, M. (2006) Cardiac hypertrophy in transgenic rats expressing a dominant-negative mutant of the natriuretic peptide receptor B. *Proc Natl Acad Sci U S A,* 103**,** 4735-40.

LEE, J., KIM, S., JUNG, M., OH, Y. & KIM, S. W. (2002) Altered expression of vascular natriuretic peptide receptors in experimental hypertensive rats. *Clin Exp Pharmacol Physiol,* 29**,** 299-303.

LEVIN, E. R., GARDNER, D. G. & SAMSON, W. K. (1998) Natriuretic peptides. *N Engl J Med,* 339**,** 321-8.

LI, Y., KISHIMOTO, I., SAITO, Y., HARADA, M., KUWAHARA, K., IZUMI, T., TAKAHASHI, N., KAWAKAMI, R., TANIMOTO, K., NAKAGAWA, Y., NAKANISHI, M., ADACHI, Y., GARBERS, D. L., FUKAMIZU, A. & NAKAO, K. (2002) Guanylyl cyclase-A inhibits angiotensin II type 1A receptor-mediated cardiac remodeling, an endogenous protective mechanism in the heart. *Circulation,* 106**,** 1722-8.

LI, Y., MADIRAJU, P. & ANAND-SRIVASTAVA, M. B. (2011) Knockdown of natriuretic peptide receptor-A enhances receptor C expression and signalling in vascular smooth muscle cells. *Cardiovasc Res,* 93**,** 350-9.

LIANG, F., O'REAR, J., SCHELLENBERGER, U., TAI, L., LASECKI, M., SCHREINER, G. F., APPLE, F. S., MAISEL, A. S., POLLITT, N. S. & PROTTER, A. A. (2007) Evidence for functional heterogeneity of circulating B-type natriuretic peptide. *J Am Coll Cardiol,* 49**,** 1071-8.

LISY, O., HUNTLEY, B. K., MCCORMICK, D. J., KURLANSKY, P. A. & BURNETT, J. C., JR. (2008) Design, synthesis, and actions of a novel chimeric natriuretic peptide: CD-NP. *J Am Coll Cardiol,* 52**,** 60-8.

LIU, C., GUAN, J., KANG, Y., XIU, H., CHEN, Y., DENG, B. & LIU, K. (2010) Inhibition of dehydration-induced water intake by glucocorticoids is associated with activation of hypothalamic natriuretic peptide receptor-A in rat. *PLoS One,* 5**,** e15607.

LOGEART, D., THABUT, G., JOURDAIN, P., CHAVELAS, C., BEYNE, P., BEAUVAIS, F., BOUVIER, E. & SOLAL, A. C. (2004) Predischarge B-type natriuretic peptide assay for identifying patients at high risk of re-admission after decompensated heart failure. *J Am Coll Cardiol,* 43**,** 635-41.

LOHMANN, S. M., VAANDRAGER, A. B., SMOLENSKI, A., WALTER, U. & DE JONGE, H. R. (1997) Distinct and specific functions of cGMP-dependent protein kinases. *Trends Biochem Sci,* 22**,** 307-12.

LUTGENS, E., DAEMEN, M. J., DE MUINCK, E. D., DEBETS, J., LEENDERS, P. & SMITS, J. F. (1999) Chronic myocardial infarction in the mouse: cardiac structural and functional changes. *Cardiovasc Res,* 41**,** 586-93.

MAACK, T. (1992) Receptors of atrial natriuretic factor. *Annu Rev Physiol,* 54**,** 11-27.

MAACK, T., SUZUKI, M., ALMEIDA, F. A., NUSSENZVEIG, D., SCARBOROUGH, R. M., MCENROE, G. A. & LEWICKI, J. A. (1987) Physiological role of silent receptors of atrial natriuretic factor. *Science,* 238**,** 675-8.

MADHANI, M., OKORIE, M., HOBBS, A. J. & MACALLISTER, R. J. (2006) Reciprocal regulation of human soluble and particulate guanylate cyclases in vivo. *Br J Pharmacol,* 149**,** 797-801.

MAISEL, A. S., CLOPTON, P., KRISHNASWAMY, P., NOWAK, R. M., MCCORD, J., HOLLANDER, J. E., DUC, P., OMLAND, T., STORROW, A. B., ABRAHAM, W. T., WU, A. H., STEG, G., WESTHEIM, A., KNUDSEN, C. W., PEREZ, A., KAZANEGRA, R., BHALLA, V., HERRMANN, H. C., AUMONT, M. C. & MCCULLOUGH, P. A. (2004) Impact of age, race, and sex on the ability of B-type natriuretic peptide to aid in the emergency diagnosis of heart failure: results from the Breathing Not Properly (BNP) multinational study. *Am Heart J,* 147**,** 1078-84.

MAISEL, A. S., KRISHNASWAMY, P., NOWAK, R. M., MCCORD, J., HOLLANDER, J. E., DUC, P., OMLAND, T., STORROW, A. B., ABRAHAM, W. T., WU, A. H., CLOPTON, P., STEG, P. G., WESTHEIM, A., KNUDSEN, C. W., PEREZ, A., KAZANEGRA, R., HERRMANN, H. C. & MCCULLOUGH, P. A. (2002) Rapid measurement of B-type natriuretic peptide in the emergency diagnosis of heart failure. *N Engl J Med,* 347**,** 161-7.

MATSUBARA, H., MORI, Y., YAMAMOTO, J. & INADA, M. (1990) Diabetes-induced alterations in atrial natriuretic peptide gene expression in Wistar-Kyoto and spontaneously hypertensive rats. *Circ Res,* 67**,** 803-13.

MATSUKAWA, K., NINOMIYA, I. & NISHIURA, N. (1993) Effects of anesthesia on cardiac and renal sympathetic nerve activities and plasma catecholamines. *Am J Physiol,* 265**,** R792-7.

MATSUKAWA, N., GRZESIK, W. J., TAKAHASHI, N., PANDEY, K. N., PANG, S., YAMAUCHI, M. & SMITHIES, O. (1999) The natriuretic peptide clearance receptor locally modulates the physiological effects of the natriuretic peptide system. *Proc Natl Acad Sci U S A,* 96**,** 7403-8.

MAURICE, D. H., PALMER, D., TILLEY, D. G., DUNKERLEY, H. A., NETHERTON, S. J., RAYMOND, D. R., ELBATARNY, H. S. & JIMMO, S. L. (2003) Cyclic nucleotide phosphodiesterase activity, expression, and targeting in cells of the cardiovascular system. *Mol Pharmacol,* 64**,** 533-46.

MCCULLOUGH, P. A., NOWAK, R. M., MCCORD, J., HOLLANDER, J. E., HERRMANN, H. C., STEG, P. G., DUC, P., WESTHEIM, A., OMLAND, T., KNUDSEN, C. W., STORROW, A. B., ABRAHAM, W. T., LAMBA, S., WU, A. H., PEREZ, A., CLOPTON, P., KRISHNASWAMY, P., KAZANEGRA, R. & MAISEL, A. S. (2002) B-type natriuretic peptide and clinical judgment in emergency diagnosis of heart failure: analysis from Breathing Not Properly (BNP) Multinational Study. *Circulation,* 106**,** 416-22.

MCKIE, P. M., CATALIOTTI, A., BOERRIGTER, G., CHEN, H. H., SANGARALINGHAM, S. J., MARTIN, F. L., ICHIKI, T. & BURNETT, J. C., JR. (2010a) A novel atrial natriuretic peptide based therapeutic in experimental angiotensin II mediated acute hypertension. *Hypertension,* 56**,** 1152-9.

MCKIE, P. M., CATALIOTTI, A., HUNTLEY, B. K., MARTIN, F. L., OLSON, T. M. & BURNETT, J. C., JR. (2009) A human atrial natriuretic peptide gene mutation reveals a novel peptide with enhanced blood pressure-lowering, renal-enhancing, and aldosterone-suppressing actions. *J Am Coll Cardiol,* 54**,** 1024-32.

MCKIE, P. M., CATALIOTTI, A., LAHR, B. D., MARTIN, F. L., REDFIELD, M. M., BAILEY, K. R., RODEHEFFER, R. J. & BURNETT, J. C., JR. (2010b) The prognostic value of N-terminal pro-B-type natriuretic peptide for death and cardiovascular events in healthy normal and stage A/B heart failure subjects. *J Am Coll Cardiol,* 55**,** 2140-7.

MCKIE, P. M., CATALIOTTI, A., SANGARALINGHAM, S. J., ICHIKI, T., CANNONE, V., BAILEY, K. R., REDFIELD, M. M., RODEHEFFER, R. J. & BURNETT, J. C., JR. (2011) Predictive utility of atrial, N-terminal pro-atrial, and N-terminal pro-B-type natriuretic peptides for mortality and cardiovascular events in the general community: a 9-year follow-up study. *Mayo Clin Proc,* 86**,** 1154-60.

MEYER, M., RICHTER, R., BRUNKHORST, R., WRENGER, E., SCHULZ-KNAPPE, P., KIST, A., MENTZ, P., BRABANT, E. G., KOCH, K. M., RECHKEMMER, G. & FORSSMANN, W. G. (1996) Urodilatin is involved in sodium homeostasis and exerts sodium-state-dependent natriuretic and diuretic effects. *Am J Physiol,* 271**,** F489-97.

MISONO, K. S., FUKUMI, H., GRAMMER, R. T. & INAGAMI, T. (1984a) Rat atrial natriuretic factor: complete amino acid sequence and disulfide linkage essential for biological activity. *Biochem Biophys Res Commun,* 119**,** 524-9.

MISONO, K. S., GRAMMER, R. T., FUKUMI, H. & INAGAMI, T. (1984b) Rat atrial natriuretic factor: isolation, structure and biological activities of four major peptides. *Biochem Biophys Res Commun,* 123**,** 444-51.

MISONO, K. S., PHILO, J. S., ARAKAWA, T., OGATA, C. M., QIU, Y., OGAWA, H. & YOUNG, H. S. (2011) Structure, signaling mechanism and regulation of the natriuretic peptide receptor guanylate cyclase. *FEBS J,* 278**,** 1818-29.

MORISHITA, R., GIBBONS, G. H., PRATT, R. E., TOMITA, N., KANEDA, Y., OGIHARA, T. & DZAU, V. J. (1994) Autocrine and paracrine effects of atrial natriuretic peptide gene transfer on vascular smooth muscle and endothelial cellular growth. *J Clin Invest,* 94**,** 824-9.

MOUAWAD, R., LI, Y. & ANAND-SRIVASTAVA, M. B. (2004) Atrial natriuretic peptide-C receptor-induced attenuation of adenylyl cyclase signaling activates phosphatidylinositol turnover in A10 vascular smooth muscle cells. *Mol Pharmacol,* 65**,** 917-24.

MUNAGALA, V. K., BURNETT, J. C., JR. & REDFIELD, M. M. (2004) The natriuretic peptides in cardiovascular medicine. *Curr Probl Cardiol,* 29**,** 707-69.

MURTHY, K. S., TENG, B. Q., ZHOU, H., JIN, J. G., GRIDER, J. R. & MAKHLOUF, G. M. (2000) G(i-1)/G(i-2)-dependent signaling by single-transmembrane natriuretic peptide clearance receptor. *Am J Physiol Gastrointest Liver Physiol,* 278**,** G974-80.

NAKAO, K., MUKOYAMA, M., HOSODA, K., SUGA, S., OGAWA, Y., SAITO, Y., SHIRAKAMI, G., ARAI, H., JOUGASAKI, M. & IMURA, H. (1991) Biosynthesis, secretion, and receptor selectivity of human brain natriuretic peptide. *Can J Physiol Pharmacol,* 69**,** 1500-6.

NAKAYAMA, T., SOMA, M., TAKAHASHI, Y., REHEMUDULA, D., KANMATSUSE, K. & FURUYA, K. (2000) Functional deletion mutation of the 5'-flanking region of type A human natriuretic peptide receptor gene and its association with essential hypertension and left ventricular hypertrophy in the Japanese. *Circ Res,* 86**,** 841-5.

NUSSENZVEIG, D. R., LEWICKI, J. A. & MAACK, T. (1990) Cellular mechanisms of the clearance function of type C receptors of atrial natriuretic factor. *J Biol Chem,* 265**,** 20952-8.

O'CONNOR, C. M., STARLING, R. C., HERNANDEZ, A. F., ARMSTRONG, P. W., DICKSTEIN, K., HASSELBLAD, V., HEIZER, G. M., KOMAJDA, M., MASSIE, B. M., MCMURRAY, J. J., NIEMINEN, M. S., REIST, C. J., ROULEAU, J. L., SWEDBERG, K., ADAMS, K. F., JR., ANKER, S. D., ATAR, D., BATTLER, A., BOTERO, R., BOHIDAR, N. R., BUTLER, J., CLAUSELL, N., CORBALAN, R., COSTANZO, M. R., DAHLSTROM, U., DECKELBAUM, L. I., DIAZ, R., DUNLAP, M. E., EZEKOWITZ, J. A., FELDMAN, D., FELKER, G. M., FONAROW, G. C., GENNEVOIS, D., GOTTLIEB, S. S., HILL, J. A., HOLLANDER, J. E., HOWLETT, J. G., HUDSON, M. P., KOCIOL, R. D., KRUM, H., LAUCEVICIUS, A., LEVY, W. C., MENDEZ, G. F., METRA, M., MITTAL, S., OH, B. H., PEREIRA, N. L., PONIKOWSKI, P., TANG, W. H., TANOMSUP, S., TEERLINK, J. R., TRIPOSKIADIS, F., TROUGHTON, R. W., VOORS, A. A., WHELLAN, D. J., ZANNAD, F. & CALIFF, R. M. (2011) Effect of nesiritide in patients with acute decompensated heart failure. *N Engl J Med,* 365**,** 32-43.

OGAWA, H., QIU, Y., OGATA, C. M. & MISONO, K. S. (2004) Crystal structure of hormone-bound atrial natriuretic peptide receptor extracellular domain: rotation mechanism for transmembrane signal transduction. *J Biol Chem,* 279**,** 28625-31.

OGAWA, H., QIU, Y., PHILO, J. S., ARAKAWA, T., OGATA, C. M. & MISONO, K. S. (2010) Reversibly bound chloride in the atrial natriuretic peptide receptor hormone-binding domain: possible allosteric regulation and a conserved structural motif for the chloride-binding site. *Protein Sci,* 19**,** 544-57.

OKAWA, H., HORIMOTO, H., MIENO, S., NOMURA, Y., YOSHIDA, M. & SHINJIRO, S. (2003) Preischemic infusion of alpha-human atrial natriuretic peptide elicits myoprotective effects against ischemia reperfusion in isolated rat hearts. *Mol Cell Biochem,* 248**,** 171-7.

OLIVER, P. M., FOX, J. E., KIM, R., ROCKMAN, H. A., KIM, H. S., REDDICK, R. L., PANDEY, K. N., MILGRAM, S. L., SMITHIES, O. & MAEDA, N. (1997) Hypertension, cardiac hypertrophy, and sudden death in mice lacking natriuretic peptide receptor A. *Proc Natl Acad Sci U S A,* 94**,** 14730-5.

OLIVER, P. M., JOHN, S. W., PURDY, K. E., KIM, R., MAEDA, N., GOY, M. F. & SMITHIES, O. (1998) Natriuretic peptide receptor 1 expression influences blood pressures of mice in a dose-dependent manner. *Proc Natl Acad Sci U S A,* 95**,** 2547-51.

PAGANO, M. & ANAND-SRIVASTAVA, M. B. (2001) Cytoplasmic domain of natriuretic peptide receptor C constitutes Gi activator sequences that inhibit adenylyl cyclase activity. *J Biol Chem,* 276**,** 22064-70.

PAN, S., CHEN, H. H., DICKEY, D. M., BOERRIGTER, G., LEE, C., KLEPPE, L. S., HALL, J. L., LERMAN, A., REDFIELD, M. M., POTTER, L. R., BURNETT, J. C., JR. & SIMARI, R. D. (2009) Biodesign of a renal-protective peptide based on alternative splicing of B-type natriuretic peptide. *Proc Natl Acad Sci U S A,* 106**,** 11282-7.

PANDEY, K. N. (1992) Kinetic analysis of internalization, recycling and redistribution of atrial natriuretic factor-receptor complex in cultured vascular smooth-muscle cells. Ligand-dependent receptor down-regulation. *Biochem J,* 288 (Pt 1)**,** 55-61.

PANDEY, K. N. (1993) Stoichiometric analysis of internalization, recycling, and redistribution of photoaffinity-labeled guanylate cyclase/atrial natriuretic factor receptors in cultured murine Leydig tumor cells. *J Biol Chem,* 268**,** 4382-90.

PANDEY, K. N., INAGAMI, T. & MISONO, K. S. (1986) Atrial natriuretic factor receptor on cultured Leydig tumor cells: ligand binding and photoaffinity labeling. *Biochemistry,* 25**,** 8467-72.

PANDEY, K. N., KUMAR, R., LI, M. & NGUYEN, H. (2000) Functional domains and expression of truncated atrial natriuretic peptide receptor-A: the carboxyl-terminal regions direct the receptor internalization and sequestration in COS-7 cells. *Mol Pharmacol,* 57**,** 259-67.

PANDEY, K. N., OLIVER, P. M., MAEDA, N. & SMITHIES, O. (1999) Hypertension associated with decreased testosterone levels in natriuretic peptide receptor-A gene-knockout and gene-duplicated mutant mouse models. *Endocrinology,* 140**,** 5112-9.

PANKOW, K., SCHWIEBS, A., BECKER, M., SIEMS, W. E., KRAUSE, G. & WALTHER, T. (2009) Structural substrate conditions required for neutral

endopeptidase-mediated natriuretic Peptide degradation. *J Mol Biol,* 393**,** 496-503.

PANKOW, K., WANG, Y., GEMBARDT, F., KRAUSE, E., SUN, X., KRAUSE, G., SCHULTHEISS, H. P., SIEMS, W. E. & WALTHER, T. (2007) Successive action of meprin A and neprilysin catabolizes B-type natriuretic peptide. *Circ Res,* 101**,** 875-82.

PAPALEO, E., RUSSO, L., SHAIKH, N., CIPOLLA, L., FANTUCCI, P. & DE GIOIA, L. (2010) Molecular dynamics investigation of cyclic natriuretic peptides: dynamic properties reflect peptide activity. *J Mol Graph Model,* 28**,** 834-41.

PARAT, M., BLANCHET, J. & DE LEAN, A. (2010) Role of juxtamembrane and transmembrane domains in the mechanism of natriuretic peptide receptor A activation. *Biochemistry,* 49**,** 4601-10.

PATEL, J. B., VALENCIK, M. L., PRITCHETT, A. M., BURNETT, J. C., JR., MCDONALD, J. A. & REDFIELD, M. M. (2005) Cardiac-specific attenuation of natriuretic peptide A receptor activity accentuates adverse cardiac remodeling and mortality in response to pressure overload. *Am J Physiol Heart Circ Physiol,* 289**,** H777-84.

PATTEN, R. D., ARONOVITZ, M. J., DERAS-MEJIA, L., PANDIAN, N. G., HANAK, G. G., SMITH, J. J., MENDELSOHN, M. E. & KONSTAM, M. A. (1998) Ventricular remodeling in a mouse model of myocardial infarction. *Am J Physiol,* 274**,** H1812-20.

PFEFFER, J. M., PFEFFER, M. A., FLETCHER, P. J. & BRAUNWALD, E. (1991) Progressive ventricular remodeling in rat with myocardial infarction. *Am J Physiol,* 260**,** H1406-14.

PFEIFER, A., ASZODI, A., SEIDLER, U., RUTH, P., HOFMANN, F. & FASSLER, R. (1996) Intestinal secretory defects and dwarfism in mice lacking cGMP-dependent protein kinase II. *Science,* 274**,** 2082-6.

PFEIFER, A., KLATT, P., MASSBERG, S., NY, L., SAUSBIER, M., HIRNEISS, C., WANG, G. X., KORTH, M., ASZODI, A., ANDERSSON, K. E., KROMBACH, F., MAYERHOFER, A., RUTH, P., FASSLER, R. & HOFMANN, F. (1998) Defective smooth muscle regulation in cGMP kinase I-deficient mice. *EMBO J,* 17**,** 3045-51.

PIGGOTT, L. A., HASSELL, K. A., BERKOVA, Z., MORRIS, A. P., SILBERBACH, M. & RICH, T. C. (2006) Natriuretic peptides and nitric oxide stimulate cGMP synthesis in different cellular compartments. *J Gen Physiol,* 128**,** 3-14.

POKREISZ, P., VANDENWIJNGAERT, S., BITO, V., VAN DEN BERGH, A., LENAERTS, I., BUSCH, C., MARSBOOM, G., GHEYSENS, O., VERMEERSCH, P., BIESMANS, L., LIU, X., GILLIJNS, H., PELLENS, M., VAN LOMMEL, A., BUYS, E., SCHOONJANS, L., VANHAECKE, J., VERBEKEN, E., SIPIDO, K., HERIJGERS, P., BLOCH, K. D. & JANSSENS, S. P. (2009) Ventricular phosphodiesterase-5 expression is increased in patients with advanced heart failure and contributes to adverse ventricular remodeling after myocardial infarction in mice. *Circulation,* 119**,** 408-16.

PORCEL, J. M. (2005) The use of probrain natriuretic peptide in pleural fluid for the diagnosis of pleural effusions resulting from heart failure. *Curr Opin Pulm Med,* 11**,** 329-33.

POTTER, L. R. (1998) Phosphorylation-dependent regulation of the guanylyl cyclase-linked natriuretic peptide receptor B: dephosphorylation is a mechanism of desensitization. *Biochemistry,* 37**,** 2422-9.

POTTER, L. R. (2005) Domain analysis of human transmembrane guanylyl cyclase receptors: implications for regulation. *Front Biosci,* 10**,** 1205-20.

POTTER, L. R., ABBEY-HOSCH, S. & DICKEY, D. M. (2006) Natriuretic peptides, their receptors, and cyclic guanosine monophosphate-dependent signaling functions. *Endocr Rev,* 27**,** 47-72.

POTTER, L. R. & GARBERS, D. L. (1992) Dephosphorylation of the guanylyl cyclase-A receptor causes desensitization. *J Biol Chem,* 267**,** 14531-4.

POTTER, L. R. & GARBERS, D. L. (1994) Protein kinase C-dependent desensitization of the atrial natriuretic peptide receptor is mediated by dephosphorylation. *J Biol Chem,* 269**,** 14636-42.

POTTER, L. R. & HUNTER, T. (2000) Activation of protein kinase C stimulates the dephosphorylation of natriuretic peptide receptor-B at a single serine residue: a possible mechanism of heterologous desensitization. *J Biol Chem,* 275**,** 31099-106.

POTTER, L. R. & HUNTER, T. (2001) Guanylyl cyclase-linked natriuretic peptide receptors: structure and regulation. *J Biol Chem,* 276**,** 6057-60.

POTTER, L. R., YODER, A. R., FLORA, D. R., ANTOS, L. K. & DICKEY, D. M. (2009) Natriuretic peptides: their structures, receptors, physiologic functions and therapeutic applications. *Handb Exp Pharmacol***,** 341-66.

PRINS, B. A., WEBER, M. J., HU, R. M., PEDRAM, A., DANIELS, M. & LEVIN, E. R. (1996) Atrial natriuretic peptide inhibits mitogen-activated protein kinase through the clearance receptor. Potential role in the inhibition of astrocyte proliferation. *J Biol Chem,* 271**,** 14156-62.

RANGASWAMI, H., MARATHE, N., ZHUANG, S., CHEN, Y., YEH, J. C., FRANGOS, J. A., BOSS, G. R. & PILZ, R. B. (2009) Type II cGMP-dependent protein kinase mediates osteoblast mechanotransduction. *J Biol Chem,* 284**,** 14796-808.

RATHINAVELU, A. & ISOM, G. E. (1991) Differential internalization and processing of atrial-natriuretic-factor B and C receptor in PC12 cells. *Biochem J,* 276 (Pt 2)**,** 493-7.

RESINK, T. J., SCOTT-BURDEN, T., BAUR, U., JONES, C. R. & BUHLER, F. R. (1988) Atrial natriuretic peptide induces breakdown of phosphatidylinositol phosphates in cultured vascular smooth-muscle cells. *Eur J Biochem,* 172**,** 499-505.

RIBEIRO, S., MAIRHOFER, J., MADEIRA, C., DIOGO, M. M., LOBATO DA SILVA, C., MONTEIRO, G., GRABHERR, R. & CABRAL, J. M. (2012) Plasmid DNA size does affect nonviral gene delivery efficiency in stem cells. *Cell Reprogram,* 14**,** 130-7.

RITTER, D., DEAN, A. D., GLUCK, S. L. & GREENWALD, J. E. (1995) Natriuretic peptide receptors A and B have different cellular distributions in rat kidney. *Kidney Int,* 48**,** 5758-66.

RONDEAU, J. J., MCNICOLL, N., GAGNON, J., BOUCHARD, N., ONG, H. & DE LEAN, A. (1995) Stoichiometry of the atrial natriuretic factor-R1 receptor complex in the bovine zona glomerulosa. *Biochemistry,* 34**,** 2130-6.

ROSENZWEIG, A. & SEIDMAN, C. E. (1991) Atrial natriuretic factor and related peptide hormones. *Annu Rev Biochem,* 60**,** 229-55.

ROST, N. S., BIFFI, A., CLOONAN, L., CHORBA, J., KELLY, P., GREER, D., ELLINOR, P. & FURIE, K. L. (2012) Brain natriuretic peptide predicts functional outcome in ischemic stroke. *Stroke,* 43**,** 441-5.

RUBATTU, S., SCIARRETTA, S., VALENTI, V., STANZIONE, R. & VOLPE, M. (2008) Natriuretic peptides: an update on bioactivity, potential therapeutic use, and implication in cardiovascular diseases. *Am J Hypertens,* 21**,** 733-41.

SANO, T., MORISHITA, Y., MATSUDA, Y. & YAMADA, K. (1992) Pharmacological profile of HS-142-1, a novel nonpeptide atrial natriuretic peptide antagonist of microbial origin. I. Selective inhibition of the actions of natriuretic peptides in anesthetized rats. *J Pharmacol Exp Ther,* 260**,** 825-31.

SANTOS-NETO, M. S., CARVALHO, A. F., MONTEIRO, H. S., FORTE, L. R. & FONTELES, M. C. (2006) Interaction of atrial natriuretic peptide, urodilatin, guanylin and uroguanylin in the isolated perfused rat kidney. *Regul Pept,* 136**,** 14-22.

SANTOS, R. A., SIMOES E SILVA, A. C., MARIC, C., SILVA, D. M., MACHADO, R. P., DE BUHR, I., HERINGER-WALTHER, S., PINHEIRO, S. V., LOPES, M. T., BADER, M., MENDES, E. P., LEMOS, V. S., CAMPAGNOLE-SANTOS, M. J., SCHULTHEISS, H. P., SPETH, R. & WALTHER, T. (2003) Angiotensin-(1-7) is an endogenous ligand for the G protein-coupled receptor Mas. *Proc Natl Acad Sci U S A,* 100**,** 8258-63.

SAWADA, Y., SUDA, M., YOKOYAMA, H., KANDA, T., SAKAMAKI, T., TANAKA, S., NAGAI, R., ABE, S. & TAKEUCHI, T. (1997) Stretch-induced hypertrophic growth of cardiocytes and processing of brain-type natriuretic peptide are controlled by proprotein-processing endoprotease furin. *J Biol Chem,* 272**,** 20545-54.

SAXENHOFER, H., FITZGIBBON, W. R. & PAUL, R. V. (1993) Urodilatin: binding properties and stimulation of cGMP generation in rat kidney cells. *Am J Physiol,* 264**,** F267-73.

SAXENHOFER, H., RASELLI, A., WEIDMANN, P., FORSSMANN, W. G., BUB, A., FERRARI, P. & SHAW, S. G. (1990) Urodilatin, a natriuretic factor from kidneys, can modify renal and cardiovascular function in men. *Am J Physiol,* 259**,** F832-8.

SCHELLENBERGER, U., NIEDERKOFLER, E. E., KIERNAN, U. A., O'REAR, J. & NELSON, R. W. (2009) (JP2009043650) METHOD, COMPOSITION AND DEVICE FOR SAMPLING NATRIURETIC PEPTIDES IN BIOLOGICAL FLUID. *Parent applied by SCIOS Inc.*

SCHOENFELD, J. R., SEHL, P., QUAN, C., BURNIER, J. P. & LOWE, D. G. (1995) Agonist selectivity for three species of natriuretic peptide receptor-A. *Mol Pharmacol,* 47**,** 172-80.

SCHULZ-KNAPPE, P., FORSSMANN, K., HERBST, F., HOCK, D., PIPKORN, R. & FORSSMANN, W. G. (1988) Isolation and structural analysis of "urodilatin", a new peptide of the cardiodilatin-(ANP)-family, extracted from human urine. *Klin Wochenschr,* 66**,** 752-9.

SCHULZ-KNAPPE, P., HONRATH, U., FORSSMANN, W. G. & SONNENBERG, H. (1990) Endogenous natriuretic peptides: effect on collecting duct function in rat kidney. *Am J Physiol,* 259**,** F415-8.

SCHWIEBS, A., WANG, Y., ZHU, X., PANKOW, K., SIEMS, W.-E. & WALTHER, T. (2011) The BNP metabolite BNP1-30 is a more potent vasorelaxant peptide than the mature BNP1-32 (Abstract). *Eur J Heart Fail,* 10 (Suppl. 1)**,** S6.

SEMENOV, A. G., TAMM, N. N., SEFERIAN, K. R., POSTNIKOV, A. B., KARPOVA, N. S., SEREBRYANAYA, D. V., KOSHKINA, E. V., KRASNOSELSKY, M. I. & KATRUKHA, A. G. (2010) Processing of pro-B-type natriuretic peptide: furin and corin as candidate convertases. *Clin Chem,* 56**,** 1166-76.

SENGENES, C., BOULOUMIE, A., HAUNER, H., BERLAN, M., BUSSE, R., LAFONTAN, M. & GALITZKY, J. (2003) Involvement of a cGMP-dependent pathway in the natriuretic peptide-mediated hormone-sensitive lipase phosphorylation in human adipocytes. *J Biol Chem,* 278**,** 48617-26.

SHI, S. J., NGUYEN, H. T., SHARMA, G. D., NAVAR, L. G. & PANDEY, K. N. (2001) Genetic disruption of atrial natriuretic peptide receptor-A alters renin and angiotensin II levels. *Am J Physiol Renal Physiol,* 281**,** F665-73.

SHI, S. J., VELLAICHAMY, E., CHIN, S. Y., SMITHIES, O., NAVAR, L. G. & PANDEY, K. N. (2003) Natriuretic peptide receptor A mediates renal sodium excretory responses to blood volume expansion. *Am J Physiol Renal Physiol,* 285**,** F694-702.

SHIMIZU, H., MASUTA, K., AONO, K., ASADA, H., SASAKURA, K., TAMAKI, M., SUGITA, K. & YAMADA, K. (2002) Molecular forms of human brain natriuretic peptide in plasma. *Clin Chim Acta,* 316**,** 129-35.

SHIOURA, K. M., GEENEN, D. L. & GOLDSPINK, P. H. (2007) Assessment of cardiac function with the pressure-volume conductance system following myocardial infarction in mice. *Am J Physiol Heart Circ Physiol,* 293**,** H2870-7.

SIMON, A., HARRINGTON, E. O., LIU, G. X., KOREN, G. & CHOUDHARY, G. (2009) Mechanism of C-type natriuretic peptide-induced endothelial cell hyperpolarization. *Am J Physiol Lung Cell Mol Physiol,* 296**,** L248-56.

SINGH, G., KUC, R. E., MAGUIRE, J. J., FIDOCK, M. & DAVENPORT, A. P. (2006) Novel snake venom ligand dendroaspis natriuretic peptide is selective for natriuretic peptide receptor-A in human heart: downregulation of natriuretic peptide receptor-A in heart failure. *Circ Res,* 99**,** 183-90.

SMITH, M. W., ESPINER, E. A., YANDLE, T. G., CHARLES, C. J. & RICHARDS, A. M. (2000) Delayed metabolism of human brain natriuretic peptide reflects resistance to neutral endopeptidase. *J Endocrinol,* 167**,** 239-46.

SOEKI, T., KISHIMOTO, I., OKUMURA, H., TOKUDOME, T., HORIO, T., MORI, K. & KANGAWA, K. (2005) C-type natriuretic peptide, a novel antifibrotic and antihypertrophic agent, prevents cardiac remodeling after myocardial infarction. *J Am Coll Cardiol,* 45**,** 608-16.

SOURJIK, V. & BERG, H. C. (2002) Binding of the Escherichia coli response regulator CheY to its target measured in vivo by fluorescence resonance energy transfer. *Proc Natl Acad Sci U S A,* 99**,** 12669-74.

STEINHELPER, M. E. (1993) Structure, expression, and genomic mapping of the mouse natriuretic peptide type-B gene. *Circ Res,* 72**,** 984-92.

SUDOH, T., KANGAWA, K., MINAMINO, N. & MATSUO, H. (1988) A new natriuretic peptide in porcine brain. *Nature,* 332**,** 78-81.

SUDOH, T., MAEKAWA, K., KOJIMA, M., MINAMINO, N., KANGAWA, K. & MATSUO, H. (1989) Cloning and sequence analysis of cDNA encoding a precursor for human brain natriuretic peptide. *Biochem Biophys Res Commun,* 159**,** 1427-34.

SUGA, S., NAKAO, K., HOSODA, K., MUKOYAMA, M., OGAWA, Y., SHIRAKAMI, G., ARAI, H., SAITO, Y., KAMBAYASHI, Y., INOUYE, K. & ET AL. (1992) Receptor selectivity of natriuretic peptide family, atrial natriuretic peptide, brain natriuretic peptide, and C-type natriuretic peptide. *Endocrinology,* 130**,** 229-39.

TAKAGAWA, J., ZHANG, Y., WONG, M. L., SIEVERS, R. E., KAPASI, N. K., WANG, Y., YEGHIAZARIANS, Y., LEE, R. J., GROSSMAN, W. & SPRINGER, M. L. (2007) Myocardial infarct size measurement in the mouse chronic infarction model: comparison of area- and length-based approaches. *J Appl Physiol,* 102**,** 2104-11.

TAMURA, N., DOOLITTLE, L. K., HAMMER, R. E., SHELTON, J. M., RICHARDSON, J. A. & GARBERS, D. L. (2004) Critical roles of the guanylyl cyclase B receptor in endochondral ossification and development of female reproductive organs. *Proc Natl Acad Sci U S A,* 101**,** 17300-5.

TAYLOR, M. E. & DRICKAMER, K. (2003) Structure-function analysis of C-type animal lectins. *Methods Enzymol,* 363**,** 3-16.

TEICHMANN, A., RUTZ, C., KREUCHWIG, A., KRAUSE, G., WIESNER, B. & SCHULEIN, R. (2012a) The Pseudo Signal Peptide of the Corticotropin-releasing Factor Receptor Type 2A Prevents Receptor Oligomerization. *J Biol Chem,* 287**,** 27265-74.

TEICHMANN, A., SCHMIDT, A., WIESNER, B., OKSCHE, A. & SCHULEIN, R. (2012b) Live cell imaging of G protein-coupled receptors. *Methods Mol Biol,* 897**,** 139-69.

THOMAS, G., SELLIN, K, BESSETTE, M, LAFRENIERE, F, LANCTOT, C, MOFFATT, P (2004) Osteocrin, a local mediator of the natriuretic system. *Proc 26th Annual Meeting of the American Society for Bone and Mineral Research, Seattle, WA (Presentation 1075),* 19.

TIAN, M. & YANG, X. L. (2006) C-type natriuretic peptide modulates glutamate receptors on cultured rat retinal amacrine cells. *Neuroscience,* 139**,** 1211-20.

TIKKANEN, I., FYHRQUIST, F., METSARINNE, K. & LEIDENIUS, R. (1985) Plasma atrial natriuretic peptide in cardiac disease and during infusion in healthy volunteers. *Lancet,* 2**,** 66-9.

TRIPATHI, S. & PANDEY, K. N. (2012) Guanylyl cyclase/natriuretic peptide receptor-A signaling antagonizes the vascular endothelial growth factor-stimulated MAPKs and downstream effectors AP-1 and CREB in mouse mesangial cells. *Mol Cell Biochem,* 368**,** 47-59.

TSAI, E. J. & KASS, D. A. (2009) Cyclic GMP signaling in cardiovascular pathophysiology and therapeutics. *Pharmacol Ther,* 122**,** 216-38.

TSIEN, R. Y. (1998) The green fluorescent protein. *Annu Rev Biochem,* 67**,** 509-44.

TSUTAMOTO, T., KANAMORI, T., MORIGAMI, N., SUGIMOTO, Y., YAMAOKA, O. & KINOSHITA, M. (1993) Possibility of downregulation of atrial natriuretic peptide receptor coupled to guanylate cyclase in peripheral vascular beds of patients with chronic severe heart failure. *Circulation,* 87**,** 70-5.

VALENTIN, J. P., SECHI, L. A., QUI, C., SCHAMBELAN, M. & HUMPHREYS, M. H. (1993) Urodilatin binds to and activates renal receptors for atrial natriuretic peptide. *Hypertension,* 21**,** 432-8.

VANNESTE, Y., MICHEL, A., DIMALINE, R., NAJDOVSKI, T. & DESCHODT-LANCKMAN, M. (1988) Hydrolysis of alpha-human atrial natriuretic

peptide in vitro by human kidney membranes and purified endopeptidase-24.11. Evidence for a novel cleavage site. *Biochem J,* 254**,** 531-7.

VIRAG, J. I. & MURRY, C. E. (2003) Myofibroblast and endothelial cell proliferation during murine myocardial infarct repair. *Am J Pathol,* 163**,** 2433-40.

VIVES, D., FARAGE, S., MOTTA, R., LOPES, A. G. & CARUSO-NEVES, C. (2010) Atrial natriuretic peptides and urodilatin modulate proximal tubule Na(+)-ATPase activity through activation of the NPR-A/cGMP/PKG pathway. *Peptides,* 31**,** 903-8.

VON BOHLEN AND HALBACH, O., WALTHER, T., BADER, M. & ALBRECHT, D. (2000) Interaction between Mas and the angiotensin AT1 receptor in the amygdala. *J Neurophysiol,* 83**,** 2012-21.

VON HAEHLING, S., JANKOWSKA, E. A., MORGENTHALER, N. G., VASSANELLI, C., ZANOLLA, L., ROZENTRYT, P., FILIPPATOS, G. S., DOEHNER, W., KOEHLER, F., PAPASSOTIRIOU, J., KREMASTINOS, D. T., BANASIAK, W., STRUCK, J., PONIKOWSKI, P., BERGMANN, A. & ANKER, S. D. (2007) Comparison of midregional pro-atrial natriuretic peptide with N-terminal pro-B-type natriuretic peptide in predicting survival in patients with chronic heart failure. *J Am Coll Cardiol,* 50**,** 1973-80.

VOORS, A. A. & VAN VELDHUISEN, D. J. (2010) Cardiorenal effects of recombinant human natriuretic peptides. *J Am Coll Cardiol,* 55**,** 1852-3.

WALTHER, T. (2007) (WO2007003594) SCREENING METHODS FOR INHIBITORS OF THE METALLPROTEASE MEPRIN.

WALTHER, T. & SCHWIEBS, A. (2012) (WO/2012/013597) SUBSTANCES AND THE USE THEREOF FOR INFLUENCING NATRIURETIC PEPTIDE RECEPTORS.

WALTHER, T., STEPAN, H., PANKOW, K., BECKER, M., SCHULTHEISS, H. P. & SIEMS, W. E. (2004a) Biochemical analysis of neutral endopeptidase activity reveals independent catabolism of atrial and brain natriuretic peptide. *Biol Chem,* 385**,** 179-84.

WALTHER, T., STEPAN, H., PANKOW, K., GEMBARDT, F., FABER, R., SCHULTHEISS, H. P. & SIEMS, W. E. (2004b) Relation of ANP and BNP to their N-terminal fragments in fetal circulation: evidence for enhanced neutral endopeptidase activity and resistance of BNP to neutral endopeptidase in the fetus. *BJOG,* 111**,** 452-5.

WANG, X., RAULJI, P., MOHAPATRA, S. S., PATEL, R., HELLERMANN, G., KONG, X., VERA, P. L., MEYER-SIEGLER, K. L., COPPOLA, D. & MOHAPATRA, S. (2011) Natriuretic peptide receptor a as a novel target for prostate cancer. *Mol Cancer,* 10**,** 56.

WANG, X., XU, W., MOHAPATRA, S., KONG, X., LI, X., LOCKEY, R. F. & MOHAPATRA, S. S. (2008) Prevention of airway inflammation with topical cream containing imiquimod and small interfering RNA for natriuretic peptide receptor. *Genet Vaccines Ther,* 6**,** 7.

WANG, Y., DE WAARD, M. C., STERNER-KOCK, A., STEPAN, H., SCHULTHEISS, H. P., DUNCKER, D. J. & WALTHER, T. (2007) Cardiomyocyte-restricted over-expression of C-type natriuretic peptide prevents cardiac hypertrophy induced by myocardial infarction in mice. *Eur J Heart Fail,* 9**,** 548-57.

WEI, C. M., KIM, C. H., MILLER, V. M. & BURNETT, J. C., JR. (1993) Vasonatrin peptide: a unique synthetic natriuretic and vasorelaxing peptide. *J Clin Invest,* 92**,** 2048-52.

WOODS, A., KHAN, S. & BEIER, F. (2007) C-type natriuretic peptide regulates cellular condensation and glycosaminoglycan synthesis during chondrogenesis. *Endocrinology,* 148**,** 5030-41.

YANCY, C. W., KRUM, H., MASSIE, B. M., SILVER, M. A., STEVENSON, L. W., CHENG, M., KIM, S. S. & EVANS, R. (2008) Safety and efficacy of outpatient nesiritide in patients with advanced heart failure: results of the Second Follow-Up Serial Infusions of Nesiritide (FUSION II) trial. *Circ Heart Fail,* 1**,** 9-16.

YASODA, A., KOMATSU, Y., CHUSHO, H., MIYAZAWA, T., OZASA, A., MIURA, M., KURIHARA, T., ROGI, T., TANAKA, S., SUDA, M., TAMURA, N., OGAWA, Y. & NAKAO, K. (2004) Overexpression of CNP in chondrocytes rescues achondroplasia through a MAPK-dependent pathway. *Nat Med,* 10**,** 80-6.

YOU, H. & LAYCHOCK, S. G. (2010) Long-term treatment with atrial natriuretic peptide inhibits ATP production and insulin secretion in rat pancreatic islets. *Am J Physiol Endocrinol Metab,* 300**,** E435-44.

YOU, H. & LAYCHOCK, S. G. (2011) Long-term treatment with atrial natriuretic peptide inhibits ATP production and insulin secretion in rat pancreatic islets. *Am J Physiol Endocrinol Metab,* 300**,** E435-44.

ZHANG, Q., MOALEM, J., TSE, J., SCHOLZ, P. M. & WEISS, H. R. (2005) Effects of natriuretic peptides on ventricular myocyte contraction and role of cyclic GMP signaling. *Eur J Pharmacol,* 510**,** 209-15.

ZHAO, D., PANDEY, K. N. & NAVAR, L. G. (2010) ANP-mediated inhibition of distal nephron fractional sodium reabsorption in wild-type and mice overexpressing natriuretic peptide receptor. *Am J Physiol Renal Physiol,* 298**,** F103-8.

ZHAO, D., VELLAICHAMY, E., SOMANNA, N. K. & PANDEY, K. N. (2007) Guanylyl cyclase/natriuretic peptide receptor-A gene disruption causes increased adrenal angiotensin II and aldosterone levels. *Am J Physiol Renal Physiol,* 293**,** F121-7.

ZHU, X., WANG, Y., SCHWIEBS, A. & WALTHER, T. (2011) Designed natriuretic peptide ACNP stimulating NPRA and NPRB, is a new promising tool for the treatment of cardiovascular diseases. *Eur J Heart Fail,* 10 (Suppl. 1).

ZOLLE, O., LAWRIE, A. M. & SIMPSON, A. W. (2000) Activation of the particulate and not the soluble guanylate cyclase leads to the inhibition of Ca2+ extrusion through localized elevation of cGMP. *J Biol Chem,* 275**,** 25892-9.

Appendices

Appendix 1: Haematological parameters within sham and MI groups
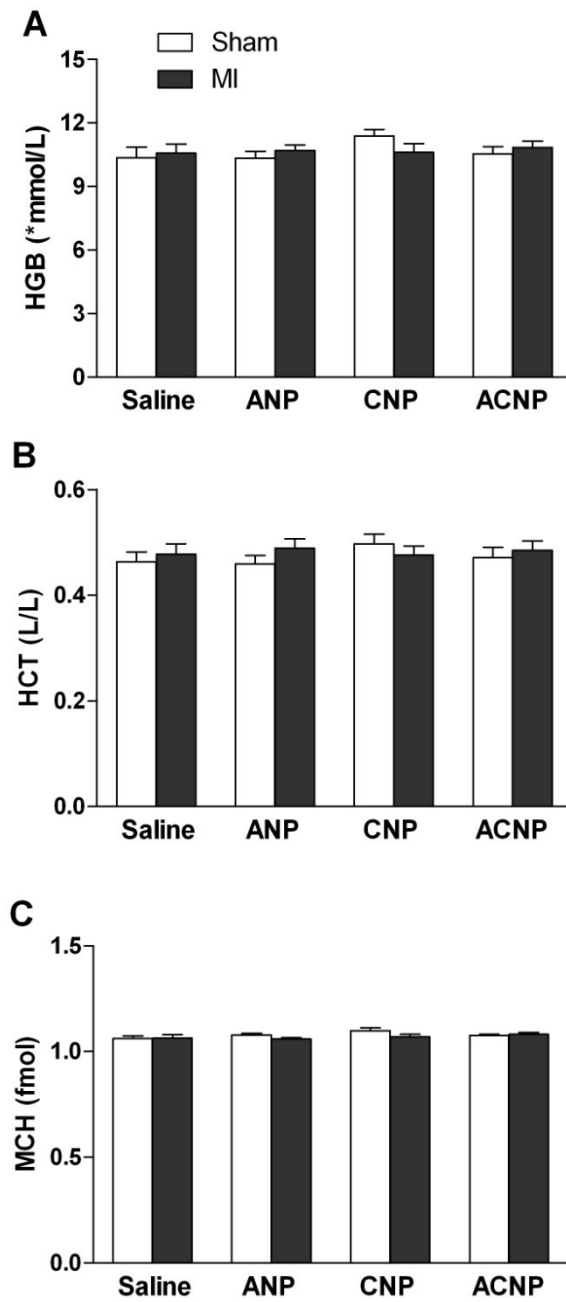
Appendix 1. Comparison of haematological parameters within sham and MI groups. **(A)** haemoglobin (HGB); **(B)** hematocrit (HCT); **(C)** mean corpuscular haemoglobin (MCH).

Appendix 2: Sequence for mouse NPRA cDNA (3174bp)

ATGCCGGGTTCCCGACGCGTCCGTCCGCGCCTAAGGGCGCTGCTGCTGC
TACCGCCGCTGCTGCTGCTCCGAAGCGGCCACGCGAGCGACCTGACCGT
GGCCGTGGTGCTGCCGCTGACCAACACCTCGTACCCGTGGTCTTGGGCG
CGTGTAGGGCCGGCGGTGGAACTGGCTCTCGGGAGGGTGAAGGCTCGGC
CGGACTTGCTGCCGGGTTGGACGGTCCGTATGGTGCTGGGCAGCAGCGA
GAACGCGGCGGGCGTCTGCTCCGACACCGCTGCACCGCTGGCCGCGGTG
GATCTCAAGTGGGAGCACAGCCCCGCGGTGTTCCTGGGCCCCGGCTGCG
TATACTCTGCTGCCCCGGTGGGACGCTTCACCGCGCACTGGCGGGTGCC
GCTGCTGACGGCTGGCGCCCCGGCTCTGGGCATCGGGGTGAAGGATGAG
TACGCGTTAACCACCCGCACAGGACCCAGCCATGTCAAGCTGGGCGACT
TCGTGACGGCGCTGCATCGACGGCTGGGCTGGGAGCACCAGGCGCTTGT
GCTCTATGCAGATCGGCTGGGCGACGACCGGCCGTGCTTCTTCATAGTGG
AGGGGCTGTACATGCGGGTGCGTGAGCGACTCAACATCACAGTAAATCA
CCAGGAGTTCGTCGAGGGCGACCCGGACCACTACACCAAGCTACTGCGG
ACCGTGCAGCGCAAGGGCAGAGTTATCTACATCTGCAGTTCTCCGGATG
CCTTCAGGAATCTGATGCTTTTGGCCCTGGATGCTGGCCTGACTGGGGAG
GACTATGTTTTCTTCCACCTGGATGTGTTTGGGCAAAGCCTTCAGGGTGC
TCAGGGCCCTGTTCCCAGGAAGCCCTGGGAAAGAGACGATGGGCAGGAT
AGGAGAGCCCGCCAGGCCTTTCAGGCTGCCAAAATTATTACTTACAAAG
AACCCGATAATCCTGAGTACTTGGAATTCCTGAAGCAGCTAAAACTCTTG
GCTGACAAGAAATTCAACTTCACCATGGAGGATGGCCTGAAAAATATCA
TCCCAGCATCCTTCCATGACGGGCTCCTGCTCTATGTCCAGGCAGTGACA
GAGACTCTGGCACAGGGGGGCACTGTCACTGATGGAGAGAACATCACTC
AGCGGATGTGGAACCGAAGCTTCCAAGGTGTGACAGGATACCTGAAAAT
TGATAGAAATGGAGATCGGGACACTGATTTCTCCCTCTGGGATATGGAC
CCCGAGACAGGTGCCTTCAGGGTTGTCCTGAACTTTAATGGTACTTCCCA
GGAGCTGATGGCTGTGTCAGAACACAGATTATACTGGCCTCTGGGATAC
CCACCTCCTGACATCCCTAAATGTGGCTTTGACAATGAGGACCCAGCCTG
CAACCAAGACCACTTTTCCACACTGGAGGTTCTGGCTTTGGTGGGCAGCC
TCTCTCTGGTTAGCTTTCTGATCGTGTCTTTCTTCATATACAGGAAGATGC
AGCTGGAAAAGGAGCTGGTCTCAGAGTTGTGGCGGGTGCGCTGGGAGGA
CTTGCAGCCCAGCAGCCTGGAGAGGCACCTTCGGAGCGCTGGCAGTCGG
CTGACCCTGAGTGGGCGAGGCTCCAATTATGGCTCCCTGCTAACCACGG
AGGGCCAGTTCCAAGTCTTTGCCAAGACAGCATACTATAAGGGCAACCT
CGTGGCTGTGAAACGTGTGAACCGGAAACGCATTGAGTTGACACGAAAA
GTCCTGTTTGAACTTAAACATATGCGGGATGTGCAGAATGAGCACTTGA
CCAGATTTGTGGGAGCTTGTACCGACCCTCCCAACATCTGTATCCTCACA

GAGTACTGTCCCCGTGGGAGCCTACAGGACATTCTAGAGAATGAGAGTA
TTACCCTGGACTGGATGTTTCGGTACTCACTCACCAATGACATTGTCAAG
GGAATGCTCTTTCTACACAACGGGGCCATTGGTTCCCATGGGAACCTCAA
GTCATCCAACTGCGTGGTAGATGGACGTTTTGTGTTAAAGATCACAGACT
ATGGGCTCGAGAGCTTCAGAGACCCGGAGCCAGAGCAAGGACACACCC
TCTTTGCCAAAAAACTGTGGACTGCACCTGAGCTCCTGCGAATGGCTTCC
CCACCTGCCCGTGGCTCCCAAGCTGGGGATGTCTACAGTTTTGGTATCAT
CCTTCAGGAAATTGCCCTAAGAAGTGGGGTCTTCTATGTGGAAGGTTTGG
ACCTCAGCCCAAAAGAGATCATTGAGCGTGTGACTCGGGGCGAGCAGCC
CCCATTCCGACCTTCCATGGATCTGCAGAGCCACCTGGAGGAACTGGGG
CAGCTGATGCAGAGGTGCTGGGCAGAGGATCCTCAGGAGCGGCCACCCT
TTCAACAGATCCGCCTGGCGCTGCGCAAGTTCAACAAGGAGAACAGCAG
CAACATCCTGGACAACCTGCTGTCACGCATGGAACAGTACGCCAACAAC
CTGGAGGAACTGGTAGAGGAGAGAACACAGGCTTATCTGGAGGAGAAG
CGCAAAGCTGAGGCCCTGCTTTACCAGATTCTGCCTCACTCTGTGGCTGA
GCAGCTGAAGAGAGGCGAGACAGTCCAGGCTGAGGCATTTGATAGTGTT
ACTATCTATTTCAGTGATATCGTGGGCTTTACAGCTCTTTCAGCAGAGAG
CACACCCATGCAGGTGGTCACCCTGCTCAATGATCTGTACACCTGTTTTG
ATGCTGTCATAGACAACTTTGATGTGTACAAGGTAGAGACCATTGGTGA
TGCTTACATGGTGGTATCAGGGCTCCCAGTGAGGAATGGACAGCTCCAT
GCCCGAGAGGTAGCCCGAATGGCACTTGCACTGCTCGATGCTGTACGCT
CCTTCCGCATCCGCCATAGGCCCCAGGAACAGCTGCGCTTGCGCATTGG
AATTCACACAGGTCCCGTGTGTGCTGGTGTGGTAGGGCTAAAGATGCCC
CGATACTGCCTCTTTGGAGACACAGTCAACACAGCTTCAAGAATGGAGT
CTAATGGGGAAGCCCTCAGGATCCACTTGTCTTCGGAGACCAAGGCTGT
GCTGGAAGAGTTCGATGGTTTTGAGCTGGAGCTCCGAGGTGACGTGGAA
ATGAAGGGCAAAGGCAAGGTTCGAACCTATTGGCTCCTCGGGGAGCGGG
GATGCAGCACTCGAGGC**TGA**

Appendix 3: Sequence for human NPRB cDNA (3144bp)

ATGGCGCTGCCATCACTTCTGCTGTTGGTGGCAGCCCTGGCAGGTGGGG
TGCGTCCTCCCGGGGCGCGGAACCTGACGCTGGCGGTGGTGCTGCCAGA
ACACAACCTGAGCTATGCCTGGGCCTGGCCACGGGTGGGACCCGCTGTG
GCACTAGCTGTGGAGGCTCTGGGCCGGGCACTGCCCGTGGACCTGCGGT
TTGTCAGCTCCGAACTGGAAGGCGCCTGCTCTGAGTACCTGGCACCGCT
GAGCGCTGTGGACCTCAAGCTGTACCATGACCCCGACCTGCTGTTAGGT
CCCGGTTGCGTGTACCTGCTGCCTCTGTGGCCCGCTTTGCCTCCCACTG
GCGCCTTCCCCTGCTGACTGCGGGTGCTGTGGCCTCTGGTTTTTCGGCTA
AGAATGACCATTATCGTACCCTGGTTCGCACTGGCCCCTCTGCTCCCAAG
CTGGGTGAGTTTGTGGTGACACTACACGGGCACTTCAATTGGACTGCCCG
TGCTGCCTTGCTGTACCTGGATGCTCGCACAGATGACCGGCCTCACTACT
TCACCATCGAGGGCGTCTTTGAGGCCCTGCAGGGCAGCAACCTCAGTGT
GCAGCACCAGGTGTATGCCCGAGAGCCAGGGGGCCCCGAGCAGGCCAC
CCACTTCATCCGGGCCAACGGGCGCATTGTGTATCTGCGGCCCTCTGG
AGATGCTGCATGAGATCCTGCTTCAGGCCCAGAGGGAGAATCTGACCAA
TGGGGATTATGTCTTCTTTTACCTGGATGTCTTTGGGGAGAGTCTCCGTG
CAGGCCCCACACGTGCTACAGGCCGGCCCTGGCAGGACAATCGCACCCG
GGAACAGGCCCAGGCCCTCAGAGAGGCCTTTCAGACTGTATTGGTGATC
ACGTACCGAGAACCCCCAAATCCTGAGTATCAGGAATTCCAGAATCGTC
TGCTGATAAGAGCCCGGGAAGACTTTGGTGTGGAGCTGGGCCCTTCCCT
GATGAACCTCATCGCTGGCTGCTTCTATGATGGGATCCTGCTATATGCTG
AAGTCCTGAATGAGACAATACAGGAAGGAGGCACCCGGGAGGATGGAC
TTCGAATTGTGGAAAAGATGCAGGGACGAAGATATCACGGTGTAACTGG
GCTGGTTGTCATGGACAAGAACAATGACCGAGAGACTGACTTTGTCCTC
TGGGCCATGGGAGACCTGGATTCTGGGGACTTTCAGCCTGCAGCCCACT
ACTCGGGAGCTGAGAAGCAGATTTGGTGGACGGGACGGCCTATTCCCTG
GGTGAAGGGGGCTCCTCCCTCGGACAATCCCCCCTGTGCCTTTGACTTGG
ACGACCCATCCTGTGATAAAACTCCACTTTCAACCCTGGCAATTGTGGCT
CTGGGCACAGGAATCACCTTCATCATGTTTGGTGTTTCCAGCTTCCTAAT
TTTCCGAAAGCTGATGCTGGAGAAGGAGCTGGCTAGCATGTTGTGGCGT
ATTCGCTGGGAAGAACTGCAGTTTGGCAACTCAGAGCGTTATCACAAAG
GTGCAGGCAGTCGCCTCACACTGTCGCTGCGGGGATCCAGTTACGGCTC
GCTCATGACAGCCCATGGGAAATACCAGATCTTTGCCAACACCGGTCAC
TTCAAGGGAAATGTTGTCGCCATCAAACATGTGAATAAGAAGCGCATTG
AGCTGACCCGGCAGGTTCTGTTTGAACTCAAACATATGAGAGATGTTCA
GTTCAACCATCTCACTCGCTTCATTGGCGCCTGCATAGACCCTCCCAACA
TTTGCATTGTCACTGAATACTGTCCTCGTGGGAGTTTACAGGATATTCTA

163

GAAAATGACAGCATCAACTTGGACTGGATGTTTCGTTATTCACTCATTAA
TGACCTTGTTAAGGGCATGGCCTTTCTCCACAACAGCATTATTTCATCGC
ATGGGAGTCTCAAGTCCTCCAACTGTGTGGTGGATAGTCGTTTTGTGCTC
AAAATCACAGACTATGGCCTGGCCAGCTTCCGATCAACTGCTGAACCTG
ATGACAGCCATGCCCTCTATGCCAAGAAGCTGTGGACTGCCCCAGAACT
GCTCAGTGGGAACCCCTTGCCAACCACAGGCATGCAGAAGGCTGACGTC
TATAGCTTTGGGATCATCCTGCAGGAGATAGCACTTCGCAGTGGTCCTTT
CTACTTGGAGGGCCTGGACCTCAGCCCCAAAGAGATTGTCCAGAAGGTA
CGAAATGGTCAGCGGCCATATTTCCGGCCAAGCATTGACCGGACCCAAC
TGAATGAAGAGCTAGTTTTGCTGATGGAGCGATGTTGGGCTCAGGACCC
AGCTGAGCGGCCAGACTTTGGACAGATTAAGGGCTTCATTCGGCGCTTT
AACAAGGAGGGTGGCACCAGCATATTGGACAACCTCCTGCTGCGCATGG
AACAGTATGCCAATAACTTGGAGAAGCTGGTGGAGGAACGCACACAGG
CCTATCTGGAGGAAAAACGCAAGGCTGAAGCTCTGCTCTACCAAATCCT
ACCCCATTCAGTGGCAGAGCAGTTAAAACGGGGAGAGACTGTACAGGCT
GAGGCCTTTGACAGTGTTACCATCTACTTCAGTGACATTGTTGGCTTCAC
AGCATTGTCAGCAGAGCACCCCCATGCAGGTAGTGACACTTCTTAAT
GACCTGTATACCTGCTTTGATGCCATAATTGACAACTTTGATGTCTACAA
GGTGGAGACGATTGGGGATGCTTACATGGTGGTATCTGGCCTCCCAGGC
CGAAATGGTCAACGCCATGCACCAGAAATTGCTCGTATGGCCCTAGCAT
TACTAGATGCAGTTTCTTCCTTTCGCATCCGCCACCGACCCCATGACCAG
CTGAGGCTACGCATAGGGGTCCATACTGGGCCAGTCTGTGCTGGGGTTG
TTGGCCTGAAGATGCCCCGTTATTGTCTTTTTGGAGACACAGTGAACACT
GCTTCTCGAATGGAGTCTAATGGTCAAGCGCTGAAGATCCATGTCTCCTC
TACCACCAAGGATGCCCTAGATGAGCTAGGATGCTTCCAGCTAGAGCTT
CGGGGGGATGTGGAAATGAAGGGAAAAGGAAAGATGCGAACATACTGG
CTCTTAGGAGAGCGGAAAGGACCTCCTGGACTCCTG**TAA**

Appendix 4: Downregulated cGMP generation by human NPs in human NPRA and rat/mouse NPRB co-transfected HEK 293 cells
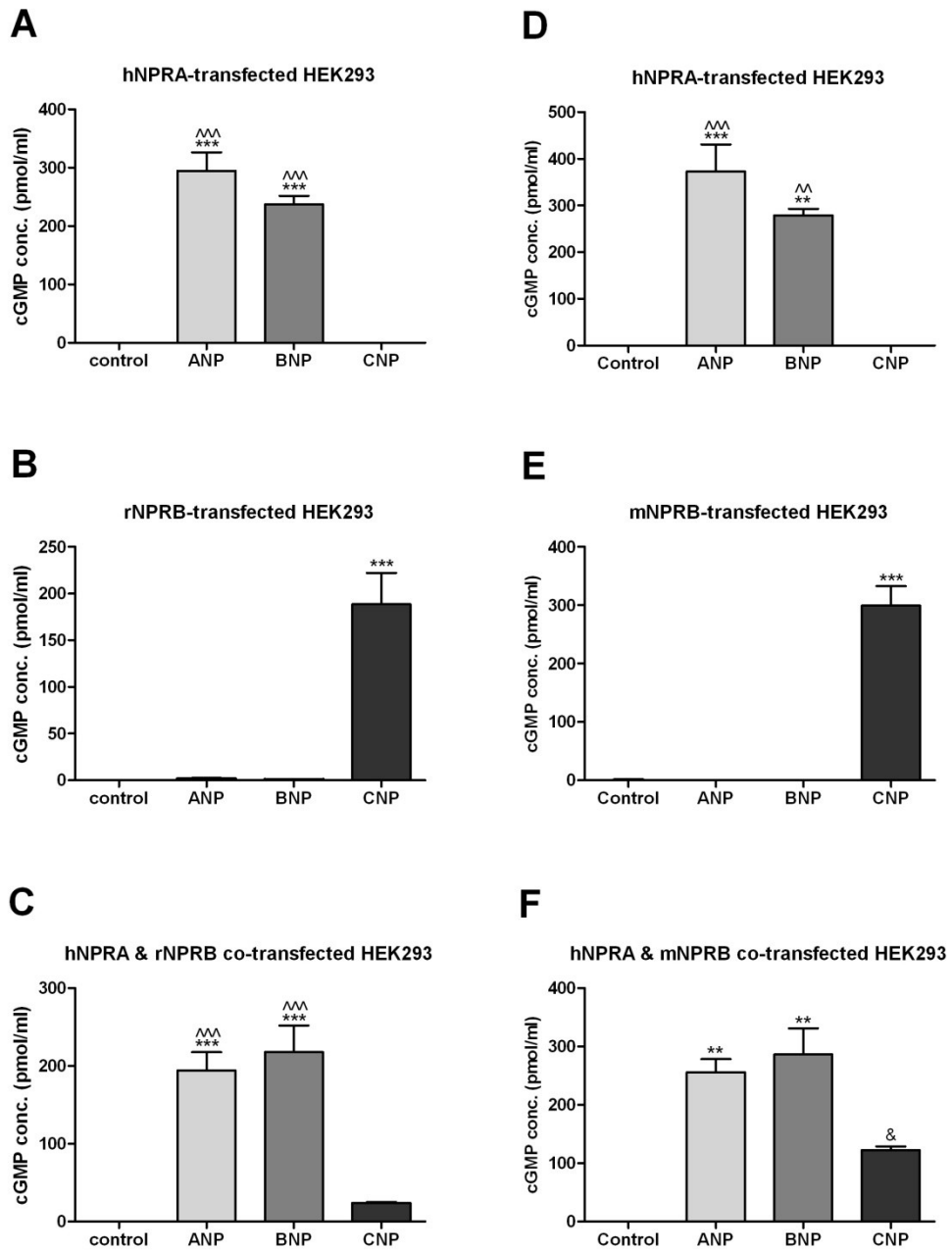
Appendix 4. cGMP generation stimulated by 10^{-7} M of human NPs in receptor transfected HEK293 cells. **(A)** Absolute values of cGMP generation in hNPRA single-transfected HEK293 cells; **(B)** Absolute values of cGMP generation in rNPRB single-transfected HEK293 cells; **(C)** Absolute values of cGMP generation in hNPRA and rNPRB double-transfected HEK293 cells; **(D)** Absolute values of cGMP generation in hNPRA single-transfected HEK293 cells; **(E)** Absolute values of cGMP generation in mNPRB single-transfected HEK293 cells; **(F)** Absolute values of cGMP generation in hNPRA and mNPRB double-transfected HEK293 cells. $**P < 0.01$, $***P < 0.001$ *vs.* control (Ctrl); $^{\&}P < 0.05$ *vs.* BNP; $^{\wedge\wedge}P < 0.01$, $^{\wedge\wedge\wedge}P < 0.001$ *vs.* CNP.

Appendix 5. No detectable immunoblot for hNPRB-CFP in untransfected/receptor transfected HEK293 cells preparations using antibody against GFP tag. Anti-calreticulin antibody were used as house-keeping protein. Numbers on the top indicate different protein fractions as follows: 1 = untransfected; 2 = 0.5 µg hNPRA; 3 = 0.5 µg hNPRB-CFP; 4 = 0.5 µg hNPRB-CFP + 0.125 µg hNPRA; 5 = 0.5 µg hNPRB-CFP + 0.25 µg hNPRA; 6 = 0.5 µg hNPRB-CFP + 0.5 µg hNPRA; 7 = 0.5 µg hNPRB-CFP + 1.0 µg hNPRA.

Appendix 6. No detectable immunoblot for hNPRA-YFP in untransfected/receptor transfected HEK293 cells preparations using antibody against GFP tag. Anti-calreticulin antibody were used as house-keeping protein. Numbers on the top indicate different protein fractions as follows: 1 = untransfected; 2 = 0.5 μg hNPRB; 3 = 0.5 μg hNPRA-YFP; 4 = 0.5 μg hNPRA-YFP + 0.125 μg hNPRB; 5 = 0.5 μg hNPRA-YFP + 0.25 μg hNPRB; 6 = 0.5 μg hNPRA-YFP + 0.5 μg hNPRB; 7 = 0.5 μg hNPRA-YFP + 1.0 μg hNPRB.

Appendix 7: Unaffected cGMP generation by mouse NPs in mouse receptor transfected HEK293 cells
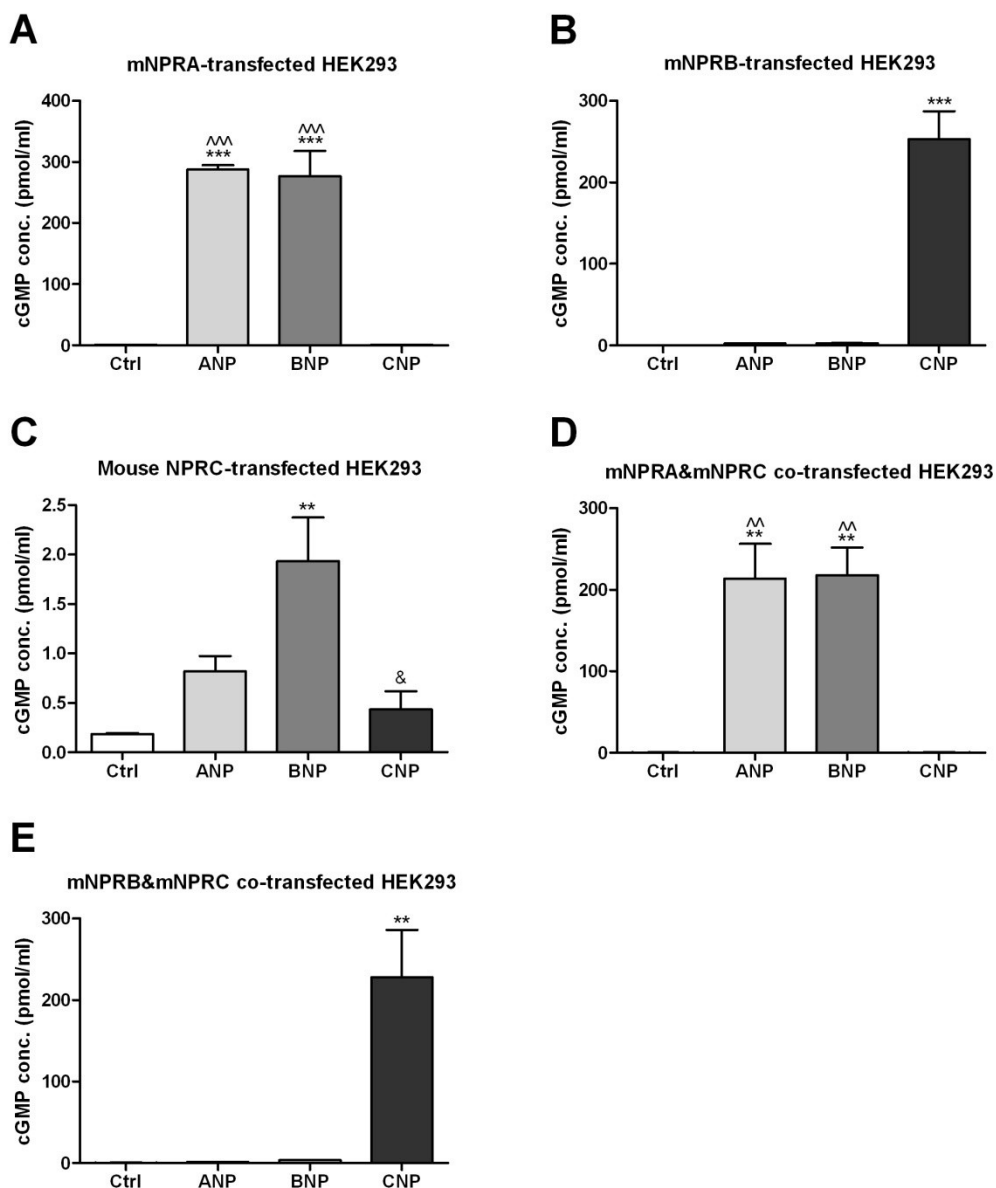
Appendix 7. cGMP generation stimulated by 10^{-7} M of mouse NPs in receptor transfected HEK293 cells. **(A)** Absolute values of cGMP generation in mNPRA single-transfected HEK293 cells; **(B)** Absolute values of cGMP generation in mNPRB single-transfected HEK293 cells; **(C)** Absolute values of cGMP generation in mNPRC single-transfected HEK293 cells; **(D)** Absolute values of cGMP generation in mNPRA and mNPRC double-transfected HEK293 cells; **(E)** Absolute values of cGMP generation in mNPRB and mNPRC double-transfected HEK293 cells. **P < 0.01, ***P < 0.001 *vs.* control (Ctrl); &P < 0.05 *vs.* BNP; ^^P < 0.01, ^^^P < 0.001 *vs.* CNP.

Appendix 8: Sequence alignment results of human NPRA, rat NPRA and mouse NPRA cDNA

```
Human_NPRA ATG CCG GGG CCC CGG CGC CCC GCT GGC TCC CGC CTG CGC CTG CTC CTG CTC CTG CTG CTG  [  60]
Rat_NPRA   ... ... ..C T.. ..A ... GT. --- --- --- ..T .C. ... ..A AGG GC. ..G ... ... ...  [  60]
Mouse_NPRA ... ... ..T T.. ..A ... GT. --- --- --- ..T .C. ... ..A AGG GC. ..G ... ... ..A  [  60]

Human_NPRA CCG CCG CTG CTG CTG CTG CTC CGG GGC AGC CAC GCG GGC AAC CTG ACG GTA GCC GTG GTA  [ 120]
Rat_NPRA   ... ... ..T ... ..A --- ... ... ... G.. ... ... A.. G.. ... ..C ..G ..T ... ..G  [ 120]
Mouse_NPRA ... ... ... ... --- ... ..A A.. G.. ... ... A.. G.. ... ..C ..G ... ... ..G  [ 120]

Human_NPRA CTG CCG CTG GCC AAT ACC TCG TAC CCC TGG TCG TGG GCG CGC GTG GGA CCC GCC GTG GAG  [ 180]
Rat_NPRA   ... ... ... A.. ..C ... ... ... ..G ... ..C ... ... ..T ..A ..G ..G ... ... ..A  [ 180]
Mouse_NPRA ... ... ... A.. ..C ... ... ... ..G ... ..G ... ... ..T ..A ..G ..G ..G ... ..A  [ 180]

Human_NPRA CTG GCC CTG GCC CAG GTG AAG GCG CGC CCC GAC TTG CTG CCG GGC TGG ACG GTC CGC ACG  [ 240]
Rat_NPRA   ... ..T ..C ..G .G. ... ... ... ..T ..G ..G ... ... ... ..T ... ... ... ... .T.  [ 240]
Mouse_NPRA ... ..T ..C .GG AG. ... ... ... ..T ..G ..G ... ... ... ..T ... ... ... ..T .T.  [ 240]

Human_NPRA GTG CTG GGC AGC AGC GAA AAC GCG CTG GGC GTC TGC TCC GAC ACC GCA GCG CCC CTG GCC  [ 300]
Rat_NPRA   ... ... ... ... ..T ..G ... ... GC. ... ... ... ..G ... ... ..C ..A ..G ... ...  [ 300]
Mouse_NPRA ... ... ... ... ..T ..G ... ... GC. ... ... ... ... ... ... ..T ..A ..G ... ...  [ 300]

Human_NPRA GCG GTG GAC CTC AAG TGG GAG CAC AAC CCC GCT GTG TTC CTG GGC CCC GGC TGC GTG TAC  [ 360]
Rat_NPRA   ... ... ... ... ... ... ... .G. ... ..G ... ... ... ... ... ... ... ... ..C ...  [ 360]
Mouse_NPRA ... ... ..T ... ... ... ... .G. ... ..G ... ... ... ... ... ... ... ..A ... ...  [ 360]

Human_NPRA GCC GCC GCC CCA GTG GGG CGC TTC ACC GCG CAC TGG CGG GTC CCG CTG CTG ACC GCC GGC  [ 420]
Rat_NPRA   T.. ..T ... ..G ... ... ... ... ... ... ... ... ... ..G ... ... ... ... ... ...  [ 420]
Mouse_NPRA T.T ..T ... ..G ... ..A ... ... ... ... ... ... ... ..G ... ... ... ..G ..T ...  [ 420]

Human_NPRA GCC CCG GCG CTG GGC TTC GGT GTC AAG GAC GAG TAT GCG CTG ACC ACC CGC GCG GGG CCC  [ 480]
Rat_NPRA   ... ... ..T ... ... A.. ..G ... ... ..T ... ... ... ..A ... ... ... A.A ..A ...  [ 480]
Mouse_NPRA ... ... ..T ... ... A.. ..G ..G ... ..T ... ..C ... T.A ... ... ... A.A ..A ...  [ 480]

Human_NPRA AGC TAC GCC AAG CTG GGG GAC TTC GTG GCG GCG CTG CAC CGA CGG CTG GGC TGG GAG CGC  [ 540]
Rat_NPRA   ... C.T .T. ... ... ... ..C ..T ... ... A.. ... ... ..T ... ... ... ... ... ..A.  [ 540]
Mouse_NPRA ... C.T .T. ... ... ... ..C ... ... ... A.. ... ... ..T ... ... ... ... ... ..A.  [ 540]

Human_NPRA CAA GCG CTC ATG CTC TAC GCC TAC CGG CCG GGT GAC GAA GAG CAC TGC TTC TTC CTC GTG  [ 600]
Rat_NPRA   ..G ... ..G G.. ... ..T ..A G.T ... .T. ..C ... ..C CG. .CT ... ... ... A.A ...  [ 600]
Mouse_NPRA ..G ... .T G.. ... ..T ..A G.T ... .T. ..C ... CG. .CG ... ... ... A.A ...  [ 600]

Human_NPRA GAG GGG CTG TTC ATG CGG GTC CGC GAC CGC CTC AAT ATT ACG GTG GAC CAC CTG GAG TTC  [ 660]
Rat_NPRA   ... ... ... .A. ... ... ..G ..T ..A ... ... ..C ..C ..A ... A.T ... .A. ... ...  [ 660]
Mouse_NPRA ... ... ... .A. ... ... ..G ..T ..G ..A ... ..C ..C ..A ..A A.T ... .A. ... ...  [ 660]

Human_NPRA GCC GAG GAC GAC CTC AGC CAC TAC ACC AGG CTG CTG CGG ACC ATG CCG CGC AAA GGC CGA  [ 720]
Rat_NPRA   .T. ... .G. ... .CG GA. ... ... C.. .A. ..A ... ... G.. G.. .G. ..A ..G ... A..  [ 720]
Mouse_NPRA .T. ... .G. ... .CG GA. ... ... ..A. ..A ... ... G.. .A. ... ..G ... A..  [ 720]

Human_NPRA GTT ATC TAC ATC TGC AGC TCC CCT GAT GCC TTC AGA ACC CTC ATG CTC CTG GCC CTG GAA  [ 780]
Rat_NPRA   ... ... ... ... ... ..T ..T ..G ... ... ... ..G .AT ..G ... ..T ... ... ... A.C  [ 780]
Mouse_NPRA ... ... ... ... ..T ..T ..G ... ... ... ..G .AT ..G ... ..T T.. ... ... ..T  [ 780]

Human_NPRA GCT GGC TTG TGT GGG GAG GAC TAC GTT TTC TTC CAC CTG GAT ATC TTT GGG CAA AGC CTG  [ 840]
Rat_NPRA   ... ... C.. AC. ... ... ... ..T ... ... ... ... ... ... G.G ... ... ... ... ..T  [ 840]
Mouse_NPRA ... ... C.. AC. ... ... ... ..T ... ... ... ... ... ... G.G ... ... ... ... ..T  [ 840]

Human_NPRA CAA GGT GGA CAG GGC CCT GCT CCC CGC AGG CCC TGG GAG AGA GGG GAT GGG CAG GAT GTC  [ 900]
Rat_NPRA   A.G A.. .CT ... ... .T. .T. ... .AG .AA ... ... A ... ..A ... ... ... ..C AGG  [ 900]
Mouse_NPRA ..G ... .CT ... ... ... .T. ... A.G .A. ... ... A ... .AC ... ... ... AGG  [ 900]

Human_NPRA AGT GCC CGC CAG GCC TTT CAG GCT GCC AAA ATC ATT ACA TAT AAA GAC CCA GAT AAT CCC  [ 960]
Rat_NPRA   ... ... ... ... ... ... ... ... ... ..T ... ..T ..C ... ..G ..T ... ... ..T  [ 960]
Mouse_NPRA ..A ... ... ... ... ... ... ... ... ..T ... ..T ..C ... ..A ..C ... ... ..T  [ 960]

Human_NPRA GAG TAC TTG GAA TTC CTG AAG CAG TTA AAA CAC CTG GCC TAT GAG CAG TTC AAC TTC ACC  [1020]
Rat_NPRA   ... ... ... ... ... ... ... C.G ... .T. T.. ..T G.C A.. A.. ... ... ... ... ...  [1020]
Mouse_NPRA ... ... ... ... ... ... ... C.. ... .T. T.. ..T G.C A.. A.A ... ... ... ... ...  [1020]

Human_NPRA ATG GAG GAT GGC CTG GTG AAC ACC ATC CCA GCA TCC TTC CAC GAC GGG CTC CTG CTC TAT  [1080]
Rat_NPRA   G.. ... ... ... ... ... AA. ..T .T. ... ... ..C ... ... ... ... ..T ... ... ...  [1080]
Mouse_NPRA ... ... ... ... ... ... AAA ..T .T. ... ... ... ... ... ..T ... ... ... ... ...  [1080]

Human_NPRA ATC CAG GCA GTG ACG GAG ACT CTG GCA CAT GGG GGA ACT GTT ACT GAT GGG GAG AAC ATC  [1140]
Rat_NPRA   G.. ... ... ... ..A ... ... ... ..G ... ... ... ..C ..A ... ..A ... ... ... ...  [1140]
Mouse_NPRA G.. ... ... ... ..A ... ... ... ..G ... ... ..C ... ..C ... ..A ... ... ...  [1140]

Human_NPRA ACT CAG CGG ATG TGG AAC CGA AGC TTT CAA GGT GTG ACA GGA TAC CTG AAA ATT GAT AGC  [1200]
Rat_NPRA   ... ... ... ... ... ... ... ... ... ..C ... ... ... ... ... ... ... ... ... ..A  [1200]
Mouse_NPRA ... ... ... ... ... ... ... ... ... ..C ... ... ... ... ... ... ... ... ... ..A  [1200]

Human_NPRA AGT GGC GAT CGG GAA ACA GAC TTC TCC CTC TGG GAT ATG GAT CCC GAG AAT GGT GCC TTC  [1260]
Rat_NPRA   .AC ..A ... ... ..C ..C ..T ... ..T ... ... G.. ..T ... ... ..A ... .CG ... ...  [1260]
Mouse_NPRA .A. ..A ... ... ..C ..T ..T ... ... ... ... ... ... ..C ... ... .CA ... ...  [1260]

Human_NPRA AGG GTT GTA CTG AAC TAC AAT GGG ACT TCC CAA GAG CTG GTG GCT GTG TCG GGG CGC AAA  [1320]
Rat_NPRA   ... ... ..C ... ... ..T ... ..T ... ... ..G ... ..A A.. ... ... ..A .AA .A. ...  [1320]
Mouse_NPRA ... ... ..C ... ... .TT ... ..T ... ... ..G ... ..A A.. ... ... ..A .AA .A. .G.  [1320]

Human_NPRA CTG AAC TGG CCC CTG GGG TAC CCT CCT CCT GAC ATC CCC AAA TGT GGC TTT GAC AAC GAA  [1380]
Rat_NPRA   T.A T.. ... ... ..T ... ... ..A ..T ..A ... ... ... G.. ..T ... ... ... ..T ..G  [1380]
Mouse_NPRA T.A T.. ... ... ..T ... ... ..A ... ..A ... ... ... ... ..T ... ... ... ..T ..G  [1380]

Human_NPRA GAC CCA GCA TGC AAC CAA GAT CAC CTT TCC ACC CTG GAG GTG CTG GCT TTG GTG GGC AGC  [1440]
Rat_NPRA   ... ... ..C ... ... ... ..C ... T.. ... ..A ... ..T ... ... ... ... ... ... ...  [1440]
Mouse_NPRA ... ... ..C ... ... ... ..C ... T.. ... ..A ... ..T ... ... ... ... ... ... ...  [1440]

Human_NPRA CTC TCC TTG CTC GGC ATT CTG ATT GTC TCC TTC TTC ATA TAC AGG AAG ATG CAG CTG GAG  [1500]
Rat_NPRA   ... ..T C.. A.T A.. T.. ... ... ..G ..T ... ... ... ... ... ... ... ... ... ..A  [1500]
Mouse_NPRA ... ..T C.. G.T A.. T.. ... ..C ..G ..T ... ... ... ... ... ... ... ... ... ..A  [1500]
```

169

```
Human_NPRA AAG GAA CTG GCC TCG GAG CTG TGG CGG GTG CGC TGG GAG GAC GTT GAG CCC AGT AGC CTT [1560]
Rat_NPRA   ... ..G ... .T. ..A ... T.. ... ... ... ... ... ... ... T.G C.. ... ..C ... ..G [1560]
Mouse_NPRA ... ..G ... .T. ..A ... T.. ... ... ... ... ... ... ... T.G C.. ... ..C ... ..G [1560]

Human_NPRA GAG AGG CAC CTG CGG AGT GCA GGC AGC CGG CTG ACC CTG AGC GGG AGA GGC TCC AAT TAC [1620]
Rat_NPRA   ... ... ..T ..T ... ..C ..T ... ... ... ... ... ... ..T ... C.. ... ... ... ..T [1620]
Mouse_NPRA ... ... ..T ... ..C ..T ... ..T ... ... ... ... ... ..T ... C.. ... ... ... ..T [1620]

Human_NPRA GGC TCC CTG CTA ACC ACA GAG GGC CAG TTC CAA GTC TTT GCC AAG ACA GCA TAT TAT AAG [1680]
Rat_NPRA   ... ... ... ... ... ..C ... ... ... ... ... ... ... ... ... ... ..C ... ... ... [1680]
Mouse_NPRA ... ... ... ... ... ..G ... ... ... ... ... ... ... ... ... ... ..C ... ... ... [1680]

Human_NPRA GGC AAC CTC GTG GCT GTG AAA CGT GTG AAC CGT AAA CGC ATT GAG CTG ACA CGA AAA GTC [1740]
Rat_NPRA   ... ... ..T ... ... ... ... ... ... ... ..G ... ... ... T.. ... ... ... ... ... [1740]
Mouse_NPRA ... ... ... ... ... ... ... ... ... ... ..G ... ... ... T.. ... ... ... ... ... [1740]

Human_NPRA CTG TTT GAA CTG AAG CAT ATG CGG GAT GTG CAG AAT GAA CAC CTG ACC AGG TTT GTG GGA [1800]
Rat_NPRA   ... ... ... ..T ..A ... ... ... ... ... ... ..G ... T.. ..A ..A ... ... ..T [1800]
Mouse_NPRA ... ... ... ..T ..A ... ... ... ... ... ... ..G ... T.. ... ..A ... ... ... [1800]

Human_NPRA GCC TGC ACC GAC CCC CCC AAT ATC TGC ATC CTC ACA GAG TAC TGT CCC CGT GGG AGC CTG [1860]
Rat_NPRA   ..T ..T ... ... ... ..C ... ..T ... ... ... ... ... ... ... ... ..A ... ..A [1860]
Mouse_NPRA ..T ..T ... ... ..T ... ..C ... ..T ... ... ... ... ... ... ... ... ... ..A [1860]

Human_NPRA CAG GAC ATT CTG GAG AAT GAG AGC ATC ACC CTG GAC TGG ATG TTC CGG TAC TCA CTC ACC [1920]
Rat_NPRA   ... ... ... ..A ... ... ... ..T ... ... ... ... ... ..T ... ... ..G ... ... [1920]
Mouse_NPRA ... ... ... ..A ... ... ... ..T ..T ... ... ... ... ..T ... ... ... ... ... [1920]

Human_NPRA AAT GAC ATC GTC AAG GGC ATG CTG TTT CTA CAC AAT GGG GCT ATC TGT TCC CAT GGG AAC [1980]
Rat_NPRA   ... ... ..T ... ... ..A ... ..C ... ... ... ... ... ..C ..T ... ... ... ... [1980]
Mouse_NPRA ... ... ..T ... ... ..A ... ..C ... ... ... ..C ... ..C ..T G.. ... ... ... [1980]

Human_NPRA CTC AAG TCA TCC AAC TGC GTG GTA GAT GGG CGC TTT GTG CTC AAG ATC ACC GAC TAT GGG [2040]
Rat_NPRA   ... ... ... ... ... ..T ... ..C ... ... ..C ... T.A ... ... ..A ... ..C ..T [2040]
Mouse_NPRA ... ... ... ... ... ... ... ..A ..T ... ... T.A ... ... ..A ... ... ... [2040]

Human_NPRA CTG GAG AGC TTC AGG GAC CTG GAC CCA GAG CAA GGA CAC ACC GTT TAT GCC AAA AAG CTG [2100]
Rat_NPRA   ..T ... ... ... ..A ... ..C. ..G ... ... ... ... ... C.C .T. ... ... ..A T.. [2100]
Mouse_NPRA ..C ... ... ... ..A ... ..C. ..G ... ... ... ... ... C.C .T. ... ... ..A ... [2100]

Human_NPRA TGG ACG GCC CCT GAG CTC CTG CGA ATG GCT TCA CCC CCT GTG CGG GGC TCC CAG GCT GGT [2160]
Rat_NPRA   ... ... ..A ... ... ... ... ... ... ..G ..A ... ..CC ..T ... ... ..A ... ..G [2160]
Mouse_NPRA ... ..T ..A ... ... ... ... ... ..C ..A ... ..CC ..T ... ... ..A ... ..G [2160]

Human_NPRA GAC GTA TAC AGC TTT GGG ATC ATC CTT CAG GAG ATT GCC CTG AGG AGT GGG GTC TTC CAC [2220]
Rat_NPRA   ..T ..G ... ... ..T ... ... ..G ... ... ... ... ..A ..A ... ... ... ... T.T [2220]
Mouse_NPRA ..T ..C ... ..T ... ..T ... ... ... ... ... ..A ... ..A ..A ... ... ... T.T [2220]

Human_NPRA GTG GAA GGT TTG GAC CTG AGC CCC AAA GAG ATC ATC GAG CGG GTG ACT CGG GGT GAG CAG [2280]
Rat_NPRA   ... ... ... ... ... ..C ... ..A ... ... ... ..T ... ..T ... ... ... ... ... [2280]
Mouse_NPRA ... ... ... ... ... ..C ... ..A ... ... ... ..T ... ..T ... ... ..C ... ... [2280]

Human_NPRA CCC CCC TTC CGG CCC TCC CTG GCC CTG CAG AGT CAC CTG GAG GAG TTG GGG CTG CTC ATG [2340]
Rat_NPRA   ... ..A ... ..A ... A.. .AT ... ..C ... ... ... ..A C... ..A. ..G ... [2340]
Mouse_NPRA ... ..A ... ..A ..T ... A.. .AT ... ... ..C ... ... ..A C... ..A. ..G ... [2340]

Human_NPRA CAG CGG TGC TGG GCT GAG GAC CCA CAG GAG AGG CCA CCA TTC CAG CAG ATC CGC CTG ACG [2400]
Rat_NPRA   ... ... ... ... ..A ... ... ... C.. ... ..C ..T ... ... ..T ... ... G.. [2400]
Mouse_NPRA ... A.. ... ... ..A ... ..T ..T ... C.. ... ..C ..T ..A ... ... ... G.. [2400]

Human_NPRA TTG CGC AAA TTT AAC AGG GAG AAC AGC AGC AAC ATC CTG GAC AAC CTG CTG TCC CGC ATG [2460]
Rat_NPRA   C.. ... ..G ..C ... .A. ... ... ... ... ... ... ... ... ... ..A ... ... [2460]
Mouse_NPRA C.. ... ..G ..C ... .A. ... ... ... ... ... ... ... ... ... ..A ... ... [2460]

Human_NPRA GAG CAG TAC GCG AAC AAT CTG GAG GAA CTG GTG GAG GAG CGG ACC CAG GCA TAC CTG GAG [2520]
Rat_NPRA   ... ... ..T ..A ... ..C ... ... ... ..A ... A.A ..A ..A ..T ..T ... ... [2520]
Mouse_NPRA ..A ... ..C ... ..C ... ... ... ... ..A ... A.A A.A ... ..T ..T ... ... [2520]

Human_NPRA GAG AAG CGC AAG GCT GAG GCC CTG CTC TAC CAG ATC CTG CCT CAC TCA GTG GCT GAG CAG [2580]
Rat_NPRA   ... ... ... ..A ... ... ... T.. ..T ... ... ..T ... ..C ... ... ... ... [2580]
Mouse_NPRA ... ... ... ..A ... ... ... T.. ... ..T ... ... ..T ... ... ... ... ... [2580]

Human_NPRA CTG AAG CGT GGG GAG ACG GTG CAG GCC GAA GCC TTT GAC AGT GTT ACC ATC TAC TTC AGT [2640]
Rat_NPRA   ... ... A.A ..C ... ..A ..C ... ..T ..G ... ..T ... ... ..T ... ..T ... [2640]
Mouse_NPRA ... ... A.A ..C ... ..A ..C ... ..T ..G ..A ... ..T ... ... ..T ... ..T ... [2640]

Human_NPRA GAC ATT GTG GGT TTC ACA GCG CTG TCG GCG GAG AGC ACA CCC ATG CAG GTG GTG ACC CTG [2700]
Rat_NPRA   ..T ... ... ..C ..T ... ..T ..T ..A ..A ..A ... ... ... ... ..T ... [2700]
Mouse_NPRA ..T ..C ... ..C ..T ... ..T ..T ..A ..A ... ... ... ... ..C ... ... [2700]

Human_NPRA CTC AAT GAC CTG TAC ACT TGC TTT GAT GCT GTC ATA GAC AAC TTT GAT GTG TAC AAG GTG [2760]
Rat_NPRA   ... ... ..T ... ... ..C ..T ... ... ... ... ... ... ... ... ... ... ..A [2760]
Mouse_NPRA ... ... ..T ... ... ..C ..T ... ... ... ... ... ... ... ... ... ... ..A [2760]

Human_NPRA GAG ACA ATT GGC GAT GCC TAC ATG GTG GTG TCA GGG CTC CCT GTG CGG AAC GGG CGG CTA [2820]
Rat_NPRA   ... ..C ... ..T ... ..T ... ... ... ... ... ..A ... ..T ..A ..AA ..C [2820]
Mouse_NPRA ... ..C ... ..T ... ..T ... ... ..A ... ... ..A ... A.. ..T ..A .A. ..C [2820]

Human_NPRA CAC GCC TGC GAG GTA GCC CGC ATG GCC CTG GCA CTG CTG GAT GCT GTG CGC TCC TTC CGA [2880]
Rat_NPRA   ... ... C.A ... ..G ... ..A ... ..A ..T ... ..A ... ... ..A ... ... ..C [2880]
Mouse_NPRA ..T ... C.A ... ... ..A ... ..A ..T ... ..C ... ... ..A ... ... ..C [2880]

Human_NPRA ATC CGC CAC CGG CCC CAG GAG CAG CTG CGC TTG CGC ATT GGC ATC CAC ACA GGA CCT GTG [2940]
Rat_NPRA   ... ... ..T A.. ... ... ..A ... ... ... ... ... ..A ..T ... ..T ..C ... [2940]
Mouse_NPRA ... ... ..T A.. ... ..A ... ... ... ... ..A ..T ... ..T ..C ... [2940]

Human_NPRA TGT GCT GGA GTG GTG GGA CTG AAG ATG CCC CGT TAC TGT CTC TTT GGG GAT ACA GTC AAC [3000]
Rat_NPRA   ... ... ..T ... ..A ..G ..A ... ... ... ..A ... ..C ... ..A ..C ... [3000]
Mouse_NPRA ... ... ..T ... ..A ..G ..A ... ... ... ..A ... ..C ... ..A ..C ... [3000]

Human_NPRA ACA GCC TCA AGA ATG GAG TCT AAT GGG GAA GCC CTG AAG ATC CAC TTG TCT TCT GAG ACC [3060]
Rat_NPRA   ... ... ..T ... ... ... ... ... ..A ... ... ..C ... ... ... ... ..A ... [3060]
Mouse_NPRA ... ..T ... ... ... ... ... ... ..C .G. ... ... ... ... ..G ... ... [3060]

Human_NPRA AAG GCT GTC CTG GAG GAG TTT GGT GGT TTC GAG CTG GAG CTT CGA GGG GAT GTA GAA ATG [3120]
Rat_NPRA   ... ... ..G ... ..A ... ..C .A. ... ... ... ... ..C ... ... ..G ... ... [3120]
Mouse_NPRA ... ... ..G ... ..A ... ..C .A. ... ..T ... ... ..C ... ..T ..C ..G ... ... [3120]

Human_NPRA AAG GGC AAA GGC AAG GTT CGG ACC TAC TGG CTC CTT GGG GAG AGG GGG AGT AGC ACC CGA [3180]
Rat_NPRA   ... ... ... ... ... ... ... ..T ... ..G ... ... C.. ..A T.. ... ..T ... [3180]
Mouse_NPRA ... ... ... ... ..A ... ..T ... ... ..C ... ... C.. ..A T.C ... ..T ... [3180]

Human_NPRA GGC TGA  [3186]
Rat_NPRA   ... ...  [3186]
Mouse_NPRA ... ...  [3186]
```

170

Appendix 9: Sequence alignment results of human NPRA, rat NPRA and mouse NPRA protein

```
Human_NPRA MPGPRRPAGS RLRLLLLLLL PPLLLLLRGS HAGNLTVAVV LPLANTSYPW SWARVGPAVE [  60]
Rat_NPRA   ...S..V--- .P..RA.... .....-...G ..SD...... ...T...... .......... [  60]
Mouse_NPRA ...S..V--- .P..RA.... .....-..SG ..SD...... ...T...... .......... [  60]

Human_NPRA LALAQVKARP DLLPGWTVRT VLGSSENALG VCSDTAAPLA AVDLKWEHNP AVFLGPGCVY [ 120]
Rat_NPRA   ....R..... .........M .........A. .......... ........S. .......... [ 120]
Mouse_NPRA ...GR..... .........M .........A. .......... ........S. .......... [ 120]

Human_NPRA AAAPVGRFTA HWRVPLLTAG APALGFGVKD EYALTTRAGP SYAKLGDFVA ALHRRLGWER [ 180]
Rat_NPRA   S......... .......... .....I.... .......T.. .HV.....T .........H [ 180]
Mouse_NPRA S......... .......... .....I.... .......T.. .HV.....T .........H [ 180]

Human_NPRA QALMLYAYRP GDEEHCFFLV EGLFMRVRDR LNITVDHLEF AEDDLSHYTR LLRTMPRKGR [ 240]
Rat_NPRA   ...V...D.L ..DRP...I. ...Y....E. ......N.Q.. V.G.PD..PK ...AVR.... [ 240]
Mouse_NPRA ...V...D.L ..DRP...I. ...Y....E. ......N.Q.. V.G.PD...K ....VQ.... [ 240]

Human_NPRA VIYICSSPDA FRTLMLLALE AGLCGEDYVF FHLDIFGQSL QGGQGPAPRR PWERGDGQDV [ 300]
Rat_NPRA   .......... ..N......N ..T...... ....V..... KSA..LV.QK .........R [ 300]
Mouse_NPRA .......... ..N......D ..T...... ....V..... ..A...V..K ...D....R [ 300]

Human_NPRA SARQAFQAAK IITYKDPDNP EYLEFLKQLK HLAYEQFNFT MEDGLVNTIP ASFHDGLLLY [ 360]
Rat_NPRA   .......... .....E.... .......... L..DKK.... V....K.I.. .......... [ 360]
Mouse_NPRA R......... .....E.... .......... L..DKK.... ....K.I.. .......... [ 360]

Human_NPRA IQAVTETLAH GGTVTDGENI TQRMWNRSFQ GVTGYLKIDS SGDRETDFSL WDMDPENGAF [ 420]
Rat_NPRA   V........Q .......... .......... .........R N...D..... ......T... [ 420]
Mouse_NPRA V........Q .......... .......... .........R N...D..... ......T... [ 420]

Human_NPRA RVVLNYNGTS QELVAVSGRK LNWPLGYPPP DIPKCGFDNE DPACNQDHLS TLEVLALVGS [ 480]
Rat_NPRA   .......... ...M...EH. .Y....... .V........ .........F. .......... [ 480]
Mouse_NPRA .....F.... ...M...EHR .Y........ .......... .........F. .......... [ 480]

Human_NPRA LSLLGILIVS FFIYRKMQLE KELASELWRV RWEDVEPSSL ERHLRSAGSR LTLSGRGSNY [ 540]
Rat_NPRA   ...ISF.... .......... ...V...... ....LQ.... .......... .......... [ 540]
Mouse_NPRA ...VSF.... .......... ...V...... ....LQ.... .......... .......... [ 540]

Human_NPRA GSLLTTEGQF QVFAKTAYYK GNLVAVKRVN RKRIELTRKV LFELKHMRDV QNEHLTRFVG [ 600]
Rat_NPRA   .......... .......... .......... .......... .......... .......... [ 600]
Mouse_NPRA .......... .......... .......... .......... .......... .......... [ 600]

Human_NPRA ACTDPPNICI LTEYCPRGSL QDILENESIT LDWMFRYSLT NDIVKGMLFL HNGAICSHGN [ 660]
Rat_NPRA   .......... .......... .......... .......... .......... .......... [ 660]
Mouse_NPRA .......... .......... .......... .......... .......... .....G.... [ 660]

Human_NPRA LKSSNCVVDG RFVLKITDYG LESFRDLDPE QGHTVYAKKL WTAPELLRMA SPPVRGSQAG [ 720]
Rat_NPRA   .......... .......... ......PE.. ....LF.... .......... ...A...... [ 720]
Mouse_NPRA .......... .......... ......PE.. ....LF.... .......... ...A...... [ 720]

Human_NPRA DVYSFGIILQ EIALRSGVFH VEGLDLSPKE IIERVTRGEQ PPFRPSLALQ SHLEELGLLM [ 780]
Rat_NPRA   .......... .........Y .......... .......... ......MD.. .......Q.. [ 780]
Mouse_NPRA .......... .........Y .......... .......... ......MD.. .......Q.. [ 780]

Human_NPRA QRCWAEDPQE RPPFQQIRLT LRKFNRENSS NILDNLLSRM EQYANNLEEL VEERTQAYLE [ 840]
Rat_NPRA   .......... .........A .....K.... .......... .......... .......... [ 840]
Mouse_NPRA .......... .........A .....K.... .......... .......... .......... [ 840]

Human_NPRA EKRKAEALLY QILPHSVAEQ LKRGETVQAE AFDSVTIYFS DIVGFTALSA ESTPMQVVTL [ 900]
Rat_NPRA   .......... .......... .......... .......... .......... .......... [ 900]
Mouse_NPRA .......... .......... .......... .......... .......... .......... [ 900]

Human_NPRA LNDLYTCFDA VIDNFDVYKV ETIGDAYMVV SGLPVRNGRL HACEVARMAL ALLDAVRSFR [ 960]
Rat_NPRA   .......... .......... .......... .......Q. ..R....... .......... [ 960]
Mouse_NPRA .......... .......... .......... .......Q. ..R....... .......... [ 960]

Human_NPRA IRHRPQEQLR LRIGIHTGPV CAGVVGLKMP RYCLFGDTVN TASRMESNGE ALKIHLSSET [1020]
Rat_NPRA   .......... .......... .......... .......... .......... .......... [1020]
Mouse_NPRA .......... .......... .......... .......... .......... ..R....... [1020]

Human_NPRA KAVLEEFGGF ELELRGDVEM KGKGKVRTYW LLGERGSSTR G* [1062]
Rat_NPRA   .......D.. .......... .......... ......C... .. [1062]
Mouse_NPRA .......D.. .......... .......... ......C... .. [1062]
```

```
Human_NPRB  ATG GCG CTG CCA TCA CTT CTG CTG TTG GTG GCA GCC CTG GCA GGT GGG GTG CGT CCT CCC  [  60]
Rat_NPRB    ... ..A ... ... ... ..C ..G ..A ... G.. ... ... ... ... ... ... ... ... ... ..G  [  60]
Mouse_NPRB  ... ..A ... ... ... ..C ..G ... ... G.. ... ... ... ... ... ... ... ... ... ..G  [  60]

Human_NPRB  GGG GCG CGG AAC CTG ACG CTG GCG GTG GTG CTG CCA GAA CAC AAC CTG AGC TAT GCC TGG  [ 120]
Rat_NPRB    ... ..A ... ... ... ... ... ... ... ... ... ... ... ... ... ... ... ... ... ...  [ 120]
Mouse_NPRB  ... ..A ... ... ... ... ... ... ... ... ... ... ... ... ... ... ... ... ... ...  [ 120]

Human_NPRB  GCC TGG CCA CGG GTG GGA CCC GCT GTG GCA CTA GCT GTG GAG GCT CTG GGC CGG GCA CTG  [ 180]
Rat_NPRB    ... ... ... ... ... ..T ..T ... ... ... ..G ... ... ... ..G ... ... ... ... ...  [ 180]
Mouse_NPRB  ... ... ... ... ... ..T ..T ... ... ... ..G ... ... ... ... ..A ... ... ... ...  [ 180]

Human_NPRB  CCC GTG GAC CTG CGG TTT GTC AGC TCC GAA CTG GAA GGC GCC TGC TCT GAG TAC CTG GCA  [ 240]
Rat_NPRB    ... ... ... ... ... ... ... ... ... ... ..A ..C ... ... ... ... ... ... ... ...  [ 240]
Mouse_NPRB  ... ... ... ... ... ... ... ... ... ... ..A ..C ... ... ... ... ... ... ... ...  [ 240]

Human_NPRB  CCG CTG AGC GCT GTG GAC CTC AAG CTG TAC CAT GAC CCC GAC CTG CTG TTA GGT CCC GGT  [ 300]
Rat_NPRB    ..A ... C.. ... ... ... ..T ... ... ... ... ... ... ... ..T ... ..G ..C ..T ...  [ 300]
Mouse_NPRB  ..A ... C.. ... ... ... ... ... ... ... ... ... ... ... ..T ... ..G ..C ... ...  [ 300]

Human_NPRB  TGC GTG TAC CCT GCT GCC TCT GTG GCC CGC TTT GCC TCC CAC TGG CGC CTT CCC CTG CTG  [ 360]
Rat_NPRB    ..T ... ... ... ... ... ... ... ..T ... ... ... ..G ... ... .A. ... ... ..C ...  [ 360]
Mouse_NPRB  ..T ... ... ..C ... ... ... ... ..T ... ... ... ..A ... ... ... ... ... ..C ...  [ 360]

Human_NPRB  ACT GCG GGT GCT GTG GCC TCT GGT TTT TCG GCT AAG AAT GAC CAT TAT CGT ACC CTG GTT  [ 420]
Rat_NPRB    ... ... ... ..A ... ... ... ..C ... G.A ... ... ... ..G ... ... ... ... ... ...  [ 420]
Mouse_NPRB  ... ... ..G ..A ... ... ... ..C ... G.A ... ... ... ..G ... ... ... ... ... ...  [ 420]

Human_NPRB  CGC ACT GGC CCC TCT GCT CCC AAG CTG GGT GAG TTT GTG GTG ACA CTA CAC GGG CAC TTC  [ 480]
Rat_NPRB    ... ... ... ... ... ..G ... ... ... ... ... ..C ..A ... ... T.. ... ... ... ...  [ 480]
Mouse_NPRB  ... ... ... ... ... ..G ... ... ... ... ... ... ..A ... ... T.G ... ... ... ...  [ 480]

Human_NPRB  AAT TGG ACT GCC CGT GCT GCC TTG CTG TAC CTG GAT GCT CGC ACA GAT GAC CGG CCT CAC  [ 540]
Rat_NPRB    ... ... ... ..T ..G ... ..T ... ... ..T ... ... ... ... ... ... ... ... ..C ...  [ 540]
Mouse_NPRB  ... ... ..A ..T ..G ... ..T ... ... ..T ... ... ... ... ... ... ... ... ..C ...  [ 540]

Human_NPRB  TAC TTC ACC ATC GAG GGC GTC TTT GAG GCC CTG CAG GGC AGC AAC CTC AGT GTG CAG CAC  [ 600]
Rat_NPRB    ... ... ... ... ... ..G ..G ... ... ... ... ... ... ... ... ... ... ... ..A ...  [ 600]
Mouse_NPRB  ... ... ... ... ... ... ... ... ... ... ... ... ... ... ... ... ... ... ... ...  [ 600]

Human_NPRB  CAG GTG TAT GCC CGA GAG CCA GGG GGC CCC GAG CAG GCC ACC CAC TTC ATC CGG GCC AAC  [ 660]
Rat_NPRB    ... ... ... A.. ... ... ... ..T ... ..T ... ..A ... ... ... ... A.A ... ... ...  [ 660]
Mouse_NPRB  ... ... ... ... ... ... ... ..T ... ..T ... ..A ... ... ... ... A.A ... ... ...  [ 660]

Human_NPRB  GGG CGC ATT GTG TAT ATC TGC GGC CCT CTG GAG ATG CTG CAT GAG ATC CTG CTT CAG GCC  [ 720]
Rat_NPRB    ... ... ... ... ... ... ... ... ..G ... ... ... ..T ... ... ... ... ... ... ...  [ 720]
Mouse_NPRB  ... ... ... ... ... ... ... ... ..C ... ... ..A ... ... ... ... ... ... ... ...  [ 720]

Human_NPRB  CAG AGG GAG AAT CTG ACC AAT GGG GAT TAT GTC TTC TTT TAC CTG GAT GTC TTT GGG GAG  [ 780]
Rat_NPRB    ... ... ... ..C ... ... ... ... ... ..C ... ... ... ... ..T ... ... ... ... ...  [ 780]
Mouse_NPRB  ... ... ... ..C ... ... ... ... ... ..C ... ... ... ... ..T ... ... ... ... ...  [ 780]

Human_NPRB  AGT CTC CGT GCA GGC CCC ACA CGT GCT ACA GGC CGG CCC TGG CAG GAC AAT CGC ACC CGG  [ 840]
Rat_NPRB    ... ..A ..A ... ... ... ... ... ..A ... ... ... ..A ... ... ... ... ..A ... .A.  [ 840]
Mouse_NPRB  ... ... ..A ... ... ... ..C ... ..A ... ... ... ..A ... ... ... ... ..A ... .A.  [ 840]

Human_NPRB  GAA CAG GCC CAG GCC CTC AGA GAG GCC TTT CAG ACT GTA TTG GTG ATC ACG TAC CGA GAA  [ 900]
Rat_NPRB    ... ..A ..T ... ... ... ... ... ... ... ... ... ..C C.. ... ... ... ... ... ..G  [ 900]
Mouse_NPRB  ... ... ... ... ... ... ... ... ... ... ... ... ... ... ... ... ..A ... ... ...  [ 900]

Human_NPRB  CCC CCA AAT CCT GAG TAT CAG GAA TTC CAG AAT CGT CTG CTG ATA AGA GCC CGG GAA GAC  [ 960]
Rat_NPRB    ... ..G ... ..C ... ... ... ... ..G ... ... ..C ..C ... ... ..C ... ... ... ...  [ 960]
Mouse_NPRB  ... ... ... ... ... ... ... ... ..G ..T ... ... ..C ... ... ..C ... ... ... ...  [ 960]

Human_NPRB  TTT GGT GTG GAG CTG GGC CCT TCC CTG ATG AAC CTC ATC GCT GGC TGC TTC TAT GAT GGG  [1020]
Rat_NPRB    ..C ..C ... ... ... ... .C. ..A ... ... ... ... ..T ..G ... ... ... ... ... ..A  [1020]
Mouse_NPRB  ... ... ... ... ... ... .C. ..A ... ... ... ... ..T ..T ... ... ... ... ... ...  [1020]

Human_NPRB  ATC CTG CTA TAT GCT GAA GTC CTG AAT GAG ACA ATA CAG GAA GGA GGC ACC CGG GAG GAT  [1080]
Rat_NPRB    ... ... ..C ... ..C C.. ... ... ... ... ... ... ... ..G ... ... ... ..A ... ...  [1080]
Mouse_NPRB  ... ... ..C ... ..C C.. ... ... ... ... ..T ... ... ..G ..T ... A.. ..A ... ...  [1080]

Human_NPRB  GGA CTT CGA ATT GTG GAA AAG ATG CAG GGA CGA AGA TAT CAC GGT GTA ACT GGG CTG GTT  [1140]
Rat_NPRB    ... ... ... ... ... ... ..G ... ... ... ... ... ..C ..T ... ... ..A ... ... ...  [1140]
Mouse_NPRB  ... ... ... ... ... ... ..G ... ... ... ... ... ..C ..T ... ... ..A ... ... ...  [1140]

Human_NPRB  GTC ATG GAC AAG AAC AAT GAC CGA GAG ACT GAC TTT GTC CTC TGG GCC ATG GGA GAC CTG  [1200]
Rat_NPRB    ..T ... ... ... ... ... ... A.. ... ... ..T ..C ... ..G ... ... ... ... T.. ...  [1200]
Mouse_NPRB  ... ... ... ... ... ... ..C ... ... ..T ..C ... ..G ... ... ... ... T.. ...  [1200]

Human_NPRB  GAT TCT GGG GAC TTT CAG CCT GCA GCC CAC TAC TCG GGA GCT GAG AAG CAG ATT TGG TGG  [1260]
Rat_NPRB    ..G ... ..C ... ... ... ... ... ..T ... ..A ... ... ... ... ... ... ... ... ...  [1260]
Mouse_NPRB  ... ... ... ... ... ... ..C ... ... ..T ... ..T ... ..A ... ... ... ... ... ...  [1260]

Human_NPRB  ACG GGA CGG CCT ATT CCC TGG GTG AAG GGG GCT CCT CCC TCG GAC AAT CCC CCC TGT GCC  [1320]
Rat_NPRB    ..A ..C ... ..A ... ... ... ... ... ... ..C ..A ..T .T. ... ..C ... ... ... ...  [1320]
Mouse_NPRB  ..A ..C ... ..A ... ... ... ... ... ... ..C ..A ..T .T. ... ... ... ... ... ...  [1320]

Human_NPRB  TTT GAC TTG GAC GAC CCA TCC TGT GAT AAA ACT CCA CTT TCA ACC CTG GCA ATT GTG GCT  [1380]
Rat_NPRB    ... ... ... ... ... ... ... ... ... ... ... ..C ..T ... ... ... ... ..C ... ..C  [1380]
Mouse_NPRB  ... ... ... ... ... ... ... ... ... ... ... ..C ..T ... ... ... ..C ... ..C  [1380]

Human_NPRB  CTG GGC ACA GGA ATC ACC TTC ATC ATG TTT GGT GTT TCC AGC TTC CTA ATT TTC CGA AAG  [1440]
Rat_NPRB    ... ... ..G ... ... ..T ... ... ... ... ... ... ... ... ... ... ... ... ... ..A  [1440]
Mouse_NPRB  ... ... ..G ... G.. ... ... ... ... ... ... ..T ... ... ... ... ... ..G ...  [1440]

Human_NPRB  CTG ATG CTG GAG AAG GAG CTG GCT AGC ATG TTG TGG CGT ATT CGC TGG GAA GAA CTG CAG  [1500]
Rat_NPRB    ... ... ... ... ... ... ... ... ... C.. ... ..C ... ... ... ... ... ... ... ...  [1500]
Mouse_NPRB  ... ... ... ... ... ... ... ... ... C.A ... ..C ... ... ... ... ... ... ... ...  [1500]
```

```
Human_NPRB  TTT GGC AAC TCA GAG CGT TAT CAC AAA GGT GCA GGC AGT CGC CTC ACA CTG TCG CTG CGG  [1560]
Rat_NPRB    ..C ... ... ..G ..T ..A ... ... ... ..G ... ... ... ... ..G ..G ... ... ...      [1560]
Mouse_NPRB  ... ... ... ..G ..T ..C ... ... ..G ... ... ... ... ... ..G ..G ... ... ...      [1560]

Human_NPRB  GGA TCC AGT TAC GGC TCG CTC ATG ACA GCC CAT GGG AAA TAC CAG ATC TTT GCC AAC ACC  [1620]
Rat_NPRB    ... ... ... ... ... ... ... ... ... ... ... ... ... ... ... ... ... ... ... ...  [1620]
Mouse_NPRB  ... ... ... ... ... ... ... ... ... ... ... ... ... ... ... ... ... ... ... ...  [1620]

Human_NPRB  GGT CAC TTC AAG GGA AAT GTT GTC GCC ATC AAA CAT GTG AAT AAG AAG CGC ATT GAG CTG  [1680]
Rat_NPRB    ... ... ... ... ... ... ..C ..T ... ... ... ... ..C ... ... ... ..C ... ...      [1680]
Mouse_NPRB  ... ... ... ... ... ... ... ..T ... ... ... ... ..C ... ... ... ..C ... ...      [1680]

Human_NPRB  ACC CGG CAG GTT CTG TTT GAA CTC AAA CAT ATG AGA GAT GTT CAG TTC AAC CAT CTC ACT  [1740]
Rat_NPRB    ... ... ..A ... ... ... ... ... ... ..C ... ... ... ..C ... ... ... ..T ...      [1740]
Mouse_NPRB  ... ... ..A ... ... ... ... ... ... ..C ... ... ... ..C ... ... ... ..T ...      [1740]

Human_NPRB  CGC TTC ATT GGC GCC TGC ATA GAC CCT CCC AAC ATT TGC ATT GTC ACT GAA TAC TGT CCT  [1800]
Rat_NPRB    ..A ... ..C ..A ..T ... ... ... ... ... ..C ... ..C ... ..C ..G ..T ... ...      [1800]
Mouse_NPRB  ... ... ..C ..A ... ... ... ... ... ... ..C ... ... ... ..C ..G ..T ... ...      [1800]

Human_NPRB  CGT GGG AGT TTA CAG GAT ATT CTA GAA AAT GAC AGC ATC AAC TTG GAC TGG ATG TTT CGT  [1860]
Rat_NPRB    ..G ... ..C ... ..A ... ... ... ... ... ... ... ..T ... ... ... ... ... ..C      [1860]
Mouse_NPRB  ..G ... ..C ... ..A ... ... ... ... ... ... ... ..T ... ... ... ... ... ..C      [1860]

Human_NPRB  TAT TCA CTC ATT AAT GAC CTT GTT AAG GGC ATG GCC TTT CTC CAC AAC AGC ATT ATT TCA  [1920]
Rat_NPRB    ..C ..G ... ... ... ... ... ..G ... ..T ... ... ... ... ... ... ... ... ...      [1920]
Mouse_NPRB  ..C ..G ... ..C ... ... ... ..G ... ..T ... ... ... ... ... ... ... ... ...      [1920]

Human_NPRB  TCG CAT GGG AGT CTC AAG TCC TCC AAC TGT GTG GTG GAT AGT CGT TTT GTG CTC AAA ATC  [1980]
Rat_NPRB    ..T ... ..A ..C ... ... ... ..T ... ..C ... ... ... ... ..A ... ... ... ... ..A  [1980]
Mouse_NPRB  ..T ... ..A ..C ... ... ... ... ... ... ... ... ..A ... ... ... ... ... ..A      [1980]

Human_NPRB  ACA GAC TAT GGC CTG GCC AGC TTC CGA TCA ACT GCT GAA CCT GAT GAC AGC CAT GCC CTC  [2040]
Rat_NPRB    ..G ..T ..C ..G ... ..T ... ... ... ... ... ... ..A ... ... ..T ... ... ...      [2040]
Mouse_NPRB  ... ..T ..C ..T ..T ... ... ... ... ... ... ..G ..C ... ... ... ... ... ...      [2040]

Human_NPRB  TAT GCC AAG AAG CTG TGG ACT GCC CCA GAA CTG CTC AGT GGG AAC CCC TTG CCA ACC ACA  [2100]
Rat_NPRB    ... ... ... ... ... ... ... ..T ... ..T ..T ... ... ... ... C.. ... ... ..G      [2100]
Mouse_NPRB  ... ... ... ... ... ... ... ..T ..C ... ... ... ... ... ... ... ... ... ...      [2100]

Human_NPRB  GGC ATG CAG AAG GCT GAC GTC TAT AGC TTT GGG ATC ATC CTG CAG GAG ATA GCA CTT CGC  [2160]
Rat_NPRB    ... ... ... ... ..G ..T ... ... ... ..CC ... ..T ... ... ..A ... ..G ..C ..A    [2160]
Mouse_NPRB  ... ... ... ..A ..A ..T ... ..C ... ..CC ... ..T ..A ... ..A ... ... ... ..A    [2160]

Human_NPRB  AGT GGT CCT TTC TAC TTG GAG GGC CTG GAC CTC AGC CCC AAA GAG ATT GTC CAG AAG GTA  [2220]
Rat_NPRB    ... ... ... ... ... ..A ... ... ... ... ..T ... ... ... ... ... ... ... ..G    [2220]
Mouse_NPRB  ... ... ... ... ... ..A ... ... ... ... ..T ... ..G ... ... ... ... ... ..G    [2220]

Human_NPRB  CGA AAT GGT CAG CGG CCA TAT TTC CGG CCA AGC ATT GAC CGG ACC CAA CTG AAT GAA GAG  [2280]
Rat_NPRB    ... ... ... ... A.. ..G ... ... ... ... ... ... ... ..A ... ... ..C ... ...    [2280]
Mouse_NPRB  ..G ... ... ... A.. ..G ... ... ... ... ... ... ... ..A ... ... ... ... ...    [2280]

Human_NPRB  CTA GTT TTG CTG ATG GAG CGA TGT TGG GCT CAG GAC CCA GCT GAG CGG CCA GAC TTT GGA  [2340]
Rat_NPRB    T.. ... ... ... ... ... A.G ..C ... ..C ... ... ... A.A ..A ..T ... ... ..G    [2340]
Mouse_NPRB  T.. ... ... ... ... ... A.. ..C ... ..C ... ... ... A.A ..A ..T ... ... ..G    [2340]

Human_NPRB  CAG ATT AAG GGC TTC ATT CGG CGC TTT AAC AAG GAG GGT GGC ACC AGC ATA TTG GAC AAC  [2400]
Rat_NPRB    ..A ..C ... ... ... ... ... ..C ..G ... ... ... ... ... ..T ... ... ... ...    [2400]
Mouse_NPRB  ..A ..C ... ... ... ... ... ..C ..G ... ... ... ..A ... ..T ... ... ... ...    [2400]

Human_NPRB  CTC CTG CTG CGC ATG GAA CAG TAT GCC AAT AAC TTG GAG AAG CTG GTG GAG GAA CGC ACA  [2460]
Rat_NPRB    ... T.. ..T ... ... ... ... ... ... ... C.. ..A ..A ... ... ... ..G ... ...    [2460]
Mouse_NPRB  ... T.. ... ... ... ... ... ... ..T ... C.. ..A ... ... ... ... ... ... ...    [2460]

Human_NPRB  CAG GCC TAT CTG GAG GAA AAA CGC AAG GCT GAA GCT CTG CTC TAC CAA ATC CTA CCC CAT  [2520]
Rat_NPRB    ... ... ..C ..A ... ..G ..G ... ... ... ..G ... ... ..G ... ... ..T ... ... ..C  [2520]
Mouse_NPRB  ... ... ..A ... ..G ... ... ..A ..G ..G ..C ... ..G ... ... ..T ... ... ...    [2520]

Human_NPRB  TCA GTG GCA GAG CAG TTA AAA CGG GGA GAG ACT GTA CAG GCT GAG GCC TTT GAC AGT GTT  [2580]
Rat_NPRB    ..T ... ... ... ... ... ... ... ... ... ..G ..T ... ..G ... ... ... ... ..C    [2580]
Mouse_NPRB  ..T ..A ... ... ... ... ..G ... ... ... ..G ..T ... ..G ... ..C ... ..C ..C    [2580]

Human_NPRB  ACC ATC TAC TTC AGT GAC ATT GTT GGC TTC ACA GCA TTG TCA GCA GAG AGC ACC CCC ATG  [2640]
Rat_NPRB    ..T ... ... ... ... ... ..C ..G ... ... ... ..G C.. ... ..T ... ... ... ...    [2640]
Mouse_NPRB  ... ... ... ... ... ... ..C ..G ... ... ... ..G C.. ... ..T ... ... ... ...    [2640]

Human_NPRB  CAG GTA GTG ACA CTT CTT AAT GAC CTG TAT ACC TGC TTT GAT GCC ATA ATT GAC AAC TTT  [2700]
Rat_NPRB    ... ..G ... ... ... ... ... ..T ... ... ... ... ... ... ..C ... ... ... ...    [2700]
Mouse_NPRB  ... ..G ... ... ... ... ... ..T ... ... ... ... ... ..T ..C ... ... ... ...    [2700]

Human_NPRB  GAT GTC TAC AAG GTG GAG ACG ATT GGG GAT GCT TAC ATG GTG GTA TCT GGC CTC CCA GGC  [2760]
Rat_NPRB    ... ... ... ... ... ..A ..C ... ... ... ..C ... ... ... ... ... ..T ..G ...    [2760]
Mouse_NPRB  ... ... ... ... ... ..A ..C ... ... ... ..C ... ... ... ... ... ..T ... ...    [2760]

Human_NPRB  CGA AAT GGT CAA CGC CAT GCA CCA GAA ATT GCT CGT ATG GCC CTA GCA TTA CTA GAT GCA  [2820]
Rat_NPRB    ... ... ... ..G ... ... ... ... ... ..A ... ..T ... ... ... ..G ... ... ..T    [2820]
Mouse_NPRB  ... ..C ... ..G ... ... ... ... ... ... ... ... ... ... ..G ... ... ... ..T    [2820]

Human_NPRB  GTT TCT TCC TTT CGC ATC CGC CAC CGA CCC CAT GAC CAG CTG AGG CTA CGC ATA GGG GTC  [2880]
Rat_NPRB    ... ... ... ..C ... ... ..T ... ..T ... ... ..C ... ... ..A ... T.. ... ..C ...  [2880]
Mouse_NPRB  ..C ... ... ..C ... ... ... ..T ... ... ... ... ... ... T.. ... ... ..T ...    [2880]

Human_NPRB  CAT ACT GGG CCA GTC TGT GCT GGG GTT GTT GGC CTG AAG ATG CCC CGT TAT TGT CTT TTT  [2940]
Rat_NPRB    ... ... ... ... ... ... ... ... ... ..G ... ... ... ... ... ..G ..C ... ... ...  [2940]
Mouse_NPRB  ... ... ... ... ... ... ... ..G ... ... ... ... ... ... ..G ..C ... ... ...    [2940]

Human_NPRB  GGA GAC ACA GTG AAC ACT GCT TCT CGA ATG GAG TCT AAT GGT CAA GCG CTG AAG ATC CAT  [3000]
Rat_NPRB    ... ... ... ..A ... ... ... ... ... ... ... ... ... ... ..T ..A ... ... ...    [3000]
Mouse_NPRB  ... ... ... ..A ... ... ... ... ... ... ..G ... ..C ... ..T ..A ... ... ...    [3000]

Human_NPRB  GTC TCC TCT ACC ACC AAG GAT GCC CTA GAT GAG CTA GGA TGC TTC CAG CTA GAG CTT CGG  [3060]
Rat_NPRB    ... ... ..G ... ... ... ... ... ..G ... ... ... ... ... ... ... ... ..A ..C ..T  [3060]
Mouse_NPRB  ... ... ..G ... ... ... ..C ... ..G ... ... ..G ... ... ... ..C ... ..C ..T    [3060]

Human_NPRB  GGG GAT GTG GAA ATG AAG GGA AAA GGA AAG ATG CGA ACA TAC TGG CTC TTA GGA GAG CGG  [3120]
Rat_NPRB    ... ... ... ..G ... ... ... ... ... ..A ... ... ..T ..T ... ... ... ... ..A    [3120]
Mouse_NPRB  ... ... ... ..G ... ... ... ... ... ..A ... ... ..T ... ... ... ..G ... .AA    [3120]

Human_NPRB  AAA GGA CCT CCT GGA CTC CTG TAA  [3144]
Rat_NPRB    ... ... ... ... ... ... ... ...  [3144]
```

173

Appendix 11: Sequence alignment results of human NPRB, rat NPRB and mouse NPRB protein

```
Human_NPRB  MALPSLLLLV AALAGGVRPP GARNLTLAVV LPEHNLSYAW AWPRVGPAVA LAVEALGRAL  [  60]
Rat_NPRB    ........V. .......... .......... .......... .......... ..........  [  60]
Mouse_NPRB  ........V. .......... .......... .......... .......... ..........  [  60]

Human_NPRB  PVDLRFVSSE LEGACSEYLA PLSAVDLKLY HDPDLLLGPG CVYPAASVAR FASHWRLPLL  [ 120]
Rat_NPRB    .......... .D........ ..R....... .......... .......... .....H....  [ 120]
Mouse_NPRB  .......... .D........ ..R....... .......... .......... ..........  [ 120]

Human_NPRB  TAGAVASGFS AKNDHYRTLV RTGPSAPKLG EFVVTLHGHF NWTARAALLY LDARTDDRPH  [ 180]
Rat_NPRB    .........A ...E...... .......... .......... .......... ..........  [ 180]
Mouse_NPRB  .........A ...E...... .......... .......... .......... ..........  [ 180]

Human_NPRB  YFTIEGVFEA LQGSNLSVQH QVYAREPGGP EQATHFIRAN GRIVYICGPL EMLHEILLQA  [ 240]
Rat_NPRB    .......... .......... ...T...... .......... .......... ..........  [ 240]
Mouse_NPRB  .......... .......... .......... .......... .......... ..........  [ 240]

Human_NPRB  QRENLTNGDY VFFYLDVFGE SLRAGPTRAT GRPWQDNRTR EQAQALREAF QTVLVITYRE  [ 300]
Rat_NPRB    .......... .......... .......... .........Q .......... ..........  [ 300]
Mouse_NPRB  .......... .......... .......... .........Q .......... ..........  [ 300]

Human_NPRB  PPNPEYQEFQ NRLLIRARED FGVELGPSLM NLIAGCFYDG ILLYAEVLNE TIQEGGTRED  [ 360]
Rat_NPRB    .......... .......... .....A.... .......... .....Q.... ..........  [ 360]
Mouse_NPRB  .......... .......... .....A.... .......... .....Q.... ..........  [ 360]

Human_NPRB  GLRIVEKMQG RRYHGVTGLV VMDKNNDRET DFVLWAMGDL DSGDFQPAAH YSGAEKQIWW  [ 420]
Rat_NPRB    .......... .......... .......... .......... E......... ..........  [ 420]
Mouse_NPRB  .......... .......... .......... .......... .......... ..........  [ 420]

Human_NPRB  TGRPIPWVKG APPSDNPPCA FDLDDPSCDK TPLSTLAIVA LGTGITFIMF GVSSFLIFRK  [ 480]
Rat_NPRB    .......... ...L...... .......... .......... .......... ..........  [ 480]
Mouse_NPRB  .......... ...L...... .......... .......... .....V.... ..........  [ 480]

Human_NPRB  LMLEKELASM LWRIRWEELQ FGNSERYHKG AGSRLTLSLR GSSYGSLMTA HGKYQIFANT  [ 540]
Rat_NPRB    .......... .......... ....D..... .......... .......... ..........  [ 540]
Mouse_NPRB  .......... .......... ....D..... .......... .......... ..........  [ 540]

Human_NPRB  GHFKGNVVAI KHVNKKRIEL TRQVLFELKH MRDVQFNHLT RFIGACIDPP NICIVTEYCP  [ 600]
Rat_NPRB    .......... .......... .......... .......... .......... ..........  [ 600]
Mouse_NPRB  .......... .......... .......... .......... .......... ..........  [ 600]

Human_NPRB  RGSLQDILEN DSINLDWMFR YSLINDLVKG MAFLHNSIIS SHGSLKSSNC VVDSRFVLKI  [ 660]
Rat_NPRB    .......... .......... .......... .......... .......... ..........  [ 660]
Mouse_NPRB  .......... .......... .......... .......... .......... ..........  [ 660]

Human_NPRB  TDYGLASFRS TAEPDDSHAL YAKKLWTAPE LLSGNPLPTT GMQKADVYSF GIILQEIALR  [ 720]
Rat_NPRB    .......... .......... .......... .......... .......... A.........  [ 720]
Mouse_NPRB  .......... .......... .......... .......... .......... A.........  [ 720]

Human_NPRB  SGPFYLEGLD LSPKEIVQKV RNGQRPYFRP SIDRTQLNEE LVLLMERCWA QDPAERPDFG  [ 780]
Rat_NPRB    .......... .......... .......... .......... .......... ...T......  [ 780]
Mouse_NPRB  .......... .......... .......... .......... .......... ...T......  [ 780]

Human_NPRB  QIKGFIRRFN KEGGTSILDN LLLRMEQYAN NLEKLVEERT QAYLEEKRKA EALLYQILPH  [ 840]
Rat_NPRB    .......... .......... .......... .......... .......... ..........  [ 840]
Mouse_NPRB  .......... .......... .......... .......... .......... ..........  [ 840]

Human_NPRB  SVAEQLKRGE TVQAEAFDSV TIYFSDIVGF TALSAESTPM QVVTLLNDLY TCFDAIIDNF  [ 900]
Rat_NPRB    .......... .......... .......... .......... .......... ..........  [ 900]
Mouse_NPRB  .......... .......... .......... .......... .......... ..........  [ 900]

Human_NPRB  DVYKVETIGD AYMVVSGLPG RNGQRHAPEI ARMALALLDA VSSFRIRHRP HDQLRLRIGV  [ 960]
Rat_NPRB    .......... .......... .......... .......... .......... ..........  [ 960]
Mouse_NPRB  .......... .......... .......... .......... .......... ..........  [ 960]

Human_NPRB  HTGPVCAGVV GLKMPRYCLF GDTVNTASRM ESNGQALKIH VSSTTKDALD ELGCFQLELR  [1020]
Rat_NPRB    .......... .......... .......... .......... .......... ..........  [1020]
Mouse_NPRB  .......... .......... .......... .......... .......... ..........  [1020]

Human_NPRB  GDVEMKGKGK MRTYWLLGER KGPPGLL*  [1048]
Rat_NPRB    .......... .......... ........  [1048]
Mouse_NPRB  .......... .........Q ........  [1048]
```

174

Appendix 12: Relevant publications

Articles in peer-reviewed scholarly journals:

Zhu, X., Wang, Y., Schwiebs, A. and Walther, T. (2012) Chimeric natriuretic peptide ACNP stimulates both natriuretic peptide receptors, the NPRA and NPRB. *Mol Cell Endocrinol.* pii: S0303-7207(12)00498-4. doi: 10.1016/j.mce.2012.11.006.

Manuscript submitted for revision:

Schwiebs, A., Wang, Y., **Zhu, X.**, Pankow, K., Siems, W. E. and Walther, T. The virtually mature BNP (BNP1-32) is a precursor for the more potent BNP1-30.

Manuscripts in preparation:

Zhu, X., *et al.* Pathophysiological role of the newly designed natriuretic peptide ACNP in myocardial infarcted mice.

Zhu, X., *et al.* The mechanism and biological consequences of the interaction between natriuretic peptide receptors, the NPRA and NPRB.

Published abstracts:

Zhu, X., Wang, Y., Schwiebs, A. and Walther, T. (2011) Designed natriuretic peptide ACNP stimulating NPRA and NPRB, is a new promising tool for the treatment of cardiovascular diseases. Eur J Heart Fail 10 (Suppl. 1), S90.

Schwiebs, A., Wang, Y., **Zhu, X.**, Pankow, K., Siems, W. E. and Walther, T. (2011) The BNP metabolite BNP1-30 is a more potent vasorelaxant peptide than the mature BNP1-32 (Abstract). Eur J Heart Fail 10 (Suppl. 1), S6.

Abbreviations

AA	amino acid
ACE	angiotensin-converting enzyme
ANF	atrial natriuretic factor
ANP	atrial natriuretic peptide
AT1	angiotensin II type 1
BAEC	bovine aortic endothelial cells
BLAST	basic local alignment search tool
BNP	brain natriuretic peptide
BSA	bovine serum albumin
bp	base pairs
BW	body weight
cAMP	cyclic 3',5'-adenosine monophosphate
cDNA	complementary deoxyribonucleic acid
CF	cardiac fibroblasts
cGMP	cyclic 3',5'-guanosine monophosphate
CHF	congestive heart failure
CIP	calf intestinal alkaline phosphatase
CNP	C-type natriuretic peptide
COS	**C**V-1 in **O**rigin, and carrying the **S**V40 genetic material cells
CREB	cAMP-response element binding protein
CVD	cardiovascular diseases
ddH$_2$O	double distilled water
DEPC	diethylpyrocarbonate
DMEM	Dulbecco's modified eagle medium
DNA	deoxyribonucleic acid
DNP	Dendroaspis natriuretic peptide
DPBS	Dulbecco's phosphate buffered saline
EBSS	Earle's balanced salts
ECD	extracellular domain
ECE-1	endothelin-converting enzyme 1

eCFP	enhanced cyan fluorescent protein
E.coli	*Escherichia coli*
EDHF	endothelium derived hyperpolarizing factor
EF	ejection fraction
ELT	expand long template
eNOS	endothelial nitric oxide synthase
ER	endoplasmic reticulum
eYFP	enhanced yellow fluorescent protein
FCS	foetal calf serum
FRET	fluorescence resonance energy transfer
GC	guanylyl cyclise
GCD	guanylyl cyclase domain
GFR	glomerular filtration rate
GPCR	G-protein coupled receptor
HDMEC	human dermal microvascular endothelial cells
HEK293	human embryonic kidney cells
HF	heart failure
HPLC	high-performance liquid chromatography
HUVEC	human umbilical vein endothelial cells
IBMX	3-isobutyl-1-methylxanthine
ICD	intracellular domain
IDE	insulin-degrading enzyme
KO	knockout
L-NAME	NG-nitro-L-arginine methyl ester
LN	liquid nitrogen
LV	left ventricle
MALDI-T of MS	matrix assisted laser desorption ionization-time of flight mass spectrometry
MAP	mean arterial pressure
MAPK	mitogen-activated protein kinases
MC	mesangial cells
MCS	multiple cloning site
MI	myocardial infarction
M-MLV RT	Moloney Murine Leukemia Virus Reverse Transcriptase

177

mRNA	messenger ribonucleic acid
NEP	neutral endopeptidase
NFAT	nuclear factor of activated T-cells
NHE-1	sodium-hydrogen exchanger-1
NO	nitric oxide
NOS	nitric oxide synthase
NPRA	natriuretic peptide receptor A
NPRB	natriuretic peptide receptor B
NPRC	natriuretic peptide receptor C
NPS	natriuretic peptide system
NPs	natriuretic peptides
ORF	open reading frame
PCR	polymerase chain reaction
pGC	particulate guanylyl cyclase
PKC	protein kinase C
PKHD	protein kinase homology domain
qRT-PCR	quantitative real-time polymerase chain reaction
RAS	renin angiotensin system
RPMI	Roswell Park Memorial Institute medium
RQ	relative quantity
RT	room temperature
RT-PCR	reverse transcriptase-polymerase chain reaction
RV	right ventricle
SEM	standard error of the mean
sGC	souble guanylyl cyclase
SMC	smooth muscle cell
SNAP	S-nitroso-n-acetylpenicillamine
SRF	serum response factor
TD	transmembrane domain
TG	transgenic
TNF-α	tumor necrosis factor-alpha
TRPC	transient receptor potential canonical
URO	urodilatin
UV	urine volume

VNP	vasonatrin peptide
VSMC	vascular smooth muscle cells
WHO	World Health Organisation
WT	wild type